The Influence Of Host Genetics And Different *Mycobacterium tuberculosis* Strains On Macrophage Functions And Clinical Outcome Of Tuberculosis Disease

Thesis

THE INFLUENCE OF HOST GENETICS AND DIFFERENT *MYCOBACTERIUM TUBERCULOSIS* STRAINS ON MACROPHAGE FUNCTIONS AND CLINICAL OUTCOME OF TUBERCULOSIS DISEASE

by

TRINH THI BICH TRAM

A thesis submitted to the Open University U.K

For the degree of Doctor of Philosophy in the field of Life Sciences

Oxford University Clinical Research Unit

Hospital for Tropical Diseases

Ho Chi Minh City, Viet Nam

Jul, 2017

ABSTRACT

Only 5-10 % of *Mycobacterium tuberculosis* (*Mtb*) infected individuals develop active pulmonary TB (PTB), and around < 1 % develop disseminated TB meningitis (TBM). Macrophages are one of the first defense barriers, but it is unclear how their antimicrobial activities influence TB presentations and clinical outcomes. Many studies have shown host and bacterial genetics are important factors in TB susceptibility and progression. I hypothesized that an impairment of macrophage phagocytic function, under the influence of genetic factors, may help explain the pathogenesis of the transition from latent to active or disseminated TB, and that the virulence of clinical *Mtb* isolates are associated with *Mtb* lineages and distinct host immune responses.

I developed assays using ligand coated beads and *Mtb* reporter strain to measure the macrophage antimicrobial activities. Our assays were able to detect the variation in macrophage activities among different individuals.

I investigated the macrophage antimicrobial functions and its association with different TB phenotypes. I measured the macrophage activities in 43 latent TB (LTB) and active TB (ATB) cases combining 54 PTB and 60 TBM patients. Our results showed that macrophages treated with ligands displayed higher antimicrobial activities in LTB than ATB, but no difference between PTB and TBM. Whereas, in *Mtb*-infected macrophages from both LTB and ATB, proteolysis was reduced due to the modulation of *Mtb* and there was no difference in their ability to control *Mtb*. Our data also indicated that the antimicrobial activities of macrophages were ligand-specific or pathway-dependent.

The influence of host genetics on TB susceptibility was examined by the association of variants on phagocytic genes using a case-control study with 450 TBM, 450 PTB and 450 controls. Heterozygotes of Macrophage receptor with collagenous structure (*MARCO)* single nucleotide polymorphisms (SNPs) were associated with increased TB susceptibility, abnormal chest X-ray, infection by Beijing strains and also with impaired macrophage phagocytosis of ligand coated beads.

The virulence of *Mtb* strains was examined by observing cell lysis of macrophages infected with 159 *Mtb* strains. Virulence phenotype was grouped as low, moderate and high. High virulence was associated with Beijing lineage, reduced TNF-α and IL-6 and increased IL-1β concentration.

Overall, this thesis provides new insights into the influence of host and bacterial factors on TB susceptibility. It also provides a foundation for further studies on factors influencing TB susceptibility.

CO-AUTHORSHIP

The works presented here were primarily performed by me under the extensive guidance of my supervisors. However, my thesis would not have been finished without the assistances from members in the TB Research group as outlined below.

In chapter 4 on Association of macrophage antimicrobial activities and outcome of TB infection:

- TBM samples were collected from a clinical trial conducted in Hospital of Tropical Disease, Ho Chi Minh city, as described in Section 4.2. Principle investigators of the trial were Dr. Guy Thwaites and Dr. Nguyen Hoan Phu.
- PTB samples were collected from a study of macrophage function in district TB control units, as described in Section 4.2. Principle investigators of study were Dr. Nguyen Thuy Thuong Thuong and Dr. Nguyen Hoan Phu.
- Screening of latent TB in 99 healthy volunteers in OUCRU using T-SPOT.TB assays was performed by me and Ms. Vu Thi Ngoc Ha.
- PBMC isolation and cryopreserved monocytes were done with the support of Ms. Vu Thi Ngoc Ha. Ms. Tran Dinh Dinh, and Ms. Nguyen Thi Thanh Tran.
- *Mtb* reporter strain was generated by Mr. Vo Sy Kiet.

In Chapter 5 on Association of phagocytic genes and TB susceptibility:

- DNA from PTB, TBM and controls were extracted from previous members of the Human Host Genetics group led by Dr. Sarah Dunstan. The genotyping for phagocytic genes was performed in collaboration with Professor Thomas Hawn (University of Washington, USA) as detailed in Section 2.10.2. The chest X-ray results were read by clinicians at district TB control units.
- *Mtb* DNA extraction was done by Ms. Do Dang Anh Thu and *Mtb* genotyping was performed by Ms. Tran Dinh Dinh
- Statistical analysis of association of SNPs and TB susceptibility was done by me and my supervisor, Dr. Nguyen Thuy Thuong Thuong.

In Chapter 6 on Virulence of *Mtb* clinical strains and its association to bacterial genotype and host immune response:

- Isolation of *Mtb* from sputum samples and preparation of *Mtb* culture were performed by Ms. Do Dang Anh Thu and Mr. Hoang Thanh Hai.
- *Mtb*-infected THP-1 and observation of host cell lysis were done with the support of Ms. Hoang Ngoc Nhung.
- *Mtb* growth rate was analysed with the assistance of Dr. Dao Nguyen Vinh.

LIST OF PUBLICATIONS

A. Publications derived from the results of this thesis

N T T Thuong, **T T B Tram**, T D Dinh, P V K Thai, D Heemskerk, N D Bang, T T H Chau, D G Russell, G E Thwaites, T R Hawn, M Caws, and S J Dunstan. MARCO variants are associated with phagocytosis, pulmonary tuberculosis susceptibility and Beijing lineage. *Genes Immun.* 17, 1–7 (2016)

B. Others publications

1. Thuong NTT, Heemskerk D, **Tram TTB**, Thao LTP, Ramakrishnan L, Ha VTN2, Bang ND, Chau TTH, Lan NH, Caws M, Dunstan SJ, Chau NVV, Wolbers M, Mai NTH, Thwaites GE. Leukotriene A4 Hydrolase Genotype and HIV Infection Influence Intracerebral Inflammation and Survival From Tuberculous Meningitis. *J Infect Dis*. 215, 1020-1028 (2017)

2. Dunstan SJ, **Tram TT**, Thwaites GE, Chau TT, Phu NH, Hien TT, Farrar JJ, Wolbers M, Mai NT. LTA4H genotype is associated with susceptibility to bacterial meningitis but is not a critical determinant of outcome. *PLoS One*. 10, e0118789 (2015)

3. Dunstan SJ, Hue NT, Han B, Li Z, **Tram TT**, Sim KS, Parry CM, Chinh NT, Vinh H, Lan NP, Thieu NT, Vinh PV, Koirala S, Dongol S, Arjyal A, Karkey A, Shilpakar O, Dolecek C, Foo JN, Phuong le T, Lanh MN, Do T, Aung T, Hon DN, Teo YY, Hibberd ML, Anders KL, Okada Y, Raychaudhuri S, Simmons CP, Baker S, de Bakker PI, Basnyat B, Hien TT, Farrar JJ, Khor CC. Variation at HLA-DRB1 is associated with resistance to enteric fever. *Nat Genet*. 46,1333-1336 (2014).

ACKNOWLEDGEMENTS

Firstly, I would like to express my deepest appreciation to my supervisors, Dr. Nguyen Thuy Thuong Thuong for her constant guidance and support during my PhD study and research as well as during my writing of this thesis. I have learnt from her not only knowledge but also the motivation and enthusiasm in doing research. Without her patient instruction, this thesis would not have been possible. I am also sincerely grateful to my co-supervisor, Professor Guy Thwaites for his review and critical feedback of the thesis.

I would very much appreciate my senior colleague Dr. Vijay Srinivasan for his superb support especially during my writing-up stage. I always enjoy and feel motivated in discussing my work with him. I would also thank Ms. Do Dang Anh Thu, Ms. Vo Thi Ngoc Ha, Mr. Hoang Thanh Hai, Ms. Hoang Ngoc Nhung, Ms. Tran Dinh Dinh for their generous help in doing laboratory, Dr. Dao Nguyen Vinh for his support in statistical analysis, Ms. Nguyen Thi Hanh for her coordination with district TB units in patient recruitment, Mr. Nguyen Van Be for rapid sample delivery. Many thanks go to clinicians and nurses who were involved in TB studies in Viet Anh ward and district TB control units as well as to other colleagues in OUCRU for their help and encouragement during my PhD journey.

I would like to express special thanks to TB patients and all OUCRU healthy volunteers who were willing to donate their blood for my study.

At last, I would like to send my big thank to my family for their unconditional support.

28 July 2017

ABBREVIATIONS

ANOVA	One-way Analysis of Variance
BCG	Bacillus Calmette-Guerin
bp	base pair
CF-SE	Carboxyfluorescein succidinimyl ester
CFU	Colonies Forming Unit
CR	Complement Receptor
CTAB	Cetyl trimethylammonium bromide
CTLR	C type lectin receptor
CXR	Chest X-ray
DC	Dendritic cell
DC-SIGN	DC-specific intercellular adhesion molecule-3 grabbing nonintegrin
DMSO	Dimethyl sulfoxide
DNA	Deoxyribonucleic acid
DQ-BSA	DQ green bovine serum albumin
ELISA	Enzyme linked immune sorbitol assay
FBS	Fetal Bovine Serum
FcγR	Fc gamma receptor
GRCh38.p10	Genome reference consortium human build 38 patch release 10
GWAS	Genome Wide Association Study
HCB	Han Chinese Beijing
HCMC	Ho Chi Minh city
HIV	Human Immunodeficiency Virus
hMDM	Human monocyte-derived macrophages
HRP	Horseradish peroxidase
HWE	Hardy-Weinberg equilibrium
IFN-ɣ	Interferon-gamma
IgG	Immunoglobulin G
IL-	Interleukin-
LAM	lipoarabinomannan
LAMP	Lysosomal-associated membrane protein
LD	Linkage disequilibrium
LJ	Löwenstein–Jensen
LPS	Lipopolysaccharide
LSP	Large sequence polymorphism
LTB	Latent tuberculosis
MAF	Minor allele frequency
MARCO	Macrophage receptor with collagenous structure
MDR-TB	Multidrug-resistant tuberculosis
MHC	Major histocompatibility complex
MINCLE	Macrophage-inducible C-type lectin
MOI	Multiplicity of infection

MR	Mannose receptor
mRNA	Messenger ribonucleic acids
Mtb	*Mycobacterium tuberculosis*
NADPH	Nicotinamide Adenine Dinucleotide Phosphate
NK	Natural Killer
NO	Nitric oxide
NRAMP1	Natural resistance-associated macrophage protein 1
OADC	Oleic Albumin Dextrose Catalase
OD_{600}	Optical density at 600nm
OUCRU	Oxford University Clinical Research Unit
OXTREC	Oxford Tropical Research Ethics Committee
PAMP	Pathogen associated molecular pattern
PBMC	Peripheral blood mononuclear cells
PBS	Phosphate-buffered saline
PE	Phycoerythrin
pks	polyketide synthase
PMA	Phorbol 12-myristate 13-acetate
PTB	Pulmonary tuberculosis
SE	Succidinimyl ester
SNP	Single nucleotide polymorphism
SR	Scavenger receptor
SSC	Side-scattered light
TB	Tuberculosis
TbD1	Tuberculosis specific deletion 1
TBM	Tuberculosis meningitis
TDM	Trehalose-6',6-dimycolate
Th1	T helper 1
Th2	T helper 2
TLR	Toll like receptor
TNF	Tumor necrosis factor
V-ATPase	Vacuolar H^+ Adenosine triphosphatase
WBC	White Blood Cells
WCL	whole cell lysis
WHO	World Health Organization
XDR-TB	Extensively drug-resistant tuberculosis

TABLE OF CONTENTS

LIST OF FIGURES

List of Tables

Chapter 1
INTRODUCTION

1.1 Tuberculosis (TB)

1.1.1 History of tuberculosis

Tuberculosis is a very old disease that was assumed to have accompanied human migrants out-of-Africa between 35,000-89,000 years ago, spreading to other parts of the world by land or coastal water travel[1]. However, a genomic study in 2014 has suggested that TB is younger than 6,000 years old and seals could be the mode of transmission of the disease from Africa to South America[2]. The disease is very common and associated with death, thus it has been known with other names such as phthisis, Robber of youth, the Captain among these men of death, or the King of evil[3]. During the 19th century, TB had become epidemic with high mortality rate among young and middle-aged adults[1].

The history of tuberculosis was changed dramatically on 24th March, 1882, when Koch discovered *Mycobacterium tuberculosis* (*Mtb*) as the causative agent[1] and explained the etiology of tuberculosis. The discovery was the greatest of the era and 24th March is recognized as the World TB day. Koch's discovery opened the way toward diagnosing and preventing tuberculosis. The other big achievements, still important today, were the development of the Pirquet and Mantoux tuberculin skin tests and Bacille Calmette-Guerin (BCG) vaccine[1]. The discovery of streptomycin, isoniazid and rifampin also began a new era of TB treatment with the hope of eliminating the disease[1]. However, despite these tools, TB remains a major public health problem, compounded by HIV-TB co-infection and multi-drug resistant strains.

1.1.2 Epidemiology of TB

Although TB incidence has been falling globally at an average rate of 1.5 % per year since 2000, TB still remains a challenge for healthcare systems worldwide with an estimated 9.6 million new TB cases in 2014. Among these, there are 56.25 % men,

33.33 % women and 10.42 % children[4]. As a disease of poverty, TB cases are predominant in low-income countries. Six countries including China, India, Indonesia Nigeria, Pakistan and South Africa collectively accounted for 60% of new cases worldwide[5]. South Africa region has the highest incidence with 281 cases per 100,000 population, which is twice the global average of 133[4]. High-income countries, including most countries in Western Europe, Canada, the United States of America, Australia and New Zealand, have very low burden with less than 10 cases per 100,000 population per year[6].

In addition, the synergistic interaction with HIV drives TB to be particularly difficult to control. The risk of developing TB in HIV-infected individuals are 26-31 times higher than those who are HIV-uninfected[7]. 13% of new incidence TB cases were estimated to be associated with HIV infection in 2014. TB has been considered as one of the leading causes of death among HIV-infected patients. The prevalence of TB and HIV co-infection was highest in Africa region. In some African countries, up to 80% active TB patients were associated with HIV infection while this number was lower in the Asian region. In 2015, about 25% of all TB deaths had HIV co-infection and about 35% of HIV deaths were due to TB[8].

Drug resistant TB presents a threat for public health globally. The number of cases with multidrug resistant (MDR-TB), defined as resistance to both isoniazid and rifampicin, slightly increase in recent years with an estimated 3.9 % of new cases and 21% of re-treatment cases[5]. According to the WHO report in 2015, there were an estimated 480,000 new cases of MDR-TB, and half of them were in China, India, South Africa and European Regions[5]. Cases with extensively drug-resistant tuberculosis (XDR-TB), defined as resistance to isoniazid, rifampin plus resistance to at least one

fluoroquinoline and a second-line injectable agent have been reported in total 105 countries[4]. About 9.7% of patients with MDR-TB have XDR-TB on average[5].

From 2015 Vietnam has been reported to have reached the global target of 50 % reduction compared to 1990 in TB prevalence and mortality. However, Vietnam is still one of 22 high TB-burden countries in the world with an estimated 140 new cases per 100,000 population. Almost 18,000 people die from TB every year. The TB incidence is geographically distributed with significantly higher rates in the Southern provinces of Vietnam, especially in Ho Chi Minh City and the greater Mekong River Delta[9,10]. Vietnam ranks 14th among 27 highest MDR-TB countries with an estimated 4% MDR-TB among new cases and 23% among the previously treated patients[4]. The proportion of HIV-positive patients with TB also slightly declined from 8.0 % in 2011 to 5.2 % in 2014[11].

1.1.3 Pathogenesis of TB

When a TB patient coughs, sneezes, or spits, 1-5 μm aerosols containing *Mtb* that causes the disease are produced; another person who inhale this air-drop may get infection. The droplet size negatively correlates to the infectiousness. The smaller sizes are likely responsible for transmission of the disease since they facilitate entry of *Mtb* to the lower lung, a place where bacteria can avoid continuous waves of microbicidal macrophages recruited by resident microflora or inhaled environmental microbes[12]. In the lower lung, the first encounter of *Mtb* with alveolar macrophages initiates a cascade of phagocytosis events, which may result in different scenarios. The macrophage response can kill the bacteria effectively and prevent progression to active disease. Otherwise, if the immune response is insufficient to control the bacterial replication, it will lead to the development of the clinical disease known as primary progressive TB in

approximately 5 % of those who get infection[13]. The disease could be remained in the lungs (first site of TB infection) or else some bacilli may move through the blood, spreading to different parts of the body to cause extra-pulmonary forms of primary TB, particularly in the meninges, bones, joints and kidneys[14]. In most infected individuals, the infected macrophages are surrounded by other immune cells including uninfected macrophages, neutrophils, T cells and B cells to form a structure known as a granuloma. *Mtb* may be kept in this structure in a dormant stage and they are unable to cause disease[15]. A person with this scenario is classified as having latent infection as evidenced by T-cell reactivity to mycobacterial antigens but they are asymptomatic and not contagious. Using an advanced image technology comprising positron emission tomography combined with computed tomography (PET-CT) provides evidence for the biological heterogeneity in the lung lesions of people with LTB[16]. Those harbouring severe abnormalities suggestive of a subclinical phase of disease, such as infiltrates, scars, or active nodules, have an increased risk to progress to symptomatic active TB. By contrast, those showing no evidence of subclinical pathology are less likely to suffer from the reactivation. Generally, about 10 % among these may develop the post-primary active disease during their lifetime. The question of whether endogenous re-activation or exogenous re-infection is the cause of the second episode of TB has been controversial. Current opinion favors reinfection being a source of adult TB in high incidence areas[17] with the proportion of cases attributed to reinfection varying from 12 % to 75 %[18]. Upon reinfection, latent TB is protective against the progressive TB while the prior active TB is associated with the post-primary disease c[13,18,19].

The determinants for containment of infection or progression to disease are not well understood and are multifactorial. Host and environment are thought to be important

variables that determine outcomes of TB disease. However, there is increasing evidence that pathogen determinants and their interaction with the host and environment are also important in understanding of TB pathogenesis[20].

1.1.4 Clinical features of TB

TB case definition for public health surveillance from WHO 2013 includes both laboratory and clinical criteria[21]. According to this definition, a TB case is confirmed when *Mtb* is detected in the clinical specimen using one of these methods: smear microscopy, culture or WHO-approved rapid diagnosis such as Xpert *MTB*/RIF[21]. In the absence of laboratory confirmation, a case can be diagnosed by clinical criteria including positive tuberculin skin test, chest X-ray, signs and symptoms compatible with TB, and response to treatment with two or more anti-TB medications.

TB cases could be classified according to the anatomical site of the disease. Pulmonary tuberculosis (PTB) refers to any cases of TB in the lung parenchyma or the tracheobronchial tree. The classic clinical features of PTB include chronic cough, fever, night sweats, loss of weight and appetite, and hemoptysis. Chest pain and difficulty in breathing as a result of parenchymal lung involvement can be present in extensive disease. Physical findings in pulmonary TB are often not helpful in defining TB. Chest X-ray examination can be used to diagnose and monitor the lesions in the lung[22]. Extra-pulmonary or disseminated TB refers to any case of TB in organs other than the lungs, for example, meninges, lymph nodes, abdomen, skin, and bones. Disseminated TB occurs in 10 % to 42 % of patients, depending on ethnicity, age, co-infection, *Mtb* strain, and immune status[20,23]. Meningeal TB is common in young children and in HIV-infected people. This is the most severe form of extra-pulmonary TB, which kills or leaves neural sequelae in half of people affected[24].

1.1.5 Treatment and prevention of TB

An early and accurate diagnosis, a screening for drug resistance, administration of appropriate antibiotics, and an adherence of patients during the treatment course are essential factors for the successful treatment for TB. The current standard treatment regimens using four first-lines dugs (isoniazid, rifampin, pyrazinamide, and ethambutol) have achieved around 90 % - 95 % cure rates in PTB treatment under provision of tuberculosis-control programs[25]. This regimen requires at least 6 months for two phases, including the intensive phase lasting 2 months of all four drugs and the continuation phase lasting 4 months of isoniazid and rifampin. In case of TB and HIV co-infection, since the early initiation of antiretroviral therapy results in a reduction in mortality especially in those with more advanced degree of immunosuppression[26], it is recommended that the antiretroviral therapy should be initiated within first 2 or 8 weeks of starting TB treatment depending on the $CD4^+$ T-cell count[27]. Patients with MDR-TB are considered incurable with conventional regimens. WHO treatment guidelines recommend that the intensive phase of regimen should last for at least 8 months, and a fluoroquinolone and a second-line injectable agent should routinely be included[28]. XDR-TB, which kills more than 70 % of patients, is extremely difficult to treat. New drugs are being investigated in trials, with several studies being conducted to access shortened regimens for drug-sensitive disease and more effective therapy for drug-resistant disease. The Nix-TB trial of three antibiotics (bedaquiline, pretomanid, and linezolid), that have not been combined before to treat TB, is investigating whether they may offer simpler, safer regimens for XDR-TB and MDR-TB treatment[29].

BCG is an anti-TB vaccine containing attenuated live bovine tuberculosis bacilli (*M. bovis*) that lost their virulence by being serially sub-cultured on bile potato medium for

years[30]. Studies of protective efficacy of BCG vaccination range from no protection to ≥ 80 % protection; this variation appears to be attributable to differences in populations, age at vaccination, nutrition status, vaccine strains, virulence of *Mtb* strains[31]. A meta-analysis study of 1,264 publications found that BCG vaccination significantly reduces the risk of TB by 50 % on average[32]. Interestingly, the vaccine successfully protects children against the most severe forms of TB such as miliary and TB meningitis, with the protective effectiveness being more than 80 %[31]. BCG is still used for infants at birth in most countries with a high TB burden. New vaccines to replace BCG, or boost BCG are being studied, offering hope for future TB control[23].

1.2 *Mycobacterium tuberculosis* - the pathogen

Mtb is one of the most successful human pathogens. The bacteria can utilize the host immune response for its survival and replication (discussed in later sections), resulting in complex clinical manifestations. The diagnosis and the treatment of the disease have been posing challenges for TB healthcare systems for more than 100 years. Therefore, understanding the bacterial genetics and its associated phenotypes could be essential for TB treatment and elimination.

1.2.1 Characteristics of *Mtb*

Mtb is an obligate pathogenic bacterial species in the *Mycobacterium* genus and the main causative agent of TB disease in humans. Koch first discovered *Mtb* in 1882 by culturing the crushed granulomas. *Mtb* is a member of *Mtb* complex which in addition includes other species that all cause disease in human and maybe in other hosts. These species include *M. africanum* causing TB in human only in certain regions of Africa; *M. bovis, M. caprae* and *M. pinnipedii* causing TB in wild and domesticated mammals; *M. microti* causing TB in voles[33]. *Mtb* has a rod-like and slightly curved shape, 0.5 μm in

diameter and 1-4 μm in length. The bacteria do not have flagellum, capsules, or spores, although some studies suggest spore formation in aged mycobacterial culture[34,35]. The cell wall of *Mtb* mainly consists of a thick layer of hydrophobic mycolic acids at its external portion. *Mtb* is not classified as a Gram positive or negative bacterium as the cell is poorly permeable to Gram staining. The unique characteristic of lipid-rich cell wall made the bacillus resistant to decolourization by acids during staining procedures. As such, *Mtb* is called an acid-fast bacillus and can be detected by red color on a stained smear, which has been taken advantage of in TB diagnosis. The characteristic of cell wall is also thought to impair the entry of nutrients, which causes slow growth of mycobacteria with the doubling time of *Mtb* being about 24 hours[36].

1.2.2 Genetic diversity of *Mtb* strains

In contrast to other bacteria, *Mtb* strains are unable to undergo horizontal gene transfer. In addition, since *Mtb* strains present over 99 % similarity at their nucleotide sequence level and have identical 16S RNAs sequences, it was believed for a long time that there is limited genetic variation among *Mtb* strains[37]. However, later studies employing different molecular typing methods, such as spoligotyping, large sequence polymorphism (LSP), whole genome sequencing, have revealed genetic variations in *Mtb* genomes[37]. Such genetic diversity is attributable to the duplication, depletion or transposition of chromosome regions as well as single nucleotide polymorphisms (SNPs). Using these genetic markers, *Mtb* strains were further subdivided into different lineages. Currently the human–adapted *Mtb* complex including *Mtb* and *M. africanum* can be classified into seven main phylogenetic lineages[38] (Figure 1.1). These lineages comprise Indo-Oceanic (also known as Lineage 1), East Asian/Beijing (also known as Lineage 2), East African-Indian (also known as Lineage 3), Euro-American (also known

as Lineage 4), *M. africanum* West Africa-1 (also known as Lineage 5), *M. africanum* West Africa-2 (also known as Lineage 6) and Ethiopian (lineage 7) lineages. Based on the presence or absence of a *Mtb*-specific deletion known as TbD1, *Mtb* complex can also be divided into ancestral or modern lineages respectively[39]. East Asian/Beijing, East African-Indian and Euro-American lineages are considered to be modern whereas Indo-Oceanic, *M. africanum* West Africa-1 and 2 lineages are ancient. Studies have also revealed a significant variation in phylogeographic distribution among major lineages, with each lineage being associated with a particular geographic region (Figure 1.2). The most widely distributed group is East Asian/Beijing lineage. This lineage occurs frequently in East Asian populations, but is also found to be present in Central Asia, Russia, and South Africa[40]. Euro-American lineage predominates in regions of Asia, Europe, Africa and America. The distribution of Indo-Oceanic and East African-Indian lineages is geographically limited to East Africa, Central-, South-, South-East Asia. The most geographically limited distributed groups are *M. africanum* West Africa-1 and 2 lineages that exclusively occur in West Africa[40] and Ethiopian lineage which to date has only been observed in Ethiopia or recent Ethiopian emigrants[41].

Among seven lineages, the East Asian/Beijing strain is considered to be emerging worldwide today[42]. This family represents 50 % of strains in East Asia and 13 % of isolates around the world. In Vietnam, there are three main lineages including Indo-Oceanic, Euro-American and East Asian/Beijing. Among these, the East Asia/Beijing lineage is highly prevalent, being responsible for 40 % of tuberculosis cases[43,44].

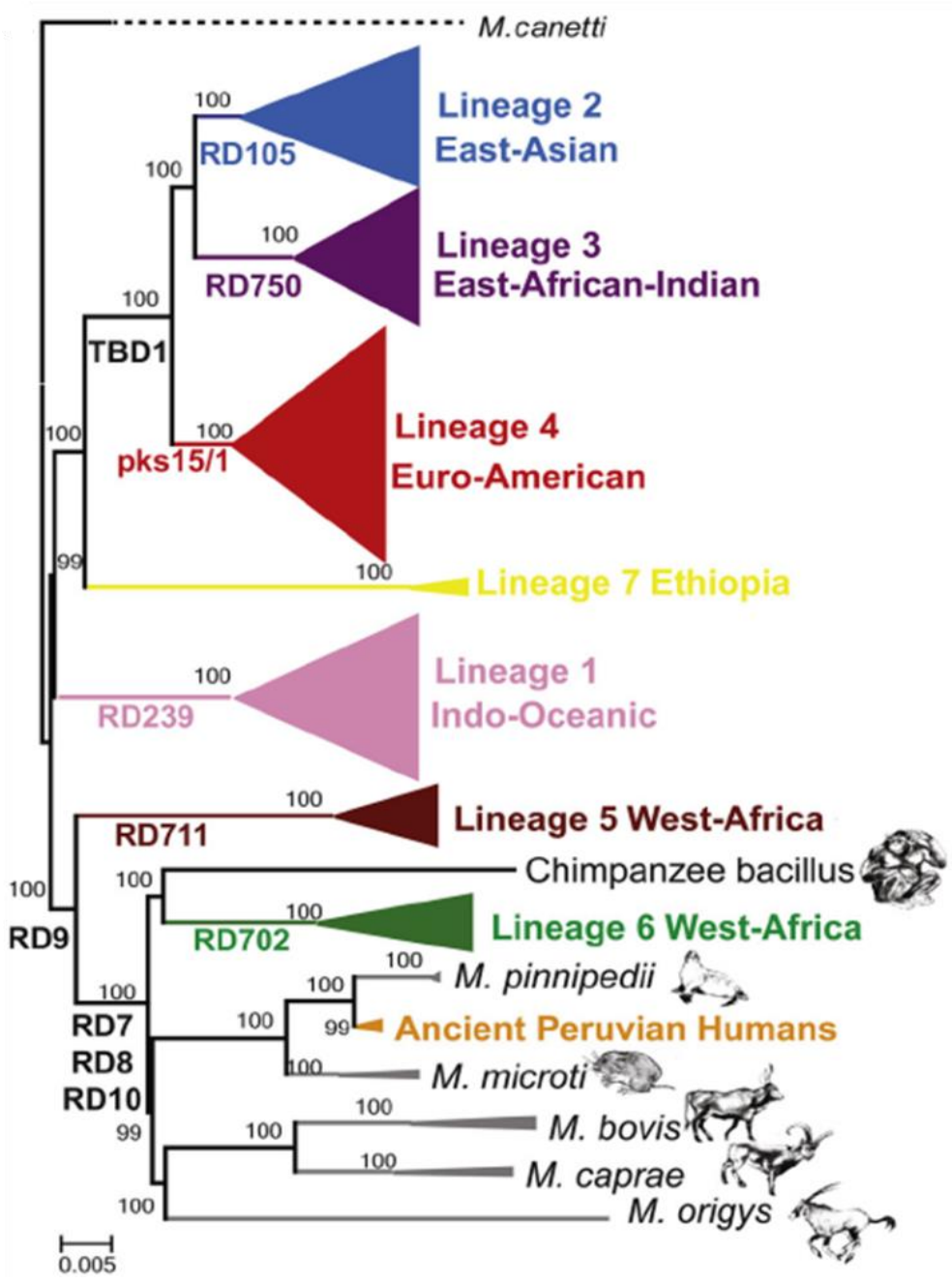

Figure 1.1 Global phylogeny of human-adapted *Mtb* complex

7 *Mtb* lineages were defined by the whole genome sequencing analyses. Node support after 1000 bootstrap replications is shown on the branches and the tree is rooted by the outgroup *M. canetti*. Region of difference (RD) on *Mtb* genome were indicated along branches. Scale bar indicates the number of nucleotide substitution per site (Coscolla et al.[45]).

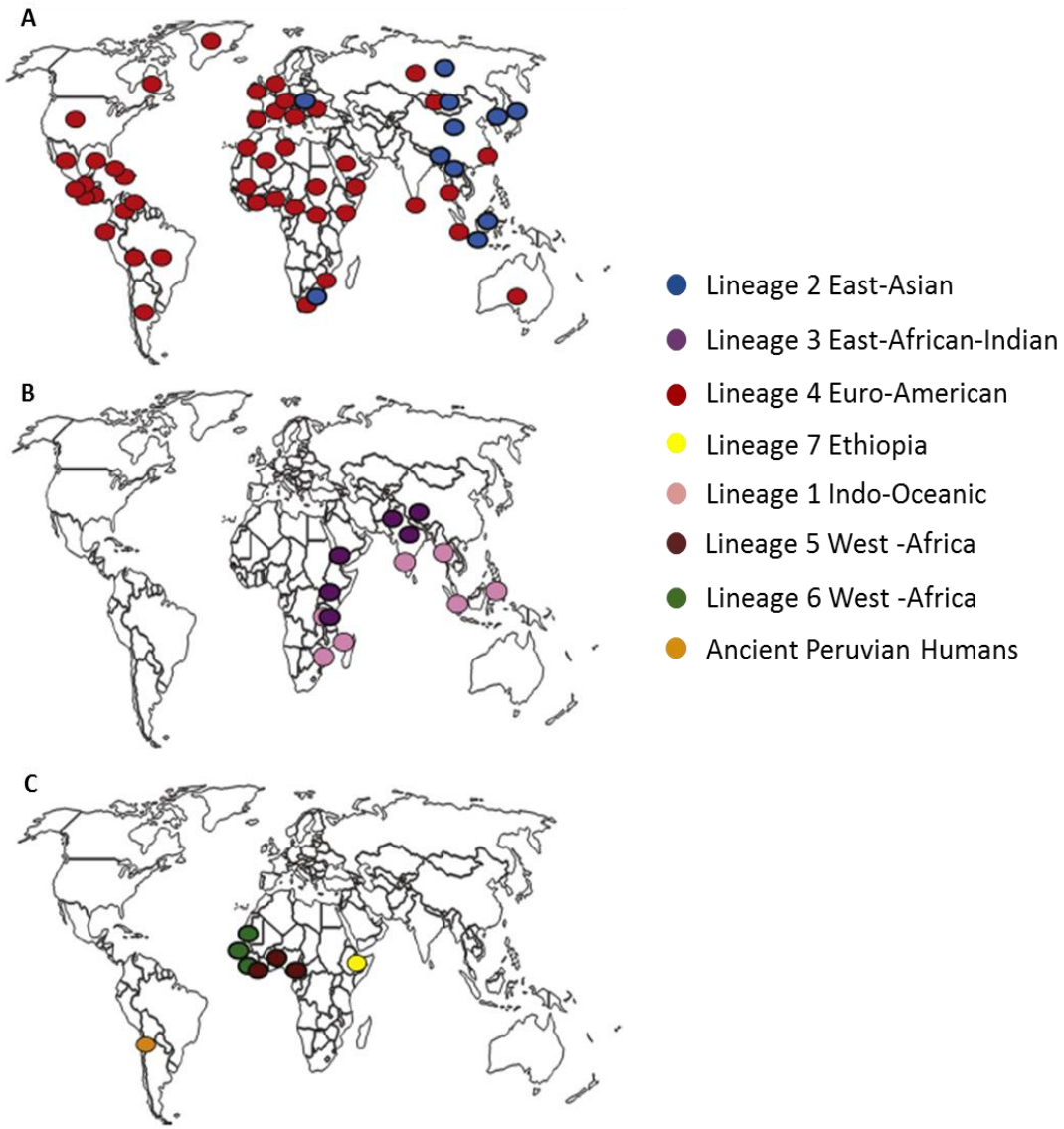

Figure 1.2 Global phylogeography of human-adapted *Mtb* complex
Dots indicate the dominant *Mtb* lineages in the country. Panel (A) shows the most geographically widespread lineages, panel (B) the intermediately distributed lineages, and panel (C) the most geographically limited distributed lineages (Gagneux *et al.*[45]).

1.2.3 Effect of genetic diversity of *Mtb* strains

During the last decades, by using various experimental models, many studies have indicated that the genetic diversity of *Mtb* lineages has translated into significant differences in the bacterial virulence and immunogenicity. The effect of *Mtb* lineage variation on clinical phenotypes has also been established.

1.2.3.1 Difference in virulence

Virulence can be defined by the ability of pathogen to cause the disease in the human host[46]. Since the development of TB disease is associated with the growth and replication of bacteria within the host, studies have assessed the virulence of *Mtb* strains by measuring the growth of bacteria in monocytes or macrophages *in vitro*[47,48], or measuring the bacterial burden in organs as well as the morbidity and mortality in animal models including guinea pigs[49,50], mice[51–53] or marmosets[54].

Difference in virulence among various *Mtb* strains have been observed very early from many decades ago[49,50]. Later studies using different molecular typing methods have demonstrated lineage-associated virulence. In general, the modern lineages including East Asian/Beijing and Euro-American lineages are considered to be higher virulence than ancestral lineages *M. africanum* West Africa-1 and 2 lineages[51]. At the level of individual lineage, East Asia/Beijing lineage is consistently demonstrated to be hypervirulent compared to other lineages in different infection models[48,51–54]. Several studies have indicated a wide variation in virulence among strains in the same lineage[48,55–58].

The high virulence phenotype of East Asia/Beijing could have resulted from intrinsic biochemical properties. Beijing lineage is suggested to show increased expression of α-crystallin and decreased expression of Hsp65, PstS1 and 47kDa protein. α-crystallin is known as a *Mtb* virulence factor while the other proteins plays a role as *Mtb* antigen. Such a reduced level of these antigen may allow Beijing lineage to evade the host response[59]. This lineage is also known to employ a different cell wall-associated lipid structure named polyketide synthase-derived phenolic glycolipid (PGL) that inhibits the

host protective immune response[60]. However, the genetic mechanisms for the lineage-specific virulence are still not clear.

1.2.3.2 Difference in host immune response

Mtb genetic diversity has also been demonstrated to induce differences in host immune response. The modern lineages (East Asian/Beijing, East African-Indian and Euro-American) induced lower inflammatory response compared to ancient lineages (Indo-Oceanic and West Africa)[61]. East Asian/Beijing strains have been most widely studied and consistently reported to induce low levels of pro-inflammatory cytokines[47,53,62,63]. The modern lineages in general, and East Asian/Beijing in particular, are shown to be virulent and globally wide-spread, suggesting that the cytokine profile might link to an effective immune evasion of these lineages[64]. As a reduced inflammatory response in host can allow a rapid intracellular growth and spread to other cells or organs, the disease can develop and transmit to new hosts. Indeed, many studies on *Mtb* strains with different transmission dynamics have demonstrated high correlation of pro-inflammatory cytokine production, virulence phenotype and transmissibility of the bacteria[65,66]. Specifically, strains that induce a low level of pro-inflammatory cytokines show increased virulence and transmission.

As with virulence phenotype, there is the variation in ability to induce immune response among strains within the same lineage[51,67,68]. Some studies indicate the contrary results for East Asia/Beijing lineage; for example, in murine macrophage model *Mtb* strains of this lineage elicit equal or high level of Tumor necrosis factor alpha (TNF-α) and Interleukin (IL)-1β compared to Indo-Oceanic or Euro-America lineages[67]. The divergent results could come from the differences in strains examined in studies[69].

1.2.3.3 Difference in clinical phenotype

Apart from the difference in virulence *in vitro*, *Mtb* genotypic diversity is associated with the variable clinical outcomes. Studies in Vietnam have indicated that the Euro-American lineage is more likely to cause pulmonary TB than meningeal TB[20] and lung consolidation is found in a high proportion of TB patients infected with this lineage[70]. Among 6 lineages, East-Asian/Beijing is the most studied strain genotype and is demonstrated to be associated with rapid disease progression and severity. In the Gambia, individuals infected with East-Asia/Beijing lineage are more likely to progress to active TB disease compared to individuals infected with *M. africanum*[71]. Vietnamese patients with TBM caused by the East Asian/Beijing lineage present shorter duration of illness to treatment and fewer cerebrospinal fluid (CSF) leukocytes than those caused by the other lineages[70]. Studies in Russia have indicated an association between East-Asian/Beijing lineage and chest radiological abnormalities[72] or extra-pulmonary forms of TB[73,74]. Infection with this lineage has also induced rapid weight loss and led to higher bacterial load in lung, liver and spleen in non-human primate model[54]. In addition, East-Asia/Beijing lineage has been reported to be associated with drug resistance[70,75], treatment failure[76,77] and disease relapse[78,79]. Whereas some of the studies in European and African countries have shown no association of East-Asia/Beijing lineage and TB clinical presentation[80,81]. The discrepancy results on the genotype-phenotype relationship could be due to the differences in sample size and patient ethnicity among the studies.

1.3 Host immune response against TB

1.3.1 The innate immunity

The innate immune response plays an important role in the protection against TB because it provides the first line of defense against *Mtb*. Many studies suggest that innate immunity could determine the outcome of infection by helping to control mycobacteria growth and shape the magnitude of adaptive immunity[82,83]. However, the innate immune response to *Mtb* is not yet completely elucidated, largely because of difficulties in studying immunity in the human lung. This part is a review on key innate cell types and processes implicated in innate host response to *Mtb* infection, which is derived mainly from *in vitro* studies or animal models.

1.3.1.1 Initial recognition and phagocytosis of *Mtb*

Alveolar macrophage is the primary cell type involved in the initial uptake of *Mtb*, after that dendritic cells and macrophages also come and take part in the phagocytosis process, mediating the subsequent host signaling to eliminate bacterial infection. The initial recognition and uptake of *Mtb* require a number of pathogen recognition receptors on the membrane of innate immune cell types, which either recognize *Mtb* directly via pathogen associated molecular patterns (PAMPs) or indirectly via opsonin with immunoglobin G (IgG) or complement on the bacterial surface. *Mtb* is an intracellular bacterium that can survive and multiply within macrophages, therefore the initial recognition and uptake is also exploited by *Mtb* for its entry into the cells and establishing infection. Below is a summary of surface receptors involved in the uptake of *Mtb*. It remains unclear whether different modes of entry into macrophage may lead to different subsequent events within the host as well as outcome of infection[84].

a. Complement receptors

The complement system comprises a number of soluble proteins that respond in a sequential manner, producing a cascade of reactions. The complement protein can be classically activated by its binding to an antigen-antibody complex or alternatively activated without antigen-antibody complex. The activated complement functions opsonizating pathogens to facilitate their phagocytosis, through chemotaxis to attract the phagocytes, or through lysis of antibody-coated bacteria. Macrophages possess various receptors for complement on their cell surface, including complement receptor (CR) 1, CR3 and CR4. Among CRs, CR3 is the principal receptor which is expressed dominantly on monocytes, macrophages, neutrophils, and natural killers.

Mtb is able to activate the complement system through the alternative pathway, resulting in the opsonization of bacteria. The opsonized *Mtb* then can bind to CRs and be phagocytosed in the phagosome. The role of CRs on macrophages in the course of *Mtb* infection has been debated. Many works indicate that lack of or blocking of CR3 results in the reduced phagocytosis of *Mtb*[85,86]; whereas other studies have shown that antibody blocking of CR3 has no effect on the binding of *Mtb*[87], the induction of anti-microbial effector mechanism or bacterial survival in macrophages[86]. Additionally, CR3-deficient mice have exhibited no defects in the control of *Mtb* infection compared to wild type[88].

b. C-type lectin receptors

C-type lectin receptors (CTLRs) consist of carbohydrate-binding C-type domains that can recognize and bind to carbohydrate-rich molecules. In addition to participating in various processes such as cell adhesion and migration or lipid scavenging, CTLRs function in the pathogen recognition and phagocytosis[89].

Mtb is recognized by a number of transmembrane CTLRs including mannose receptor (MR), Dendritic cell-specific intercellular adhesion molecule-3 grabbing non-integrin (DC-SIGN), MINCLE, and DECTIN-1. MR can be found on most types of tissue macrophages but not on circulating monocytes[90]. DC-SIGN is expressed mainly on the surface of dendritic cells (DCs) but also on the macrophage surface. These receptors are reported to bind lipoarabinomannan (LAM)[91] or mannose-capped LAM (ManLAM)[92], components on *Mtb* cell wall, to induce the bacterial phagocytosis. The binding of LAM or ManLAM are also reported to inhibit the phagosome-lysosome fusion in the infected macrophage[92], prevent the T cell-mediated immune response by inhibiting the maturation of infected DCs, and induce the production of anti-inflammatory cytokine IL-10[93]. These conditions promote host immunosuppression and may contribute to *Mtb* survival.

c. Scavenger receptors

Scavenger receptors (SRs) comprise a large family of integral membrane proteins belonging to at least 8 different subclasses (A-H) based on their tertiary structure[94,95]. These receptors are known to bind a variety of ligands including modified or oxidised low-density lipoproteins, apoptotic cells and pathogens[94].

Both class A including scavenger A (SRA) and macrophage receptor with collagenous structure (MARCO), and class B SRs are involved in *Mtb* recognition and uptake. Many studies have indicated that these SRs participate in phagocytosis of mycobacterial species, including *M. leprae*[96], *M. avium*[97], *M. bovis* BCG[98], and *Mtb*[87,99] and are required for production of pro-inflammatory cytokines against mycobacterial infection. Blocking class A SRs almost abolishes all the *Mtb* binding and phagocytosis that persist

after CR and MR are blocked[87]. This also leads to a reduction in TNF-α production mediated by mycobacterial lipopeptides[100,101].

d. Fcγ receptors

There are two types of Fcγ receptors (FcγRs), including activation receptors and inhibitory receptors that contain an immunoreceptor tyrosine activating motif or inhibitory motif, respectively. While DCs and macrophages express both activating and inhibitory receptors, natural killer (NK) cells only express activating FcγRs and B cells are limited to inhibitory FcγRs. All FcγRs mediate the internalization but the type of receptors will determine the subsequent processes. The internalization by activating FcγRs favors effector responses for antigen processing and presentation that results in activation of T cells, while the internalization by inhibitory FcγRs favors preserving the intact antigen for presenting to B cells[102].

The uptake of *Mtb* opsonized with antibody against TB via FcγRs is shown to lead to a rapid phagosome-lysosome fusion[103], an enhanced oxidative burst and production of pro-inflammatory cytokine in infected macrophages[104]. There is no difference in the intracellular growth rate after internalization between opsonized and non-opsonized tubercule bacilli, indicating that entry by FcγRs or alternative does not affect the intracellular survival of bacteria[103].

e. Toll like receptors

Toll like receptors (TLRs) are transmembrane proteins with an extracellular leucine-rich domain to recognize bacterial products. TLRs that are known to be involved in *Mtb* recognition include TLR2, TLR4, TLR9 and possible TLR8[36]. TLR2 can recognize a number of lipoglucans and lipids on mycobacterial cell walls, including LAM, LAM-precursor lipomannan (LM) and mannosylated phosphatidylinositol (PIM). Such ability

to recognize different bacterial structures could be explained by the unique ability of TLR2 to cooperate with is co-receptors including TLR1, TLR6, CD14, or CD36[105,106]. Treatment of mice macrophages with PIM, LAM or LM leads to an increased production of pro-inflammatory cytokines[107]. TLR4, a receptor in concert with CD14 binding to LPS of Gram negative bacteria, recognizes *Mtb* cell wall lipids, glycoproteins, and secreted proteins[108]. The intracellular TLR9 that is located on the phagosomal membrane can recognize *Mtb* DNA and induce TNF-α production[109]. The significant role of TLRs in TB infection is not always consistent *in vivo*. TLR2 and TLR4 are demonstrated to be required for the control of *Mtb* infection in mice[110,111] but other studies have shown the unnecessary role of these receptors in immunity against *Mtb* infection[112,113]. Nevertheless, many genetic studies have shown the association of polymorphisms in TLR genes and TB susceptibility[114].

f. Other receptors

In addition to these important receptors, other receptors and proteins can recognize and mediate the interaction of innate immune cells and *Mtb*. Surfactant proteins A in the lung can coat *Mtb*, enhancing macrophage binding and *Mtb* uptake by binding to surfactant protein A receptors on the macrophage[115] or to other receptors such as FcγRs, complement receptors[116], and probably mannose receptors[117]. CD14 can also recognize and bind *Mtb* via LAM[118] and chaperonin 60.1[119], which mediate the bacilli internalization of macrophages[120].

1.3.1.2 Innate immune cells

The major innate immune cells that are studied in human TB include macrophages, neutrophils, DCs and natural killer cells.

a. Macrophages

This is one of the first immunity cell types to encounter *Mtb* in the lung following aerosol inhalation. A range of macrophage activities for elimination of infection have been investigated, including bacterial phagocytosis, induction of antimicrobial pathways and cytokine production. However, macrophages also serve as a major cellular niche for bacterial proliferation during early infection as well as a reservoir for persistent bacteria within the lung granuloma during chronic infection. The multifaceted functions as well as the interaction of macrophages and bacteria in TB infection will be further discussed in the upcoming sections.

b. Neutrophils

Neutrophils are among the first cell types migrating to the site in response to infection. Dissection of mice infected with *Mtb* has revealed a number of neutrophils in the lungs after one week of infection[121]. A number of studies in mice have demonstrated the protective role of neutrophils in TB infection[122,123]. When neutrophils encounter *Mtb*, the cells rapidly phagocyte bacteria and release antimicrobial molecules contained in their granules into the *Mtb*-containing phagosome following its fusion with granules, resulting in bacterial killing and digestion[124]. Neutrophils also kill bacteria efficiently via reactive oxygen species which are produced by a membrane-integrated enzyme, the phagocyte nicotinamide adenine dinucleotide phosphate (NADPH) oxidase in the *Mtb* containing-phagosome[125]. Furthermore, neutrophils are known to function as a modulator for the effector mechanisms of macrophages. After macrophages phagocytose *Mtb*, contents of neutrophil granules are transferred to the *Mtb*-containing vacuole, which augments the antimicrobial activities of infected macrophage, reducing intracellular growth[126]. In addition, the release of heat shock protein (Hsp72) by

neutrophils has recently been found to be able to enhance the inflammatory response in the infected macrophage[127]. Neutrophils also produce a number of specific cytokines that help recruit and activate other immune cells, contributing to cellular immunity against *Mtb*.

However, there is conflicting evidence on the role of neutrophils in protection against TB. Neutrophil accumulation is thought to contribute to the development of severe lung pathology. Gopal *et al*. has revealed that lung inflammatory lesions from patient with active TB harbor high number of neutrophils[128]. *In vivo* studies in mice show that numbers of infiltrating neutrophils correlate with the susceptibility of mice and with the necrotic pathology[121]. Thus, a strict regulation of neutrophil influx in infected tissues may be essential to prevent tissue damage[121].

c. Dendritic cells (DCs)

DCs are the key immune cells involved in bridging innate and adaptive immunity due to their ability to capture, process and present antigen. The contribution of DCs in immune response against *Mtb* infection is well-studied. Following *Mtb* infection, DCs are quickly recruited to the site of infection, which are even more dominant than alveolar or recruited macrophages, to phagocytose the bacteria[129]. Infection of DCs with *Mtb* has resulted in the upregulation of MHC class I and II and costimulatory molecules as well as high levels of cytokines such as TNF-α and IL-12 that help induce T cell proliferation[130]. Therefore, DCs can generate efficient adaptive immunity against *Mtb* infection through a successfully antigen presentation to T cells in lymph nodes[131]. In line with these findings, depletion of DCs significantly causes a delay in $CD4^+$ T cells activation that in turn has impaired the control of bacterial replication, resulting in high bacterial burdens in the lungs and spleen[132]. On the contrary, *Mtb* has been shown to

develop mechanisms to prevent DC migration and maturation, reduce IL-12 production and inhibit ability of DCs to stimulate T cell immunity[133,134]. These findings highlight the complexities in the interactions between *Mtb* and the host innate immune system.

d. Natural Killer (NK) cells

NK cells are unable to phagocytose the pathogen but they can function in controlling the infection using cytotoxicity mechanisms. Various proteases and antimicrobial proteins inside NKs cytoplasmic granules are released into the target cytoplasm, resulting in directly lysis of the target cells (microbes or infected cells) or initiating apoptosis[135]. NK cells can also produce cytokines such as interferon-gamma (IFN-γ) and TNF-α[136] which not only enhance their lytic function,[137] but also help to activate macrophages.

A number of works have suggested the protective role of NK cells against mycobacterial infection. In mice whose NK cell activity is depleted by injection of anti-NK antibody, increased *M. avium* growth in the spleens is observed[138]. NK cells from peripheral blood mononuclear cells (PBMC) of healthy donors have been shown to significantly reduce the bacterial intracellular growth in *Mtb*-infected monocytes[139,140]. This growth inhibition has been partially mediated by IFN-γ and TNF-α produced by NK cells[140]. NK cells have been shown to be capable of killing *Mtb* by releasing cytolytic proteins of granules, which requires the direct contact of NK cells and bacteria[141].

1.3.1.3 Cytokine production

Recognition of *Mtb* by phagocytes leads to cell activation and cytokine production, which in turn induces further activation, cytokine production and effector functions of immune cells in both innate and adaptive immunity[14]. Cytokines could be categorized according to the immune response pathways where cytokines are produced, including

type-1 immunity driven by T helper 1 (Th1) cells and type-2 immunity driven by T helper 2 (Th2) cells[142]. Depending on the nature of infection Th1 or Th2 pathway will develop, with Th1 responding against intracellular pathogens and viruses while Th2 protecting against extracellular pathogen such as parasites[143]. The Th1 pathway produces IFN-ɣ, IL-2 and TNF-α which activate macrophages and are responsible for cellular immunity, resulting in inflammatory and cytotoxic reactions. Whereas Th2 cells produce IL-10, IL-4, IL-5 and IL-13, which are responsible for production of antibody as well as inhibition of macrophage functions and inflammatory response. Over activation of a particular pathway can cause the disease, such as autoimmune disorder[142]. Therefore, cytokines from one pathway can cross-inhibit the response of other pathway, and vice versa, to keep the Th1/Th2 balance. Besides Th1 and Th2, there are several cytokines that are produced by other T cells that also function in the inflammatory or anti-inflammatory response[144].

As an intracellular pathogen, the efficient Th1 immune response is decisive for the protection against *Mtb* infection. However, the overexpression of Th1 cytokines such as TNF-α may result in tissue damage, which may advance the disease development[145]. Therefore, the balance between Th1 and Th2 response is very important in TB pathogenesis. Below is summary of several cytokines produced in response to *Mtb* infection, including TNF-α, IFN-ɣ, IL-1β, IL-6 and IL-10.

TNF-α is a pro-inflammatory cytokine, which is induced by monocytes, macrophages, DCs[146], NK cells, T cells[140] when these cells are stimulated with mycobacterial products. TNF-α plays a key role in controlling *Mtb* infection by induction of reactive oxygen species[147] or increasing phagosome-lysosome maturation macrophages[148,149]. TNF-α also recruits immune cells to the infection site, contributing to the granuloma

formation that may help in preventing disease progression[150,151]. The TNF level may determine the outcome of infection, since either too low or too high TNF levels are associated with necrosis of infected macrophages that result in the exuberant bacterial growth[152]. In humans, TNF-α is produced at a local infection site[153] and its spillover correlates with the destruction of lung tissue[145], suggesting the contribution of TNF-α in the immunopathology of TB.

IL-1β is a pro-inflammatory cytokine, which is also mainly produced by monocytes, macrophages, and dendritic cells. IL-1β is produced at the site of infection during TB, as shown by IL-1β expression in granulomas in the lungs of TB patients[154] or in bronchoalveolar lavage cells obtained from the infected lung of TB patients[153]. Studies in mice have suggested important roles of IL-1β in host resistance to tuberculosis since an increased bacterial load and defective granuloma formation were observed in IL-1α knockout mice infected with *Mtb*[155,156]. In humans, IL-1β has been shown to induce rapid differentiation of monocytes into macrophages with enhanced phagocytic and antigen-presentation activities[157]. Genetic studies have shown the association of polymorphisms on *IL-1β* genes and pulmonary TB in African populations[158,159].

IL-6 is a cytokine that has both pro- and anti-inflammatory properties. Like TNF-α, IL-1β, IL-6 is produced at the site of infection[145,153] by macrophages, neutrophil and dendritic cells[131]. Many studies have supported the protective roles of IL-6 against *Mtb*; for example, absence of IL-6 leads to the increased bacterial loads in lungs[160] and early death of infected mice[161]. Such functions of IL-6 could be involved in the early IL-6–mediated IFN-ɣ production, which enhances the antimicrobial function of macrophage[160]. As with TNF-α, IL-6 may be involved in TB immunopathology because IL-6 levels in the lavage fluid of TB patients correlate with the lung damage[145].

IFN-γ is a pro-inflammatory cytokine that has been long known for protective function against *Mtb*. This cytokine is produced primarily by $CD4^+$ and $CD8^+$ T cells and NK cells[162]. IFN-ɣ plays an essential role in macrophage activation which enables them to exert antimicrobial functions. IFN-ɣ-stimulated macrophages increase the phagosome-lysosome fusion and production of intermediate nitrogen species, leading to efficiently killing of intra-macrophage mycobacteria[163–168]. Individuals bearing mutations in the IFN-γ or receptor gene have been shown to be extremely susceptible to TB disease[169,170]. Genetics studies also indicate the association of polymorphisms in the IFN-γ gene and TB.

IL-10 is an anti-inflammatory cytokine, which is produced by macrophages and T lymphocytes during *Mtb* infection. IL-10 is demonstrated to limit T cell responses against *Mtb* infection because this cytokine inhibits the production of pro-inflammatory cytokines such as IFN-γ, TNF-α and IL-12[171]. It also prevents the traffic of the complexes of *Mtb* peptide and MHC-II to the plasma membrane for $CD4^+$ T cell presentation[172]. In addition, IL-10 can inhibit the phagosome maturation, resulting in enhanced intracellular survival and growth of bacteria[173]. Taken together, the data have suggested that IL-10 suppresses the protective immunity and promotes the bacterial survival.

1.3.2 The adaptive immunity

The adaptive immune response to *Mtb* infection is delayed, starting after approximately two weeks in infected animals[14] and 8-10 weeks in humans upon *Mtb* infection (based on the fact that skin test may be inaccurate before 8-10 weeks from exposure[174]). The adaptive immune response initiates following the antigen presentation of infected DCs to T cells in the lymph node[134]. Although DCs are infected from early, *Mtb* impairs the

antigen presentation and migration of DC, thereby leading to such a delay of adaptive immune response[134]. Following antigen presentation, naïve T cells are activated and proliferated into effector T cells, of which there are two main subsets with different functions, including $CD8^+$ T cytotoxic cells and $CD4^+$ T helper cells. Memory $CD4^+$ T cells and $CD8^+$ T cells also form upon *Mtb* infection[175]. These activated T cells then migrate to the site of infection by the attraction of cytokines that are produced by infected phagocytes.

$CD4^+$ T cells play an important role in the protective immune response against *Mtb*, which is indicated by experimental studies. The primary role of $CD4^+$ T cells in host immunity is thought to induce production of cytokines. Depending on the cytokine environment, the $CD4^+$ T cells can produce either Th1 response or Th2 response. The function of these responses in TB infection has been mentioned in Section 1.3.1.3. In practice, the increased risk of TB in HIV patients also establishes the critical role of $CD4^+$ T cells in immunity to *Mtb* infection. Depletion of $CD4^+$ T cell has resulted in the increased severity of the primary disease[176], failure in granuloma formation[177], developing extra-pulmonary dissemination[176], and causing disease reactivation in animals with latent TB[176,178]. Even though the amount of $CD8^+$ T cells increase to compensate for the lack of $CD4^+$ T cell, the response of $CD8^+$ T cells has not been sufficient to control the bacterial burden in the lung of infected mice[178].

$CD8^+$ T cells contribute in controlling *Mtb* infection since they function as killer cells for *Mtb*-infected cells[179]. The killing mechanism is dependent on the release of granular contents into the infected cell targets, which directly lyses the infected cells[173]. In addition, $CD8^+$ T cells function by producing a variety of cytokines, including IFN-γ

and TNF-α, which enhance the antimicrobial activities of macrophages, resulting in reduced intracellular mycobacterial growth[174].

There is increasing evidence for the role of B lymphocytes and a humoral response in protection against TB, although functional variation in antibody responses exists[182]. Opsonization of *Mtb* with *Mtb*-specific IgG from person with latent TB enhances the bacterial killing of human macrophage by inducing phagosome maturation, suggesting a protective role for antibodies against active TB[104]. Recently Lu *et al.* have found that antibodies obtained from individuals with latent TB are more effective in inhibiting the growth of intracellular *Mtb* than those from persons with active TB[183]. However, by analyzing serum antibodies and recombinant monoclonal antibodies that are made by cells isolated from *Mtb*-exposed health workers and persons with pulmonary TB, Zimmermann *et al*. have indicated that *Mtb*-specific IgG promotes the infection of human epithelial-like and macrophage-like cell lines, whereas IgA opsonization inhibits the *Mtb* infection[184]. The difference in functional response of IgG could be attributed to different experimental cell types[182].

1.3.3 Granuloma

Upon *Mtb* infection, the innate and adaptive immune cells migrate to the site of infection by the attraction of cytokines and chemokines, and locate around the infected macrophages. Such a structure is called a granuloma, which may help an infected person with *Mtb* remain in the stage of latency or may contribute to *Mtb* proliferation, dissemination and persistence[185]. There are many different cell types to form granulomas, including macrophages (main cell type), natural killer cells, neutrophils, DCs, T and B cells[129,186], and epithelial cells[187]. At the early granuloma, uninfected macrophages continuously migrate to the site of infection, which in turn become

infected by phagocytosing the infected macrophages. At the late stage of granuloma formation, a fibrous cuff is present to surround and strengthen the structure[188]. In the heart of the granuloma, there is a necrotic and caseous structure that is thought to be the mixture of bacteria and the lipid released by the necrotic breakdown of *Mtb*-infected lipid-rich macrophages (foamy macrophages)[188]. Along with limiting the spread of infection by walling off the bacteria and infected macrophages, granulomas may contain and inhibit the bacterial growth by stressing them with starvation, reactive oxygen and nitrogen species, and hypoxia[189]. However, it has been revealed that mycobacteria can survive and overcome stresses by utilizing the host cell lipid as nutrition[188,190]. When the granuloma structure is weak under certain immune-comprising conditions such as depletion of $CD4^+$ T cells[176–178], bacteria can exit from granulomas, and spread through the body to cause clinical disease.

1.3.4 Host genetic susceptibility to TB

TB has high prevalence at some parts of the world such as South Asia, Africa and South Africa. The difference in the rate of TB occurrence among particular populations, ethnicities and families indicates the involvement of host genetics in TB susceptibility. Results from early twin studies showed higher TB incidence among monozygotic than dizygotic twins. Family-based genome-wide association studies showing the association of several loci on chromosome and TB susceptibility have supported the influence of host genetics on infection outcome[191]. Over the past decades, technical advances have allowed us to study the association of genetic variants and the disease at the level of whole genome. The use of different approaches such as candidate gene studies and genome wide association studies has led to a significant increase in understanding of the genetic basis of TB susceptibility.

1.3.4.1 Candidate gene studies

There are up to 30,000 genes in the human genome and the probability that a gene selected randomly will influence TB disease is very low. Therefore, it is important to have genes selected for study[192]. The candidate genes are mostly selected based on their possible function on disease pathogenesis. For instance, genes of the TLR family, which play roles in *Mtb* recognition[193], were examined for associations with TB[114]. Candidate genes are also discovered from experimental animal models. For example, through a genetic screen in zebrafish, *lta4h* has been identified as a susceptibility locus to mycobacterial infection. From this, the association of this gene and human TB was uncovered[194]. Host genetic variations can be identified by gene sequencing or SNP genotyping selected among hundreds of SNPs in the gene. Linkage disequilibrium (LD) is a phenomenon that indicates the non-random association of alleles at different loci on chromosome[195]. The SNPs that are in high LD will mainly be inherited together. These SNPs can be tagged and presented by a selected SNP among them, which can be referred to tag SNP[195]. In candidate gene studies, selection of tag SNP is very useful because genotyping a few but carefully selected tag SNPs can provide sufficient information about other SNPs remaining in the region of interest[196]. In addition, SNPs in the coding region which result in a change in encoded protein sequence and SNP in the regulatory region (such as promoter) of gene are considered for selection. SNP typing on candidate genes has been cheap and quick compared to different genetic association studies, comprising genotyping the gene variants (often SNPs) in candidate genes in unrelated cases (TB patients) and controls (healthy individuals).

1.3.4.2 Whole genome wide association studies

The objective of whole genome wide association studies (GWAS) is to examine the genetic variants in the entire genome to identify variants associated with a trait (a disease or phenotype). In contrast with candidate gene association studies, GWAS is a non-candidate gene approach. This approach employs the different types of commercial chips which can be used to genotype up to 500,000, 600,000 or 250 million SNPs in human genome. The chip selection will take into account the level of genomic coverage, the possible sample size and the allowable budget[197].

1.3.4.3 Association of host genetics and TB

By exploiting different approaches, variants in many genes involved in immune response to TB have been demonstrated to be associated with TB susceptibility[114,159,198–201]. For example, as listed in Tables 1.1[202], SNPs in receptor genes involved in recognition of TB including TLR family (TLR1, 2, 4, 8, and 9) or C-type lectin receptors (MR, DG-SIGN) are associated with TB susceptibility in different populations. For SNPs known to be associated with TB, there is very limited understanding concerning the underlying molecular mechanisms of how these variants affect the disease susceptibility (Table 1.1[202]). The use of the latest approach of next generation DNA or RNA sequencing that provides the whole genomic data could advance knowledge on the influence of gene variants on disease susceptibility at the level of transcriptomics or proteomics[195]. A thorough understanding on host genetics could be translated to better diagnostic, prevention and treatment therapy for TB disease.

Table 1.1 Association studies on host innate immune genes related to TB pathogenesis (extracted from the work of Azad *et al.*[202])

Gene	Polymorphism(s) (genetic location)	Population(s)[a]	Association with TB[b]	Molecular mechanism known?
MR	1186G/A (exon)	China	Yes	No
DC-SIGN	−336G/A (promoter)	South Africa	Yes	No
		Colombia, Tunisia	No	
		SSA, Gambia	Yes	No
		India, China	No	
	−871G/A (promoter)	South Africa	Yes	No
		China	No	
Dectin-1	Not identified			
TLR1	N248S, S602I (exon)	USA (African-American)	Yes	No
		Europe (Caucasian)	Yes	No
TLR2	R753Q (exon)	Turkey	Yes	No
	R677W (exon)	Tunisia	Yes	No
	Insertion/deletion (promoter)	Guinea-Bissau, USA (Caucasian)	Yes	No
TLR4	D299G (exon)	Gambia, Guinea-Bissau	No	
TLR8	rs3764880 (exon)	Indonesia, Russia	Yes	No
TLR9	rs352143, rs574386 (exon)	USA (Caucasian), USA (African-American)	Yes	No
TIRAP	S180L (exon)	West Africa	Yes	Yes
		Indonesia, Russia, Ghana	No	
		Meta-analysis (China)	No	
CR1	Q1022H (exon)	Malawi	Yes	Yes
CR3	Not identified			
NOD1	Not identified			
NOD2	P268S, R702W, A725G (exon)	USA (African-American)	Yes	No
CD14	−159C/T (promoter)	Mexico	Yes	No
		Korea	Yes	Yes
P2X7	1513A/C (exon)	Gambia, China	No	
		Mexico, Russia	Yes	No
		India	Yes	No
		Meta-analysis (China)	Yes	No
		Meta-analysis (China)	No	
	−762T/C (promoter)	Gambia, India	Yes	No
		Mexico, Russia, China	No	
		Meta-analysis (China)	No	
VDR	ApaI (exon)	Guinea-Bissau	Yes	No
		Tanzania	No	
	BsmI (exon)	Meta-analysis (Asia)	Yes	No
		Meta-analysis (Africa)	No	
	FokI (exon)	China	Yes	No
		Tanzania	No	
	TaqI (exon)	Gambia	Yes	No
		Cambodia, Tanzania	No	
	FokI-BsmI-ApaI-TaqI haplotype	West Africa	Yes	No
		South Africa	Yes	No
SP-A1	1416C/T (intron)	India	Yes	No
	307G/A,776C/T (exon)	Ethiopia	Yes	No
SP-A2	1382C/G (intron)	India	Yes	No
	355C/G, 751A/C (exon)	Ethiopia	Yes	No
MBL	O allele	India	Yes	No
	O, X alleles	Denmark	Mixed	
	B allele	USA (African-American)	Yes	No
	O allele	USA (Caucasian)	No	
	O,H,L,X,Y,P,Q alleles	China	No	
	AO genotype	Tanzania	No	
	HYA/HYA, LYB/LYD haplotypes	Italy	Yes	No

[a] SSA, sub-Saharan Africa.
[b] Refers to mainly pulmonary TB.

1.4 Macrophages

1.4.1 Function and activation

Macrophages are large mononuclear cells and play an important role in the immune system. Macrophages function as professional phagocytes that have capacity to engulf particles larger than 0.5 μm, including microbes[203]. The term of macrophage means "big eater" in Greek. Monocytes are the precursors of macrophages, which circulates in the blood stream. When infection occurs, monocytes are recruited into sites of infection and then differentiate into macrophages that have increased phagocytic capacity, different morphology and adhesive properties[204]. In a resting state, the role of the macrophages is to phagocyte apoptotic cells and cell debris in a quiet manner without inflammation to minimize tissue damage[205]. During infection, macrophages function as immune effector cells that ingest and destroy pathogens, activate and recruit other immune cells, process and present antigens to T cells in adaptive immunity. In order to perform such activities, macrophages must first be activated. The classical activation of macrophages requires two signals: priming signal followed by triggering signal[206]. The role of priming signal is to enhance the responsiveness of macrophages to the triggering signal; without priming signal, the macrophages respond to the activating stimuli in a weaker capacity. The priming signal is typically IFN-γ while the triggering signal is bacterial products such as LPS. Upon activation, the macrophage induces competent microbial activity for effective bacterial elimination, although several intracellular pathogens, such as *Mtb* or *Salmonella*, have developed strategies to modulate this response[207–209].

1.4.2 Phagocytosis

Macrophages have evolved a number of strategies to uptake extracellular material, including pinocytosis, receptor-mediated endocytosis, and phagocytosis. Pinocytosis is the process to uptake fluid and solutes, while receptor-mediated endocytosis is used to uptake macromolecules, viruses, and small particles. These two pathways usually occur independently of actin polymerization[210].

Phagocytosis refers to the uptake of particles, cells or pathogens, which are larger than 0.5 μm, into a plasma membrane-derived vesicle. Phagocytosis can be performed by professional phagocytes including macrophages, neutrophils and dendritic cells. These cells use similar mechanisms, however there are the important differences existing among them, which depend on the roles that each cell type performs in the immune response[210]. In general, phagocytosis process may be divided into two steps (1) internalization of particles into phagosome, and (2) phagosome maturation. Here I focus on the phagocytosis process performed by macrophages.

1.4.2.1 Phagosome formation and particle internalization

The first step of phagocytosis is mediated by PPRs that can recognize and bind pathogens directly via PAMPs comprising surface carbohydrates, peptidoglycans or lipoproteins, or indirectly via opsonization with IgG or components of the complement system. There is a diversity of receptors capable of stimulating phagocytosis on a macrophage surface, for example, receptors listed in the Section 1.3.1. Receptors are activated upon binding of particles, which produce signals to reorganize the actin network of the cell membrane. Subsequently the area around the particle is remodeled, to form a phagocytic cup. The cell membrane then extends over the particle to enclose

the cup, leading to the internalization of particles into the cytoplasm. The vesicle containing particle upon internalization is termed a phagosome.

1.4.2.2 Phagosome maturation

Maturation of phagosomes starts immediately once a phagosome is formed. After release from the surface membrane to cytoplasm, the phagosome sequentially fuses with early and late endosomes and finally with lysosomes to become a mature phago-lysosome vesicle. During this phagosome development, there are changes in the phagosome's content and membrane composition. It is suggested that the fusion between phagosome and the intracellular organelles is a kind of "kiss-and-run" interaction in which the content markers are transferred but the intermixing of membrane contents are limited[211].

There are three stages of phagosome during maturation: early phagosome, late phagosome, and phago-lysosome. The early phagosome indicates the new formed phagosome that are capable of fusion with sorting and recycling endosomes but not lysosomes[212]. An environment inside the early phagosome is mildly acidic with a pH around 6.3, poor hydrolytic, and contains membrane-bound proteins, such as the Rho-GTPase Rab5, which are required for fusion of early phagosome with early endosomes[203,213]. After this fusion, the phagosome fuse with late endosome to form the late phagosome, which in turn undergoes a drop in pH caused by the pumping of H^+ into the phagosome due to the increasing number of vacuolar H^+-ATPases (V-ATPases)[203,214]. The late phagosome is acidic with pH of 5.5 and enriched in proteases that are acquired from the late endosome. The phagosome has loss of Rab5 and instead contains lysosomal-associated membrane proteins (LAMPs) and Rab7a, which are the

markers for this organelles and are known to mediate the fusion with a lysosome[203,214–216].

The final stage of phagosome maturation is the formation of the phagolysosome that is generated by the fusion of phagosome with lysosome through a Rab7a-dependent process[203]. This organ is highly acidic with pH about 4.5-5 and filled with active hydrolases as well as other antimicrobial substances. These microbicidal properties grant the phagosome the ability to effectively kill an ingested microorganism. However, several intracellular pathogens are capable of circumventing the phagosome maturation, thereby evade the hydrolase-mediated destruction and are able to live within phagosomes[217,218]. Their mutants that fail to modulate the killing programme of macrophage have impaired intracellular growth[219,220].

1.4.3 Antimicrobial activities of macrophages

The phagosome is central to macrophage activity against infection. During the maturation process, phagosomes acquire a number of microbicidal features, including acidification of the phagosome, activation of reactive oxygen and nitrogen species, as well as antimicrobial peptides and degradative proteins. The antimicrobial agents employed by macrophages can efficiently kill many pathogens, ranging from Gram negative and positive bacteria, fungi *Candida sp*, *Cryptococcus neoformans*, non-tuberculosis mycobacteria[203,221,222] to *Mtb*[223].

1.4.3.1 Acidification of the phagosome

The acidification of phagosomes may be generated by the accumulation of V-ATPases in the phagosome membrane during its maturation[218]. V-ATPases are comprised of a membrane-bound sector and a cytosolic sector; the assembly of these components forms

an active enzyme that can hydrolyse the energy-rich adenosine triphosphate (ATP) and pump protons H^+ into the phagosome[224]. Acidification is central for macrophage antimicrobial activity. An acidic environment itself directly destroys pathogens through an inhospitable environment where essential nutrient is extruded and microbial metabolism is impaired[203]. In addition, an acidic pH is required for the fusion of phagosomes with vesicles[218] and favors the activity of phagosomal hydrolytic enzymes which have acidic pH optima[225]. An inhibition of the V-ATPase activity by concanamycin A affects the phagosomal acidification, formation of phagolysosome and the hydrolytic activity[226]. Furthermore, by pumping H^+ into phagosome, the V-ATPase facilitates superoxide production (O_2^-) as H^+ can counteract the negative charges transported by the NADPH oxidase. The oxidase products can subsequently react with the phagosomal H^+, generating more complex reactive oxygen species[203].

1.4.3.2 Reactive oxygen and nitrogen species

Macrophages can destroy pathogens through reactive oxygen species generated by membrane-integrated NADPH oxidase NOX_2 although this mechanism is the most prominent and well-studied in neutrophils[125,227]. The activation of NADPH oxidase requires the assembly of different subunits within the phagosome[228]. The activated NADPH oxidase donates electrons from NADPH at the cytoplasm surface to O_2 in the phagosome, thereby producing a superoxide anion (O_2^-). This superoxide serves as a precursor for other toxic reactive oxygen species such as hydrogen peroxide (H_2O_2), hypochlorous acid (HOCl) and hydroxyl radical, which can kill the pathogens effectively[229,230].

Inducible nitric oxide synthase (iNOS) is synthesized upon stimulation of macrophages with bacterial products[231]. The function of this enzyme is to catalyze the

production of nitric oxide (NO) from L-arginine and O_2[232]. Unlike superoxide, NO is synthesized in the cytoplasm, outside of phagosome but it later can be delivered into the phagosome[231]. In the phagosomal lumen, when NO encounters oxygen species it is subsequently converted to reactive nitrogen species. Reactive oxygen and nitrogen species can synergize to produce highly toxic effects on intraphagosomal pathogens, by which the microbe is damaged, protein is inactivated and lipid is converted[203]. The importance of reactive nitrogen species in protection against infection of different pathogens in mouse macrophages has been well studied[163,229,233]. The role of these antimicrobial substances in human macrophage infection is controversial because it is difficult to detect the expression of iNOS or NO in human macrophages[234,235].

1.4.3.3 Antimicrobial peptides and proteins

The phagosome after maturation possesses many microbicidal peptides and proteins which contribute to the destruction of intraphagosomal pathogens. These agents can either prevent microbial growth by limiting the nutrient source inside the phagosome or compromise the integrity of microbes[203].

For instance, iron scavenger lactoferrin and cation exporter natural resistance-associated macrophage protein 1 (NRAMP1) extrude iron and other cations such as Zn^{2+} and Mn^{2+} from phagosomal lumen, thus affecting the activity of bacterial enzymes required for their DNA synthesis and mitochondrial respiration[236]. Antimicrobial agents that are more directly to disrupt the integrity of microbes by inducing microbial membrane permeabilization include defensins, cathelicidins, hepcidin, lysozymes, and lipases and various proteases[203,237]. These hydrolases can also help degrading the pathogen. In neutrophils, these antimicrobial agents are packed in granules while in macrophages

they are delivered to phagosome from multiple vesicles through the phagosome maturation process or from other cell types such as neutrophils upon activation[126,222].

1.4.4 Interaction of macrophages and *Mtb*

Macrophages are thought to be the first host defense against *Mtb* infection. As discussed in Section 1.3.1, there are a wide range of receptors on macrophage surface that facilitate the internalization of *Mtb*. Following entry, the phagosome undergoes a maturation process, where after *Mtb* in phagosomes is exposed to a range of antimicrobial mechanisms to kill or inhibit the intracellular growth of mycobacteria. However, *Mtb* has been found to have developed different strategies to escape the killing mechanisms within phagosomes, exploiting macrophages as a niche for its survival and replication.

1.4.4.1 Controlling intracellular mycobacterial growth

A number of studies indicate that the antimicrobial mechanisms of macrophages are able to inhibit the growth of *Mtb* and other mycobacterial species in macrophages. Activation of monocytes or macrophages by cytokines such as IFN-ɣ or microbial product of LPS, results in the reduced intracellular bacteria burden[121,164,166,233,238]. It has been shown that the mycobacteria are efficiently killed by the production of reactive oxygen and nitrogen species[233], or by successful maturation of phagosome that delivers bacteria to a hostile acidic environment enriched with numerous hydrolases[164–166,223]. A recent study has indicated that the *Mtb*-containing phagosome is even more toxic with enhanced superoxide burst[239] that contributes to the killing of bacteria.

1.4.4.2 Inhibition of microbicidal mechanisms

a. Inhibit phagosome maturation

The inhibition of phagosomal maturation mediated by *Mtb* is well-characterized, which results from its ability to interfere with the recruitment of V-ATPase[218,240,241] and the fusion events of phagosomes. *Mtb* is shown to be capable of preventing the fusion of phagosomes with vesicles through modulating the delivery or elimination of proteins required for phagosome maturation to or from the phagosome membrane[242,243]. *Mtb*-containing phagosomes in mice and human macrophage cell lines shows a delayed acidification that maintains at pH of ~ 6.4 compared to pH ~ 4.5-5 in successfully acidified phagosome[244]. In the clinical setting, *Mtb*-containing phagosomes of *Mtb*-infected alveolar macrophages from patients with TB and HIV co-infection fail to fuse with the lysosome and are not acidified [245].

The arrest of phagosome maturation seems to have a correlation with the viability of infecting bacteria. In the infected mouse macrophage, *Mtb* carrying mutants that are defective in arresting phagosomal acidification have reduced growth [219,220]. Several molecules of *Mtb* have been indicated to modulate the maturation of phagosomes. For instance, cell wall ManLAM[246] and trehalose 6,6'-dimycolate (TDM)[247] are able to block phagolysosome fusion. Stimulation of human or murine macrophages with cytokines override the arrest of maturation of the mycobacterium-containing phagosomes, resulting in a reduced intracellular growth of mycobacteria and increased antigen presentation[164,165,248,249].

b. Escape from phagosome

Mtb was believed to reside exclusively in the membrane-enclosed vacuole in the macrophage for a long time but this consensus has been changed due to advances in

technology. Previous study has shown that at early time point *Mtb* is localized in the phagosome that is not acidified, but at least two days after infection, *Mtb* is found to translocate from phagolysosome to the cytosol of DC and macrophages in a manner dependent on 6kDa early secretory antigenic target (ESAT-6) protein produced by *Mtb*[250]. This phenomenon was argued not merely due to the outgrowth of bacteria in phagosomes and not a result of membrane disruption during apoptosis of infected cells. Later studies utilizing the fluorescent-based methods have indicated that at the late stage of infection, *Mtb* is capable of rupturing the phagosomal membrane to translocate to cytosol where it can mediate the host cell death[251]. ESX-1- dependent translocation could be the factor that determines the virulence of the mycobacteria[252]. By exploiting transmission electron microscopy (TEM), the cytosolic translocation of *Mtb* is shown to occur at very early stage of infection and there is the strain-specific heterogeneity in ability to induce phagosomal escape[253]. In addition host factors could affect the translocation of *Mtb*. Mice deficient in functional Nramp-1, a phagosomal bivalent cation transporter who functions in phagosomal acidification and pH regulation, leads to an enhanced *Mtb*-mediated phagosomal rupture[254].

c. Other survival strategies

Apart from strategies employed by *Mtb* to avoid antimicrobial properties of macrophage described above, there are several other strategies. In hMDM, *Mtb* favors its intracellular survival by down-regulating the expression of Cathepsins, one of proteases who have many functions in protection against the infection, including pathogen killing, protein processing and antigen presentation[255]. *Mtb* also reprograms the host lipid metabolism by accumulating lipid droplet in the *Mtb*-containing phagosome that could be served as bacterial nutrition[239]. Furthermore, *Mtb* can inhibit the expression of

MHC class II in mouse macrophages to prevent antigen presentation to $CD4^+$ T cells, thereby avoiding an Th1 immune response[256].

1.4.4.3 *Mtb*-induced macrophage cell death

In response to *Mtb* infection, the initial purpose of immunity response is to help the body defend against and recovery from the infection through activation of inflammatory pathways, complement system, production of antimicrobial mechanisms and recruitment of different immune cell types to the site of infection. However, if the condition is unresolved, infected cells may undergo cell death.

There are two common types of cell death following productive *Mtb* infection of human or murine *in vitro*: apoptosis and necrosis[257]. Apoptosis is a form of death in which cell is shrunk, nuclear is condensed and fragmented but plasma membrane integrity is preserved; whereas necrosis is characterized by the plasma membrane disruption[257]. Recently, it has become apparent that the mode of death of infected host cells has decisive role in the control of *Mtb* infection and, later on, in the development of disease[47,258]. Apoptosis is generally considered to be a part of protective mechanism of host immune response since the apoptotic *Mtb*-infected macrophages are engulfed by uninfected macrophages through efferocytosis, in which *Mtb* are effectively killed[258]. Whereas, necrosis is considered to provide first a niche for *Mtb* replication, then cause cell lysis and facilitates bacterial dissemination[47,259]. It is suggested that *Mtb* strains differ in their ability to induce the mode of cell death. The virulent *Mtb* strains are able to induce the necrosis rather than apoptosis[47,260]. *Mtb* is shown to be able to manipulate host cell death by multiple mechanisms. *Mtb* can inhibit host cell apoptosis by upregulation of host cell anti-apoptosis signaling proteins such as Bcl-2 or suppression the apoptosis signaling pathway[261]. In addition, *Mtb* is capable of causing EXS-1

dependent phagosome rupture which results in the host cell necrosis[251]. Another pathway *Mtb* exploits to induce necrotic death of host cell is involved in the increased level lipid mediator lipoxin A_4 (LXA_4)[262]. Zebrafish model shows that increased level of LXA_4 inhibits the production of TNF-α. As a result, there is an exuberant number of *Mtb*, leading to the necrosis of infected cells[194].

1.5 Aims of the thesis

Although there have been many studies on host genetics, immune response against *Mtb* and its genome related to TB susceptibility, a number of critical questions remain, that require clear answers to improve the prevention and treatment of TB. Some of the critical questions are (1) why do only 10% of individuals among 2 million people with latent TB develop active disease and (2) what markers predict disease severity and treatment outcomes?

Macrophages are important for the defense against TB infection. They play an essential role in regulating the recruitment and the activation of other immune cells through cytokine and chemokine secretion. More importantly, macrophages can phagocytose *Mtb* and function as an effector cell. Phagosomes are known to be central to the antimicrobial function of macrophages, where they can kill pathogens by producing reactive oxygen and nitrogen species, delivering internalized microbes to low-pH, hydrolytically active environment during the phagosome maturation. With such important roles, defects in macrophage antimicrobial function may have major consequences in TB infection. However, to date there is limited understanding of the influence of macrophages to clinical outcomes of TB infection.

Substantial data have shown the influence of genetic variations of host immune genes on the susceptibility to TB. Phagocytosis of *Mtb* by macrophages is mediated by a variety of membrane receptors on macrophage that can recognize different molecular structures on pathogens. But knowledge is lacking whether the genetic variation of these receptors influences the recognition of *Mtb*, phagosomal function of macrophages and thus outcomes of *Mtb* infection.

In view of the knowledge lacuna above, I hypothesized that the impairment of macrophage phagocytic function under the influence of host genetics could explain the different clinical phenotypes of TB. I established intracellular assays to directly measure the extent of antimicrobial capacity of macrophage from TB patients to examine the association between phagosomal activities and TB clinical phenotypes.

Many studies demonstrate that *Mtb* is able to arrest the phagosome maturation to avoid multiple antimicrobial responses inside the phagosome. As a consequence, *Mtb* can survive and proliferate inside the macrophage, which could result in infection establishment and progression to clinical complications. There is mounting evidence for the influence of diversity of *Mtb* strains on their virulence, modulation of host immunity, clinical phenotype and disease transmission. Most of the studies examined lab strains or clinical isolates but in a limited number, resulting in certain discrepancy in the results. Therefore, it is important to investigate, with a large number of clinical isolates, how the strain variation influences their virulence and modulates host immune response, which will lead to better understanding of TB pathogenesis. The aims of my thesis are:

1. To establish intracellular assays to measure antimicrobial function of macrophages from TB patients

2. To investigate the association of macrophage antimicrobial function and TB clinical phenotypes.

3. To determine whether polymorphisms in phagocytic function genes are associated with TB susceptibility and underlying molecular mechanism of the association

4. To study the virulence of different *Mtb* strains and its association with host immune response and *Mtb* genotype

Chapter 2
METHODOLOGY

2.1 Subjects with TBM, PTB and LTB

The subjects were recruited for the macrophage study in chapter 4 and the genetic case-control study in chapter 5. The detail of recruitment is described in detail in each chapter. In general, they could be divided into 4 groups: subjects with TBM, subjects with PTB, subjects with LTB and controls. All subjects with TBM, PTB and LTB were adults and HIV negative.

2.1.1 Subjects with TBM

TBM patients, as previously described[263,264] had clinical meningitis, which was defined as the combination of nuchal rigidity and abnormal cerebrospinal fluid parameters, and/or acid fast bacilli seen in the cerebrospinal fluid by Ziehl-Neelsen stain or culture.

2.1.2 Subjects with PTB

PTB patients had sputum positive with acid fast bacilli by Ziehl-Neelsen stain and chest X-rays that were consistent with active PTB, but not miliary or extra-pulmonary TB. In study of antimicrobial activity of macrophages in chapter 4, PTB patients had no previous history of TB treatment.

2.1.3 Subjects with LTB

These subjects had no history of active disease and were recruited from healthy Vietnamese volunteers who are working at OUCRU. They had positive tests in ESAT-6 and CFP-10 specific IFN-ɣ T-SPOT.TB assays (see section 2.4).

2.1.4 Controls

The controls for the genetic association study were newborn babies born in 2003 and between 2006 and 2007 at Hung Vuong Obstetric Hospital, HCMC, which were a

subset of our laboratory's collection of 1000 umbilical cord blood samples. This group was also used as a genetic control for Vietnamese population to assess the association of human genetic factors and other infectious diseases[265–267].

2.1.5 Ethical approval and informed consent

All study protocols related to this research were approved by Ethics and Scientific Committees at hospitals where the human subjects were recruited, including Hospital for Tropical Diseases, Pham Ngoc Thach Hospital and Hung Vuong Hospital. Ethical approvals were also granted by the Oxford Tropical Research Ethics Committee UK.

Prior enrollment to any study in this research, written informed consent was obtained from each participant or an accompanying relative if he/she could not provide consent independently.

2.2 Media for cell culture and bacteria growth

2.2.1 Media for cell culture

In this study, I used three different cell types, including macrophage cell lines from murine J774 and human THP1 as well as primary human monocyte-derived macrophages (hMDM). The macrophage cell lines were used for optimizing the experimental conditions because cell lines are easy to culture, sustain and they have constant genetic and phenotypic features which may differ from their original tissues. Unlike cell lines, the primary hMDM are able to maintain most of cellular functions and used to examine antimicrobial activity of macrophage in response to *Mtb* infection. The cells were cultured in optimal medium. All cell culture media were sterilized by using vaccuum filtration system through 0.22 µm membrance (Merk Millipore, Germany).

a. Medium for J774 and THP1 cell lines: RPMI (Sigma, Germany) was suplemented with 2 mM L-glutamine (Sigma, Germany)**,** 100 units of penicillin and streptomycin (Sigma, Germany)**,** 10% (v/v) Fetal Bovine Serum (FBS, Sigma, Germany). This medium was used for culturing J774 and THP1 cells.

b. Antibiotic-free medium for J774 and THP1 cell lines: This medium was prepared as described in (a.) without adding antibiotics and was used to infect cell lines with *Mtb*.

c. Serum-free medium for PBMCs: RPMI was suplemented with 2 mM L-glutamine, 100 units of penicillin-streptomycin**,** 1 mM Sodium pyruvate. This medium was used for monocyte isolation by adherence.

d. Complete medium for hMDM: RPMI was suplemented with 2 mM L-glutamine**,** 100 units of penicillin-streptomycin**,** 1 mM Sodium pyruvate, 10 % (v/v) heat-inactivated FBS. This medium was used for culturing hMDM.

e. Antibiotic-free medum for hMDM: This medium was prepared as described in (d.) without adding antibiotics and was used to infect hMDM with *Mtb*.

2.2.2 Media for *Mtb* growth

a. 7H9T: 4.7 g 7H9 (BD Diagnostic System) was dissolved in 900 ml, then 0.5 ml Tween 80 (Sigma) was added. This suspension was autoclaved at 121 ^{o}C, 10 min, then let to cool at room temperature. When media temperature was about 50 ^{o}C (that could be touched by hand), 100 ml Middlebrook OADC Growth Supplement (BD Diagnostic System) was added.

b. 7H9G: The preparation of 7H9G medium was similar to that of 7H9T. However, 2 ml of glycerol was added into the medium instead of using 0.5 ml Tween 80. This medium is mainly used to culture *Mtb* for archive.

c. Selective medium 7H10 agar plates: 2.35 g 7H10, 0.85 g Glucose (Merck), 0.5 g Casitone (Merck), and 10 g Agar powder (BD) were dissolved in 500 ml, then 0.5 ml Tween 80 was added. This suspension was autoclaved at 121 ^{o}C, 10 min, and then let to cool at room temperature. When medium temperature reached about 50 ^{o}C, 50 ml Middlebrook OADC was added, and Kanamycin was also added to a final concentration of 30 µg/ml. This medium was used to screen *Mtb* colonies transformed with mCherry plasmid (see Section 2.8.1).

d. LJ: was provided by BD Diagnostic System. The components of this medium contain 2.5 g monopotassium phosphate, 0.24 g magnesium sulfate, 0.6g sodium citrate, 3.6 g L-asparagine, 30 g potato flour, 0.4 g malachite green, 12 ml glycerol, 1000 ml whole egg and 600 ml purified water. This medium is often used to isolate and cultivate *Mtb*.

2.3 PBMC isolation

PBMC were separated from heparinized whole blood by Lymphoprep (Asix-Shield, Norway) gradient centrifugation in accordance with the manufacture's protocol. 20 ml of blood was diluted in 20 ml of PBS (ratio of 1:1), then slowly added to the tube containing 20 ml of Lymphoprep (ratio of 2:1), and centrifuged at 1300 g for 24 min at room temperature without brake (brake adjusted to zero). The buffy coat layer of PBMC was transferred to a new tube and washed 3 times with cold PBS supplemented with 3 % FBS at 4 ^{o}C, 600 g for 7 min to remove platelets.

2.4 T-SPOT.TB assay

This assay is used as an aid in diagnosis of *Mtb* infection based on the principle that T cells of individuals, who get infected with *Mtb*, have ability to produce IFN-γ *in vitro* when they are stimulated with *Mtb* antigen. In this assay, individual TB-specific

activated T cells can be enumerated by using a simplified ELISPOT method that is remarkably sensitive because IFN-γ is captured directly around the secreting cell, before it is captured by receptors of neighboring cells or degraded in the supernatant[268]. In this assay, *Mtb* antigens used are ESAT-6 and CFP-10 peptides that are specific for the *Mtb* complex (*Mtb*, *M. bovis*, *M. africanum*, *M. microti*, and *M. canetti*). Therefore, the assay only detects *Mtb* complex and reduces cross-reactivity to the BCG vaccine and to most environmental mycobacterium. The assay was performed in accordance with the manufacturer's instructions (TSPOT.TB, Oxford Immunotec, UK). The 96 wells coated with a mouse monoclonal antibody against IFN-γ were allowed to equilibrate to room temperature. Each patient sample required the use of 4 individual wells, namely Nil control, Panel A, Panel B, and a Positive Control. 50 µl of complete media for PBMCs, 50 µl solution of ESAT-6 antigens, 50 µl solution of CFP-10 antigens, and 50 µl solution of phytohaemagglutinin were respectively added to the assigned well for Nil control, Panel A, Panel B, and Positive Control. 2 x 10^5 PBMCs in serum-free media were added to each well of the 4 wells to be used for a patient sample. The plate was incubated in a humidified incubator at 37 °C with 5 % CO_2 for 16-20 h, and then washed 4 times with 200 µl PBS per well to remove nonspecific binding. 50 µl of alkaline phosphatase-conjugated mouse monoclonal antibody to IFN-γ diluted 200 fold in PBS (150 mM NaCl, 7 mM Na_2HPO_4, 2.8 mM NaH_2PO_4 at pH 7.2) was added to each well. After 2 h incubation at 2-8 ^oC, the plate was washed again with 200 µl PBS per well for 4 times, and the antibody-cytokine-antibody sandwich complex was detected by incubating in 50 µl of substrate solution at room temperature for 7 min. The plate was then thoroughly washed with distilled or deionized water to stop the detection reaction and was air-dried. The number of distinct and dark blue spots in each well was

counted by using a dissecting microscope: positive test wells would have at least 20 spots while the negative control wells would have less than 10 spots. T-SPOT.TB test results were interpreted by subtracting the spot count in the Nil Control well from the spot count in each of the Panels, the result was positive when (Panel A minus Nil Control) or (Panel B minus Nil Control) would have at least 8 spots, and negative when (Panel A minus Nil Control) or (Panel B minus Nil Control) would have less than 5 spots. If the highest of (Panel A minus Nil Control) or (Panel B minus Nil Control) was 5, 6, and 7 spots, the result was considered borderline and it is recommended to re-test the individual[268]. In our study, the results were read independently by two researchers following the manufacturer's manual.

2.5 Preparation of resting macrophages

2.5.1 Human primary monocyte-derived macrophages

For phagocytosis, $9x10^5$ PBMC were plated in each well of cell culture treated 48-well plates (Corning, USA) in serum-free media to screen adhered monocytes. Cells were incubated at 37^oC, in 5 % CO_2 for 2 h and the non-adhered cells were gently washed off twice with warm PBS containing 3 % FBS. Then, cells were re-suspended in 0.4 ml complete media containing 10 ng/ml human m-CSF (R&D Systems, USA), and incubated at 37 ^oC, 5 % CO_2 for 6 days to derive macrophages. The complete media containing 10 ng/ml human m-CSF were changed at day 4, and phagocytosis assay was performed at day 7.

For other assays, the remaining PBMCs were plated in cell-culture treated 60 mm x 15 mm petri dishes (Corning, USA) with $6 – 8 \times 10^6$ cells per dish. Cells were incubated at 37 ^oC, in 5 % CO_2 for 2 h and the non-adhered cells were gently washed off 3 times

with PBS containing 3 % FBS. Then, cells were re-suspended in 2 ml complete media containing 10 ng/ml human m-CSF, and incubated at 37 ^{o}C, 5% CO_2. On the following day, they were gently washed off twice with PBS containing 3 % FBS, harvested in 1 ml cold PBS using scrapper, then centrifuged at 4 ^{o}C, 600 g for 7 min. The pellet was re-suspended in 2 ml complete media supplemented with 10 ng/ml human m-CSF. Then some of the cells were plated in cell culture-treated black flat bottom 96-well plate (Corning, USA) at $8x10^4$ cells per well for acidification and proteolytic assays, the remaining cells were cryopreserved in FBS containing 10 % dimethyl sulfoxide (DMSO) (Sigma-Aldrich) for further *Mtb* infection. The adhered cells in 96-well plate were incubated for 6 days at 37 ^{o}C, 5 % CO_2 to differentiate into macrophages. The complete media was changed at day 4, and acidification and proteolysis assays were performed at day 7.

For *Mtb* infection, frozen monocytes were rapidly thawed at 37 ^{o}C and washed twice in the complete media. Cells were then plated in cell culture-treated black flat bottom 96-well plate at $8x10^4$ cells per well and derived as described above. Macrophages were infected with *Mtb* at day 7 after thawing.

2.5.2 Cell lines

J774 murine (ATCC® TIB-67™) and THP1 (ATCC® TIB-202™) human macrophages were obtained from ATCC (USA) and maintained in the media at 37 ^{o}C, 5 % CO_2. THP-1 cells were non-adherent cells, which were passed 1:4 dilution into new media every 3 to 4 days with the final concentration of $2x10^5$ cells/ml[269]. To prepare cells for experiments, THP1 monocytic cells were transferred to 96-well plates at 6 x 10^4 cells per well to establish a confluent monolayer. These cells were incubated with 50 ng/ml phorbol 12-myristate 13-acetate PMA (Sigma) for 2 days for macrophage

differentiation. Cells were then washed and incubated in fresh media for at least 12 h before experiment.

J774 cells were cultured in a 75 cm^2 flask. These cells are adherent to tissue culture-treated surface; hence, subcultures are prepared by scrapping. To subculture cells, 10 ml of culture media were removed. Cells were then incubated in cold PBS for 5 min, then scraped and collected by centrifugation at 600 g for 5 min. Subsequently, cells were dispensed into new flasks with a subcultivation ratio of 1:3 to 1:6. Media was replaced or added two or three times weekly[270]. To prepare cells for the experiments, they were plated to 96-well plate at 4 x 10^4 cells, or to 48-well plate at 8 x 10^4 cells per well one night before conducting the experiments.

2.6 Preparation of phagosomal beads

To investigate phagocytosis, acidification and proteolysis activities of macrophages from TB patients, phagosomal bead-based assays have been adapted and modified for our purposes.

In general, the carboxylated 3 μm diameter silica beads were used because of their high density and homogeneity which ensures the synchronized contact with the macrophage monolayer at the bottom of the test well[271]. Acidification and proteolysis beads were constructed with chemical coatings which always contain three elements: a fluorogenic substrate, a fluorophore of calibration and a ligand while phagocytosis beads were only constructed with the two latter components (Figure 2.1). The roles of these three elements are as follows.

(1) **A fluorogenic substrate** or reporter is used to specifically detect the enzymatic activity of interest or change of phagosomal pH. In line with previous protocols

published by Yates *et al.*[244], I used pH-sensitive fluorochrome carboxyfluorescein-succidinimyl ester (CF-SE) for measuring phagosomal acidification and DQ green bovine serum albumin (DQ-BSA) for proteolysis. In presence of proteases, DQ-BSA gets easily digested to release fluorescent fragments that can be measured.

(2) **A fluorophore of calibration** or calibrator remains unchanged through the assay and is used to normalize the readout in case of measuring acidification and proteolysis. There are a number of fluorescent dyes to select according to the compatibility of the existing measuring instrument. It is necessary to ensure that the excitation-emission spectra of fluorogenic substrate and the calibrator do not overlap. For acidification assay, the emission intensity of fluorogenic substrate when excited at pH-insensitive wavelength was used to normalize the readout. For phagocytosis beads, the labeling with calibrator facilitates the bead visualization that helps to discriminate the cell population internalizing or not internalizing the beads.

(3) A **ligand** is to facilitate phagocytosis and to programme the pathway of the innate immune response through its receptor.

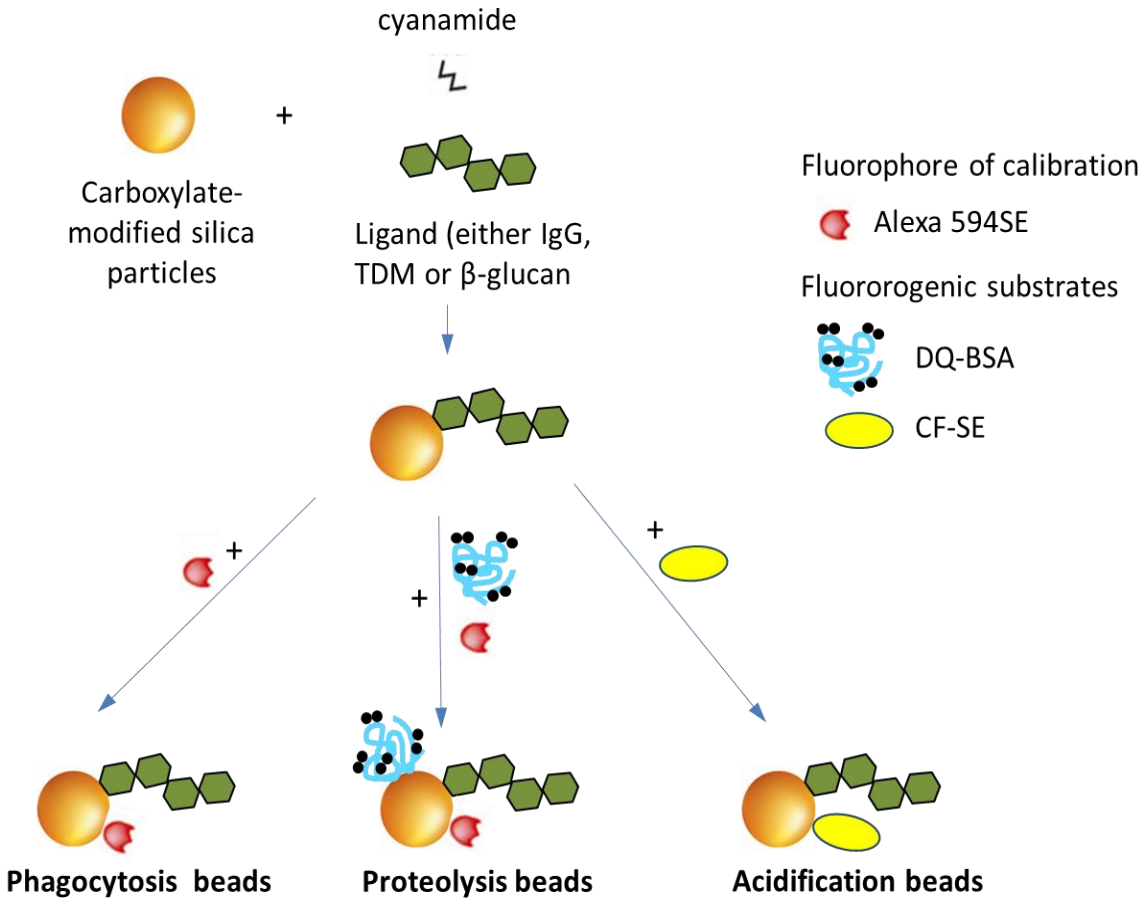

Figure 2.1. A schematic diagram for preparation of phagocytosis, proteolysis and acidification beads.

All three kinds of bead were coated with ligands (either IgG, TDM or β-glucan) that were coupled with carboxylate-modified silica beads through covalent binding, mediated by crosslinker cynamide. In addition, phagocytosis beads were labeled with calibrator Alexa 594SE. Similarly, proteolysis beads were coated with fluorogenic substrate DQ-BSA and a calibrator Alexa 594SE. Acidification beads were coated with CF-SE that was used as both fluorogenic substrate and calibrator. More clearly, the emission intensity of this substrate when excited at pH-insensitive wavelength was used to normalize the readout. The location of different components on bead was for illustrative purpose only.

2.6.1 Phagocytosis beads

In protocol published by Yates *et al*. in 2005[244], the beads are coated with IgG or α-D-mannosylated-PITC-albumin, two ligands recognized by FcγR and mannose receptors on the macrophage surface, to facilitate the bead uptake by phagocytosis. Then the bead phagocytosed is visualized by labeling with Alexa Fluor 594 succidinimyl ester (SE). In this study, beside IgG, the beads were coated with either TDM (a cord factor derived from *Mtb*, Enzo Life Science) or β-glucan (derived from *S. cerevisiae*, InvivoGen), which are recognized by specific receptors, to study the phagocytosis induced by different pathways. The cells with internalized beads were detected by the fluorescent dye Alexa Fluor 594. Below is our detailed protocol for preparation of phagocytosis beads.

Five hundred microliter of 3 μm carboxylate-modified silica particles (Kisker Biotech, Germany) were washed three times in 1 ml of PBS by vortexing and centrifuged at 2000 g for 1 min. The beads were re-suspended in PBS with 25 mg/ml of the crosslinker cynamide (Sigma-Aldrich, USA), which works as a cross-linker, and agitated for 15 min at room temperature. Following this, the beads were washed twice in 1 ml of PBS and once in 1 ml of coupling buffer (50 mM borate buffer in PBS, pH 8.0) to remove excess cynamide. Next, they were re-suspended in 0.5 ml coupling buffer with 1.0 mg defatted BSA (Sigma-Aldrich) and 0.1 mg human IgG (Molecular Probes) or 0.25 mg ligands [TDM (Enzo Life Sciences) or β-glucan/ whole glucan particles (Invitrogen)] then incubated for 12 h with agitation. Next, the beads were washed three times in 1 ml of quenching buffer (250 mM glycine (Sigma-Aldrich) in PBS, pH 7.2) to quench unreacted cyanamide. The beads were then re-suspended in 1 ml coupling buffer containing 10 μl of 5 mg/ml Alexa Fluor 594 SE (Molecular Probes) in DMSO and

agitated for 1 hr. Then, the beads were washed three times in 1 ml quench buffer, re-suspended in 1 ml PBS with 0.02 % sodium azide and stored at 4 ^{o}C.

2.6.2 Acidification beads

Our acidification beads were prepared similarly to that in studies by Yates *et al.*[244]. However, I generated the bead by coating with not only IgG, but with TDM or β-glucan ligands to study the acidification via different pathways. Our procedure to generate acidification beads were detailed as below.

First steps to prepare the cynamide-bound beads were followed exactly as described in the procedure above for the preparation of phagocytosis beads. The cynamide-bound beads were re-suspended in 500 µl of coupling buffer with 1 mg defatted BSA, 0.1 mg human IgG or 0.5 mg/ml of ligands (either TDM or β-glucan), and incubated with agitation for 12 h. Then, they were washed twice with 1 ml of quenching buffer to quench unreacted cyanamide and twice with 1ml of coupling buffer. Following this, the beads were re-suspended in 1 ml of coupling buffer containing 10 µl of the 5 mg/ml stock of the CF-SE (Molecular Probes) dissolved in DMSO. The beads were agitated for 2 h to allow the albumin-bound particles to be sufficiently labeled with the amine-reactive fluor, and then were washed three times in 1 ml of quenching buffer. The acidification beads were stored in 1 ml of PBS with 0.02 % sodium azide at 4 ^{o}C.

2.6.3 Proteolytic beads

Proteolysis beads were prepared similarly to that in published protocol[272]. Instead of coating the beads with ligands of IgG and mannose as Yates *et al.* did, I generated the proteolysis beads by coating with either IgG, TDM or β-glucan ligands to study the proteolysis via different pathways.

The cyanamide-bound beads were prepared as describe above in Section 2.6.1. The beads were then re-suspended in 500 µl of coupling buffer with 1mg of DQ-BSA (Molecular Probes, USA) and 0.1 mg human IgG or 0.5 mg/ml of ligands (either TDM or β-glucan), and were incubated with agitation for 12 h. Next, they were washed three times in 1 ml of quenching buffer to quench unreacted cyanamide, and were re-suspended in 1 ml of coupling buffer containing 10 µl of the 5 mg/ml stock of the calibration fluor Alexa Fluor 594-SE (Molecular Probes, USA) in DMSO. Following this, the beads were agitated for 1 h to allow the albumin-bound particle to be sufficiently labeled with the amine-reactive fluor, and then they were washed three times in 1 ml of quenching buffer. The proteolytic beads were stored in 1 ml of PBS with 0.02 % sodium azide at 4 ^{o}C.

2.7 Phagosomal beads assays

2.7.1 Phagocytosis assays

Resting macrophages in 48-well plate were checked by microscope to ensure that a monolayer with about 80 % confluence had been achieved. New media was changed with 200 µl per well. Stored phagocytosis beads were washed three times in PBS with vortexing, then 10 µl of beads was added into each well with concentration to achieve an average of 1–2 beads internalized per macrophage[244]. Binding and uptake of the beads were performed by incubating of macrophages with a suspension of the beads at 37 ^{o}C, 5 % CO_2 for 10 min. The cells were washed three times in PBS with 3 % FBS to remove unbound beads, then were harvested by scraping in cold PBS with 1 % para-formaldehyde and transferred into a tube for flow cytometry analysis.

Phagocytosis of macrophages was determined by the percentage of phagocytes which internalized Alexa Fluor 594 SE-labeled beads. Samples were run using BD FACS Canto II and FACS Diva acquisition software, and fluorescent intensity was analyzed using FlowJo analysis software (FLOWJO, LLC).

2.7.2 Acidification and proteolysis assays

Stored acidification or proteolysis beads were washed in PBS twice with vortexing, and were re-suspended in PBS[273]. Confluent monolayer of resting macrophages was washed and 50 µl assay buffer (1 mM $CaCl_2$, 2.7 mM KCl, 0.5 mM $MgCl_2$, 5 mM dextrose, 10 mM HEPES, 10 % FBS in PBS) were added. Next, 10 µl of the beads were added into each well with concentration to achieve an average of 4–5 beads internalized per macrophage[239]. Subsequently, cells were transferred to 37 ^{o}C in a fluorescent microplate reader (SynergyH4, BioTek) to initiate the fluorescence data acquisition in real-time. This acquisition lasted 90 min for acidification assay and 210 min for proteolytic assay. During this time period, data were collected with an interval of 1.30 min. The relative pH within phagosome was calculated by the ratio between fluorescent intensities emitted at 520 nm when excited at pH-sensitive 490 nm and at pH-insensitive 450 nm. Proteolysis was expressed by the calibrated fluorescent intensity of hydrolyzed DQ-BSA substrate emitted at 520 nm when excited at 490 nm. To compare the macrophage acidification or proteolysis activity between different groups of patients, activity index was used as reported previously[274,275]. Acidification Activity index of macrophages at 30, 60, 70, and 90 min was calculated by ratio of relative pH at 10 min over that at 30, 60, 70, and 90 min respectively. Likewise, proteolysis Activity index at 60, 120, 180 and 210 min was calculated by dividing proteolysis at these time-points respectively by that at 10 min.

Three wells were used for each experimental condition and the mean was determined. Three independent experiments were conducted for testing consistency of proteolysis and acidification activities of J774 murine macrophage and the mean was determined.

Proteolysis activity of hMDM infected with *Mtb* was assessed at day 2 post infection (see Section 2.8.3).

2.8 Macrophage and *Mtb* interaction

The interaction of macrophage and *Mtb* was assessed by the intracellular growth of bacteria and the *Mtb*-induced cell death of macrophages.

2.8.1 Preparation of *Mtb* reporter strain

The gold standard method to examine the growth of *Mtb* within the macrophages is lysing macrophages, plating then counting colony-forming units CFU. However, this method is laborious and time consuming. Alternatively, fluorescent reporter strains can be used to assess the bacterial intracellular growth because of rapid detection, high sensitivity and real time detection[276]. Therefore, to study antimicrobial function of macrophages from TB patients, I generated the *Mtb* reporter strain that enables to express mCherry fluorescent protein. Correlations of mCherry intensity and bacterial growth measured by optical density (OD) at 600nm (OD_{600}) or CFU were assessed and presented in chapter 3.

a. Generating *Mtb* reporter strain

Plasmid pVV16 containing hsp60 promoter and a gene encoding for fluorescent protein mCherry (pVV16-mCherry plasmid) was kindly provided by Professor DG. Russell (Cornell University, USA). This construct was transformed to *Mtb* by using a Micropulser Electroporator (Biorad, USA). To prepare the competent cells for

electroporation, *Mtb* clinical strain isolated from TB patient was cultured with shaking in 10 ml 7H9T medium at 37 ^{o}C to log phage OD_{600} 0.5 - 1 for 15 - 18 days. 1 ml of 2 M glycine solution was added to culture 24 h before harvesting the cells. Bacteria were harvested at 3200 g for 10 min at room temperature. The cells were washed in 50 ml of pre-warmed 10 % glycerol, re-suspended well in 500 µl of 10% glycerol through a sterile syringe equipped with 23-gauge needle to form single cell suspension, then aliquoted and kept at -20 ^{o}C as glycerol stocks until further use. 0.2-0.5 µg of pVV16-mCherry plasmid were mixed with 200 µl competent cells and left for 10 min at room temperature. Then, this mixture was transferred to a 0.2 cm electroporation capped cuvette. Electroporation was conducted at a pulse of 2.5 kV, 25 µF. Cell suspension was transferred to pre-warmed 7H9T and incubated at 37 ^{o}C for at least 48 h. Cell suspension was then plated on selective media containing 30 µg/ml kanamycin and incubated at 37 ^{o}C for 3 weeks. *Mtb* carrying the pVV16-mCherry plasmid was selected from pink colonies growing in the selective media (Figure 2.1) and cultured in 7H9T media containing kanamycin at 37 ^{o}C with shaking until OD600 0.8 – 1 for 15 – 18 days. Bacteria were harvested at 3200 g for 10 min at room temperature, washed in 50 ml of pre-warmed 10 % glycerol, re-suspended in 10% glycerol, aliquoted and stored at -20^{o}C for further use.

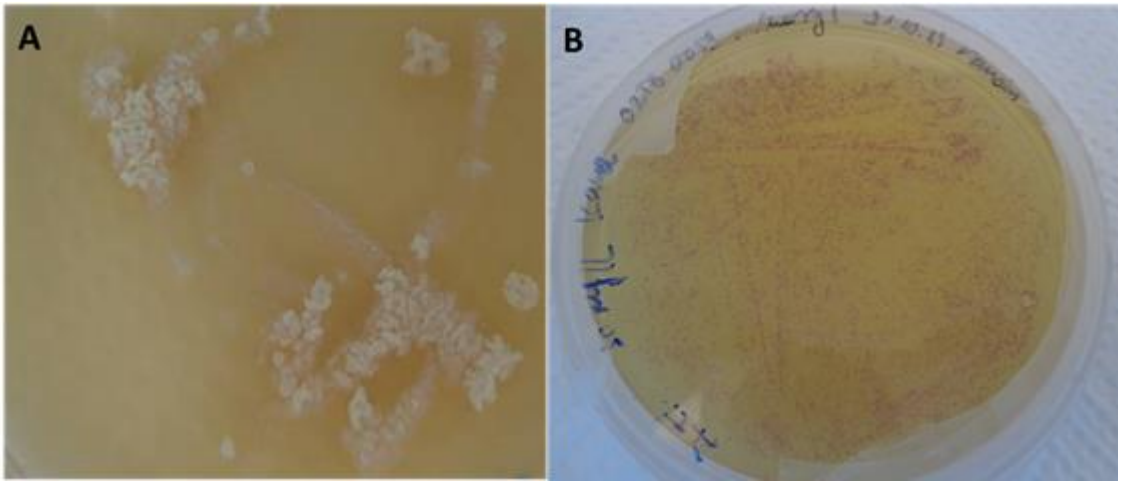

Figure 2.2 Generating *Mtb* reporter strain

(A) *Mtb* carrying the pVV16 plasmid (white colonies) as a negative control. (B) *Mtb* carrying the pVV16-mCherry plasmid (pink colonies)

b. Culture of *Mtb* reporter strain

Mtb reporter strain was cultured from -20 ^{o}C stock above in 7H9T containing 30 µg/ml kanamycin at 37 ^{o}C with shaking to OD_{600} of 1 - 2 for 15 - 20 days. The bacteria was sub-cultured in 7H9T containing 30 µg/ml kanamycin at 37 ^{o}C with shaking, and was ready for infection experiment when OD_{600} reached 0.5 – 1.

c. CFU of *Mtb* reporter strain

The bacterial culture having OD_{600} of 0.5 - 1 was serially diluted 10-fold from 10^{-1} up to $10^{-4,}$ then two-fold from $2^{-1}x10^{-4}$ to $2^{-4}x10^{-4}$. 100 µl of each dilution from 10^{-4} to $2^{-4}x10^{-4}$ was transferred to plate of selective medium containing 30 µg/ml kanamycin and spread onto the plate. The plates were incubated at 37 ^{o}C for 3 weeks for CFU counts. Within 3-4 weeks after plating, the plates were taken out and CFU was calculated from the number of colonies of *Mtb* on the plates, taking into account the dilution factors.

d. Fluorescent intensity of *Mtb* reporter strain

The bacterial culture having OD_{600} of 0.5 - 1 was serially two-fold diluted. 100 µl of each dilution was transferred to black flat-bottom plate and mCherry intensity was measured at emission wavelength of 620 nm after excitation at 575 nm using the fluorescent microplate reader.

2.8.2 Isolation of *Mtb* from sputum sample

Sputum (N= 159) were collected from patients who had less than three days of TB treatment. To decontaminate the sputum sample, an equal volume of N-acetyl-L-cysteine and 2% NaOH were added to the sputum (approximately 10 ml each), mixed in screw capped tube and vortexed. The mixture was incubated at room temperature for 15 min with occasional shaking. PBS (pH 6.8) was added to the mixture to get a final volume of 50 ml, then the mixture was centrifuged at 3200 g for 15 min. Supernatant was discarded carefully and the pellet was dissolved in 0.5 to 1 ml of PBS. This suspension was used for culturing *Mtb* on LJ medium at 37 ^{o}C**,** then after 3-4 weeks, *Mtb* was sub-cultured in 7H9G from single colony. When the culture reached OD_{600} of 0.5-1, it was centrifuged at 1800 g for 15 min, then the pellet was re-suspended in 7H9G, aliquoted and stored at -20 ^{o}C for further experiments.

To prepare culture for infection, *Mtb* was re-cultured from -20 ^{o}C stock above in 7H9T at 37 ^{o}C with shaking to OD_{600} of 1 - 2 for 15 - 20 days. The bacteria were sub-cultured in 7H9T at 37 ^{o}C with shaking, and were ready for infection experiment when OD_{600} reached 0.5 – 1.

2.8.3 Experimental infection of macrophage with *Mtb*

Resting macrophages were recharged with 100 µl antibiotic-free medium. Cells then were infected with *Mtb* at different desired MOI of 1, 2, or 3 and incubated at 37 ^{o}C, 5 % CO_2. Four hours after infection, macrophages were washed with pre-warmed medium without antibiotics and incubated at 37 ^{o}C, 5 % CO_2. Next, infected cells were incubated at 37 ^{o}C, 5 % CO_2, and cell supernatants were collected at 24 h after infection for cytokine measurement. Infected cells were then further incubated in new media at 37 ^{o}C, 5 % CO_2 to examine the bacterial growth or phagosomal activities.

2.8.4 Measurement of in vitro bacterial growth rate

To assess the bacteria growth rate of 159 clinical *Mtb* isolates, $6x10^6$ bacilli were cultured in 10 ml 7H9T at 37 ^{o}C without shaking. The OD_{600} was measured every two days during 20 days of culture. The $\log_2$ of OD_{600} value of each isolate was plotted and the bacterial growth rate was expressed as the slope of this line.

2.8.5 Measurement of intracellular bacterial growth

The intracellular growth of *Mtb* reporter strain was assessed over 5-7 days, by using the fluorescence microplate reader, through fluorescent intensity of mCherry protein, emitted at wavelength of 620 nm after excitation at 575 nm. Three wells were used for each *Mtb* strain and the mean was determined.

2.8.6 Observation of macrophage lysis

The interaction of macrophage and *Mtb* clinical isolates was assessed by macrophages lysis. The percentage of lysed macrophages was daily estimated using conventional microscopy. The result was read by two independent staff without noticing sample

position on the plates. Three wells were used for each *Mtb* strain and the mean was determined.

2.9 Molecular and Immunological assays

2.9.1 Stimulation for mRNA gene expression and cytokine production

For mRNA expression, monocytes from healthy volunteers were plated to 24-well plate at concentration of 10^6 cell per well. Cells were incubated at 37 °C with 5% CO_2 overnight in the complete media. Following day, media was changed and cells were subsequently stimulated with either whole cell lysis (WCL) of *Mtb* H37Rv (Colorado State University, USA) at 5 µg/ml, lipopolysaccharides (LPS) from *Escherichia coli* (Sigma-Aldrich) at 100 ng/ml or media. After 5 h of incubation at 37 °C with 5 % CO_2, the old medium was removed and 0.5 ml Trizol (Life technologies^{TM}) was added in order to disrupt the cells, dissolve the cell components and release RNA. This suspension was transferred to the 1.5 ml RNA-free tube and stored at -80 ^oC for further extraction (see Section 2.9.2).

For cytokine production, PBMCs from healthy volunteers were plated in 96-well plates at concentration of 10^5 cells / well in the complete media. Cells were stimulated with either H37Rv WCL at 25 µg/ml, TDM at 100 µg/ml, LPS 100 ng/ml or media. For stimulation, TDM was coated on the plate and air-dried in the cabinet the day before, while other ligands were added directly into the medium after cell plating. Cells were incubated at 37 ^oC, 5 % CO_2 for 24 h and supernatants were collected, kept at -80 ^oC. All samples were then processed and cytokines were measured from stored supernatants at the same time.

2.9.2 mRNA gene expression

a. mRNA extraction

mRNA was extracted by Trizol method following the manufacturer's instruction (Ambion, Life technologies^{TM}). Briefly, the samples stored at -80 ^{o}C were thawed, then cell suspension was transferred to 1.5 ml tube; 100 µl of chloroform was added to separate the solution into an aqueous phase and an organic phase by centrifugation at 10000 g, 4 ^{o}C for 15 min. The aqueous phase which contained RNA was transferred to a new tube. 500 µl of isopropanol was added to precipitate the RNA by centrifugation at 12000 g for 10 min at 4 ^{o}C. Then the supernatant was discarded and the RNA pellet was washed with 1 ml of 75% ethanol by centrifugation at 7500 g for 5 min at 4 ^{o}C, air-dried, dissolved in 10 µl RNase- free water and stored at -80 ^{0}C until use.

RNA concentration was measured by absorbance at 260 nm using a spectrophotometer (Nanodrop ND-1000, Germany). The nucleotide bases absorb UV light of approximately 260 nm of wavelength. An OD of 1 corresponds to 40 ng/µl for RNA at 260 nm. The ratio between the reading of 260 nm and 280 nm (OD_{260}/OD_{280}) shows an estimate of the purity of the nucleic acid. Pure preparation of RNA has an OD_{260}/OD_{280} value of 2.

b. Reverse transcription

I synthesized cDNA from total RNA template by reverse transcription. 10 µl RNA were mixed with 1µl of 50 ng/µl random primers (Roche) and 1 µl of 10mM dNTPs on ice. This sample mixture was incubated at 65^{o}C for 5 min by Mastercycler and immediately incubated on ice for at least 1 min. Master mix was prepared on ice for each reaction with 1 µl of 200 U/ µl of SuperScript™ III RNase H Reverse Transcriptase (Invitrogen), 4 µl of 5X First-Strand buffer (Invitrogen), 2 µl of 100 mM DTT (Invitrogen), and 1 µl

of 40 U/µl RNAase OUT (Invitrogen). The master mix was added to the sample mixture, mixed well and incubated at 25 ^{0}C for 10 min, 50 ^{o}C for 1 h, 72 ^{o}C for 15 min and held at 4 ^{o}C for 2 min. After thermal cycling, all cDNA samples were stored at -20 ^{o}C until use.

c. Preparing and running Taqman® real-time PCR

Glyceraldehyde-3-phosphate dehydrogenase *GAPDH* was used as a house-keeping gene to normalize the samples. The primers and probes of *MARCO* and *GAPDH* adapted from previous study[277] and PhD thesis of Dr. Thuong Nguyen (Open University, 2008) respectively were listed in Table **2.1**. Real-time PCR reaction was performed in 20 µl master mix consisting of 1 µl of 10 µM of each primer, 0.5 µl of 5 µM of each probe, 10 µl of 2X reaction buffer (LightCycler480 Probe Master, Roche), 2.5 µl distilled water and 2.5 µl of cDNA from reverse transcription product.

Table 2.1 *MARCO* and *GAPDH* primers and probes

Type	Gen	Sequence (5'-3')
Primers (Sigma)	*MARCO*-forward	CTGGTGGTCCAAGTTCTGAATCT
	MARCO-reverse	TCAGCCGCCAGAGTGTCA
	GAPDH-forward	CCACATCGCTCAGACACCAT
	GAPDH-reverse	ACCAGGCGCCCAATACG
Probes (Tib Molbiol)	*MARCO*	Cyan500-CTCCGGGTCCTGGAGATGTATTTCCTCA-BHQ1'
	GAPDH	Cy5-CAAATCCGTTGACTCCGACCTTCACCTT-BBQ'

The reaction was loaded to a thermocycler (LightCycler480, Roche) and run as follow: 95 ^{o}C for 5 min; and 45 cycles of 95 ^{o}C for 15 seconds, 60 ^{o}C for 45 seconds. The

fluorescent signals were read at wavelengths of 440-488 nm and 618-660 nm for *MARCO* and *GAPDH*, respectively.

d. Data analysis

I used relative quantification to determine a change in the expression of the *MARCO* mRNA in ligand or WCL-stimulated monocytes relative to an untreated-monocyte *MARCO* mRNA expression. Each reaction was repeated twice and the mean was calculated. Analyses were performed using LightCycler 480 release 1.5.1.62 Relative Quantification software (Roche). The expression of target genes was normalized to *GAPDH* expression.

2.9.3 Measurement of cytokine production

a. Using Bio-Plex Precision Pro Assays

The concentrations of TNF-α, IL-1β and IL-10 from stimulated PBMC (see section 2.9.1) were quantified using Bio-Plex Precision Pro Assays, Human cytokine 10-Plex (Biorad). This is a bead-based immunoassay whose principle is similar to sandwich ELISA. A wide range of fluorescent dyed-beads are used to quantify the level of different cytokines in the sample. Each kind of dyed-bead is coated with monoclonal antibodies specific for a desired target cytokine. After several washes, bound cytokine is detected by a biotinylated detection antibody specific for a different epitope. Then streptavidin- PE is added to bind to the biotinylated detection antibodies; the fluorescent intensity produced indicates the relative quantity of target cytokine.

The procedures were carried out in accordance with the manufacturer's instructions. Briefly, after 96-well filter plate was pre-wetted with 200 µl of assay buffer, 50 µl of the beads were added to each well and vacuum-filtered. After washing the plate twice, 50 µl

of standard or sample were added to each well and incubated with gentle shaking for 1 h in the dark at room temperature. Then, the plate was washed and incubated with 25 µl 1X detection antibody at room temperature in the dark for 30 min with gentle shaking. The bead-cytokine-antibody complex was detected by incubating with 50 µl of 1X streptavidin-PE for 10 min in the dark at room temperature. Following this, 125 µl of assay buffer were added to each well and the assay plate was shaken for 30 seconds at 1100 rpm before acquiring data using a multiplex array reader from Luminex Systems (Luminex-200 system from Luminex).

The cytokine concentrations were calculated using Bio-Plex Manager Software (Biorad). The limits of detection for TNF-α, IL-1β, and IL-10 were 0.14, 0.23 and 0.96 (pg/ml), respectively.

b. Using DuoSet® ELISA

Concentration of TNF-α, IL-1β, and IL-6 secreted by macrophages infected with *Mtb* (see section 2.8.3) were measured using the DuoSet® ELISA for desired cytokines (R&D). The procedure of this assay was performed in accordance with the manufacturer's manual. First, 96-well plate was coated with 100 µl of diluted mouse antibody to particular cytokine at working concentration in PBS and incubated overnight at room temperature. After 3 times of washes with wash buffer to remove the unbound antibody, the plate was blocked by adding 300 µl of PBS containing 1% BSA to each well and incubated at room temperature for a minimum of 1 h. After washing 3 times, 100 µl of samples or recombinant standards were added and incubated with gentle shaking at room temperature for 2 h. The plate was washed 3 times to remove unbound materials, and then incubated with 100 µl of the biotinylated goat antibody to particular cytokine with gentle shaking at room temperature for 2 h. After washing, to

detect the cytokine-antibody complex, 100 µl of the working dilution of Streptavidin-HRP were added and incubated for 20 min at room temperature in the dark. The unbound streptavidin-HRP was washed away and the plate was added with 100 µl of Tetramethylbenzidine (TMB) substrate solution, incubated for 20 min at room temperature in the dark. A blue color developed in proportion to the amount of targeted cytokine present in the sample. 50 µl of stop solution was added, turning the color in the well to yellow. The optical density of well was determined using a microplate reader (680XR, Biorad) at the wavelength of 450 nm together with a correction wavelength of 540 nm.

The cytokine concentrations were calculated using Microplate manger version 5.2.2 (Biorad). The limits of detection for TNF-α, IL-1β and IL-6 are 15.6, 3.91 and 9.38 (pg/ml), respectively.

2.10 Human SNP genotyping

2.10.1 SNP selection

At the time of conducting this study, the whole genome sequence of Vietnamese population in project of 1000 Genomes was still ongoing, hence I used genetic information from Han Chinese Beijing (CHB) population as our reference. All SNPs across entire *MARCO*, *DECTIN1*, and *MINCLE* genes and 20 kb from their upstream and 10 kb from downstream region were obtained based on the HapMap reference data (has been retired from June 2016) for CHB population. Criteria I used to choose SNPs for genotyping were allele frequency, tag SNPs and functionality of SNPs. Tag SNPs were selected to serve as multi-marker tagging algorithm with the criteria of r^2 cut off of 0.8 for linkage disequilibrium and a minor allele frequency (MAF) cut off of 5 %.

Haploview 4.2 (Broad Institute of MIT and Harvard, USA) was used to calculate r^2 and D' for linkage disequilibrium. Functional information of SNPs was obtained from Genome Bioinformatics Site of University of California Santa Cruz (UCSC, http://genome.ucsc.edu/cgi-bin/hgGateway), from Genome Variation Server 147 (GVS, http://gvs.gs.washington.edu/GVS147/) or from SNP database (dbSNP, https://www.ncbi.nlm.nih.gov/snp/?term=). SNPs that were known to change amino acids of protein (missense SNPs) were also selected to be genotyped.

2.10.2 Procedure of SNP genotyping

a. Human genomic DNA isolation

DNA from blood samples was extracted by Qiagen DNA extraction kits (Qiagen, UK) or Nucleon BACC Genome DNA extraction kits (GE Healthcare, Sweden) in accordance with manufacturer's instruction. Briefly, 3 ml blood was diluted to 5 ml in PBS then 6 ml lysis buffer were added to the blood mixture. Such mixture was thoroughly mixed and left at 70 ^{o}C for 10 min. Next, 5 ml of ethanol (96-100%) was added and the sample was mixed well to increase the efficient binding. This lysate was then loaded twice to the QIAamp Maxi column and centrifuged at 1200 g for 3 min. The column was washed two times, then 600 µl elution buffer or distilled water was added to elute DNA binding to the membrane. The column was incubated at RT for 5 min and then centrifuged at 5000 g for 5 min to obtain DNA. For Nuleon BACC kit, 3 ml blood was incubated with 12 ml reagent A for 20 min at RT to lyse the red blood cell. The pellet was collected after centrifugation of sample at 1700 g for 7 min. The white blood cells were further disrupted by incubating the pellet with 1ml buffer B for 10 min at 37 ^{o}C. Next, 400 µl of sodium perchlorate solution were added for deproteinization. Next, 2 ml chloroform was added to denaturate proteins and the sample was mixed thoroughly

by inverting the tube. Following, 220 µl of nucleon resin was added and the mixture was centrifuged at 1500 g for 7 min. The upper phase of nucleon layer was harvested and two volumes of cold absolute ethanol was added to precipitate DNA. The solution was mixed well, then centrifuged at 13000 g for 5 min at 4^{o}C. DNA was washed in cold 70% ethanol and then air-dried to remove the ethanol. DNA was then re-dissolved in 400 µl of distilled water.

b. SNP genotyping

Genotyping of SNPs was performed in collaboration with Professor Thomas Hawn (University of Washington, USA) using GoldenGate assay (Illumina, San Diego, USA). The principle of this method has been well described[278]. Firstly, genomic DNA is activated by biotinylation to bind to paramagnetic particles, then the activated DNA is combined with the assay oligonucleotides, buffer for hybridization, and paramagnetic particles in the hybridization step. Three oligonucleotides are designed for each SNP site. Two oligos are specific to each allele of the SNP site and are called Allelic-Specific Oligos (ASOs). A third oligo hybridizes several bases downstream from the SNP site and is called the Locus-Specific Oligo (LSO). All these oligos contain regions of genomic complementarity and universal PCR primer sites allowed PCR reaction to occur; the LSO also contained a unique address sequence that targeted a particular bead type. The next step was the extension reaction of ASO towards the LSO, which was then ligated. The product after ligation was amplified by PCR with fluorescent labeled primers. The dye-labeled PCR products were hybridized to beads carrying the complementary sequence to their unique address sequence. After hybridization, a high-throughput scanner was used to detect the fluorescent beads and decode the information used to generate genotype clustering and calling.

2.10.3 Quality control for genotyping

The controls do not have the disease so they should follow Hardy–Weinberg equilibrium (HWE) principle, which states that allele and genotype frequencies in a population will remain constant from one generation to the next in the absence of other evolutionary influences. The influences include mate choice, mutation, selection, gene flow, genetic drift, and meiotic drive. In the population, if frequency of allele A is a and allele B is b = 1- a, then the frequencies of AA, AB and BB genotypes should be a^2, 2ab and b^2. Deviation from HWE in controls could result from genotyping problems (such as a mutation in the PCR primer or miscalling heterozygotes as homozygotes[279]) or different biases in sampling, such as heterozygous population (the controls may comprise different populations with different allele frequencies) or small sample size[280]. Therefore, the HWE should be checked, particularly in the control group. SNPs on *DECTIN1*, *MINCLE* and *MARCO* were tested for HWE in control subjects using a Chi-square test. SNPs were excluded if they had > 5% missing genotype calls, MAF < 10 % or HWE P value < 0.05.

2.11 Chest radiography

Chest X-rays (CXR) were examined at the time of TB diagnosis, with reports provided by clinicians from district TB control units. Abnormal features on a chest radiograph were recorded comprising of nodules, infiltrates, consolidation, cavities and miliary TB. To grade chest radiograph severity, the abnormal features were assessed and classified as mild if abnormal features were present in one lobe, intermediate if abnormal features were present in one lung, and severe if abnormal features were present in both lungs.

2.12 *Mtb* lineage identification

Mtb lineages were identified by large sequence polymorphism (LSP) typing that has been shown to classify isolates to geographical-related clades[40].

Firstly, *Mtb* DNA was extracted from cultures on LJ media (BD, USA) by cetyltrimethyl ammonium bromide (CTAB) method which kills bacteria by heat then lyses the microorganisms by a combination of heat, lysozyme, proteinase and detergent. CTAB solution (5% CTAB and 0.5M NaCl) forms an insoluble complex with nucleic acid and selectively precipitates DNA, which can be separate from carbohydrates, proteins and other components. Briefly, bacteria were dispersed in 600 µl TE buffer (10 mM Tris pH 8.0 and 1 mM EDTA**)**, followed by heating the tube at 80^{o}C for 20 min. 50 µl lyzozyme 10mg/ml was added; the cell suspension was mixed well by vortexing and incubated overnight at 37^{o}C. Next, to denature the proteins 10µl proteinase K (10mg/ml) and 35µl of SDS 20% were added and incubated at 55 ^{o}C for 30 min. Following this, the suspension was added with 100 µl 5M NaCl and 100 µl 5% CTAB solution, and incubated at 60 ^{o}C for 15 min. Two phases of DNA and protein-cell debris were separated by adding 700 µl chloroform and centrifugation at 12000 g for 5-10 min. The DNA phase was taken and precipitated with 0.6 volume of isopropanol by centrifugation at 13000 g for 15 min. DNA was washed with 70% ethanol, air-dried and re-suspended in 40-80 µl TE buffer or distilled water.

LSPs were then defined following the method of Tsolaki *et al.*[20,281]. Isolates were first characterized for RD239 and RD105 deletion by PCR as the majority of isolates were anticipated to contain one of these two deletions. Isolates bearing RD239 deletion were defined as Indo-Oceanic genotype while isolates bearing RD105 deletion were defined as East-Asia/Beijing genotype. The primers used to screen RD239 were RD239F 5'-

GGCCAACATCGACCACCTACCC-3' and RD239R 5'-ATCCTCGCTACCGGCACCTCAT-3 while for RD105 deletion were RD105F 5'-GGAGTCGTTGAGGGTGTTCATCAGCTCAGTC-3' and RD105R 5'-CGCCAAGGCCGCATAGTCACGGTCG-3'. The PCR reaction for RD239 deletion contained 0.5 mM each primer, 0.2 mM dNTPs, 1.5 mM MgCl2, 0.5U Taq polymerases (Bioline), 1x buffer, 10.25 µl ELGA water and 15 ng DNA in a final volume of 15 µl. The PCR programme started with a denaturation of 95 ^{o}C for 3 minutes, followed by 25 cycles of 94 ^{o}C for 30 seconds, 64 ^{o}C for 30 seconds and 72 ^{o}C for 30 seconds, finished with an extension of 72 ^{o}C for 6 minutes. The PCR mix for RD105 deletion was prepared similarly with RD239, except that 0.3 mM each primer and 1U Expand™ High Fidelity enzyme (Roche) was used. The PCR programme for RD105 started with a denaturation of 95 ^{o}C for 3 minutes, followed by 25 cycles of 94 ^{o}C for 15 seconds, 64 ^{o}C for 15 seconds and 72 ^{o}C for 4 min, finished with an extension of 72 ^{o}C for 6 min. The amplification using RD105 primers produced a product of 4 kb in the control H37Rv while it was shorter with 850 kb in isolates bearing RD105 deletion. Likewise, product from amplification using RD239 primers was 1.8 kb in control H37Rv and was shorter in isolates bearing RD239 deletion. Isolates without RD105 or RD239 were further defined for the Euro-American lineage by PCR to detect the deletion of 7 bp in the pks 15/1 gene using primers pks1i 3'-GCAGGCGATGCGTCATGGGG-5' and pks1j 3'-TCTTGCCCACCGACCCTGGC-5' and an internal primer pks1insR 3'-ACGGCTGCGGCTCCCGATGCT-5'[20]. The PCR reaction contained 0.1 mM pks1i, 0.1 mM pks1j, 0.2 mM pks1insR, 0.2 mM dNTPs, 1.5 mM MgCl2, 0.5 U Hotstart Taq (Qiagen), 1x buffer, 10.85 µl ELGA water and 15 ng DNA in a final volume of 20 µl. The PCR programme started with a denaturation of 95 ^{o}C for 15 minutes, followed by

30 cycles of 94 ^{o}C for 30 seconds, 67 ^{o}C for 30 seconds and 72 ^{o}C for 30 seconds, finished with an extension of 72 ^{o}C for 2 minutes. Isolates bearing a deletion of 7 bp produced 2 bands of 520 bp and 259 bp whereas isolates without the deletion produced a single band of 520 bp.

2.13 Statistical analysis

2.13.1 Association of host genetic variants and disease susceptibility

For alleles of SNPs, the majority allele is coded by 1, the minority allele by 2. Hence for genotypes, the majority homozygote is 11, the minority homozygote is 22 and the heterozygote is 12. In order to assess the association of single SNP and disease susceptibility or clinical presentation or infecting *Mtb* strains, I primarily performed genotypic model that compared the genotype frequencies (11, 12, and 22) and allelic model that compare allele frequencies (allele 1 and 2) in cases and controls. In secondary analysis, SNPs were investigated for associations under the additional genetic models (dominant, recessive and heterozygote). Dominant model is used to compare the frequencies of the 11 and 12 combined versus 22 genotype in cases and controls. Recessive model is used to compare the frequencies of the majority homozygote 11 versus 12 and 22 combined in cases and controls. Heterozygous advantage model is used to compare the frequencies of 12 versus 11 and 22 combined in cases and controls. These 5 models were based on the Chi-squared test using R program, version 3.3.1 (https://www.r-project.org/). The association is considered statistically significant when the P value is ≤ 0.05. For multiple SNPs comparisons, Bonferroni correction was applied by multiplying the P value by the number of SNPs.

2.13.2 Other comparisons

For continuous variables with normal distribution, student t-test or ANOVA test was used for comparison of two or three groups respectively. Continuous variables without normal distribution were analyzed using Mann-Whitney U test or Kruskal-Wallis test to compare the 2 or 3 groups respectively. Categorical variables were analyzed using Chi-square test. P value ≤ 0.05 was considered statistically significant. Correlations between acidification and proteolysis activity index were calculated by use of Spearman's rank correlation coefficient imputed by GraphPad Prism version 6.04 for Windows, (GraphPad Software, La Jolla California USA, www.graphpad.com).

2.13.3 Graphs

Graphs were generated using GraphPad Prism version 6.04 (www.graphpad.com) or R program, version 3.3.1 (https://www.r-project.org/).

Chapter 3

DEVELOPMENT AND EVALUATION OF INTRACELLULAR ASSAYS TO MEASURE MACROPHAGE ANTIMICROBIAL ACTIVITIES

3.1 Introduction

Macrophages play a central role in innate immunity via the phagocytosis process that is initiated by recognizing and internalizing the invading pathogen into its phagosome. The recognition can be promoted either directly by utilizing conserved structures on the pathogen surface, such as LPS or peptidoglycan, or indirectly by opsonization of the pathogen with serum complement, and immunoglobulins[203]. Once formed after pathogen engulfment, the phagosome undergoes a process termed maturation, in which both its membrane and lumen contents were modified by the means of fission and fusion with other cellular compartments[203]. During this process, phagosome develops into a toxic environment by acidifying, acquiring a range of hydrolytic enzymes and producing toxic radical compounds. Phagosome acidification is prerequisite to optimal function of hydrolytic enzyme and degradation of phagosomal content. Furthermore, acidic pH establishes a hostile environment for an internalized pathogen. Acidification commences early in phagosome maturation and predominantly results from recruitment of V-ATPase to the phagosomal membrane. The hydrolytic enzymes can directly kill bacteria by interrupting the integrity of mycobacterium membrane but also help in degrading the pathogen. Antigen generated from such degradation is presented to T lymphocyte via MHC class II molecule, bridging the innate and adaptive immunity.

It is reported that an impairment in phagocytic capacity of macrophages could lead to the development of several pulmonary diseases that are caused by *Haemophilus influenza*, *Streptococcus pneumoniae*[282,283,284], or *Coxiella burnetii*[285]. Several professional intracellular bacteria such as *Mtb, Listeria monocytogenes*, and *Legionella pneumophila* have evolved the mechanisms to avoid phagosome maturation, so that bacteria can replicate within macrophage and establish the infection[203]. It is likely that

the outcome of infection depends on the innate interaction between bacteria and macrophage[286]; any defects in the phagosomal function of macrophage could have major impact on the establishment of the infection. Therefore, it is important to assess the macrophage phagosomal function, which may help to understand not only the contribution of macrophage in host defense and susceptibility to the disease but also the macrophage manipulation by the pathogen.

Many assays have been developed to examine the phagosome maturation within macrophages. Most approaches use immunofluorescence colocalization with well-characterized markers[285,287,288,289]. The most common markers are Ras-related proteins (Rab5 or Rab7 for early and late endosomal markers), LAMP-1, LAMP-2 (phagosomal markers), and Cathepsin D (lysosomal marker). The expression of these markers in a compartment indicates how aggressive this compartment might be towards an invading microbe. These methods have been widely used, however they are very subjective, have low sensitivity and do not completely reflect the environment within the phagosome [205,290].

To overcome these disadvantages, Russell and colleagues have developed the platform of different assays to measure directly and quantitatively functionally-relevant parameters of phagosomal luminal biology, allowing researchers to design their own experiments to address the interesting biological questions on phagosomal maturation in response to microbial infection[271,273,275,291]. These assays exploit the model of beads coated with microbe-derived ligands that facilitate particle uptake and also mimic the conditions of infection *in vivo*. Different phagosomal activities in live macrophages can be quantified using specific fluorogenic substrates that are coated on the particles. For example, pH-sensitive fluorochromes such as CF-SE or Oregon Green can be used to

access phagosomal acidification while DQ-BSA that is highly sensitive to the digestion of various proteases is used to detect the proteolysis. The fluorescent output can be assessed on different analytical platforms, including (i) flow cytometry, (ii) confocal microscopy, and (iii) fluorescence microplate; each has both strengths and limitations. The flow cytometry provides detail at individual cell level within and between cell populations. Visualization by microscope provides excellent spatial and temporal details at the level of single phagosome. These methods are time-consuming, lacking statistical power, and only handle limited experiment conditions at a time; whereas the microplate reader can allow monitoring of multiple conditions with many replicates. Depending on the research question and the existing infrastructure, single platforms can be used or different platforms can be combined to complement one another for speed, sensitivity, and resolution[271].

The efficiency of phagosomal functions of macrophages could be also evaluated by measuring the bacterial killing ability of macrophages upon infection[292]; hence counting the viable bacterial numbers becomes an important read-out for the host response. Viable bacteria have the capacity to form colonies, hence the most commonly used method for measuring the viable bacterial numbers after infection is by plating and culturing defined volumes of lysed cells followed by the counting of colony-forming units (CFU) on agar plates. To analyze colony-forming units, bacteria need to replicate multiple times before colonies start to appear. However, this becomes a major drawback when studying very slow-growing bacteria such as *Mtb*, since it takes 2-3 weeks for a colony of *Mtb* to appear. Furthermore, CFU plating is rather labor-intensive and it is difficult to handle a large number of samples. Therefore, fluorescent reporter strains of

bacteria can be used as a valuable alternative tool in intracellular growth studies because of rapid detection, high sensitivity and real time detection[276].

In order to study the association of macrophage phagosomal functions and susceptibility to TB disease, in this chapter I generated the beads and established the bead-based assays to measure the macrophages' activities including phagocytosis (uptake ability), acidification and bulk proteolysis. I also generated the *Mtb* reporter strain that expresses fluorescent protein mCherry to study the outcome of interaction between macrophages and bacteria to measure the bacterial survival.

3.2 Results

3.2.1 Generation of beads for assays measuring macrophage antimicrobial activities

The resting macrophage plays vital homeostatic roles, including daily clearance of erythrocytes and removal of tissue debris or apoptosed cells; such processes occur quietly with little or no production of cytokines[275]. When macrophages are classically activated by immunogenic components from the pathogen or by IFN-ɣ, the cells function as immune effectors which have enhanced microbicidal activities and antigen presentation. These immune responses are accompanied with the induced inflammatory signals[275,293]. In an attempt to study the phagosomal functions of macrophages in response to *Mtb* infection, I have adapted the bead construction from the Russell group for our purposes. The beads are principally coated with three components, including a fluorogenic substrate, a fluorophore of calibration, and a ligand (see Section 2.6). However to study macrophage antimicrobial activities regarding different signaling pathways, I modified the beads by coating them separately with two ligands including TDM from *Mtb* and β-glucan from yeast that are recognized by scavenger receptor[294]

and C-type lectin[36,295] respectively. IgG-coated beads are used to assess macrophages activities in resting state.

Following the instructions (see section 2.6), the beads were incubated in an excess of IgG, TDM and β-glucan that ensure the coating of these ligands on the bead surface[244]. To examine coating efficiency of components on the beads, fluorogenic substrate and fluorophore of calibration were analysed by flow cytometry. For phagocytosis beads, I observed a complete shift toward the higher fluorescence signal of ligands-beads coated with Alexa 594 SE compared to the control uncoated bead (Figure 3.1A), indicating that the phagocytosis beads were successfully coated. The proteolysis beads exhibited the signal of proteolysis substrate DQ-BSA (FITC) and signal of the calibrator (Alexa 594) in comparison with the control uncoated beads, indicating the successful attachment of these components to the proteolysis beads (Figure 3.1B). Likewise, the acidification beads were completely coated with fluorogenic carboxylated-SE indicated by increased FITC signal on the bead surface (Figure 3.1C).

Next, I tested the consistency of the assays exploiting the beads generated above. I used J774 murine macrophages for this purpose since cell lines are genetically stable and easy to handle. The flow cytometry was used to examine the phagocytosis while the microplate reader was used to measure the proteolysis and acidification.

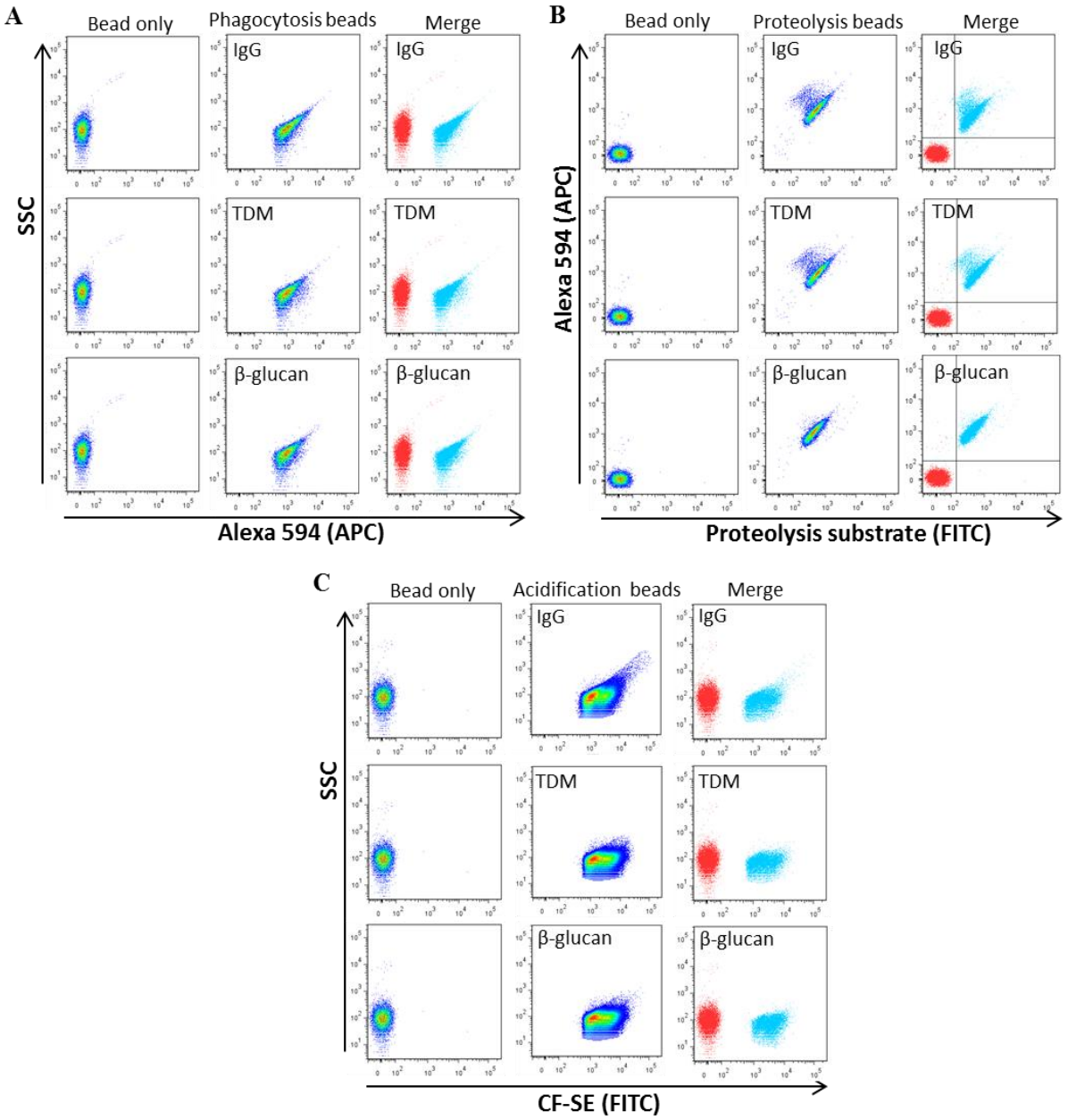

Figure 3.1 Cytometry analysis of phagocytosis, proteolysis and acidification beads
(A) Phagocytosis beads are beads coated with a ligand including IgG, TDM or β-glucan and Alexa 594 SE dye. The dots represent beads only or phagocytosis beads, and were plotted against side-scattered light (SSC) and APC channel for Alexa 594. (B) Proteolysis beads are beads coated with a ligand, proteolysis substrate and calibrator Alexa 594 SE. The dots represent beads only or proteolysis beads, and were plotted against APC channel (for Alexa 594) and FITC channel (for proteolysis substrate). (C) Acidification beads are beads coated with a ligand and CF-SE. The dots represent beads only or acidification beads, and were plotted against SSC and FITC channel for acidification indicator CF-SE.

3.2.2 Evaluation of consistency in phagocytosis assay

Previous studies that exploit bead-based assay to measure macrophage activities by flow cytometry have revealed that the phagocytosis by macrophages occurs efficiently during 10 min after adding of beads so that the change of macrophage phagosomal activities can be easily assessed[274,275]. Therefore, in this study I also examined the phagocytosis (bead uptake) of J774 macrophages at 10 min after feeding the cells with phagocytosis beads at the concentration of 1-2 beads per cell[244]. As shown in Figure 3.2A, flow cytometry of cells treated with beads revealed two discriminated populations. By comparing with un-treated J774 (negative signal for Alexa 594) and phagocytosis beads alone (positive signal for Alexa 594), the population of J774 that was positive for Alexa 594 SE was considered as population of cells that phagocytose the beads. The phagocytosis ability of J774 macrophage was indicated by the proportion of this cell population. After 10 min of bead incubation, approximately 92.5% ± 2.1% of cells phagocytosed the IgG beads, 88.2% ± 2.7 % of cells phagocytosed the TDM beads and 86.9% ± 4.0 % of cells phagocytosed the β-glucan beads (Figure 3.2B). These results were averaged from three repeated experiments; the SD was small, indicating the consistency of the assay. There was no significant difference in the phagocytosis ability of J774 in response to IgG, TDM or β-glucan beads ($P = 0.17$).

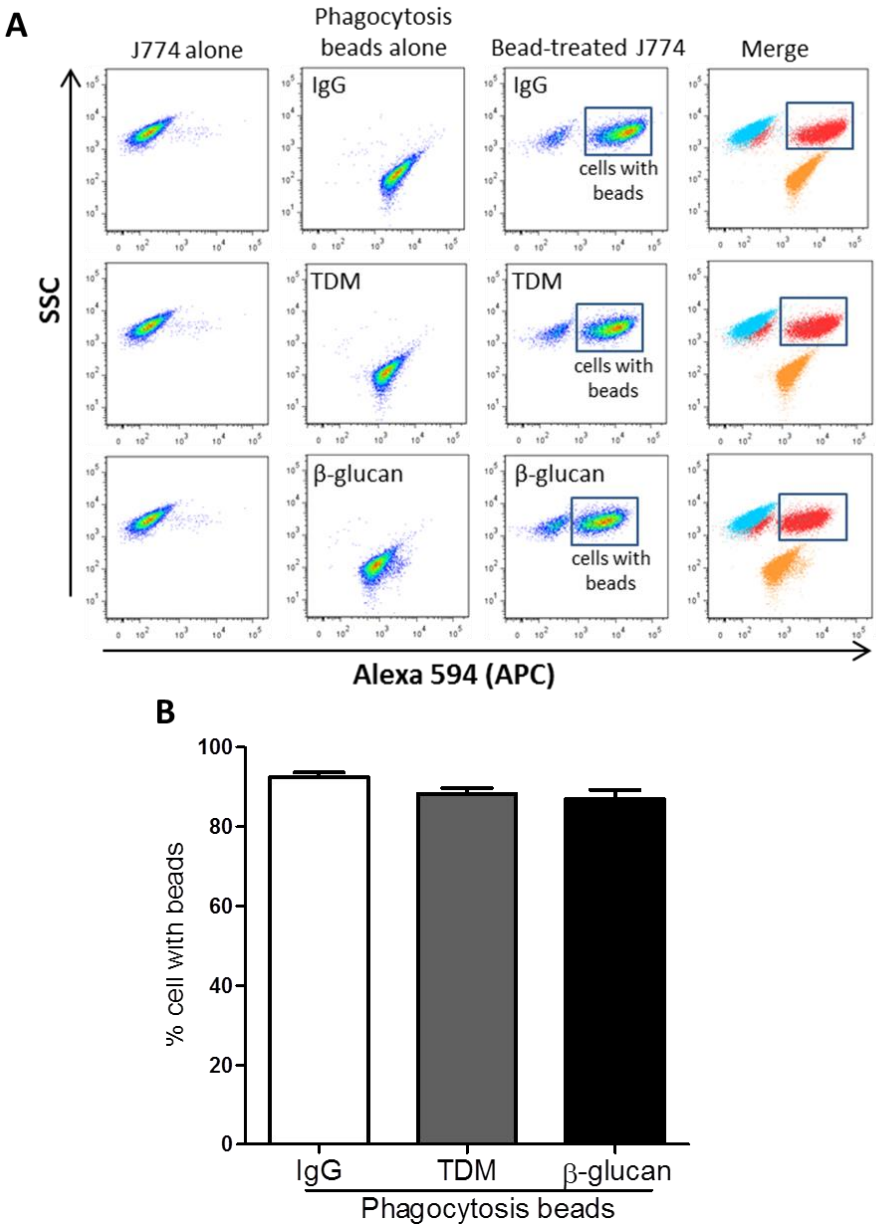

Figure 3.2 Phagocytosis assays in J774 murine macrophages

J774 cells were treated with Alexa 594 beads coated with either IgG, TDM or β-glucan and phagocytosis was assessed by flow cytometry. (A) Signals of Alexa 594 (detected by APC channel) were plotted against SSC. The dots represent J774 cells alone, phagocytosis beads alone or J774 treated with beads. The phagocytosis ability was determined by the percentage of J774 positive with Alexa 594 dye (gated cells and named "cell with beads"). (B) Proportion of J774 cells phagocytosed beads. Data are mean ± standard deviation (SD) from 3 independent experiments. P value was determined using Kruskal-Wallis test for comparison across three groups.

In the phagocytosis assay, the phagocytosis ability of macrophages was identified by the percent of cells positive for Alexa 594 after 10 min of bead treatment. This method could be argued to not distinguish the fluorescent signal produced by beads attached to the cell surface from that produced by bead ingestion (phagocytosis). However, the unbound or loosely attached beads were removed by washing the cells three times before harvesting for the analysis. The bead location was then verified using phase contrast microscope, and I found that the majority of the beads were engulfed after 10 min. Our observation was further confirmed by little increase in population of cells positive with Alexa 594 when I examined the phagocytosis of macrophages after 30 min of bead treatment (10 min vs. 30 min: 90- 93 % vs. 90.4- 94.6 % (IgG beads), 85-91 % vs. 85.5- 90.9 % (TDM beads), 82- 90 % vs. 82.9- 90.9 % (β-glucan beads)). The uptake of beads after 10 min of bead treatment was further examined by proteolysis assay to measure the proteolysis of macrophage following the bead uptake using flow cytometry. In this assay, after 10 min of incubation to allow bead uptake, the unbound beads were washed three times and proteolysis of macrophage was examined at 180 min later (Figure 3.3). The percentage of cells with beads (that were positive with Alexa 594) after 10 min and 180 min were not much different (88 % vs. 86 %), indicating that beads were ingested early at 10 min. The increase in FITC fluorescent intensity after 180 min (Figure 3.3) once again added more evidence for beads ingestion after 10 min, since the signal was only produced when the beads were internalized into the phagosome and the fluorogenic substrate coated on the beads were cleaved by proteases there.

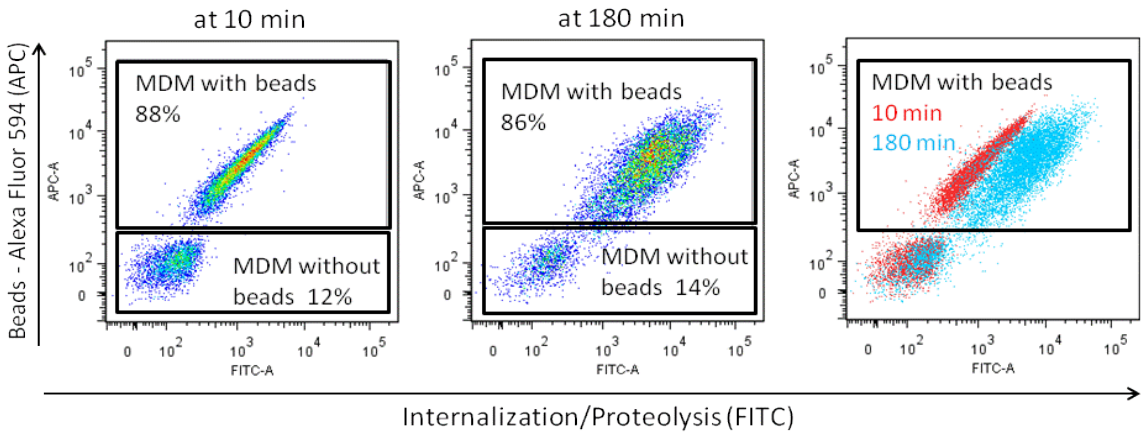

Figure 3.3 Assessment of hMDM for phagocytosis and proteolysis by flow cytometric analysis

Beads were coated with (1) Alexa Fluor 594 [y axis] and (2) DQ Green BSA substrate (Molecular Probes) [x axis]. Bright green fluorescence is achieved when beads are internalized by hMDM and DQ Green BSA substrate is cleaved by proteolysis to release green fluorescent protein fragments. hMDM were incubated with beads for 10 minutes to allow uptake, then the cells were washed three times to remove loosely attached or unbound beads. Green fluorescence was measured at early (10 minutes) and late (180 minutes) time points.

Since I wanted to study the phagocytosis ability of macrophages from individuals with different TB outcomes, I next examined whether the phagocytosis assays worked in hMDM model. hMDM from three independent healthy volunteers were fed with phagocytosis beads coated with either IgG, TDM or β-glucan. Proportions of macrophages phagocytosed the beads were ~ 95% for IgG, 75- 80 % for TDM and ~ 80 % for β-glucan beads (Figure 3.4). I also observed small variations in phagocytosis ability of macrophages from different individuals, especially in response to TDM coated beads.

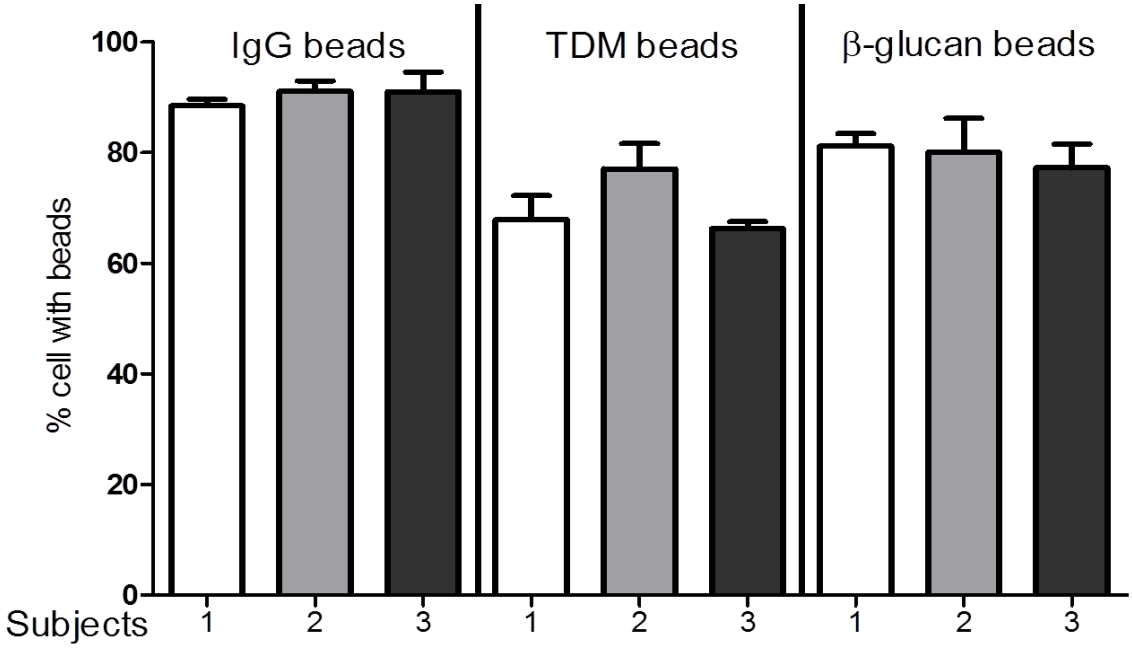

Figure 3.4 Phagocytosis in hMDM

hMDM from 3 independent healthy volunteers were treated with phagocytosis beads. Phagocytosis ability was indicated by percentage of cells with beads via flow cytometry analysis. Data are mean and ± SD of triplicated wells.

3.2.3 Evaluation of acidification assay in macrophages

Microplate reader allows many samples to be simultaneously measured with many replicates which help to increase the accuracy of the measurement; hence I used microplate reader to measure acidification and proteolysis of macrophages from TB patients and LTB in different experimental conditions simultaneously. At first, I examined the stability and consistency of acidification assay using microplate reader.

J774 murine macrophages were treated with the acidification beads at a concentration of 4 beads per macrophage as per previous study[239]; the pH change in the phagosomal lumen was measured in real-time during 90 min. The relative pH in phagosome was expressed by the ratio of fluorescent intensity at pH-sensitive and -insensitive wavelengths, with a decreased ratio indicating a drop in pH (Figure 3.5A). Conversion

from the fluorescent ratio value to pH could be achieved through polynomial regression of a standard curve generated by the calculation of the fluorescent ratio in environments of known pH (Figure 3.5B). In macrophages treated with beads, pH reduced significantly within an hour from pH 6.9 to 5.5, and had slightly changed afterwards (Figure 3.5A). To compare acidification activity, I used an activity index that was the ratio of relative pH at early time point of 10 min (when most of the macrophages phagocytosed beads) over that at time-points of interest. After 30 min of bead treatment, or later time points of 60 or 90 min, I did not observe any difference in acidification capacity among J774 mouse macrophages treated with IgG- and TDM- and b-glucan-coated beads (Kruskal-Wallis test, 30 min: P= 0.19, 60 min: P= 0.73, and 90 min: P= 0.73) (Figure 3.5C). These experiments were repeated three times independently and the results were similar, which confirmed the consistency of the assays.

I next examined the acidification assay in an hMDM model. hMDM from three independent healthy volunteers were treated with acidification beads coated with either IgG, TDM or β-glucan. As in J774 macrophages, bead-treated hMDM from all three subjects showed a decreased phagosomal pH by time and the bead-containing phagosomes were acidified completely after 60 min of bead treatment (Figure 3.6 A, C, E). Consistently, by calculating the activity index, I observed an increased activity at 60 min and 90 min compared to 30 min in bead-treated macrophages from all three subjects (Figure 3.6 B, D, F). For example, from subject 1 the activities at 30 min, 60 min, and 90 min in IgG-treated macrophages were 1.087 ± 0.016, 1.183 ± 0.016 and 1.209 ± 0.028 respectively.

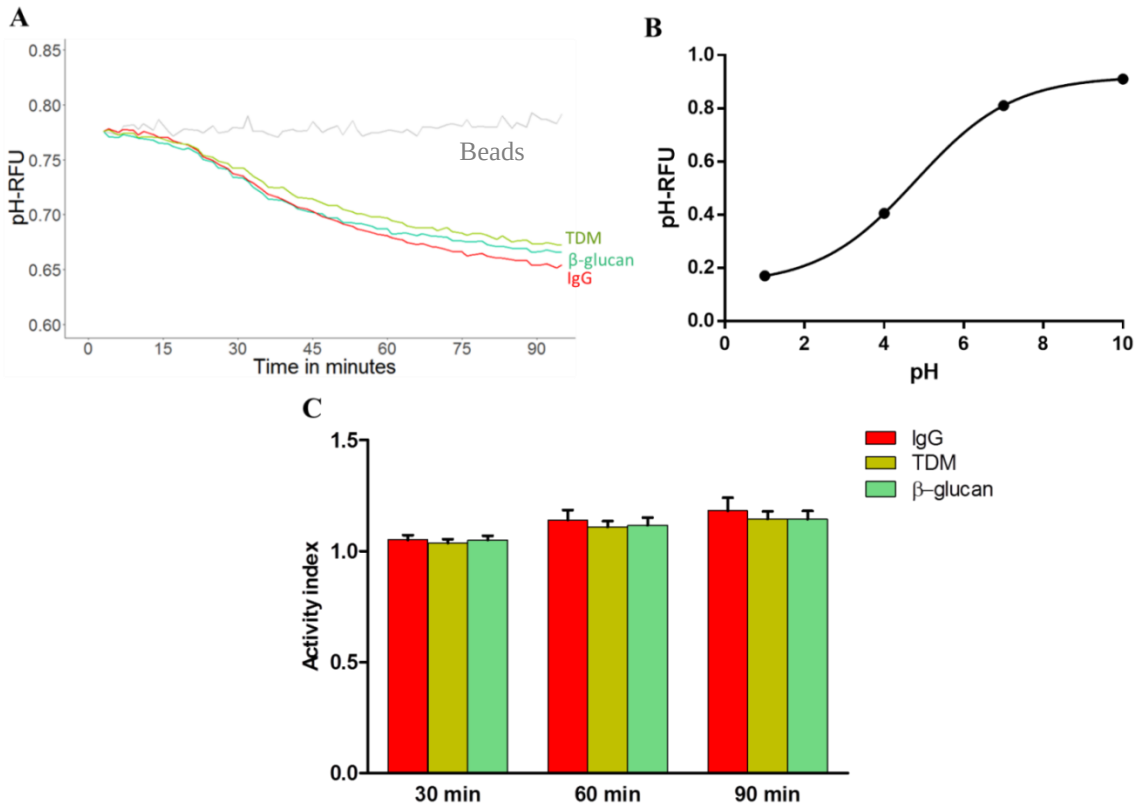

Figure 3.5 Acidification activity of J774 murine macrophages

Macrophages were treated with acidification beads coated with either IgG, TDM or β-glucan. (A) The kinetics of phagosomal pH, plotted as the ratio of fluorescence emitted at 520 nm upon excitation wavelengths of 490 nm and 450 nm. Bead: pH beads in assay buffer without macrophages. (B) The relationship of fluorescent ratio and pH of acidification beads when beads were added in standard pH solutions. (C) Acidification activity index of macrophages at selected time points 30, 60 and 90 minutes, calculated by the ratio of relative fluorescent unit (RFU) at 10 min over RFU at 30, 60 or 90 min. The data in (C) were expressed as the mean ± (SD) from 3 independent experiments. P value was determined using Kruskal-Wallis test for comparison across three groups. At 30 min, P= 0.19; at 60 min, P= 0.73; at 90 min, P= 0.56.

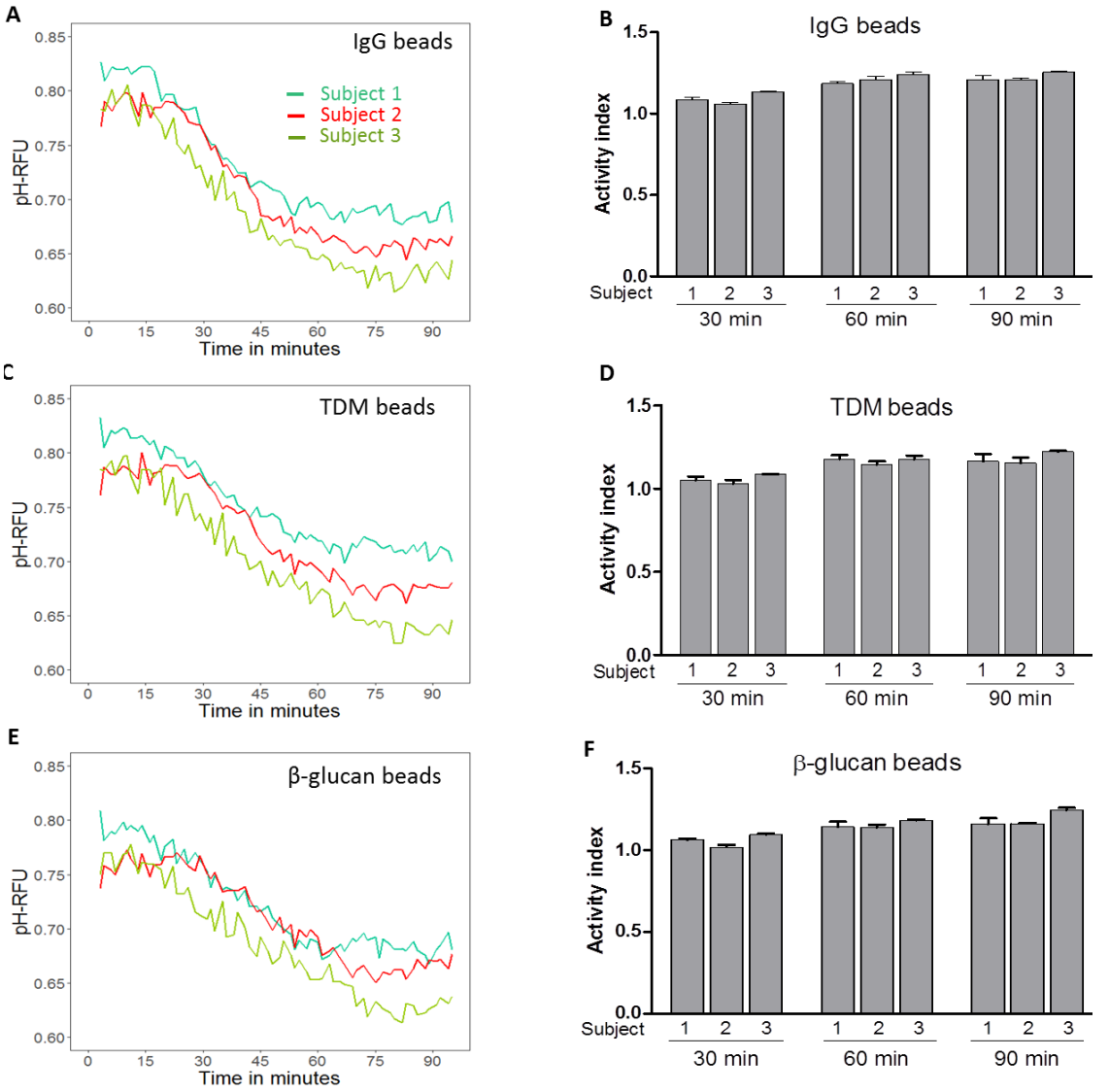

Figure 3.6 Phagosomal pH in hMDM

hMDM macrophages from 3 independent healthy volunteers were treated with acidification beads coated with either IgG, TDM or β-glucan. (A, C, E) The kinetics of phagosomal pH was plotted as the ratio of fluorescence emitted at 520 nm upon excitation with wavelengths of 490 nm and 450 nm. (B, D, F) Acidification activity index of hMDM, that was calculated by the ratio of relative fluorescent unit (RFU) at 10 min over RFU at 30, 60 or 90 min. The data were expressed as the mean ± SD from triplicated wells.

3.2.4 Evaluation of proteolysis assay in macrophages

To measure the proteolytic activity, ligand beads coated with fluorogenic substrate DQ green BSA were added to J774 macrophages at 4 beads per macrophage. The increase in fluorescence generated by cleavage of substrate indicated the more proteolytic activity. Macrophages treated with beads showed an acquisition of proteolysis at 40-50 min, followed by an increase in activity (Figure 3.7A). To compare the proteolysis in response to different ligand coated beads, I then calculated the activity index that was the ratio of proteolysis at time-points of interest over early time point of 10 min when most of macrophages had phagocytosed the beads. J774 macrophage treated with TDM and β-glucan beads showed a decrease in proteolytic activity index at 60 min or afterwards after bead treatment compared to resting macrophages treated with IgG beads (Kruskal-Wallis test, P= 0.05, 0.03, 0.03, 0.03 at 60, 120, 180 and 210 min respectively) (Figure 3.7B). The macrophage treated with TDM-coated beads showed the lower activity compared to macrophage treated with β-glucan beads (paired t-test, P = 0.01, 0.01. 0.01, and 0.02 at 60, 120, 180 and 210 min) (Figure 3.7B), suggesting the pathway-dependent variation of cell proteolysis. These experiments were repeated three times independently and the results were similar, indicating a consistent tendency in proteolytic activity.

As with other assays, I also examined the proteolysis beads in the hMDM models. hMDM from three independent healthy volunteers were treated with proteolysis beads coated with either IgG, TDM or β-glucan. There was an increased proteolysis in bead-treated hMDM from all three subjects (Figure 3.8A, C, and E), indicating the proteolysis assays also worked in hMDM. Variations in the activity of hMDM from 3 donors at 180 min or 210 min (IgG, subject 1: 14.760 ± 0.450, subject 2: 16.520 ±

0.484, and subject 3: 20.296 ± 4.660; TDM, subject 1: 14.250 ± 0.987, subject 2: 14.220 ± 0.920, and subject 3: 21.700 ± 5.680; and β-glucan, subject 1: 15.045 ± 0.234, subject 2: 14.511 ± 1.376, and subject 3: 26.440 ± 0.511) suggested a possible diversity activity among individuals (Figure 3.8B, D, F).

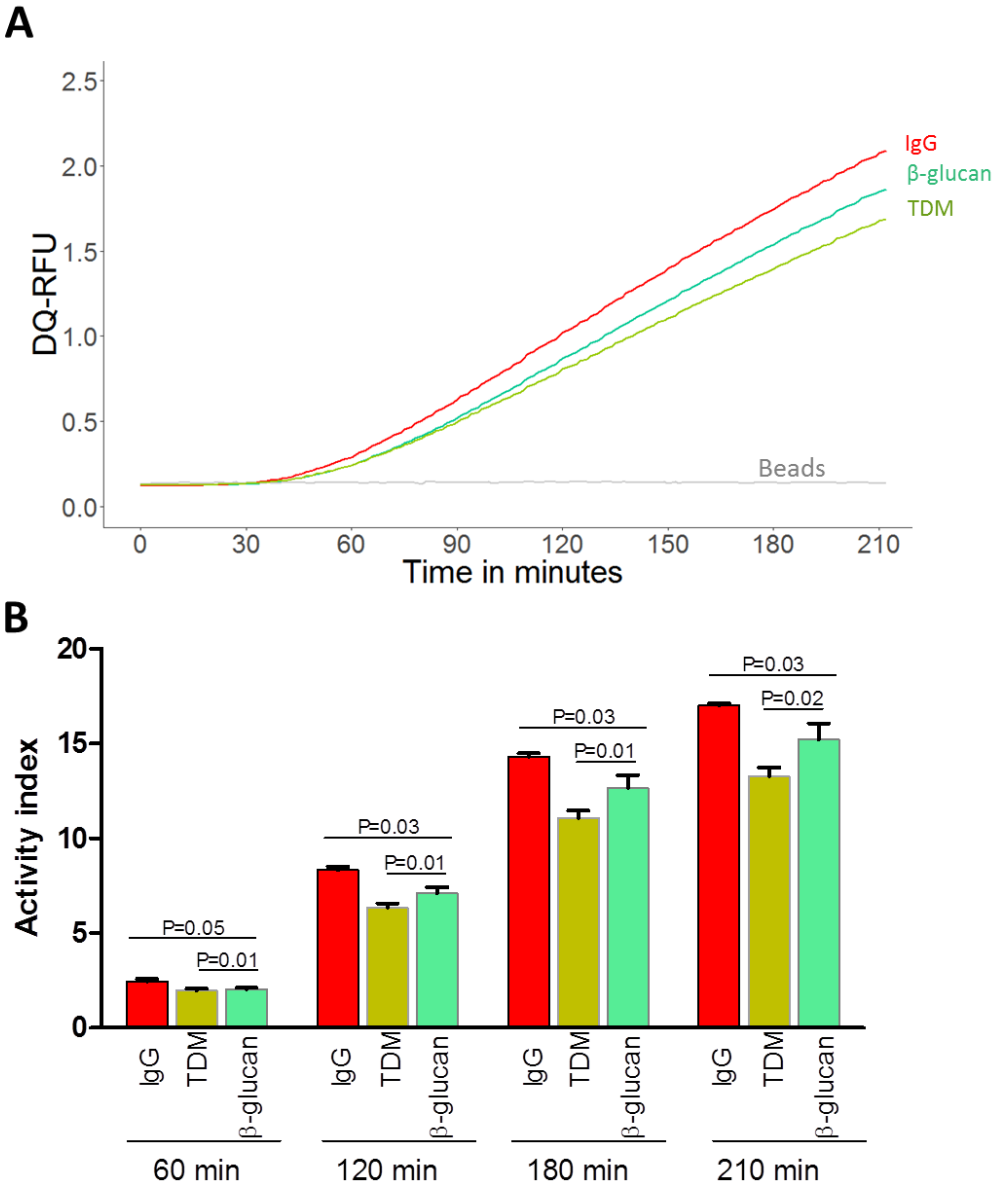

Figure 3.7 Proteolytic activity of J774 murine macrophages

J774 macrophages were treated with proteolytic beads coated with either IgG, TDM or β-glucan. (A) The kinetics of proteolysis, plotted as the ratio of DQ-BSA green fluorescence and calibration fluorescence. Beads: beads in assay buffer without macrophages. (B) Proteolysis activity index at different time-points, which was generated from (A). Activity index was calculated by the ratio of RFU at 60, 120, 180, or 210 min over RFU at 10 min. The data in (B) were expressed as the mean ± SD from 3 independent experiments. P value was determined using Kruskal-Wallis test for comparison across three groups or paired t-test for comparisons two groups of TDM and β-glucan.

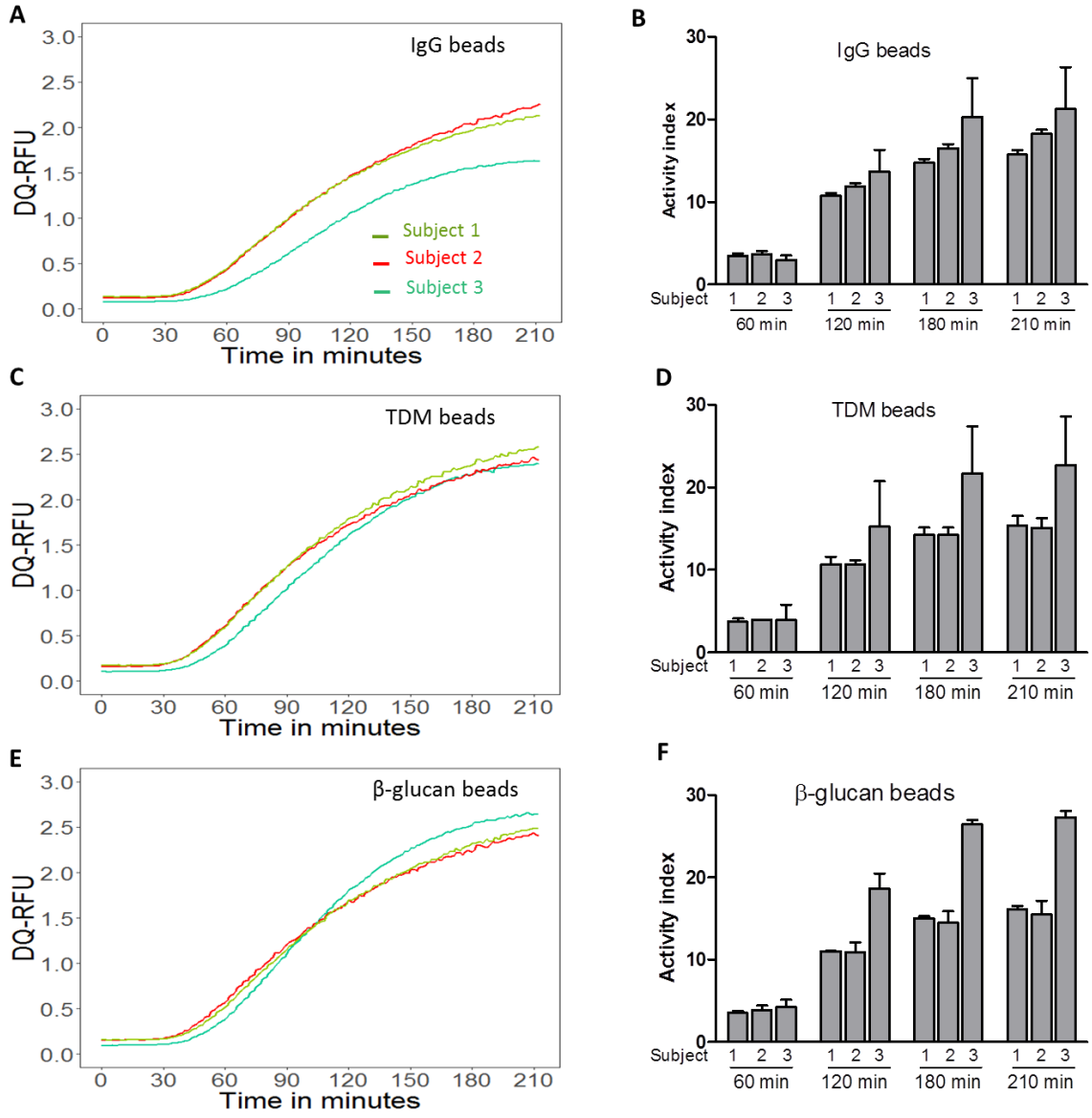

Figure 3.8 Proteolysis in hMDM

hMDM macrophages from 3 independent healthy volunteers were treated with acidification beads coated with either IgG, TDM or β-glucan. (A, C, E). The kinetics of proteolysis, plotted as the ratio of DQ-BSA green fluorescence and calibration fluorescence. (B, D, F) Proteolysis activity index of hMDM. The data were expressed as the mean ± SD from triplicate wells.

3.2.5 Mycobacterial killing capacity of macrophages

To study the variations in *Mtb* killing capacity of macrophages from patients with different TB phenotypes, I generated *Mtb* reporter strain expressing fluorescent protein so that the intracellular growth of bacteria could be assessed by the fluorescent intensity. mCherry is very bright, shows no photobleaching, being stable during continuous excitation[276,296] and tolerant to acidic pH[297]. Due to the acidic environment within phagosome, this fluorescence is an optimal option for constructing intracellular bacteria expressing fluorescence. *Mtb* Beijing strain is known to have high prevalence in Vietnam. In this study, I used a clinical Beijing strain isolated from a TB patient to investigate the interaction between bacteria and macrophages. The mCherry plasmid was transformed to this *Mtb* strain. As described previously[276], the strains bearing mCherry were shown to bear no defect in growth or virulence (data not shown). To examine whether mCherry could be used as an indicator for intracellular bacterial growth, I firstly tested the correlation of mCherry fluorescence and bacterial viability. The bacterial culture was serially diluted 2-fold and the fluorescent intensity of mCherry was measured at emission wavelength of 620 nm when excited at 575 nm using microplate reader. I found that there is a linear correlation between intensity of mCherry and bacterial cell density with a goodness-of -fit value R^2 of 0.9994 (Figure. 3.9A). The fluorescence was still measurable at mycobacterial cell density as low as $4x10^5$ cells (OD_{600} = 0.015). By quantifying CFUs per volume unit of bacteria, our data showed that optical density was likely to be correlated with the number of viable bacteria in linear regression with a R^2 value of 0.9043 (Figure. 3.9B). Altogether, these results demonstrated that the fluorescent intensity of mCherry could be used to measure the number of viable bacteria.

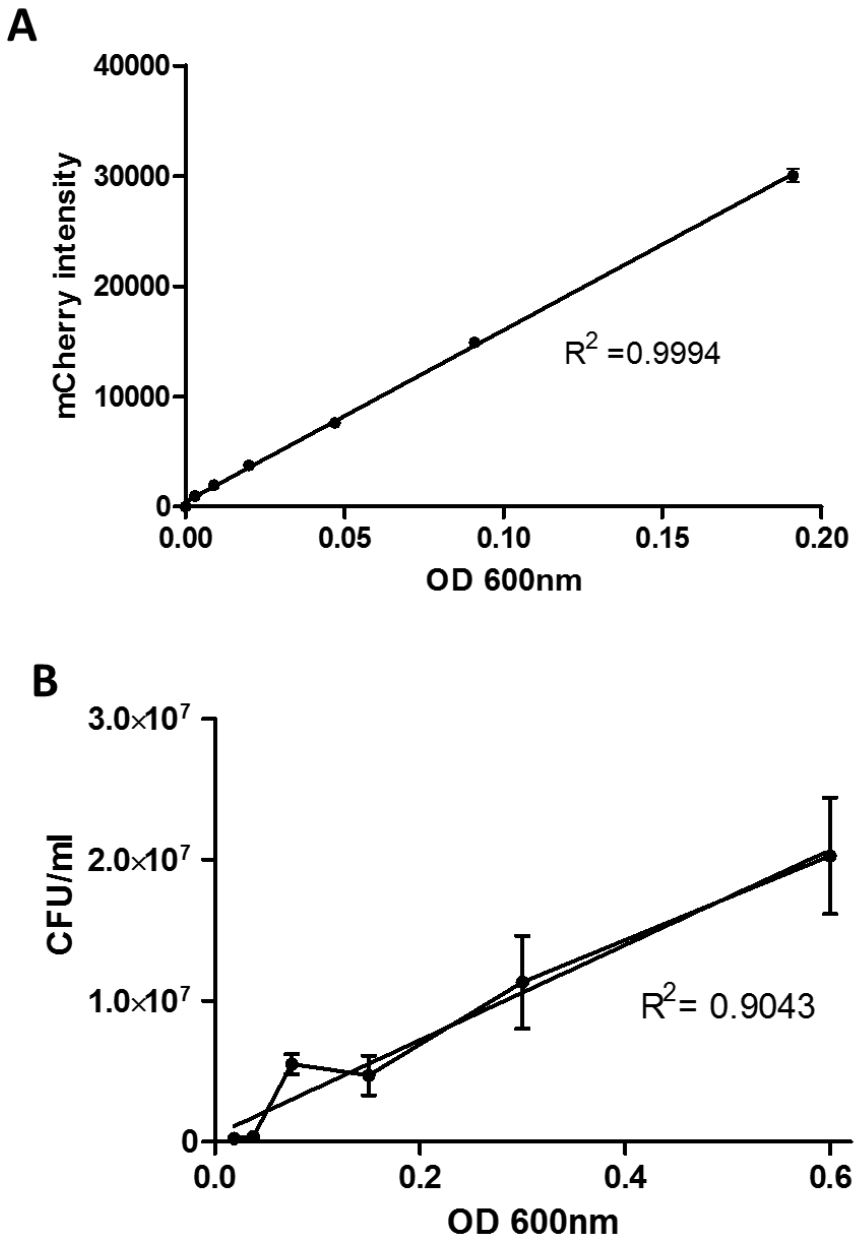

Figure 3.9 mCherry fluorescence and *Mtb* viability

(A) Correlation of fluorescent intensity and bacterial number. (B) Correlation of optical density and the number of viable bacteria. Data were mean and ± SD of triplicated wells.

The infection of murine macrophage with virulent *Mtb* commonly leads to the necrosis-like death of infected cell[260]; cells first swell, and then the cell membrane collapses and cells are rapidly lysed[298]. In this study, I assessed the lysis of infected cells by examining the cell lysed under conventional microscopy. To investigate the interaction

between bacteria and macrophages through bacterial growth and macrophage lysis, I infected mouse J774 and human THP1 macrophages with the *Mtb* reporter strain at different MOI of 1, 2, and 3. The intracellular growth of bacteria was assessed by the increase of fluorescence intensity of mCherry over time and the time-point when macrophage lysis occurred was noticed. Infection of macrophages with *Mtb* at different MOI resulted in variations in bacterial intracellular growth and the fate of infected cells. When J774 macrophages were infected with *Mtb* at MOI 1, the bacteria replicated slowly and infected macrophages still remained viable during 5 days post infection; whereas infection at higher MOI resulted in rapid bacterial replication and cell lysis (Figure 3.10A). The two times increase of mCherry intensity in macrophages infected with *Mtb* at MOI 2 in comparison to that in macrophages infected at MOI 1 suggested the double number of intracellular bacteria in macrophage infected at MOI 2, which may also resulted in the commencement of cell lysis at day 4. Infection at MOI 3 resulted in effective bacterial replication that killed cells very early at day 2 (Figure 3.10A). Similar scenarios were observed in THP1 human macrophage infected with *Mtb* (Figure 3.10B). There was a rapid increase in bacterial number overtime in cells infected with *Mtb* at MOI 2 and 3 while a slow increase in bacterial number was seen in those infected at MOI 1. Cell death occurred rapidly in infected human cell lines that could be observed at day 1 after infection at MOI 3, at day 2 at MOI 2 and day 3 at MOI 1 (Figure 3.10B). These results were reproducible for three independent experiments. Infection of murine and human cell lines suggested that the susceptibility of these cell lines to *Mtb* is different, with THP1 being more susceptible than J774. As MOI 1 did not cause cell lysed in short period of time like other higher MOI, which allowed us to

study the host-bacterial interaction over a long time period, I decided to infect macrophages with bacteria at MOI 1 for further infection experiments.

I then tested the killing capacity of hMDM from several healthy subjects by infecting macrophages with *Mtb* reporter strain at MOI 1 for 5 days (Figure 3.10C). I observed variations in the mCherry intensity from inoculation of *Mtb*-infected hMDM from different subjects, with hMDM from subject 1 being highest and subject 2 being lowest. The lysis of infected macrophages from subject 1 and 3 occurred at day 3 while it occurred at day 5 for subject 2. Altogether, these results suggested the variations in the killing capacity of human macrophages from different individuals.

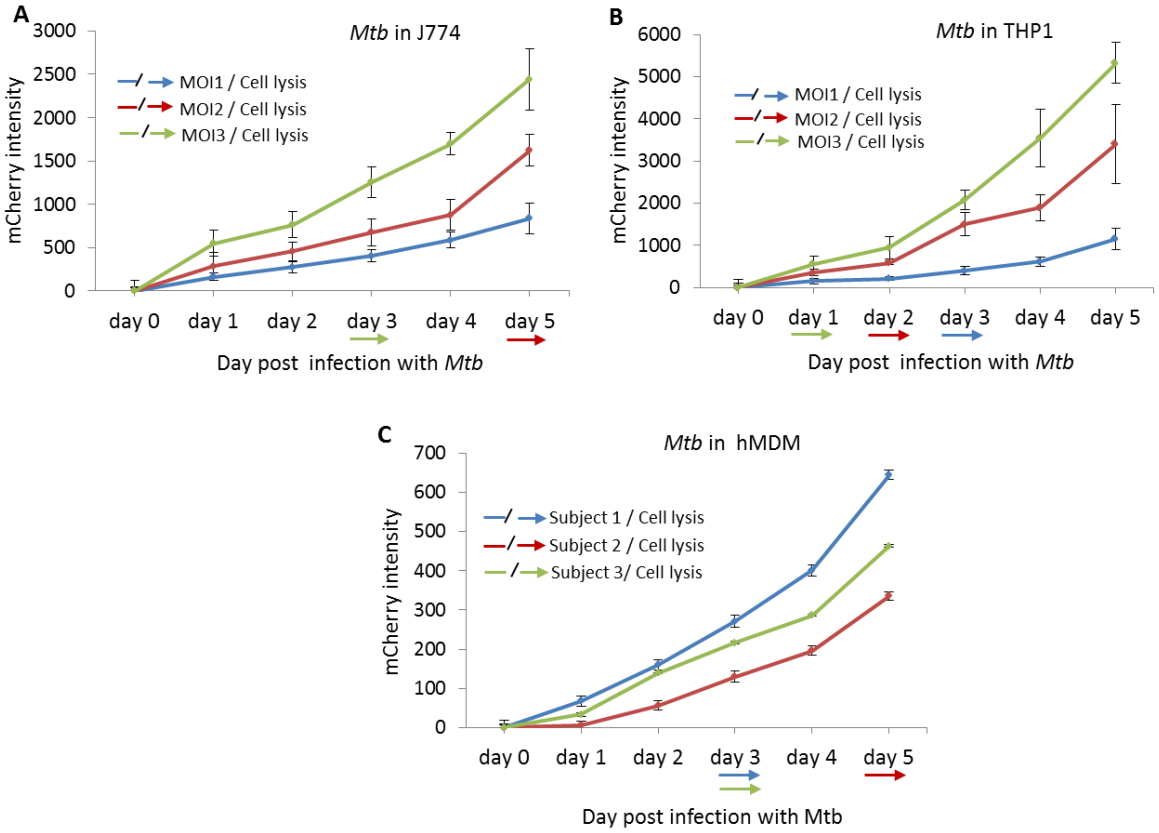

Figure 3.10 Intracellular replication of *Mtb* strain in macrophages

Mouse J774, human THP1 macrophages and hMDM were infected with *Mtb* expressing mCherry for 5 days. The growth of bacteria was assessed by the fluorescent intensity of mCherry that was measured every day using microplate reader. (A, B and C) The intracellular growth curves of bacterial infection with J774 cells (A) and THP1 cells (B) at MOI of 1, 2, and 3. (C) The intracellular growth curve of bacteria in infected hMDM from 3 individuals at MOI 1. The figures showed the mean and ± SD of fluorescence intensity from 4 repeated wells. The arrow indicated the day when the cell lysis occurred.

3.3 Discussion

In this chapter I established the bead-based assays to measure the phagocytosis ability of macrophage as well as its antimicrobial activities including acidification and proteolysis. At first I successfully generated the beads coated with ligands and substrates specific for assays of interest. I then exploited the stability of macrophage cell

line to use it as a model to set up and optimize the bead-based assays. In such models, the assays were shown to work well giving consistent results. I observed the decrease in phagosomal pH and the occurrence of proteolysis in macrophage treated with beads. I found that stimulation of macrophages with TDM or β-glucan led to a significantly decreases in proteolytic activities in comparison to resting macrophage. Interaction between macrophages and bacteria could be investigated by infection of macrophages with *Mtb* expressing mCherry. Our assays also worked in the hMDM model which displayed variations in antimicrobial activities of macrophages from different subjects. The bead-based assays were originally developed to study the physiological changes in phagosome of macrophage that can help to explain its plastic functions in both homeostasis and during immune response. Therefore, it is suggested that this new approach can be applied in clinical settings to identify the macrophage-associated pathologies[275,273,226,299]. The bead-based measurement of antimicrobial activities of AM in HIV patients have suggested the possible association of the impairment in AM activities and the increasing susceptibility to upper respiratory disease[274]. Furthermore, this new approach has helped to provide the insight to the global modification in hMDM activities in response to *Mtb* infection[239].

The beads used in these studies were only opsonized with IgG to facilitate the uptake by macrophages. It remains unclear whether different routes of entry into macrophages may lead to differences in subsequent events within the host such as signal transduction, immune activation, and intracellular survival of *Mtb* as well as outcome of infection[14]. The beads developed in our study were novel since they were coated with specific antigens such as TDM and β-glucan, which could further help us to dissect the

contribution of the signaling pathways specific for these ligands in controlling macrophage antimicrobial activities in response to *Mtb* infection.

By exploiting the beads labeled with pH-sensitive fluorochrome carboxyfluorescein SE, I have seen a rapid redution in phagosomal pH, which had been observed in previous studies[239], from neutral to 5.5 within 1 h in resting macrophage. The bulk protease activity of macrophages was assessed by the beads coupled with DQ green BSA. I observed an increase in fluorescence signal generated by degradation of this substrate overtime, indicating the occurrence of proteolysis in phagosome. J774 macrophages treated with TDM- or β-glucan- coated beads showed a reduced proteolysis activity compared with resting macrophage. The beads are coated with an excess amount of ligands (IgG/TDM or β-glucan) so that they are optimal for recognition and phagocytosis which is further indicated by the comparable phagocytic ability of macrophages towards IgG, TDM or β-glucan beads. Therefore, the variations in proteolysis activity of macrophages treated with different ligands-coated beads could come from the nature of ligands. Different ligands mediate their specific pathways that would induce different macrophage responses. The decreased activity in macrophages treated with TDM- or β-glucan beads was similar to that observed previously upon activation of macrophages with LPS[272]. These results suggest a shift in macrophage function from its role in homeostasis to the role in immunity. More clearly, the homeostatic function of macrophages is to remove dead cells or cell debris, hence their hydrolytic activity is programmed to occur with high efficiency for complete degradation of those materials. Whereas, under activation by cytokines or bacterial components the hydrolytic activity is reduced to ensure the balance of effectively killing

and efficient antigen processing for presenting to T cells. The consistency in our data and previous data also provided a validation for the reliability of our bead-based assays.

The *Mtb* strain expressing mCherry provided a sensitive and rapid tool in a study of macrophage-mycobacterial interaction. As other reporter *Mtb* strains generated in previous study, our strain showed a strong correlation between mCherry intensity and bacteria viability[276]. mCherry signal was very sensitive, so the signal could be detected at a very low cell density of *Mtb*. It has been revealed that the fate of *Mtb*-infected macrophage is different due to the intracellular burden of bacteria[300], cells with heavily burden progressing to necrosis. The reporter fluorescence in our study facilitated the assessment the correlation of intracellular growth of *Mtb* and the macrophage lysis when bacteria were infected to murine and human macrophage cell lines at different MOI. In consistent with the previous study[290], I also observed the rapid increase of intracellular *Mtb* growth at MOI 2 and 3 that leads to early host cell lysis in comparison to MOI 1 in both J774 and THP1 models. Because of slow bacterial growth and delay in host cell lysis, I propose that the infection of macrophage at MOI 1 is applicable for examining the host-pathogen interactions in detail.

In summary I have successfully established the assays to examine the phagosomal antimicrobial activities as well as killing ability of macrophages; these assays showed consistent results during experimental replications. In the next chapter, I apply these assays developed here to study the association of macrophage antimicrobial activities and different manifestations of TB.

Chapter 4

ASSOCIATION OF MACROPHAGE ANTIMICROBIAL ACTIVITIES AND OUTCOME OF *MTB* INFECTION

4.1 Introduction

Mtb is an intracellular bacterium whose infection leads to different scenarios and manifestations. One third of the human population is infected with *Mtb*, of which 5-10% develop TB within 2-5 years from first infection[301,302] and 90% of the remaining have latent TB that mostly lasts during the person's life time without any symptoms. The primary site of TB is in lung, however it can disseminate by the bloodstream to form extra-pulmonary TB in other organs. TBM is the most severe form, causing many deaths or neurological sequelae in survivors. The factors that lead to containment of infection or progression to the disease are multifactorial[303] and not well understood.

Alveolar macrophages in the lung are one of the first immune cell types to encounter *Mtb* when the bacilli are inhaled. After the bacterial recognition via various receptors on the surface, macrophages phagocytose the bacteria into the phagosome, which is central to its antimicrobial function. During a maturation process, the phagosome is acidified by recruitment of V-ATPases and sequentially fuses with multiple intra-vesicles. At the last stage of this endocytic pathway, the phagosome fuses with a lysosome to form a phago-lysosome which is well-known for antimicrobial properties. The environment inside this vesicle is very acidic, with pH of 4.5, and enriched with an assortment of endopeptidases, exopeptidases and hydrolases, which can kill bacteria and process antigens for presentation to T cells. Indeed, a previous study has shown the association between phagosomal acidification and *Mtb* growth restriction[290]. Inhibition of acidification or protease activity within the phagosome using V-ATPases or protease inhibitors, respectively, results in an increased *Mtb* replication[290]. An increased maturation of phagosomes in macrophages activated with IFN-ɣ leads to an efficiently mycobacterial killing[164,166,233,238].

Many previous works indicate that the phagosome maturation is modulated in *Mtb* infection[205,218,245,304,305]. *Mtb* prevents the incorporation of V-ATPases into the phagosomal membrane as well as the fusion of phagosome-lysosome. Therefore *Mtb* can reside in the phagosome with pH of 6.3 and low content of mature lysosomal hydrolases. These evasion mechanisms allow bacteria to replicate efficiently and subsequently to spread to other cells. As a consequence, active TB (ATB) may ensue. In contrast, *Mtb* strains that are defective in arresting acidification and phagosomal maturation have reduced intracellular growth[219,220]. The fact that *Mtb* develops evasion mechanisms to modulate the phagosome maturation for its survival and replication again emphasizes the importance of phagosomal function of macrophages in controlling *Mtb* infection.

Although macrophages have the capacity to defend the host early in the *Mtb* infection, how variation in their innate antimicrobial activity influences TB development has not been previously investigated. I hypothesized that the antimicrobial function of macrophages is associated with different TB clinical phenotypes. By using the bead-based assays developed in chapter 3, I assessed the phagocytosis, acidification and proteolytic activities of resting versus activated monocyte-derived macrophage from Vietnamese individuals with LTB or ATB. Ability of macrophages in killing *Mtb* was investigated in LTB and ATB by infecting macrophages with *Mtb* reporter strain as described in chapters 2 and 3.

4.2 Human subjects and study design

Individuals with LTB and ATB, comprising of PTB and TBM, were recruited to this study (Figure 4.1). TBM patients originated from a clinical trial conducted at HTD, HCMC, Vietnam from Sep 2014 to Feb 2016. PTB patients were recruited from two

District Tuberculosis Units (DTUs), HCMC from Jan 2015 to Feb 2016. The inclusion criteria for TBM and PTB were detailed in Section 2.1. To identify LTB, 99 healthy volunteers, who had no history of TB and were working at OUCRU, were screened for latent *Mtb* infection using T-SPOT.TB assays (see Section 2.4). 46 (46.5%) individuals were positive while 32 (32.3%) had negative results. The test scores of 21 (21.2%) individuals were borderline (see Section 2.4). Because of limited numbers of LTB subjects (n= 37) (others leave OUCRU), among those with borderline results, 8 people whose test scores were nearest to the positive cut-off (see Section 2.4) were recruited to the study in the LTB group (Figure 4.1). Finally, I recruited 45 LTB and 147 ATB subjects that included 70 with PTB and 77 with TBM. Among them, baseline data were missing for 13 individuals with LTB.

The demographics of subjects with LTB and ATB are described in Table 4.1. The majority of ATB patients were male (71.4%), with a median age of 43 (range 32-50) while LTB group had an equal male to female ratio, and were younger with a median age of 36 (range 32 - 42.5). ATB patients had a significantly higher absolute number of WBC, neutrophils and monocytes than LTB subjects (all $P< 0.0001$). The absolute lymphocyte number of ATB patients was lower than that of LTB subjects ($P< 0.0001$). There was a slightly difference in other blood elements count between LTB and ATB subjects.

To minimize the influence of plate-to-plate variation on the comparison among groups, TBM, PTB and LTB subjects were recruited simultaneously as much as possible. That is, when I received a TBM sample I arranged to also obtain a PTB and LTB sample on the same day and ran the assays on the three samples at the same time. From 20 ml blood taken, PBMCs were isolated and monocytes selected (Figure 4.1). Approximately

25 x 10^5 monocytes were differentiated to hMDM to assess phagocytosis and antimicrobial functions using bead-based assays (see Section 2.5, 2.6 and 2.7). The remainder were cryopreserved for further killing assays (see Section 2.8). The number of individuals with LTB or ATB for the assessment of phagocytosis, acidification, proteolysis and bacterial control were detailed in Figure 4.1.

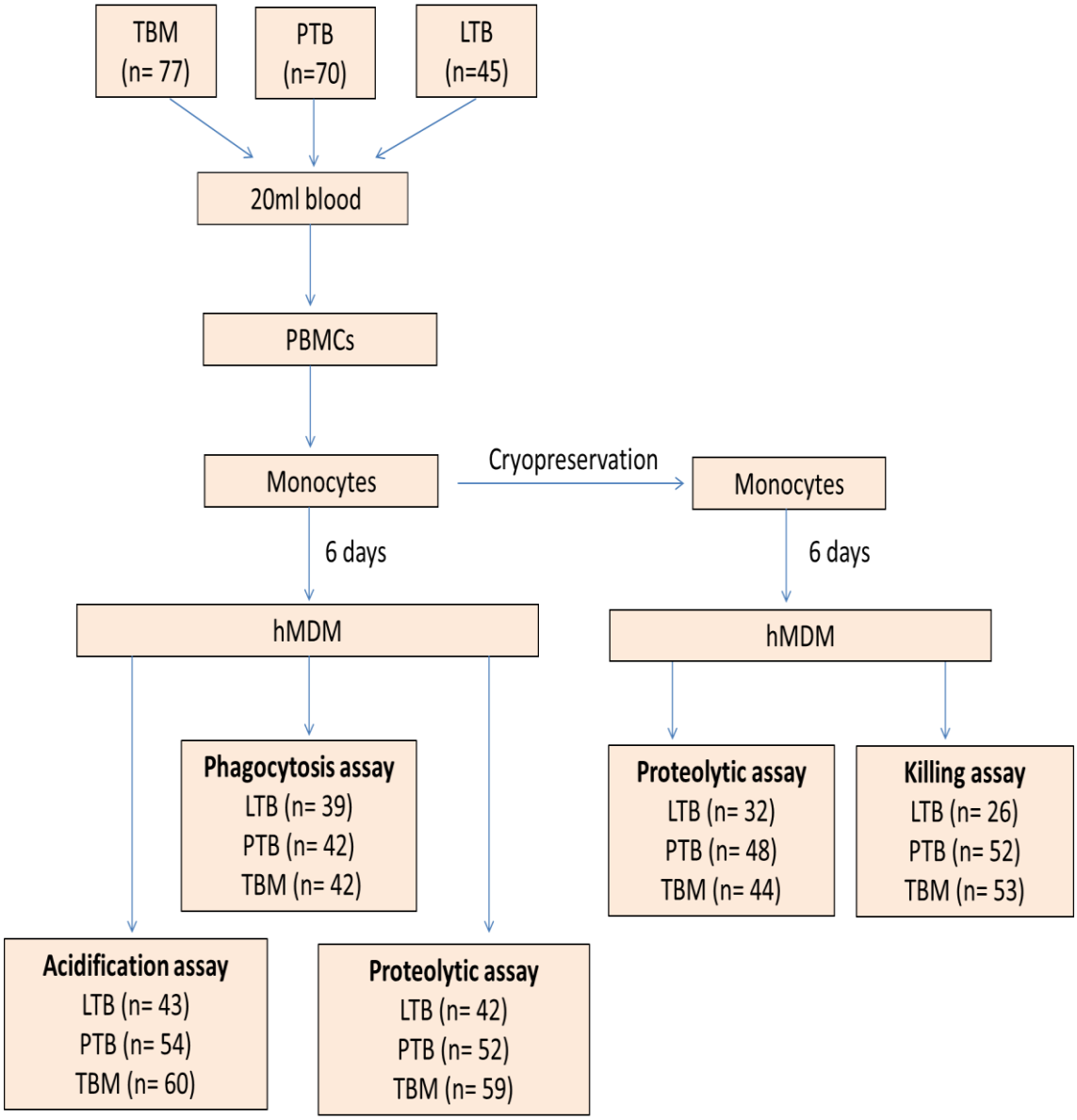

Figure 4.1 Study design of antimicrobial function of macrophage from LTB and ATB

Table 4.1 Baseline characteristic of study population

TB phenotypes	**LTB (n= 32)**	**PTB (n= 70)**	**TBM (n= 77)**	**ATB (n= 147)**	**P**
Male sex - no. (%)	16 (50)	58 (82.8)	47 (61)	105 (71.4)	**0.019**
Age - yr	36 (32-42.5)	45 (33-51)	41 (32-50)	43 (32-50)	0.069
White blood cells - K/µl	5.90 (5.03 - 6.88)	9.73 (8.06 - 11.72)	9.42 (7.20-12.03)	9.44 (7.74-11.75)	**<0.0001**
Neutrophil - K/µl	3.38 (2.95-3.88)	6.57 (5.31 -8.33)	7.27 (4.82 -9.96)	6.87 (5.05-9.59)	**<0.0001**
Lymphocyte - K/µl	1.89 (1.64 - 2.35)	1.82 (1.48 - 2.40)	1.13 (0.73-1.66)	1.55 (0.98-2.02)	**<0.0001**
Monocyte - K/µl	0.33 (0.27 - 0.46)	0.71 (0.55 - 0.93)	0.60 (0.46-0.82)	0.62 (0.50-0.86)	**<0.0001**
Red blood cell - M/µl	4.94 (4.46 -5.25)	4.94 (4.36 - 5.41)	4.69 (4.11-4.99)	4.77 (4.28-5.23)	0.3867
Hemoglobin - g/dL	14.20 (12.68 - 15.55)	13.50 (12.20 - 14.75)	12.90 (12.10-14.20)	13.10 (12.20-14.35)	**0.017**
Hematocrit - %	42.15 (38.23 - 45.60)	41.55 (37.98 - 44.45)	39.50 (36.70-42.10)	40.30 (37.15-43.45)	0.061
Platelets - K/µl	263.50 (219.50 - 287.00)	316.00 (264.75 - 391.25)	244.00 (193.00-342.00)	294.00 (219.50-371.50)	0.0714

Data for age and blood cell types were expressed as median (interquartile range)

P: P value, was determined using Mann-Whitney U test for comparisons of LTB and ATB

ATB: data combined from PTB and TBM

4.3 Results

4.3.1 Phagocytosis of macrophages was not associated with TB phenotypes

Phagocytosis facilitates the delivery of pathogens into phagosomes where pathogens are killed by antimicrobial activities during phagosome maturation. Therefore, impairment in macrophage phagocytosis could result in the failure of macrophages to clear the pathogen, which may influence the outcome of *Mtb* infection. To examine whether there was association between the macrophage phagocytosis and TB, I assessed the phagocytosis ability of macrophages isolated from individuals with LTB (N= 39) and ATB (N= 84) using bead-based internalization assays. IgG-, TDM- or β-glucan-coated beads were added to hMDM and at 10 min after adding beads the percentage of macrophages with or without beads was measured using flow cytometry (Figure 4.2). The phagocytosis ability was expressed by the percentage of cells with beads. Regardless to the disease phenotypes, I observed a high proportion of hMDM that internalized the IgG bead. There was a wide heterogeneity in phagocytosis of hMDM incubated with TDM- or β-glucan beads, ranging from 60 % to 95 % cells with beads.

I then compared the phagocytosis of IgG-, TDM-, and β-glucan-coated beads between macrophages from LTB and ATB. I did not find any significant association between phagocytic activity and TB phenotype (IgG bead, P= 0.46; TDM bead, P= 0.88; β-glucan bead, P= 0.86) (Figure 4.2). The hMDM from individuals with either LTB or ATB phagocytosed more IgG-coated beads than β-glucan and TDM-coated beads (P< 0.0001). This result was different with the observations in J774 whose phagocytosis was similar in response to IgG-, TDM- and β-glucan-coated beads.

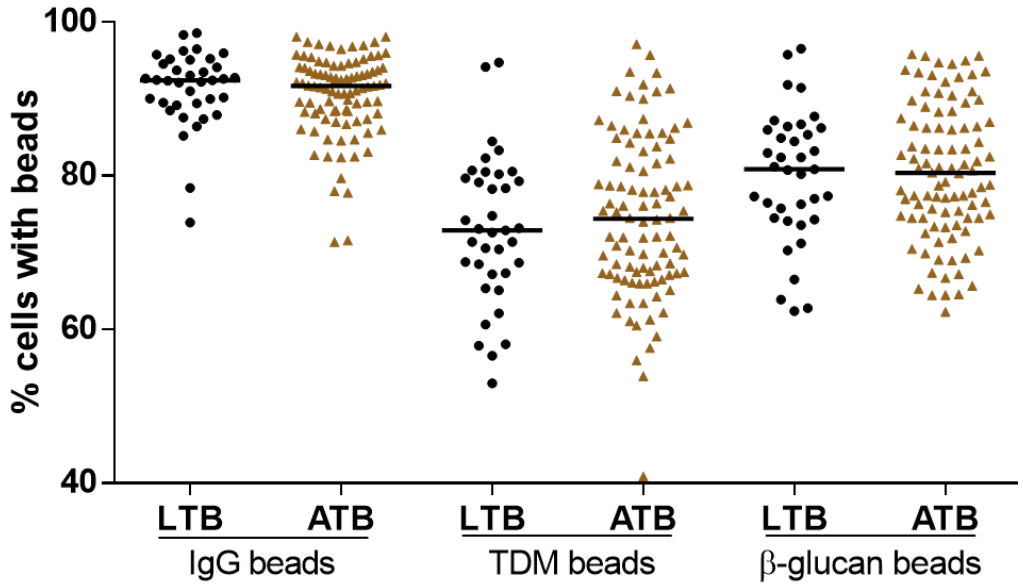

Figure 4.2 Phagocytosis of macrophages from LTB and ATB subjects

Monocyte-derived macrophages from subjects with LTB (n= 39), ATB (n= 84) at day 7 were treated with reporter beads that were coated with either IgG, TDM or β-glucan. Phagocytosis ability was assessed by percentage of cells with beads, analyzed using flow cytometry. Bars in the plot represent median values. P-value was determined using Mann-Whitney U test.

4.3.2 Deactivation of hMDM from TB patients after in vitro differentiation

To study antimicrobial activities of macrophages in different TB clinical forms, it is important to understand the state of hMDM from TB patients. Macrophages isolated from ATB could be still activated by *Mtb* infection. I hypothesized that after 7 days in culture, hMDM from ATB patients before treatment were deactivated and have returned to resting state. To test this I compared the macrophage Activity index for proteolysis and acidification from TBM patients (n= 19) at their enrollment to study and after 8 months of TB treatment (Figure 4.3). I did not observe any difference in the acidification or proteolysis Activity index before and after treatment in response to any kind of beads (Figure 4.3A, B). These results suggested that after *in vitro* culturing, hMDM from ATB patients before treatment were in the same status as cells after

treatment and that the cell status was not influenced by the disease stage. Hence the role of hMDM activities in TB development can be studied by comparing across TB clinical forms.

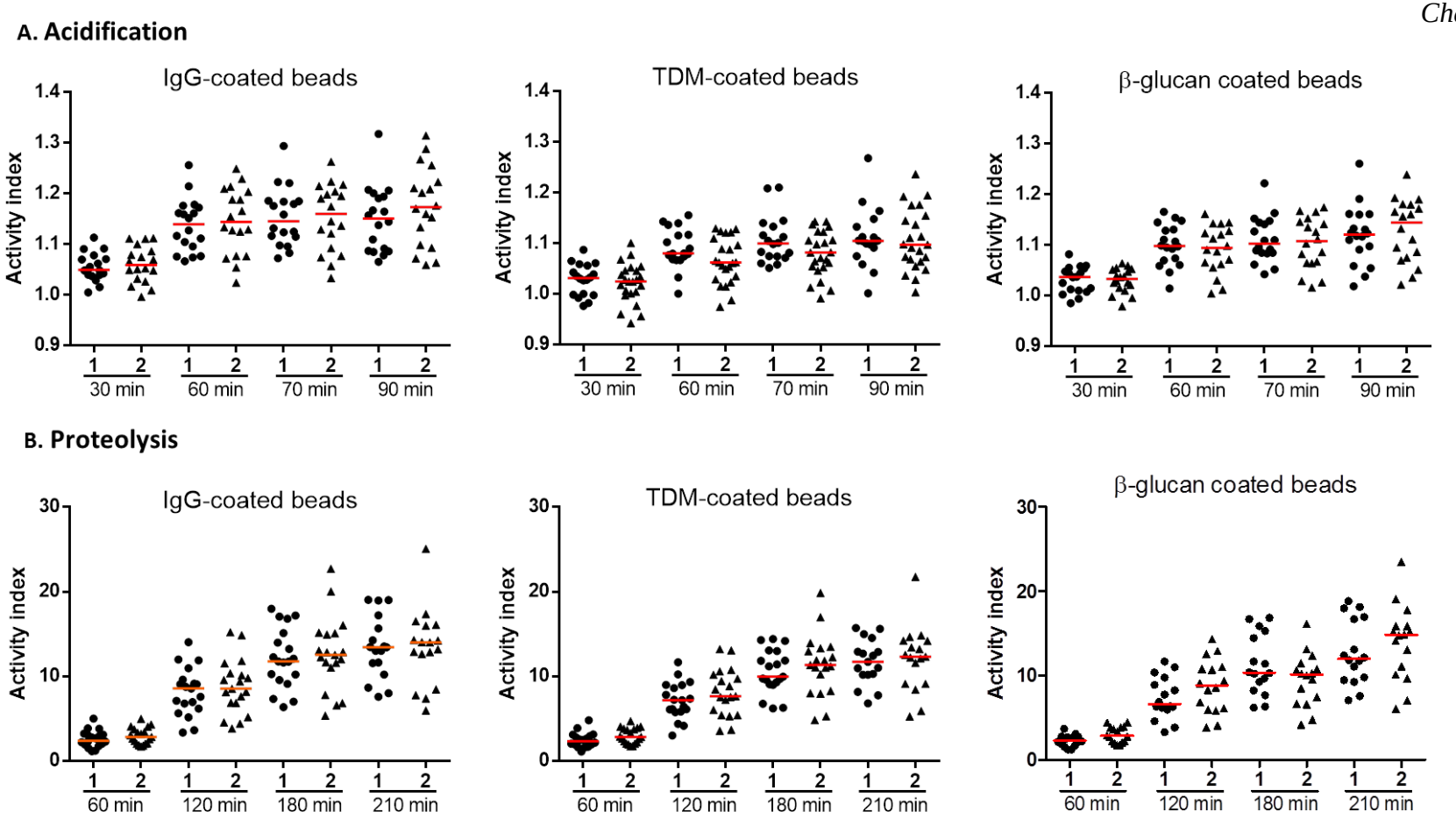

Figure 4.3 Acidification and proteolysis of MDMs from TBM subjects before and after anti-TB treatment

hMDM from TBM subjects (n= 19) before and after 8 months of TB treatment at day 7 of culturing were treated with acidification or proteolysis beads. The acidification Activity index (A) and proteolysis Activity index (B) at different time-points upon bead treatment were plotted. 1: TBM patients before TB treatment, 2: TBM patients after 8-month TB treatment. Bars in the plot represent median values. P-value was determined using paired student t-test; $P > 0.05$ in all comparisons.

4.3.3 Increased macrophage acidification and proteolytic activities associated with ATB

Next I examined the antimicrobial activities which were comprised of acidification and proteolysis of macrophages between LTB and ATB groups. hMDM from subjects with LTB (n= 43) and ATB (n= 114), who were recruited simultaneously by phenotype as much as possible, were treated with pH-sensitive carboxyfluorescein-coated beads and DQ-BSA–coated beads. After 10 min of bead treatment, approximately 80% of macrophages internalized these beads (Figure 4.4). In macrophages from LTB individuals, the onset of acidification was ranging from first 10 min to 15 min upon the treatment of either IgG-, TDM- or β-glucan-coated beads. The similarity was observed in hMDM from ATB treated with beads (Figure 4.4). Most of hMDM took 75- 90 min to acidify completely, which were indicated by the stabilization of the kinetics curves. However, in both LTB and ATB groups, macrophages from different individuals showed heterogeneity in the acidification activity, reflected by readouts varying from 0.6 to 0.8 RFU when treated with either IgG-, TDM- or β-glucan-coated beads (Figure 4.4). I then compared the acidification Activity index, where the activity at later time-point is normalized with the activity at early time-point of 10 min (see Section 2.7.2), of macrophages from groups of LTB and ATB at different time-points across the acidification kinetics (Figure 4.6A). When the acidification of phagosomes started entering a stabilization phase around 60 min, I observed a significantly higher activity in resting macrophages (IgG-bead treatment) from ATB groups compared to that from LTB group (P= 0.01). This difference was still observed when acidification was in stable phase at 70 min (P= 0.02) or 90 min (P= 0.04) (Figure 4.6A). However, I did not observe any difference in acidification activity of macrophages from groups of LTB and

ATB when macrophages were treated with TDM beads (P= 0.32, 0.08, 0.17, 0.09 at 30, 60, 70, and 90 min respectively). As with resting macrophages, macrophages treated with β-glucan beads from ATB had higher acidification activity than that from LTB (P= 0.02, 0.03, 0.03 for 60, 70, and 90 min respectively).

Unlike the rapid process of acidification, proteolysis in hMDM occurred slowly within first 60 min, then rapidly increased and likely became saturated after 180 min upon bead treatment (Figure 4.5). The readout for proteolysis varied from 0.5 to 4.0 RFU, showing the heterogeneity in proteolytic activity between individuals from either LTB or ATB groups. The difference in proteolysis activity of macrophages from LTB and ATB was assessed using Activity index where the activity at later time-point is normalized with the activity at early time-point of 10 min (see Section 2.7.2). At time-point of 60 min there was not difference in activity of resting macrophages treated with IgG beads from ATB and LTB groups (P= 0.07) (Figure 4.6B). At later time-points across the proteolysis kinetics, I found a significantly increased activity in resting macrophages from ATB patients compared to that from LTB subjects (120 min, P= 0.04; 180 min, P= 0.02; 210 min, P= 0.02) (Figure 4.6B). The difference in macrophage activity between ATB and LTB was also observed in the late stage of proteolysis when macrophages were treated with TDM- or β-glucan-coated beads (TDM beads, P= 0.05, 0.05, 0.03; β-glucan beads, P= 0.06, 0.04, 0.03 at 120, 180 and 210 min respectively) (Figure 4.6B).

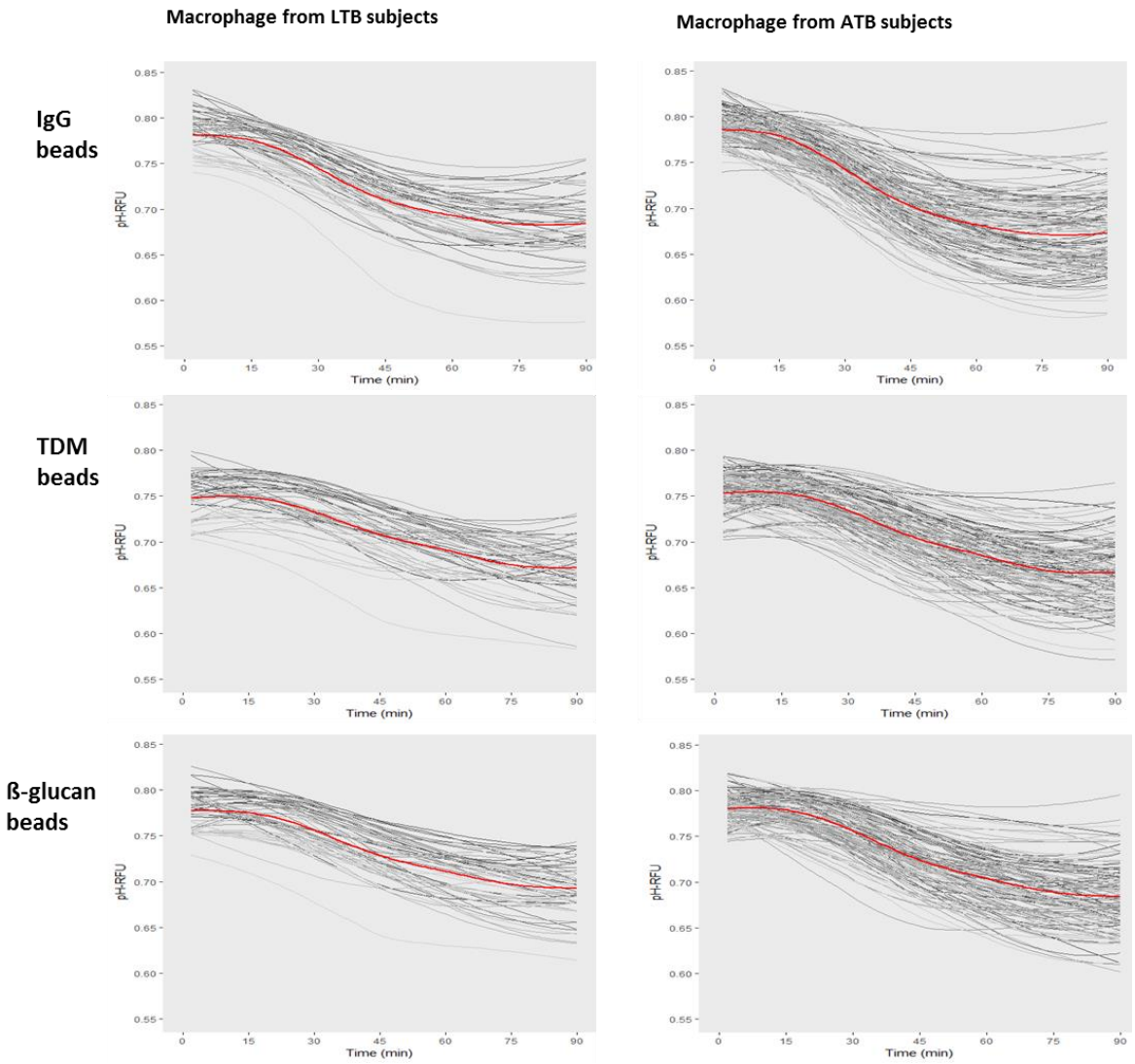

Figure 4.4 Kinetics of acidification in phagosomes of macrophages from LTB and ATB subjects

hMDM from subjects with LTB (n= 43) and ATB (n= 114) at day 7 were treated with reporter beads coated with either IgG, TDM or ß-glucan. The kinetics of acidification was plotted from LTB (A) or from ATB (B) subjects during 90 minutes. The red line represents the smoothed median, while each grey line represents an individual's values.

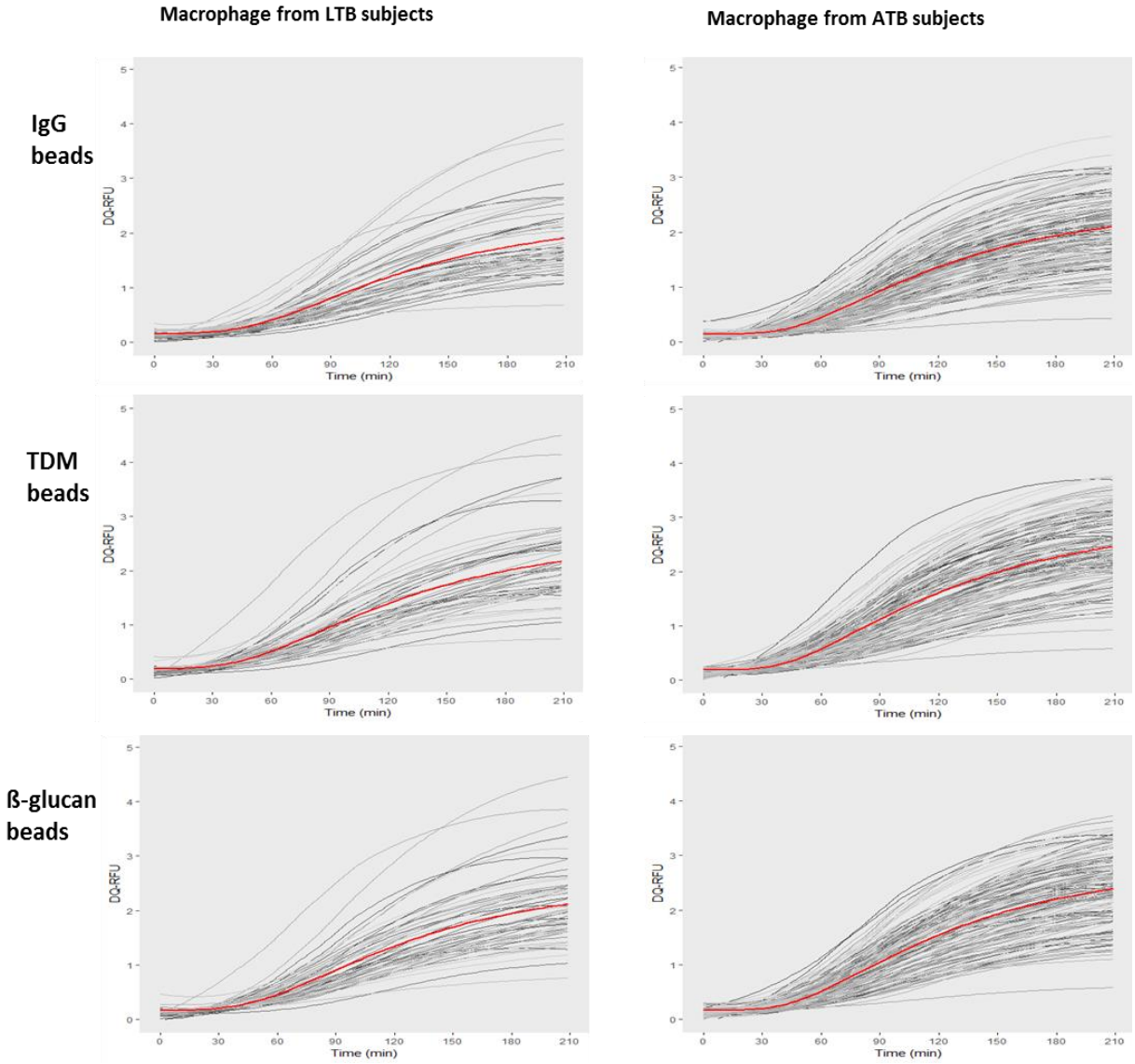

Figure 4.5 Kinetics of proteolysis in phagosome of macrophages from LTB and ATB subjects

hMDM from subjects with LTB (n= 42) and ATB (n= 111) at day 7 were treated with reporter beads coated with either IgG, TDM or β-glucan. The kinetics of proteolysis was plotted from LTB (A) or from ATB (B) subjects during 210 minutes. The red line represents the smoothed median, while each grey line represents an individual's values.

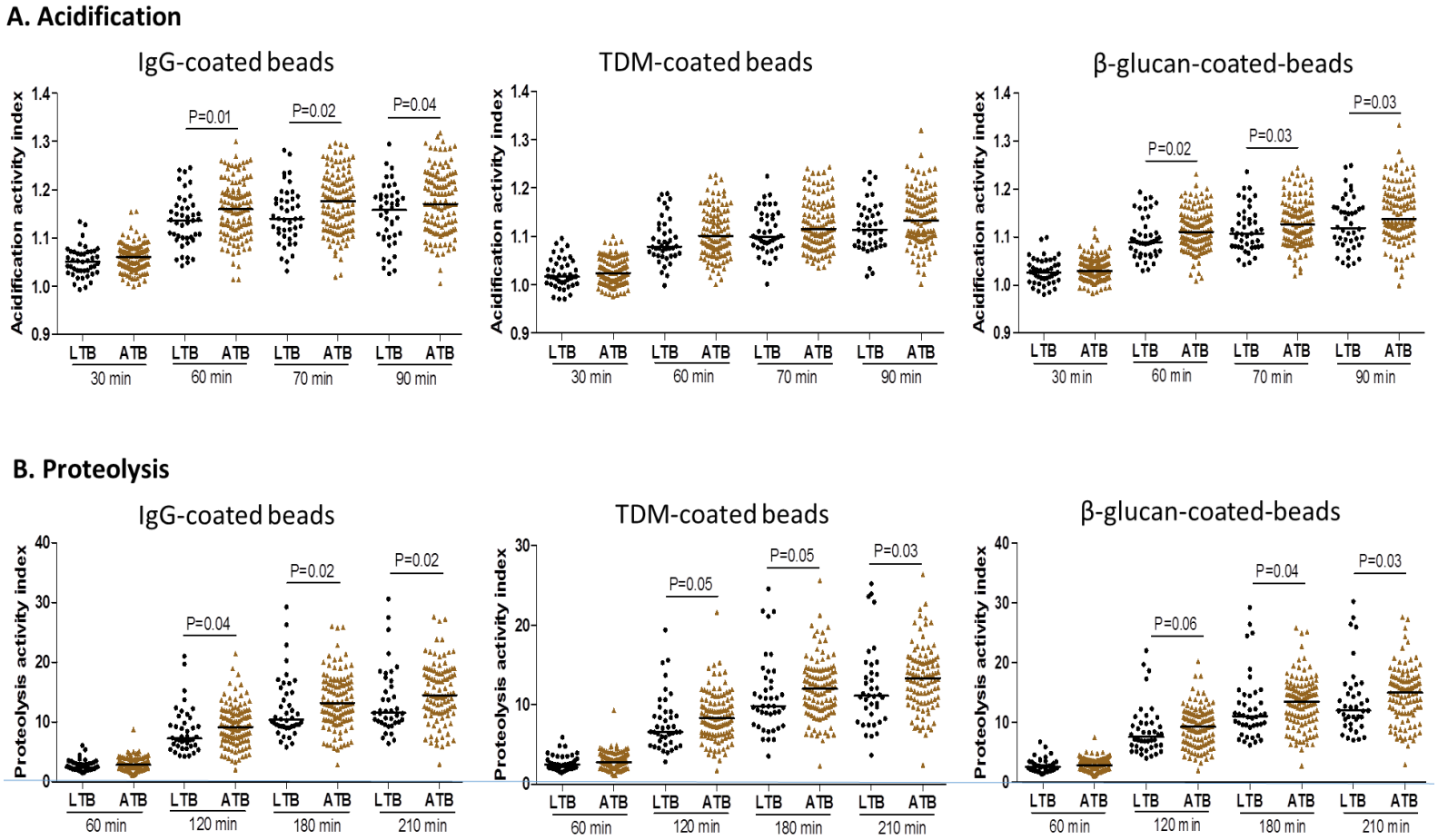

Figure 4.6 Acidification and proteolysis of macrophages from LTB and ATB subjects

(A) Acidification Activity index at 30, 60, 70 and 90 min across kinetics presented in Figure 4.2

(B) Proteolytic index at 60, 120, 180, and 210 min across kinetics presented in Figure 4.3

Bars represent median values. P value was determined using Mann-Whitney U test.

Since acidification is a prerequisite for the fusion of phagosome with lysosome, which is enriched with hydrolases as well as many proteases to have optimal working condition at acidic pH, the acidic environment within phagosome directly affects the acquisition and the activities of phagosomal hydrolytic enzymes. In mice, incubation of IgG bead-treated macrophages with concanamycin A that blocks lysosomal acidification reduces proteinase activity[226]. This prompted us to examine whether there was a correlation between acidification and proteolytic activity in macrophages of ATB patients or LTB individuals. The acidification process within phagosome saturated around 90 min after bead treatment (Figure 4.4), accordingly I assessed the correlation of acidification activity and proteolysis at this time-point. I found a moderate positive correlation between these two activities in IgG bead-treated macrophages from either LTB or ATB groups or when two groups were combined (Spearman's correlation r= 0.55, 0.58 and 0.59 respectively) (Figure 4.7A, B, C). The similar level of correlation was observed in macrophages treated with TDM (r= 0.58, 0.58 and 0.55 for LTB, ATB and combined respectively) (Figure 4.7D, E, F) or β-glucan beads (r= 0.61, 0.57 and 0.56 for LTB, ATB and combined respectively) (Figure 4.7G, I, J).

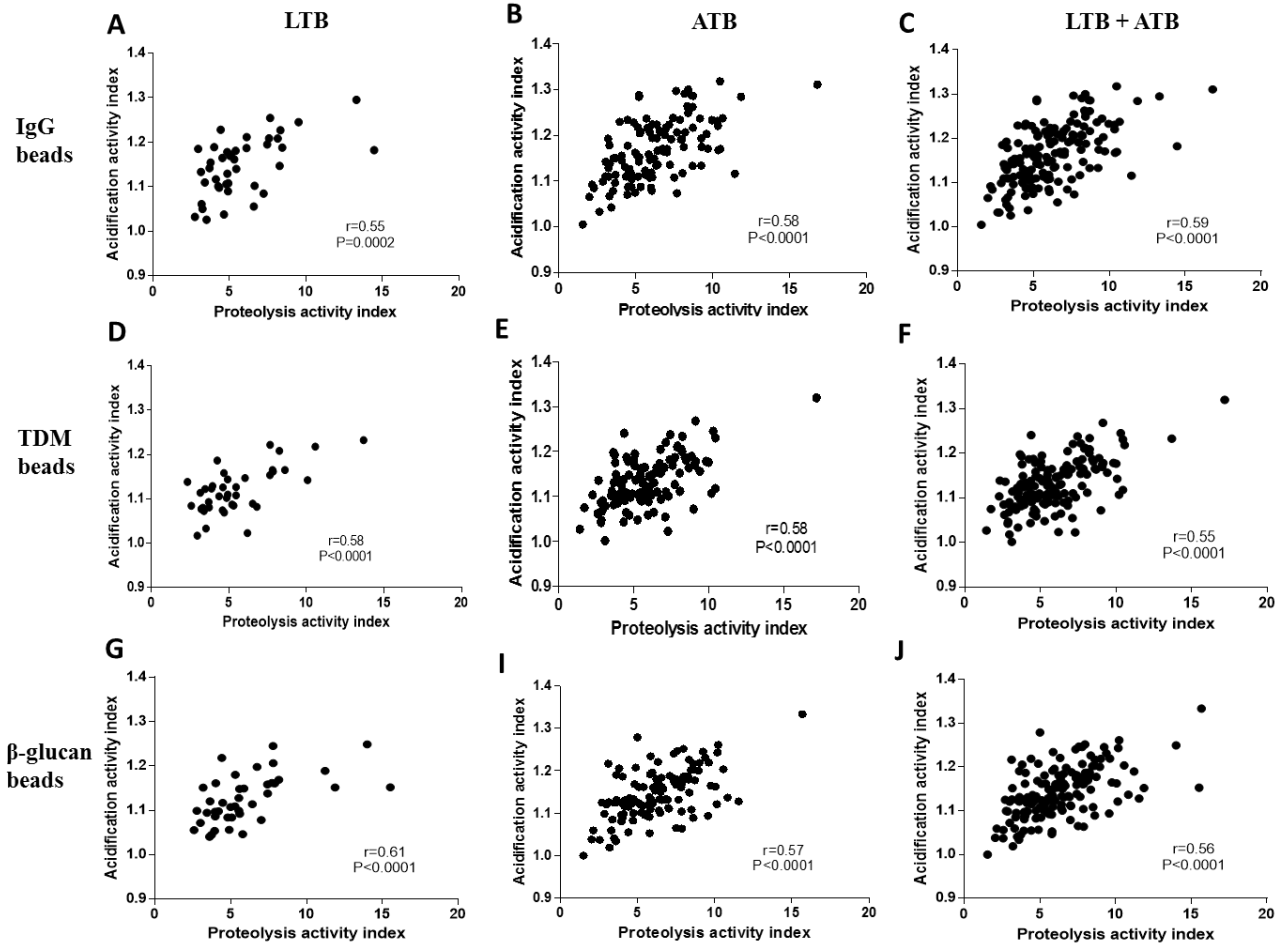

Figure 4.7 Correlation between proteolysis and acidification activities in macrophages treated with beads coated with either IgG (A-C), TDM (D-F) or β-glucan (G-I)

Macrophages were from subjects with LTB (A, D, G), or ATB (B, E, I) or both LTB and ATB combined (C, F, J). r: correlation coefficient. P: P value, P <0.05 indicating that the observed correlation between acidification and proteolysis is not due to a randomly sampling.

4.3.4 Influence of *Mtb* infection on the proteolytic activity of macrophages from ATB and LTB subjects

To advance their intracellular survival, *Mtb* is able to delay macrophage acidification and proteolysis, as well as prevent the phagosome-lysosome fusion[239,245]. I next examined how the macrophages from LTB and ATB subjects respond to *Mtb* infection. Because of limited cell numbers, only proteolysis activity was assessed. Macrophages, differentiated from cryopreserved monocytes that were isolated from LTB subjects (n= 32) and ATB patients (n= 92), were infected with *Mtb* reporter strain at MOI 1 for 48 h then treated with proteolytic beads coated with IgG to measure the activity. Activity index of macrophages was calculated at 210 min upon bead treatment. I first tested whether cryopreservation of monocytes influence the macrophage activity. In both LTB and ATB groups there was a slightly reduced activity in uninfected macrophages derived from cryopreservation compared to fresh macrophages (data obtained from Section 4.3.3) but this reduction was not significant (Mann-Whitney U test; LTB group, P= 0.24; ATB group, P= 0.07) (Figure 4.8). I then compared the activity of uninfected macrophage derived from cryopreserved monocytes isolated from LTB and ATB individuals (Figure 4.8). I again observed a lower proteolytic activity in macrophages from LTB subjects than that from patients with ATB (P= 0.02), which confirmed the above finding. Upon *Mtb* infection, the activity of macrophages from the two groups decreased approximately a half compared with uninfected cells (LTB group: 5.87 vs. 10.21; ATB group: 6.87 vs. 12.44; P< 0.0001) (Figure 4.8). Surprisingly, the observed difference in activity of uninfected macrophage from LTB and ATB individuals was abolished upon *Mtb* infection (P= 0.12). The reduction in activity from infected macrophages was not due to cell death, as macrophages of both ATB and PTB

individuals were still viable at day 2 post infection, as evident by the cell survival assay mentioned below. These data demonstrated that *Mtb* has the capacity to manipulate the host cell defense. The reduction of proteolysis activity to the same extent, driven by *Mtb* infection, in macrophages from ATB and LTB individuals, showed no difference in macrophage proteolysis function in response to the *Mtb* infection between ATB and LTB.

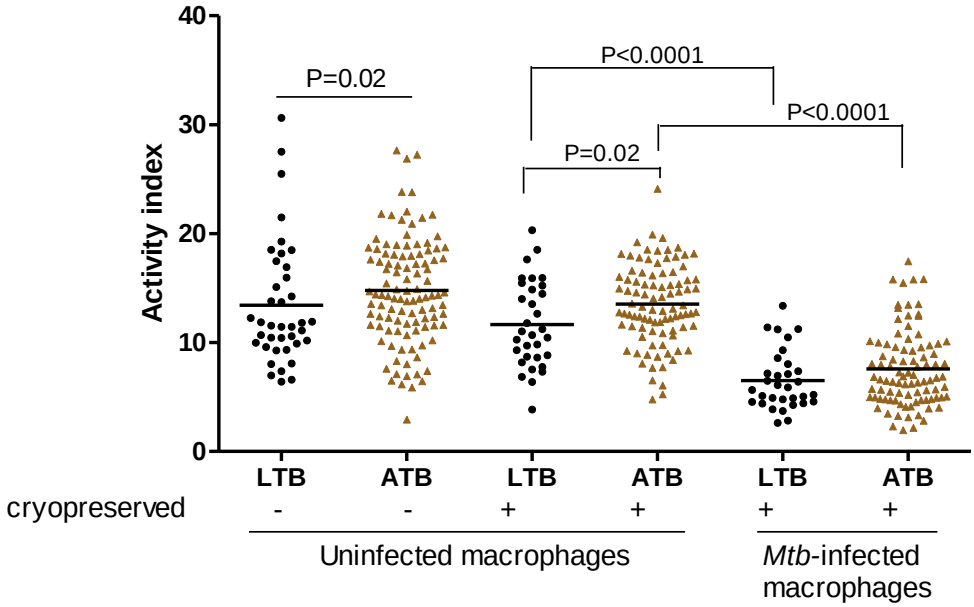

Figure 4.8 Proteolytic activity of *Mtb*-infected macrophages from LTB and ATB subjects

The first two columns were Activity index at 210 min upon IgG-bead treatment of monocyte-derived macrophages from LTB and ATB individuals. For the remaining columns, macrophages derived from cryopreserved monocytes from subjects with LTB (n= 32), and ATB (n= 92) were infected with *Mtb* reporter strain at MOI 1 or left uninfected. At day 2 post infection, macrophages were treated with reporter beads coated with IgG and the proteolytic activity index was assessed at 210 min upon bead treatment. (-): macrophage derived from fresh monocytes, (+): macrophage derived from cryopreserved monocytes. Bars in the plot represent median values. P: P value, determined using Mann-Whitney U test.

4.3.5 Survival of *Mtb* in macrophages from LTB and ATB subjects

Upon *Mtb* infection, macrophages from LTB individuals showed similar proteolysis activity as compared to macrophages from ATB patients, hence, I further examined the bacterial control of macrophages from these two groups (26 LTB and 105 ATB). Macrophages derived from cryopreserved monocytes were infected with the *Mtb* reporter strain at MOI 1. The lysis of infected macrophages in both LTB and ATB were 20% by day 6 of infection, and the extracellular bacteria interfered with the mCherry intensity of intracellular bacteria. Hence, I assessed the bacterial intracellular growth through mCherry intensity along with macrophages viability for the first 5 days of infection (Figure 4.9A, B). During first two days after infection I observed an intracellular replication of bacteria indicated by the increase of mCherry intensity (Figure 4.9A). There was also no difference in control ability of macrophages between LTB and ATB subjects; all macrophages remained adherent and intact (Figure 4.9B). From day 3 of infection, *Mtb* growth from LTB group seemed to be higher than ATB group but it was not a significant difference (day 3, P= 0.4; day 4, P= 0.7; day 5, P= 0.07) (Figure 4.9A). The macrophage lysis from LTB and ATB was observed from day 3 post infection. There was even more macrophage lysis among LTB subjects than among ATB patients at day 4 or 5 (P= 0.02) (Figure 4.9B), which could have resulted from differences in the interaction of bacteria and macrophages from LTB compared to ATB. In conclusion, there was no difference in control of intracellular *Mtb* growth in macrophages from individuals with LTB and ATB.

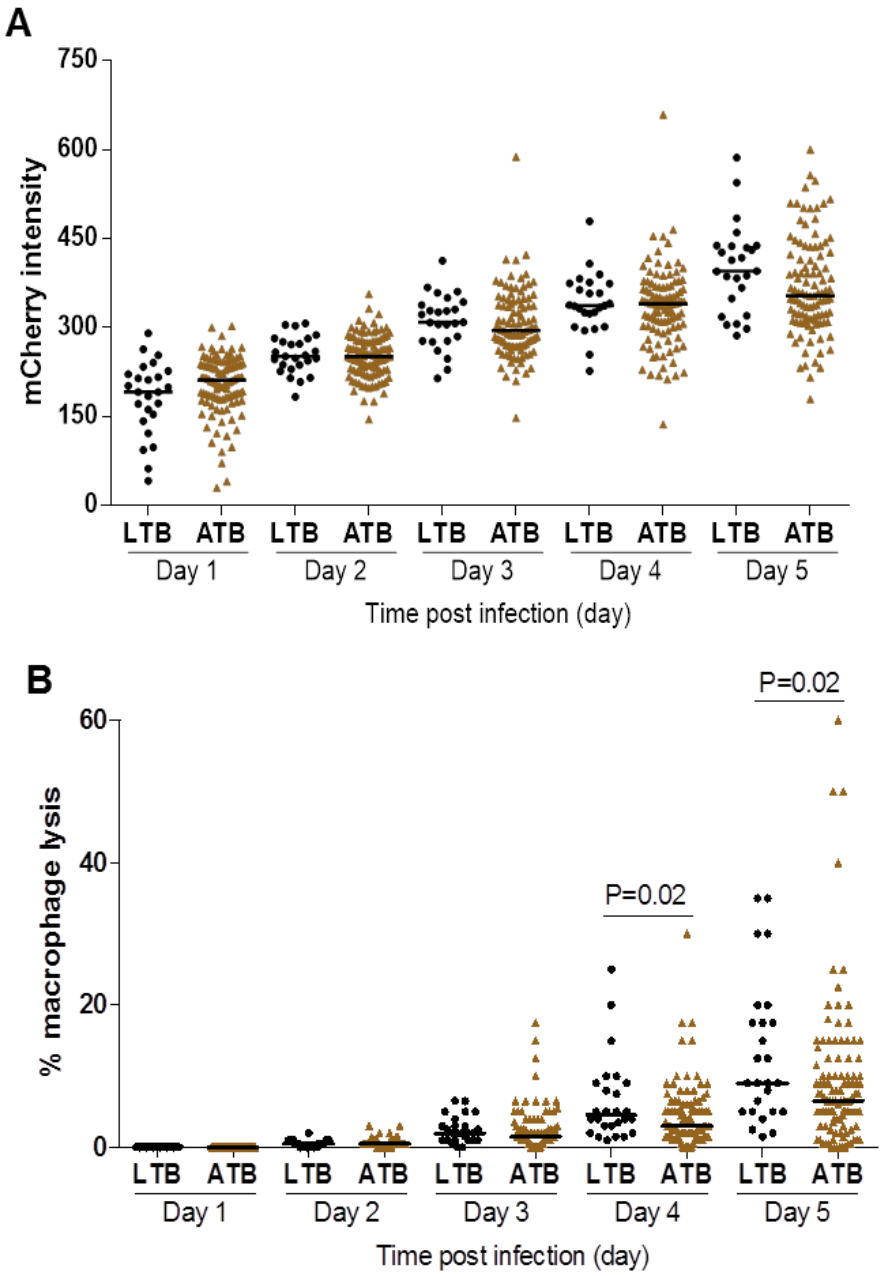

Figure 4.9 Intracellular replication of *Mtb* in macrophages from LTB and ATB subjects

hMDM from subjects with LTB (n= 26) and ATB (n= 105) were infected with the *Mtb* reporter strain at MOI 1. The bacterial intracellular growth during 5 days of infection was assessed by the mCherry intensity readout (A) and the viability of infected macrophages (B). Bars in the plots represent median values. P value was determined using Mann-Whitney U test.

All antimicrobial activities of macrophages were shown above to be associated with ATB group that includes both PTB and TBM, I then examined whether there was any difference in antimicrobial functions between localized PTB and disseminated TBM. The activities of macrophages from PTB were similar to that from TBM in all measurements; including phagocytosis, acidification, and proteolysis (see Supplementary figure 4.1). There was also no difference in proteolysis activity of macrophages as well as their ability in controlling intracellular *Mtb* growth between PTB and TBM individuals (see Supplementary figure 4.2).

4.3.6 Macrophage antimicrobial activities were modulated by different ligands triggering phagocytosis

To study the phagocytosis and phagosomal functions of macrophages, I generated the reporter beads that were coated with different ligands including IgG, TDM and β-glucan. IgG is recognized by FcγRI, TDM is recognized by MINCLE and MARCO receptors[294,306] while β-glucan is recognized by DECTIN-1[295]. These receptors then induce signaling to facilitate the phagocytosis and further activities inside the phagosome. The beads were coated with an excess amount of ligands so that the ability to be recognized and bind to their receptors was similar. In fact, there was no difference in phagocytosis of these ligand beads in J774 (Chapter 3), suggesting that there would be equivalency of attachment among ligands and receptors. Hence, the ligand-coated beads could allow us to study the variations of macrophage antimicrobial activities facilitated by different phagocytic receptors.

The data for phagocytosis, acidification and proteolysis were pooled from LTB and ATB individuals from above (n= 179) and stratified by each kind of ligand coated to the beads. There was difference in the macrophage activities induced by distinct ligands

coated on the bead (phagocytosis and acidification, $P < 0.0001$; proteolysis, $P= 0.01$) (Figure 4.10A, B, and C.). In a closer look, macrophages treated with IgG beads phagocytosed more beads (Figure 4.10A) and induced higher acidification (Figure 4.10B) as well as proteolysis (Figure 4.10C) compared to macrophages treated with other ligand coated beads. The phagocytosis of macrophages against β-glucan beads was higher than TDM beads (75% vs. 80%, $P< 0.0001$) (Figure 4.10A). Likewise, the acidification and proteolysis activity were higher in macrophages treated with β-glucan than with TDM beads (acidification, $P= 0.06$; proteolysis, $P= 0.01$) (Figure 4.10B and C). There was no correlation between the phagocytosis activity and acidification or proteolysis activities against specific ligands (see Supplementary figure 4.3). These results altogether suggested that the phagosomal activities of macrophages were regulated by ligands and the corresponding receptors.

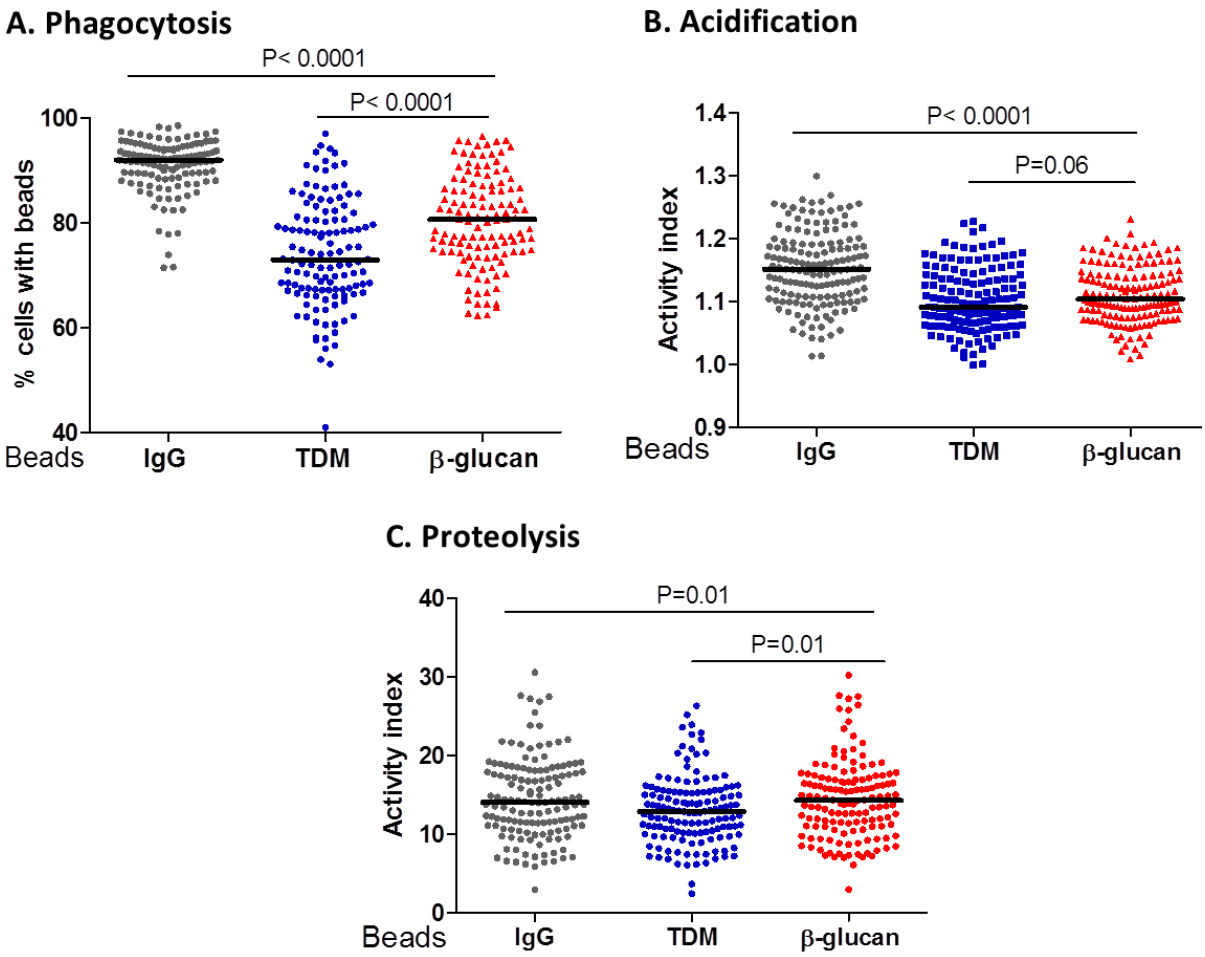

Figure 4.10 Phagocytosis and antimicrobial activities of macrophage treated with different ligand beads

hMDM combined from subjects with LTB and ATB at day 7 were treated with reporter beads coated with either IgG, TDM or β-glucan. (A) Phagocytosis stratified by ligand in macrophages from 123 individuals, (B) Acidification Activity index at 60 min in macrophages from 157 individuals, and (C) Proteolysis Activity index at 210 min in macrophages from 153 individuals. P value was determined using Kruskal-Wallis test for comparison across three groups or using Mann-Whitney U test for two groups.

4.4 Discussion

Macrophages are thought to play an essential role in controlling the bacterial clearance of *Mtb*, however whether the efficiency of this performance is related to the establishment and development of different manifestations of TB infection is unknown. To understand the contribution of macrophages in TB pathogenesis, I examined the phagocytosis and phagosomal function of macrophages including acidification and proteolysis from individuals with LTB and ATB. I found that although the phagocytosis ability remained similar between LTB and ATB macrophages, the macrophages from LTB had reduced acidification and proteolytic activity compared to ATB in resting state (IgG–bead treatment) or in activated state (by immunologic component β-glucan[307]). In case of TDM beads treatment, I observed only reduced proteolytic activity in LTB than ATB macrophages. However, when macrophages were infected with live *Mtb*, proteolysis of macrophages from individuals with LTB and ATB were modulated to the same extent. The infected macrophages from LTB individuals did not show any difference in controlling *Mtb* intracellular growth compared to macrophages from ATB patients. Besides, I did not observe any difference in the phagosomal activities as well as ability to control *Mtb* in macrophages from localized PTB and disseminated TBM. These results suggest that macrophage antimicrobial functions were not associated with different TB clinical phenotypes. In addition, our study also indicated that different ligands had distinct effect on the phagocytosis and antimicrobial activities of human macrophages.

For acidification, I only observed reduced macrophage activities in LTB compared to ATB when cells were treated with either IgG or β-glucan beads. Whereas, I observed the reduced proteolysis activity in macrophages from LTB in treatment of IgG, TDM or

β-glucan beads. Although I observed a moderate correlation between acidification and proteolysis activities of macrophages, and acidification has been suggested to be requisite for hydrolytic activity within phagosomes, there could be other factors which may independently regulate proteolysis activity and show different level of activity between LTB and ATB. A previous study has indicated the phagosomal proteolysis activity of macrophages could be regulated by NADPH oxidase in an pH-independent manner[308].

Along with the ligand-coated beads model, I also used the live *Mtb* infection model to study the antimicrobial activities of macrophages. In the ligand bead model, the beads were coated with single immunogenic components from *Mtb*, hence this model can help us understand how specific ligand and its corresponding pathway influences the antimicrobial functions. The approach is also important to understand the link of host genetic association and macrophage antimicrobial functions. That is, whether the polymorphisms in receptor gene are associated with the susceptibility of TB because they alter the macrophage antimicrobial functions induced by its ligand. But ligand beads are limited as the antimicrobial functions of macrophages against the ligand beads may be different with macrophage functions in response to live *Mtb*. Using macrophages infected with the live *Mtb* enables us to highlight the complicated interaction of *Mtb* and macrophage by its ability in manipulating the functions of macrophage. The proteolysis activity in *Mtb*-infected macrophages from LTB and ATB were reduced by 50% compared to the level in resting macrophages, resulting in no difference between LTB and ATB in proteolysis activity.

In this study, macrophages from LTB and ATB showed similarity in their proteolysis activity in response to *Mtb* infection as well as in the ability of *Mtb* control that was

indicated by the same extent of *Mtb* intracellular growth. It is observed that T cell response can activate antimicrobial functions of macrophage and contribute to protection against TB, as HIV-infected people who have low CD4 count have high risk of getting active TB from latent infection. Similarly, recent studies have shown that humoral immune response is different between individuals with LTB and ATB, and specific antibody in LTB persons can enhance the phagocytosis of *Mtb* by macrophages[183]. Our results further confirm these observations as macrophage antimicrobial functions alone cannot determine for TB protection to remain in LTB stage or for TB development. The macrophage infection model may be further improved by the inclusion of other adaptive immune components from individuals with LTB and ATB. For example, *Mtb* could be opsonized with the antibodies specific for LTB and ATB, then were infected to macrophages from individuals with LTB and ATB to determine the macrophage antimicrobial functions of two groups.

Our results from ligand-coated beads model suggest for a possible ligand-specific antimicrobial functions of macrophages. The reduction in antimicrobial function of macrophages treated with TDM compared to IgG or β-glucan suggests for a survival mechanism of *Mtb* which may contribute to the disease development. Reduced phagocytosis mediated by TDM may prevent *Mtb* from the antimicrobial activities within macrophage phagosome. Likewise, the decrease in proteolysis and acidification against the TDM-coated beads may favor bacterial intracellular growth to establish the infection. In line with our results, previous studies show that TDM may inhibit phagosome - lysosome fusion events to enhance intracellular survival of *Mtb* during infection[247,309]. Removal of surface lipids of *Mtb* leads to enhanced trafficking of bacteria to acidified compartments and reduced number of intracellular bacteria while

reconstitution of delipidated *Mtb* with purified TDM is sufficient to restore ability to delay phagosome acidification and fusion[309].

Our study is the first study assessing the macrophage phagosomal function from individuals with different TB phenotypes, which contributes to the understanding of the contribution of macrophages in TB control. The bead-based models suggest that the antimicrobial functions of macrophages from both ATB and LTB vary regarding to specific ligands and their pathways. While using live *Mtb* model, I found that *Mtb* is able to modulate antimicrobial functions of macrophages for its survival, resulting no difference in antimicrobial function as well as the bacterial control of macrophages from LTB and ATB. Further study on interaction of humoral response and macrophages in controlling *Mtb* between LTB and ATB could provide the insights into the TB development and progression.

Chapter 5

ASSOCIATION OF PHAGOCYTIC GENES AND TB SUSCEPTIBILITY

5.1 Introduction

In Chapter 4, I observed that there was a wide range of phagosomal activity in macrophages from different individuals (Figure 4.2 and 4.6). These results suggest an involvement of host genetic variation, especially in genes involved in phagocytosis, in the heterogeneity of phagosomal activity which may influence the susceptibility to TB disease.

A number of studies provided strong evidences for the crucial roles of receptors comprising DECTIN-1, MINCLE and MARCO in mycobacterial recognition, phagocytosis and initiating immunity against mycobacteria infection. DECTIN-1 is encoded by *DECTIN-1* or aliases C-type Lectin Receptor 7A (*CLEC7A*) on chromosome 12. This receptor is expressed not only on monocytes but also on macrophages, dendritic cells and neutrophils[310]. It is found to be a phagocytic receptor for β-glucan-containing particles, including zymosan and live *Candida albicans*[295]. In fungal infection models, binding of ligands to DECTIN-1 is shown to induce a number of cellular process, including ligand phagocytosis, respiratory burst, production of cytokines and chemokines[311,312]. DECTIN-1 can recognize *Mtb* but the precise PAMP has been uncharacterized yet. Several studies show that DECTIN-1 in concert with TLR2 is required for phagocytosis of nontuberculous *M. abcessus*[313] and *M. ulcerans*[314]. *Mtb* internalization by human alveolar cells is partially blocked when DECTIN-1 expression is silenced by siRNA[315]. In addition, DECTIN-1 is found to be the key receptor for the induction of pro-inflammatory cytokines and antimicrobial effects in response to mycobacterial infection in both mice and humans[315–317]. Blockage of DECTIN-1 receptor results in the enhanced survival and growth of *Mtb*[315]. MINCLE is encoded by *MINCLE,* also named as C-type Lectin Receptor 4E (*CLEC4E*), on

chromosome 12p31 and predominantly expressed on macrophages, neutrophils and DCs[318,319]. The role of MINCLE in host response to mycobacterial infection was investigated in both *in vitro* and *in vivo* analysis. The expression of this receptor on the alveolar macrophage surface was up-regulated following exposure to mycobacteria[320]. MINCLE was identified as a main receptor recognizing mycobacterial cord factor TDM, which in turn activated the inflammatory pathway and induced antimycobacterial immunity[306,320,321]. Macrophages from mice deficient of *Mincle* show impaired production of pro-inflammatory cytokines and nitric oxide after stimulation with TDM or its synthetic analog, trehalose 6,6-dibehenate (TDB)[306]. Moreover, treatment of *Mincle* knockout mice with TDM results in significantly reduced TNF-α and IL-6 production. In other studies, *Mincle*-deficient mice exhibited an increased bacterial loads in lung after BCG or *Mtb* infection[320,322], suggesting a role of MINCLE in mycobacterial clearance.

Another surface receptor, MARCO, a class A SR, has been implied for the host defense against mycobacterial infection. MARCO is encoded by *MARCO* gene located on chromosome 2. MARCO is shown to be highly expressed on the macrophages in mice BCG-induced granuloma from very early stages during infection with BCG[323]. In another study, MARCO-expressing macrophages appear to phagocytose more BCG than the neighboring macrophages that do not express MARCO[324]. This observation suggests that MARCO functions as a receptor to recognize mycobacteria, facilitates the uptake and induces immune response. More specifically, it has been demonstrated that *Mtb* is captured by MARCO *in vivo* via its cell wall cord factor (TDM), which increases pro-inflammatory cytokine response through the interaction with Toll-like receptors and CD14[294]. As such, macrophages from *Marco*-deficient mice produce less cytokines in

response to *Mtb* infection than wild type[294]. The experiment with *M. marinum* in zebrafish further supports the hypothesis that the phagocytosis of mycobacteria is MARCO-dependent[325]. Recently, MARCO is shown to associated with the increased susceptibility to TB[326,327].

Despite the important role of *DECTIN-1*, *MINCLE*, and *MARCO* in TB pathogenesis, the role of these phagocytic genes in TB susceptibility is not fully understood or specifically clarified in different populations including ones with high prevalence of TB, such as the Vietnamese. Our previous studies have revealed the association of polymorphisms on a number of innate immune genes on TB susceptibility and I found that these associations are predominant to either PTB or TBM[114,198,199,328]. Therefore, in this study I aimed to investigate the association of phagocytic gene variants and different clinical forms of TB.

I hypothesized that (1) the polymorphisms in phagocytic genes including *DECTIN-1*, *MINCLE*, and *MARCO* are associated with susceptibility to tuberculosis and influence clinical presentations and treatment failure, (2) the associated polymorphisms if available in (1) could regulate the macrophage phagocytosis, gene expression and cytokine response. A number of results related to the work presented in this chapter have been recently published with the title of "*MARCO* variants are associated with phagocytosis, pulmonary tuberculosis susceptibility and Beijing lineage"[329].

5.2 Study design

I used tagging SNP to select SNP markers on *MINCLE*, *MARCO*, and *DECTIN-1* genes for association studies (see Section 2.10). To examine the association of gene variants with clinical TB, I used a case-control study. I genotyped candidate polymorphisms

across *DECTIN-1*, *MINCLE*, and *MARCO* in 900 cases including 450 TBM and 450 PTB, and 450 cord blood controls (see Section 2.10). TBM patients were recruited for several clinical trials and observational studies from 2001-2013 from either Pham Ngoc Thach Hospital for Tuberculosis and Lung Disease or the HTD, HCMC. PTB patients were recruited through the network of district TB control units from 2003-2011[114,199,329]. Criteria for recruitment of TBM, PTB and controls were detailed in Section 2.1.

The association between gene variants and clinical presentations in TB patients (see Section 2.11) as well as genotypes of infecting *Mtb* strains (see Section 2.12) were examined. The phagocytosis, cytokine response and mRNA expression of *MINCLE*, *MARCO,* and *DECTIN-1* were determined in macrophages from a cohort of individuals with healthy volunteers (N= 41) (Section 2.7.1 and 2.9). The influence of gene variants on macrophage phagocytosis, cytokine production and gene expression was then examined.

5.3 Results

5.3.1 Selection of candidate SNPs for genotyping *DECTIN-1*, *MINCLE* and *MARCO*

A tagging SNP represents for a groups of SNPs that have strong linkage with each other, hence genotyping tagging SNPs in the region can predict genetic association of the remaining SNPs in the region. I selected tagging SNPs for *DECTIN-1*, *MINCLE* and *MARCO* as detailed in Section 2.10.1. The SNPs in the gene region that showed the association with TB in other population from previous works were also considered. In addition, functional nonsense or missense SNPs that change the amino acid sequence of protein encoded by the gene were investigated.

5.3.1.1 Selection of *DECTIN-1* SNPs

DECTIN-1 has a length of 14,492 bp and includes 5 exons. This gene is located on chromosome 12 from position of 10,116,777 to 10,130,258 (GRChr38.p10) (Figure 5.1). Because regions surrounding the main gene could contain promoter or enhancer that have effect on the gene function, I investigated the SNPs across this gene and span of 20 kb extra from the upstream (toward the 5'end) and of 16 kb from the downstream (toward 3' end) of the gene. There were 108 SNPs genotyped within this region from HCB population, many of them (n= 37) were present in the *DECTIN-1* gene and distributed throughout the gene (Table 5.1 and Figure 5.1A). However, around half of the SNPs within the gene region as well as surrounding areas were monomorphic or had low MAF (< 5 %) (Table 5.1). I then investigated the association of 48 SNPs with MAF ≥ 5 %. By setting the cut off of r^2 for LD of 0.8, I found 6 tagging SNPs. I also selected two SNPs which showed potential association on our previous study (rs7137840, rs11053624) and two SNPs in the upstream region. Finally, ten SNPs in *DECTIN-1* region were selected for genotyping (Table 5.1 and Figure 5.1B).

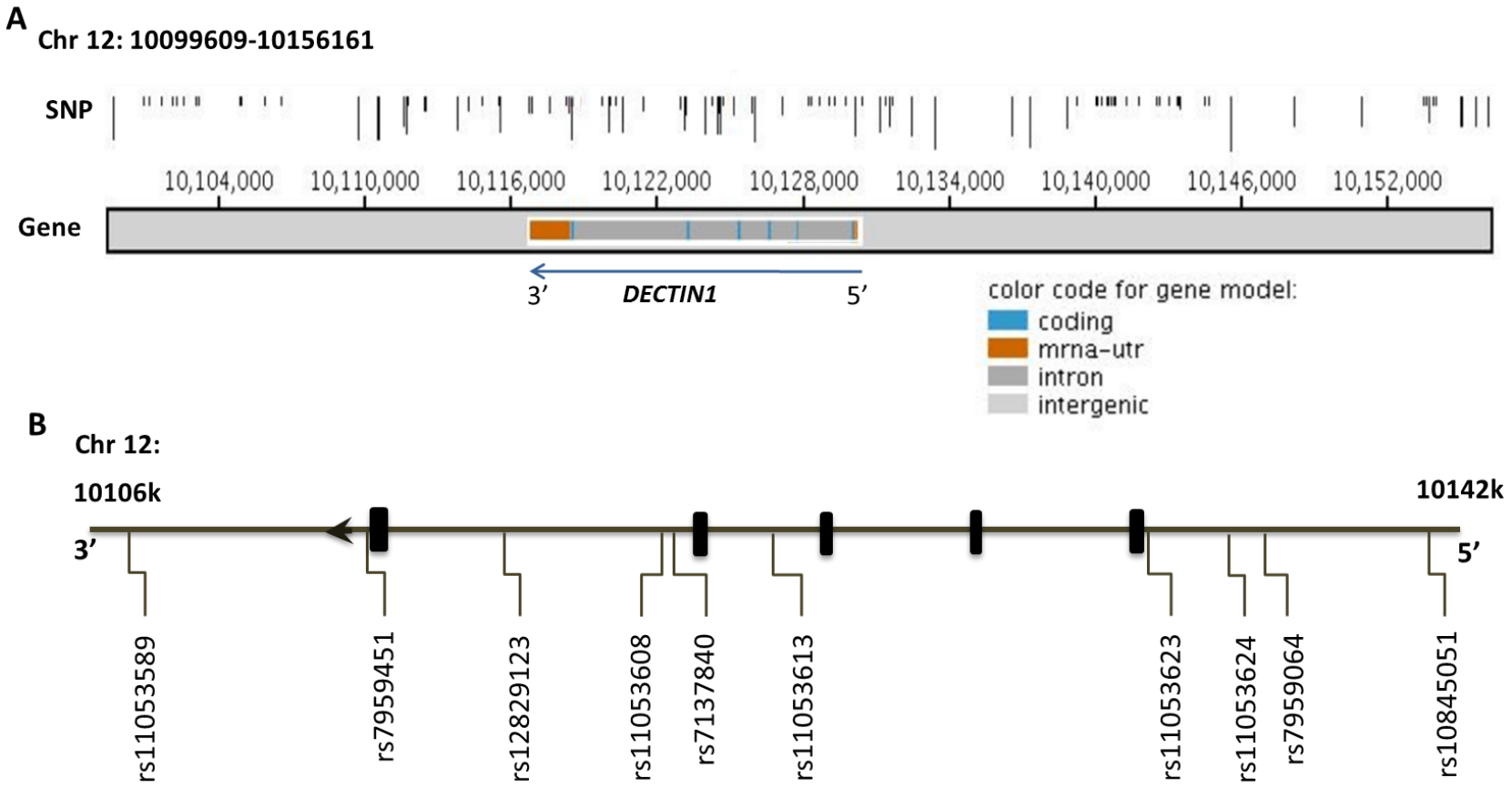

Figure 5.1 Chromosomal location and polymorphisms across *DECTIN-1* region

(A) *DECTIN-1* gene region and its 20 kb upstream and 10 kb downstream on chromosome 12 . SNPs across the region from HCB population from International HapMap Project were presented as lines; the SNP line lengths are proportional to the minor allele frequency in the population. Figure was originated from http://gvs.gs.washington.edu build 147 based on human genome assembly GRCh38.p10. (B) Chromosomal map of candidate SNPs in *DECTIN-1* region for genotyping. Tagging SNPs and other potential SNPs in Table 5.1 were mapped. Boxes showed exonic regions.

Table 5.1 SNPs information on *DECTIN-1* region from HCB population

Location with respect to gene	Function	Total SNPs (N=108)	Monomorphic SNPs (N= 55)	Rare SNPs (MAF< 5 %) (N= 5)	Common SNPs (≥ 5 %) (N= 48)	Tagging SNPs (No. of tagged SNP)	Other potential SNPs for genotyping
Downstream	Intergenic	29	12	4	13	rs11053589 (5)	
3'-UTR	3'-UTR	6	1	-	5	rs7959451 (2)	
Gene region	Intronic	28	14	-	14	rs12829123 (6) rs11053613 (11)	rs11053608 rs7137840[a]
5'-UTR	5'-UTR	3	1	-	2	rs11053623 (3)	
Upstream	Intergenic	42	27	1	14	rs10845051 (8)	rs11053624[b] rs7959064

MAF: Minor allele frequency

Intergenic: A variant located in the intergenic region, between genes

3'-UTR: A variant of the 3' Untranslated region

5'-UTR: A variant of the 5' Untranslated region

Intronic: A transcript variant occurring within an intron

[a] GWAS, P= 0.013

[b] data from our collaboration showed association of this SNP with TB

Monomorphic SNP: a SNP with only one type of allele (no other variant) was identified

5.3.1.2 Selection of *MINCLE* SNPs

MINCLE is a 6-exon gene that is located on chromosome 12 with length of 7,7 kb (from 8,533,305 to 8,540,963) (Figure 5.2). As with *DECTIN1*, the SNPs across *MINCLE* and 30 kb upstream and 15 kb downstream of the gene were investigated. There were 95 SNPs across the spanning region of *MINCLE*; however *MINCLE* was highly conserved with very few SNPs (n= 8) in the gene while most of SNPs were distributed in the upstream region (Figure 5.2A). Approximately one third of SNPs in the region were monomorphic or had MAF < 5% (Table 5.2). 62 SNPs with MAF > 5 % were examined and 10 tagging SNPs were identified (Table 5.2). Finally 12 SNPs across *MINCLE* region were selected for genotyping (Table 5.2 and Figure 5.2B). All SNPs were in the non-coding regions including either introns or intergenic upstream of gene.

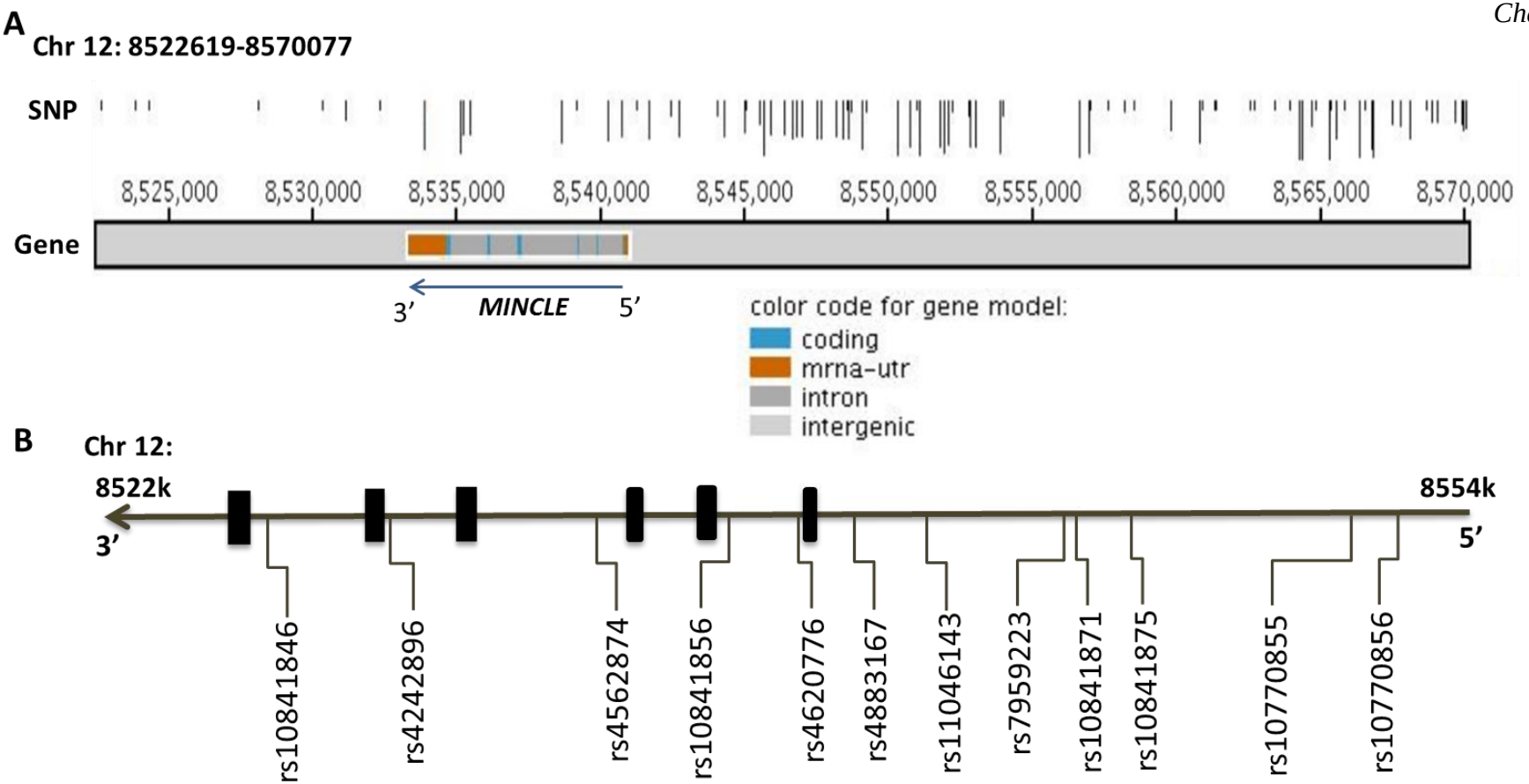

Figure 5.2 Chromosomal location and polymorphisms across *MINCLE* region

(A) *MINCLE* gene region and its 20 kb upstream and 10 kb downstream on chromosome 12. SNPs across the region from HCB population from International HapMap Project were presented as lines; the SNP line lengths are proportional to the minor allele frequency in the population. Figure was originated from http://gvs.gs.washington.edu build 147 based on human genome assembly GRCh38.p10. (B) Chromosomal map of candidate SNPs in *MINCLE* region for genotyping. Tagging SNPs and other potential SNPs in Table 5.2 were mapped. Boxes showed exonic regions.

Table 5.2 SNPs information on *MINCLE* region from CHB population

Location with respect to gene	Function	Total SNPs (N= 96)	Monomorphic (N= 26)	Rare SNPs (MAF< 5 %) (N= 8)	Common SNPs (≥ 5 %) (N= 62)	Tagging SNPs (No. of tagged SNP)	Other potential SNPs for genotyping
Downstream	Intergenic	7	6	-	1	-	-
3'-UTR	3'UTR	1		-	1	-	-
Gene region	Intronic	8	1	-	7	rs10841846 (2) rs4562874 (2) rs10841856 (2) rs4620776 (7)	rs4242896
Upstream	Intergenic	80	19	8	53	rs4883167 (7) rs11046143 (2) rs7959223 (7) rs10841875 (12) rs10770855 (8) rs10770856 (8)	rs10841871

MAF: Minor allele frequencies

3'-UTR: A variant of the 3' Untranslated region

5'-UTR: A variant of the 5' Untranslated region

Intergenic: A variant located in the intergenic region, between genes

Intronic: A transcript variant occurring within an intron

Monomorphic SNP: a SNP with only one type of allele (no other variant) was identified

5.3.1.3 Selection of *MARCO* SNPs

MARCO is located on the chromosome 2 with length of 52,5 kb (from 118,942,166 to 118,994,660) and has 17 exons (Figure 5.3). As with two of the above genes, I searched for the candidate SNPs across 20 kb upstream and 10 kb downstream of *MARCO* gene using the data from HCB population. There were 130 SNPs in this region, 78 of which were in the *MARCO* and concentrated in the region containing exons toward 5' end of the gene (Figure 5.3A and Table 5.3). I also observed a number of variants in the upstream toward 3' end of the gene. Out of 130 *MARCO* SNPs, 46 SNPs were monomorphic or had frequency < 5 %. Among 84 SNPs with MAF ≥ 5 %, 12 tagging SNPs were identified (Table 5.3). The rs6761637, a missense mutation in exon 10 was selected for genotyping. Finally, I had 14 *MARCO* SNPs for genotyping, all of which except rs6761637 were located in non-coding regions and their effect to the MARCO function has been unknown (Table 5.3 and Figure 5.3B).

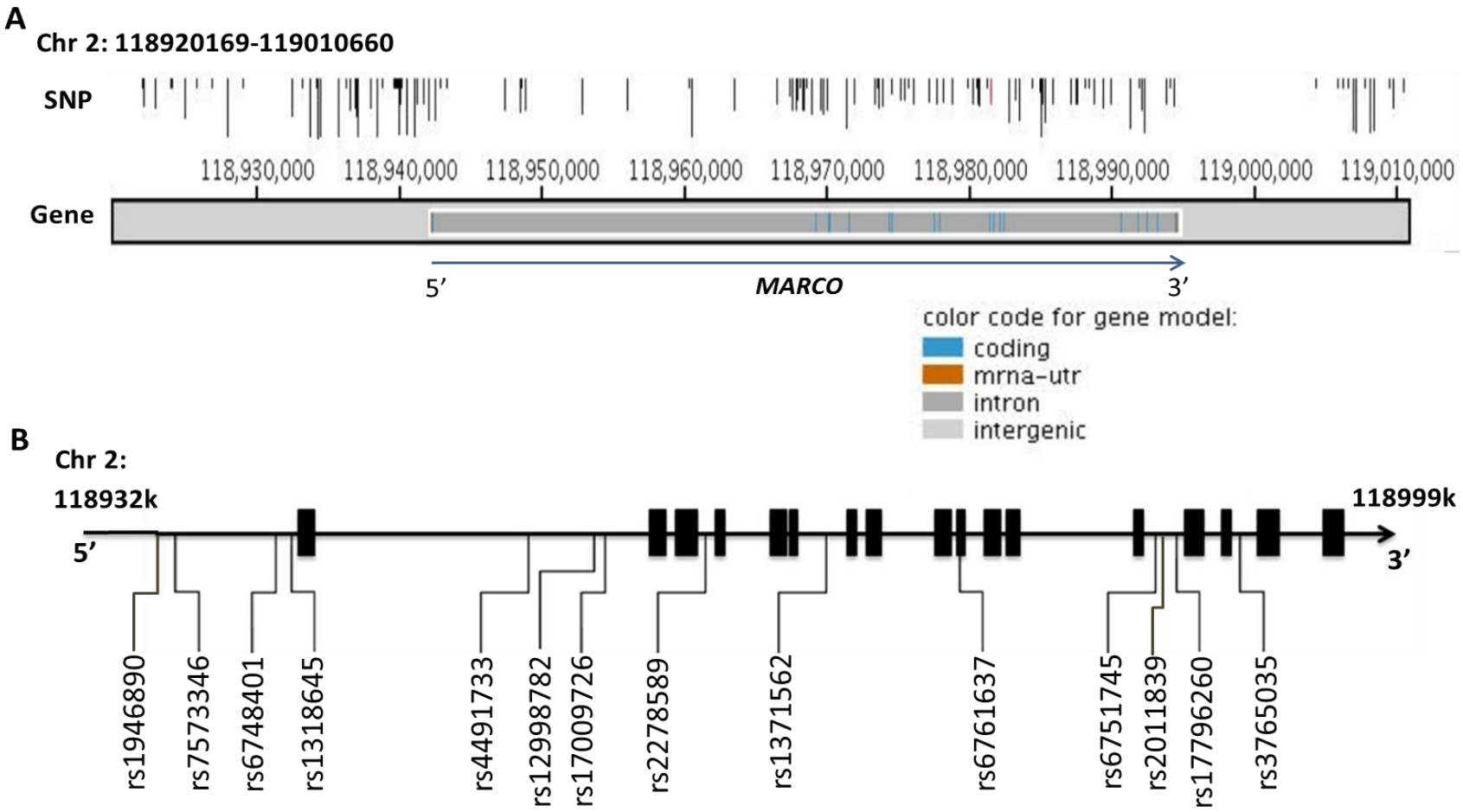

Figure 5.3 Chromosomal location and polymorphisms across *MARCO* region

(A) *MARCO* gene region and its 20 kb upstream and 10 kb downstream on chromosome 12. SNPs across the region from HCB population from International HapMap Project were presented as lines; the SNP line lengths are proportional to the minor allele frequency in the population. Figure was originated from http://gvs.gs.washington.edu build 147 based on human genome assembly GRCh38.p10. (B) Chromosomal map of candidate SNPs in *MARCO* region for genotyping. Tagging SNPs and other potential SNPs in Table 5.3 were mapped. Boxes showed exonic regions.

Table 5.3 SNPs information on *MARCO* region in CHB population

Location with respect to gene	Function	Total SNPs (N= 130)	Monomorphic (N= 42)	Rare SNPs (MAF< 5 %) (N= 4)	Common SNPs (≥ 5 %) (N= 84)	Tagging SNPs (No. of tagged SNP)	Other potential SNPs for genotyping
Upstream	Intergenic	39	16	1	22	rs1946890 (5) rs7573346 (11) rs3806496 (11) rs1318645 (5)	
Gene region	Introgenic Missense F (TTC)--> S (TCC)	78 1	20	2 1	56	rs4491733 (11) rs12998782 (10) rs17009726 (26) rs2011839 (2) rs1371562 (2) rs6751745 (4) rs17796260 (4) rs3765035 (2)	rs2278589 rs6761637
Downstream	Intergenic	12	6		6		

MAF: Minor allele frequencies

3'-UTR: A variant of the 3' Untranslated region

5'-UTR: A variant of the 5' Untranslated region

Intergenic: A variant located in the intergenic region, between genes

Monomorphic SNP: a SNP with only one type of allele (no other variant) was identified

F: Phenylalanine, S: Serine

5.3.2 Association of SNPs in phagocytic genes and TB susceptibility

I genotyped 10 SNPs in *DECTIN-1*, 12 SNPs in *MINCLE* and 14 SNPs in *MARCO* in TB cases and controls. SNPs were excluded if they had missing genotype calls> 5%, MAF< 10%, or P value for deviation from HWE of controls< 0.05 (see Section 2.10.3). After checking for quality, 1 SNP in *DECTIN-1* (rs11053589) and 3 SNPs in *MINCLE* (rs4562874, rs10841871 and rs10841875) showed P value for HWE in control< 0.05; in *MARCO*, 1 SNP (rs1946890) was monomorphic and 1 SNP (rs2011839) had 30% missing data. Finally, 9 *DECTIN-1* SNPs, 9 *MINCLE* SNPs and 12 *MARCO* SNPs, were analyzed for associations between SNPs and susceptibility to different TB clinical phenotypes (Table 5.4, 5.5, and 5.6).

5.3.2.1 Association of *DECTIN-1* SNPs and TB susceptibility

I first examined the association of *DECTIN-1* SNPs and TB susceptibility using phenotypic and allelic models. By comparing the genotype frequencies of *DECTIN-1* SNPs in TB patients and controls, I found that none of the 9 SNPs associated with PTB (P> 0.05) while 2 of them (rs7959451 and rs7137840) were associated with TBM (P= 0.027 and 0.044, respectively) (Table 5.4). However, the association did not remain significant after applying Bonferroni correction for multiple tests (rs7959451: 0.027 x 9 SNPs = 0.243, rs7137840: 0.044 x 9 SNPs = 0.396). As with the genotypic model, when I compared the allele frequency of SNPs in TB patients and controls in allelic model, none of the 9 SNPs were associated with PTB (P> 0.05) while 3 SNPs including rs7959451, rs7137840 and rs11053613 were associated with TBM (P = 0.008, 0.012, and 0.018, respectively) (Table 5.4). The association did not remain significant after applying Bonferroni correction for multiple tests of 9 SNPs.

Table 5.4 Summary of genotyped SNPs in *DECTIN-1* in Vietnamese population

rs ID **Location**	**Cases (N)** **PTB/TBM**	 **11/12/22**	**Controls (N)** **11/12/22**	 **HWE-P**	**Genotypic** **P**	**Allelic** **P**
rs7959451	PTB	244/176/24	249/173/14	0.073	0.632	0.455
UTR-3’	TBM	216/196/31			**0.027**	**0.008**
rs12829123	PTB	314/119/11	308/123/8	0.282	0.752	0.978
Intron 4	TBM	300/126/15			0.316	0.294
rs11053608	PTB	314/119/13	307/122/8	0.298	0.542	0.788
Intron 4	TBM	303/125/15			0.335	0.334
rs7137840	PTB	104/240/102	376/59/3	0.682	0.653	0.402
Intron 4	TBM	374/70/3			**0.044**	**0.012**
rs11053613	PTB	373/70/3	376/61/3	0.761	0.745	0.484
Intron 3	TBM	354/85/6			0.060	**0.018**
rs11053623	PTB	234/179/33	227/173/35	0.800	0.937	0.828
UTR-5’	TBM	213/184/48			0.257	0.110
rs11053624	PTB	234/179/33	225/176/36	0.848	0.887	0.671
900 bp upstream	TBM	213/183/48			0.345	0.169
rs7959064	PTB	268/156/23	267/147/24	0.526	0.905	0.867
1.3 Kb upstream	TBM	258/163/25			0.629	0.422
rs10845051	PTB	254/170/21	264/150/25	0.547	0.417	0.602
8.5 Kb upstream	TBM	249/172/22			0.347	0.426

1: majority allele; 2: minority allele. 11, 12, and 22: genotypes from different allelic combination.

HWE: Hardy Weinberg equilibrium; P: P value

Genotypic is the comparison of genotype frequencies (11, 12, and 22) between cases and controls; Allelic is the comparison of allele frequencies (allele 1 and 2) between cases and controls

Numbers in bold in Genotypic P and Allelic P columns represent P value < 0.05

5.3.2.2 Association of *MINCLE* SNPs and TB susceptibility

I did not observe the association of any 9 SNPs in this gene with either TBM or PTB using the genetic model (Table 5.5). Whereas in the allelic model, I found 2 SNPs (rs10770855 and rs10770856) were associated with TBM but not PTB (TBM: P= 0.017, 0.028 respectively) (Table 5.5). However, after applying Bonferroni correction, none of the 2 SNPs remained the significant association.

Table 5.5 Summary of genotyped SNPs in *MINCLE* in Vietnamese population

rs ID	**Cases (N)**		**Controls (N)**		**Genotypic**	**Allelic**
Location	**PTB/TBM**	**11/12/22**	**11/12/22**	**HWE-P**	**P**	**P**
rs10841846	PTB	119/227/98	129/219/87	0.733	0.574	0.296
Intron 5	TBM	123/229/84			0.779	0.502
rs4562874	PTB	143/219/84	147/222/71	0.400	0.569	0.385
Intron 3	TBM	146/220/79			0.814	0.632
rs10841856	PTB	143/219/84	197/196/45	0.299	0.452	0.312
Intron 1	TBM	177/206/66			0.689	0.477
rs4620776	PTB	168/216/61	162/218/57	0.219	0.646	0.997
Intron 1	TBM	175/208/62			0.913	0.764
rs4883167	PTB	181/208/53	176/213/49	0.195	0.875	0.994
700 bp upstream	TBM	179/201/60			0.477	0.667
rs11046143	PTB	413/35/1	413/29/0	0.476	0.388	0.346
1.4 Kb upstream	TBM	412/36/0			0.397	0.397
rs7959223	PTB	174/214/59	167/220/53	0.131	0.782	0.968
4 Kb upstream	TBM	180/205/57			0.561	0.670
rs10770855	PTB	154/229/62	180/201/60	0.744	0.145	0.150
11Kb upstream	TBM	150/218/78			0.057	**0.017**
rs10770856	PTB	170/228/48	197/196/45	0.714	0.109	0.093
11.8 Kb upstream	TBM	177/206/66			0.075	**0.028**

1: majority allele; 2: minority allele. 11, 12, and 22: genotypes from different allelic combinations

HWE: Hardy Weinberg equilibrium; P: P value

Genotypic is the comparison of genotype frequencies (11, 12, and 22) between cases and controls; Allelic is the comparison of allele frequencies (allele 1 and 2) between cases and controls

Numbers in bold in Genotypic P and Allelic P columns represent P value < 0.05

5.3.2.3 Association of *MARCO* SNPs and TB susceptibility

For *MARCO*, none of the 12 SNPs were associated with TBM, while 3 of them were associated with PTB using the genotypic model (rs6748401, P= 0.039; rs2278589, P= 0.004; rs6751745, P= 0.011) (Table 5.6). However, the allelic model did not show any association of the *MARCO* SNPs and TB (Table 5.6). In genotypic model, only rs2278589 remained significant after Bonferroni correction for multiple tests (0.004 x 12 SNPs= 0.048). When I analyzed the linkage disequilibrium of the *MARCO* SNPs, I found that among these 3 associated SNPs, rs2278589 was in high LD (D'= 1, r^2= 0.88) with rs6751745 but not with rs6748401 in our Vietnamese Kinh control population (Figure 5.4A, B). I further investigated the association of two SNPs in high LD mentioned above with PTB using additional genetic models including heterozygote, dominant and recessive. I found that the heterozygous advantage model displayed a significant association of rs2278589 and rs6751745 heterozygous genotypes with susceptibility to PTB (rs2278589; P= 0.001, OR= 1.6 and rs6751745; P= 0.009, OR= 1.4; Table 5.7). Associations between these 2 SNPs with PTB in this model remained significant after Bonferroni correction (Table 5.7).

Collectively, there was no association of *DECTIN-1* and *MINCLE* SNPs with susceptibility to clinical TB phenotypes while the heterozygote genotypes of two SNPs in the *MARCO* gene were associated with PTB, but not with TBM. Therefore, I mainly focused on these *MARCO* SNPs for functional studies.

Table 5.6 Summary of genotyped SNPs in *MARCO* in Vietnamese population

rs ID Location	Cases (N) PTB/TBM	 11/12/22	Controls (N) 11/12/22	 HWE-P	Genotypic P	Allelic P
rs7573346 4.9 Kb upstream	PTB TBM	131/233/84 127/216/101	122/213/105	0.524	0.175 0.913	0.159 0.679
rs6748401 1.5 Kb upstream	PTB TBM	108/245/90 115/223/109	120/215/100	0.845	**0.039** 0.788	0.063 0.495
rs1318645 3 bp upstream	PTB TBM	109/246/92 115/223/109	119/215/100	0.879	0.057 0.815	0.079 0.525
rs4491733 intron 1	PTB TBM	104/240/102 120/222/101	114/228/93	0.290	0.593 0.782	0.342 0.909
rs12998782 intron 1	PTB TBM	228/184/34 239/168/33	243/160/31	0.510	0.345 0.883	0.207 0.634
rs17009726 intron 1	PTB TBM	331/110/8 342/99/5	340/94/6	0.863	0.456 0.911	0.211 0.100
rs2278589 intron 3	PTB TBM	165/245/35 194/203/47	194/190/48	0.885	**0.004** 0.871	0.286 0.878
rs1371562 intron 6	PTB TBM	289/141/15 286/140/15	284/138/15	0.724	0.998 0.998	0.996 0.978
rs6761637 exon 10	PTB TBM	323/114/8 333/101/6	335/89/9	0.289	0.202 0.519	0.169 0.761
rs6751745 intron 13	PTB TBM	194/225/27 223/178/39	210/181/43	0.663	**0.011** 0.752	0.807 0.451
rs17796260 intron 13	PTB TBM	293/139/13 292/136/14	283/135/18	0.708	0.622 0.739	0.566 0.573
rs3765035 intron 15	PTB TBM	145/251/49 183/199/60	152/220/60	0.164	0.210 0.149	0.949 0.155

1: majority allele; 2: minority allele. 11, 12, and 22: genotypes from different allelic combinations

HWE: Hardy Weinberg equilibrium; P: P value

Genotypic is the comparison of genotype frequencies (11, 12, and 22) between cases and controls; Allelic is the comparison of allele frequencies (allele 1 and 2) between cases and controls. Numbers in bold in Genotypic P and Allelic P columns represent P value < 0.05

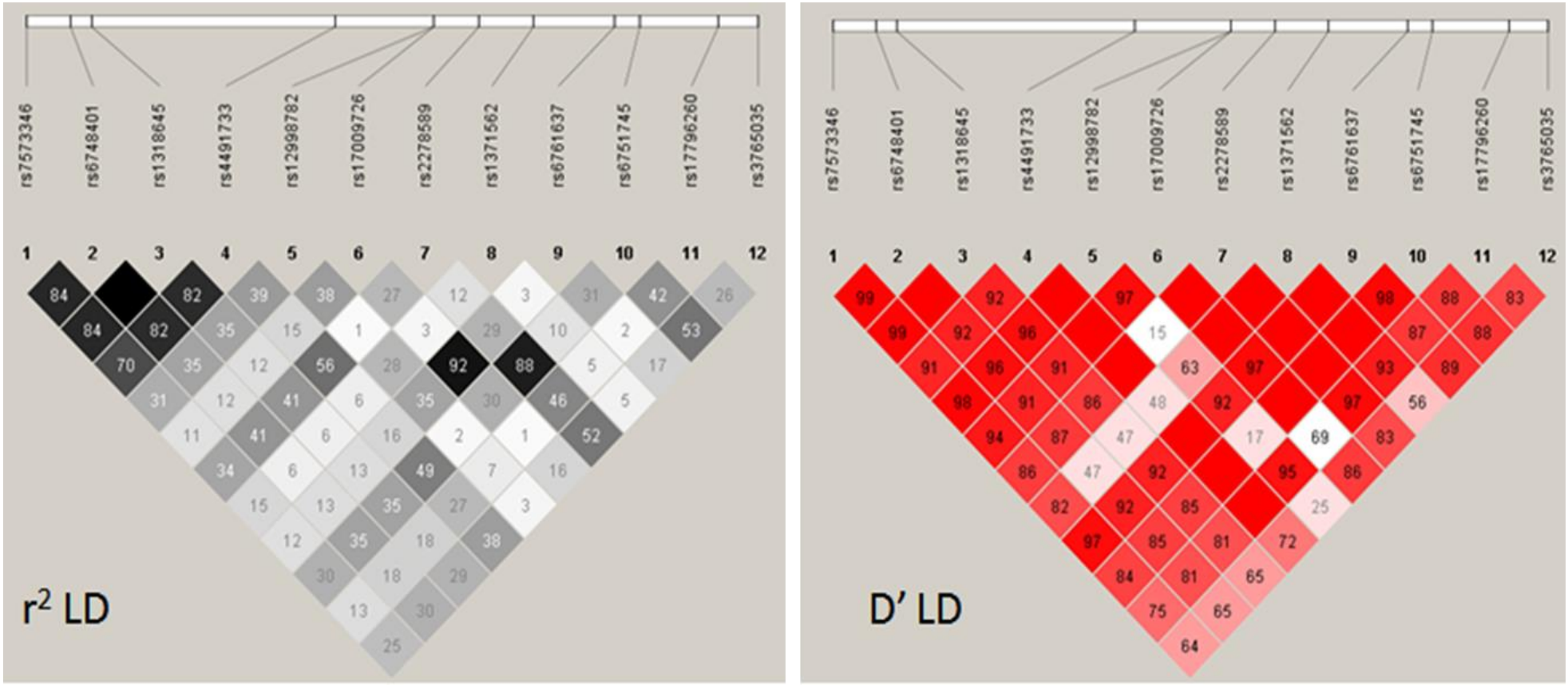

Figure 5.4 Linkage disequilibrium of *MARCO* polymorphisms in a Vietnamese cohort

(A, B) Linkage disequilibrium values (r^2 and D') between SNPs were generated by Haploview 4.2 using the genotype data from the control population (Vietnamese Kinh). Empty squares indicate complete linkage disequilibrium (r^2 or D'=1).

Table 5.7 *MARCO* SNPs rs2278589 and rs6751745 are associated with PTB

SNP	**rs2278589**			**rs6751745**		
Genotypes	11 (N, %)	12 (N, %)	22 (N, %)	11 (N, %)	12 (N, %)	22 (N, %)
Control	194 (0.45)	190 (0.44)	48 (0.11)	210 (0.48)	181 (0.42)	43 (0.10)
PTB	165 (0.37)	245 (0.55)	35 (0.08)	194 (0.43)	225 (0.50)	27 (0.06)
Comparison models	P	P*	OR (95%CI)	P	P*	OR (95%CI)
Dominant	0.101	0.202	1.5 (0.9-2.3)	**0.035**	0.070	1.7 (1.0-2.8)
Recessive	**0.018**	**0.036**	0.7 (0.5-0.9)	0.146	0.292	0.8 (0.6-1.1)
Heterozygous	**0.001**	**0.002**	1.6 (1.2-2.0)	**0.009**	**0.018**	1.4 (1.1-1.8)

1: majority allele; 2: minority allele; 11, 12, and 22: genotypes from different allelic combinations

Dominant is the comparison of (11+12) vs. 22 between cases and controls; Recessive is the comparison of 11 vs (12+22) between cases and controls; Heterozygous is the comparison of (11+22) vs. 12 between cases and controls

P: P value

P*: corrected P value, Bonferroni correction by 2 SNPs (P value x 2)

OR (95%CI): odds ratio (95% confidence interval)

5.3.3 *MARCO* polymorphisms are associated with chest X-ray presentation

To investigate whether *MARCO* polymorphisms influence clinical presentation or disease outcome, I examined the relationship between the two associated SNPs (rs2278589 and rs6751745), pre-treatment CXR abnormalities, and 8-month treatment outcomes. Patients enrolled in this study were sputum smear-positive for pulmonary TB before treatment. Pre-treatment CXR showed 427/429 (99.5%) were abnormal with evidence of nodules (139, 32.4%), infiltrates (407, 94.9%), consolidation (40, 9.3%), and cavities (139, 32.4%).

SNPs rs2278589 and rs6751745 were associated with severity of CXR abnormality. SNP rs2278589 was associated with intermediate and severe CXR abnormality in the heterozygote model (P= 0.008 intermediate; P= 0.007 severe, OR= 1.6; Table 5.8). SNP rs6751745 was also associated with severe CXR abnormality in the heterozygote model (P= 0.007, OR= 1.6; Table 5.8).

There was no association between rs2278589 and rs6751745 genotype and poor treatment outcome (29/429, 6%), which was defined by death, or failure to convert to sputum smear negativity, however this may be due to the lack of events in this dataset and consequent lack of statistical power.

Table 5.8 *MARCO* SNPs rs2278589 and rs6751745 are associated with level of CXR abnormality in PTB patients

Abnormality level	Genotype (N, %)			Genotypic	Heterozygous	
	GG	AG	AA	P	P	OR (95%CI)
rs2278589						
Controls	194 (0.45)	190 (0.44)	48 (0.11)			
Mild	26 (0.38)	39 (0.57)	4 (0.06)	0.112	0.052	1.7 (1.0-2.7)
Intermediate	67 (0.37)	101 (0.56)	13 (0.07)	**0.022**	**0.008**	1.6 (1.1-2.3)
Severe	60 (0.35)	96 (0.56)	15 (0.09)	**0.026**	**0.007**	1.6 (1.1-2.3)
rs6751745						
Controls	210 (0.48)	181 (0.42)	43 (0.10)			
Mild	31 (0.44)	35 (0.50)	4 (0.06)	0.314	0.193	1.4 (0.8-2.3)
Intermediate	82 (0.45)	90 (0.50)	9 (0.05)	0.055	0.068	1.4 (1.0-2.0)
Severe	68 (0.40)	92 (0.54)	11 (0.06)	**0.026**	**0.007**	1.6 (1.1-2.3)

CXR: Chest X-ray; P: P value; OR (95%CI): odds ratio (95% confidence interval)

Genotypic is the comparison of genotype frequencies (genotype GG, AG and AA) between cases with Mild/Intermediate/Severe CXR and controls; Heterozygous is the comparison of (GG+AA) vs. AG between cases with Mild/Intermediate/Severe CXR and controls

Mild: abnormal features (nodules, infiltrates, consolidation, cavities or miliary TB) on a chest radiograph were present in one lobe; Intermediate: abnormal features were present in one lung; Severe: abnormal features were present in both lungs

Numbers in bold represent P value <0.05

5.3.4 MARCO polymorphisms are associated with Beijing lineage

Our previous studies have reported association between lineages of *Mtb*, particularly the modern East Asian/Beijing lineage, with TB clinical phenotypes[20,70]. Given a worldwide emergence of *Mtb* East Asian/Beijing strains[42], I hypothesized that variation in the scavenger receptor gene *MARCO* might be preferentially associated with a specific lineage. Therefore, I next examined whether the rs2278589 and rs6751745 genotypes are associated with infection caused by a particular bacterial lineage and whether this relationship influences disease phenotype.

The genotypic frequencies of rs2278589 and rs6751745 in all PTB patients (N= 445) and in those patients where the lineage of the infecting *Mtb* isolate was determined (N= 370), were compared with controls (Table 5.9). There was no significant association between the two SNPs and infection with either Indo-Oceanic or Euro-American lineage, or when combined as non-Beijing lineages (Table 5.9). However, I found a significant association between these SNPs and infection with East Asian/Beijing isolates in a genotypic comparison (rs2278589, P= 0.005; rs6751745, P= 0.033), and in a heterozygous model (rs2278589, P= 0.001, OR= 1.7; rs6751745, P= 0.012, OR= 1.5; Table 5.9).

Table 5.9 *MARCO* SNPs rs2278589 and rs6751745 are associated with the Beijing strain

Group	**Genotype (N, %)**			**Genotypic**	**Heterozygous**	
	GG	**AG**	**AA**	**P**	**P**	**OR (95%CI)**
rs2278589						
Controls	194 (0.45)	190 (0.44)	48 (0.11)			
PTB	165 (0.37)	245 (0.55)	35 (0.08)	**0.004**	**0.001**	1.6 (1.2-2.0)
All isolates	135 (0.36)	205 (0.55)	30 (0.08)	**0.005**	**0.001**	1.6 (1.2-2.1)
Non-Beijing	61 (0.42)	77 (0.53)	8 (0.05)	0.060	0.066	1.4 (1.0-2.1)
East Asian/Beijing	74 (0.33)	128 (0.57)	22 (0.10)	**0.005**	**0.001**	1.7 (1.2-2.3)
rs6751745						
Controls	210 (0.48)	181 (0.42)	43 (0.10)			
PTB	194 (0.43)	225 (0.50)	27 (0.06)	**0.011**	**0.009**	1.4 (1.1-1.9)
All isolates	161 (0.47)	187 (0.48)	23 (0.05)	**0.021**	**0.014**	1.4 (1.1-1.9)
Non-Beijing	68 (0.47)	70 (0.48)	8 (0.05)	0.174	0.188	1.3 (0.9-1.9)
East Asian/Beijing	93 (0.41)	117 (0.52)	15 (0.07)	**0.033**	**0.012**	1.5 (1.1-2.1)

P: P value; OR (95%CI): odds ratio (95% confidence interval)

Genotypic is the comparison of genotype frequencies (genotype GG, AG and AA) between cases stratified by *Mtb* lineage and controls; Heterozygous is the comparison of (GG+AA) vs. AG between cases stratified by *Mtb* lineage and controls

Numbers in bold represent P value <0.05

5.3.5 Association of *MARCO* SNPs with macrophage phagocytosis, mRNA expression and cytokines in response to *Mtb*

MARCO is a phagocytic receptor on macrophages which binds bacteria and facilitates phagocytosis to control and clear the pathogens[325,330,331]. Therefore, I examined whether *MARCO* SNPs are associated with susceptibility to TB and disease severity since these SNPs influence macrophage phagocytosis, gene expression, and cytokine profiles.

I genotyped twelve *MARCO* tagging SNPs from 41 volunteers and performed phagocytosis assays (this data was a subset of LTB dataset in Chapter 4). 10 SNPs in *MARCO* that were not associated with PTB were also not associated with phagocytosis of any IgG, TDM or β-glucan beads except for rs4491433 (β-glucan beads, P= 0.02) (Figure 5.5). The genotypes of both rs2278589 and rs6751745, were associated with phagocytosis of either TDM or β-glucan beads, but were not associated with phagocytosis of IgG beads (Figure 5.6A, 5.6B). Since the heterozygote genotypes of these two SNPs displayed significant association with susceptibility to PTB, I wondered whether the heterozygotes could influence the phagocytosis. Our results showed that heterozygous genotypes of both SNPs were associated with reduced phagocytosis of TDM and β-glucan beads (rs2278589, P= 0.04 and 0.03; rs6751745, P= 0.01 and 0.007) (Figure 5.6A, 5.6B).

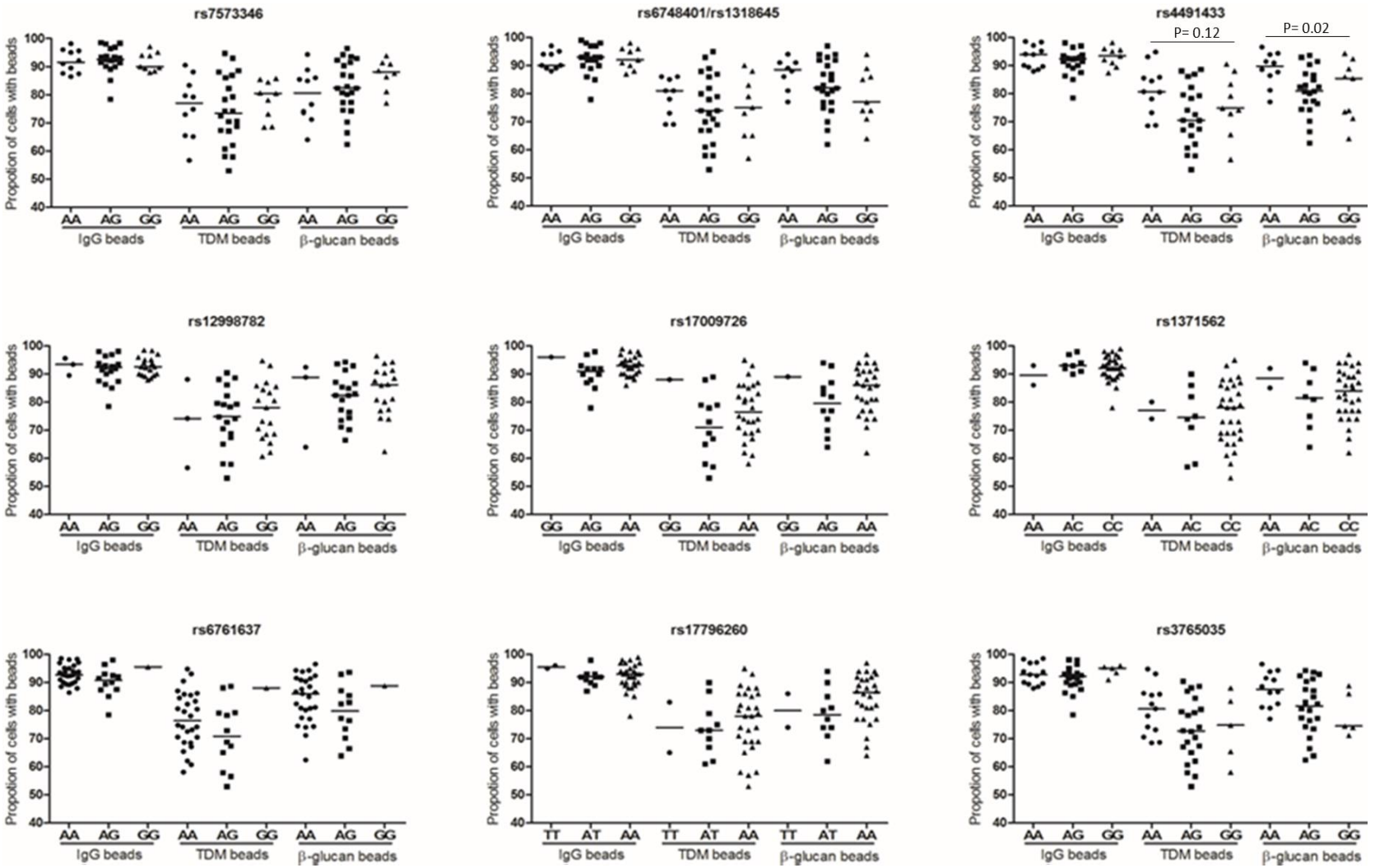

Figure 5.5 Phagocytic ability of macrophages from healthy subjects

Macrophage phagocytosis of IgG, TDM and β-glucan beads was plotted by *MARCO* SNP genotype. Data is shown for 10 tagging SNPs in 41 healthy subjects. Bars in plots represent median values. Comparisons across three groups of genotypes were performed by using one-way ANOVA.

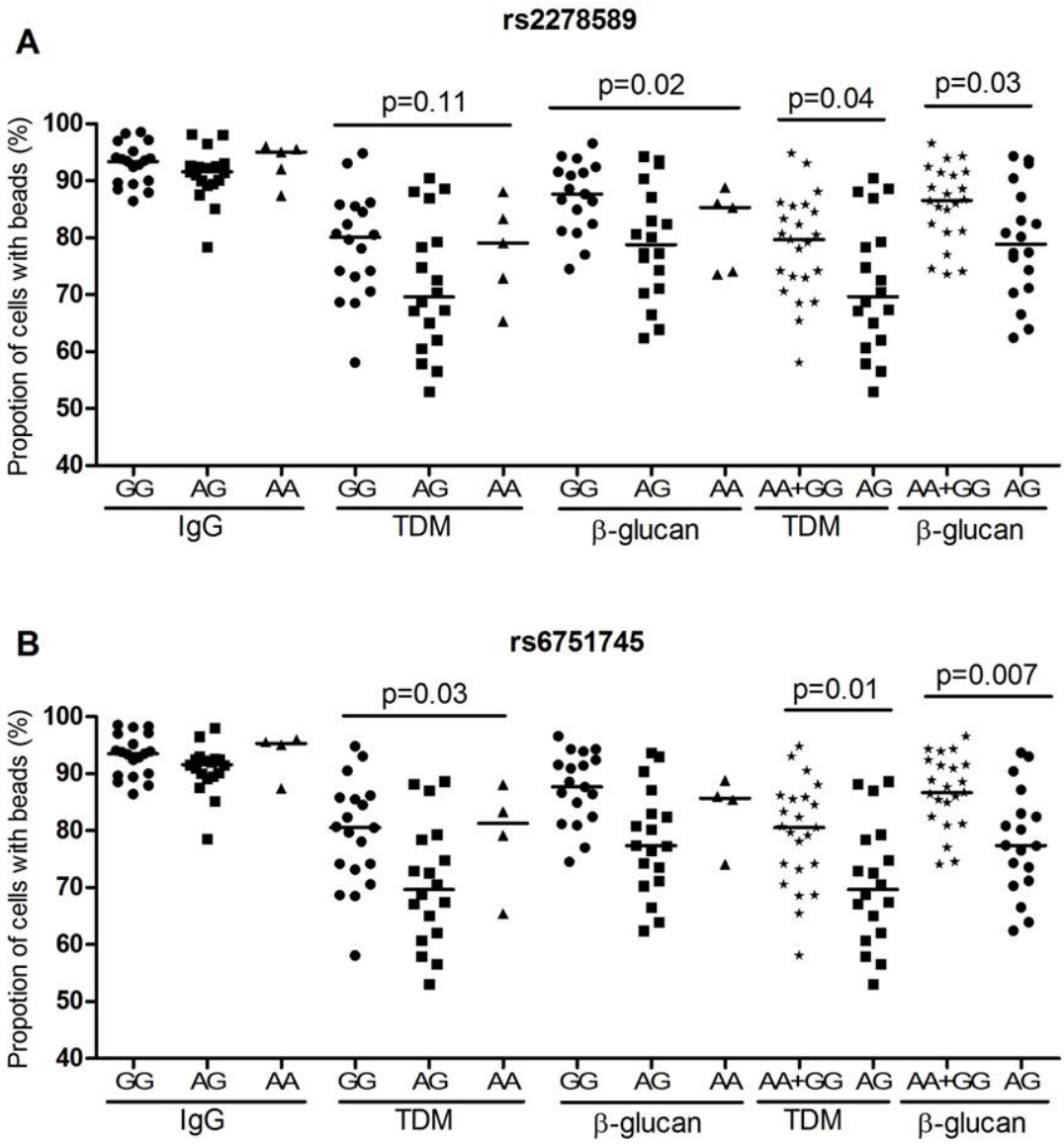

Figure 5.6 Phagocytic ability of macrophages from healthy subjects

Macrophage phagocytosis of beads was assessed according to *MARCO* SNP genotypes in healthy subjects; (A) rs2278589 (18 GG, 18 AG, 5 AA) and (B) rs6751745 (19 GG, 18 AG, 4 AA). Bars in plots represent median values. Comparisons across three groups of genotypes were performed by using one-way ANOVA, or two groups by using Mann-Whitney U test.

I also examined the association of *MARCO* SNPs rs2278589 and rs6751745 with mRNA expression or cytokines in PBMCs from 31 healthy subjects. *MARCO* mRNA

levels were up-regulated approximately 2 fold in PBMCs stimulated with LPS or *Mtb* whole cell lysate compared with un-stimulated cells (Figure 5.7A). The genotypes of rs2278589 and rs6751745 were marginally associated with *MARCO* mRNA expression in cells stimulated with *Mtb* (Figure 5.7B) (P= 0.068 and 0.039 respectively). For the heterozygous model, the AG genotype of these two SNPs was not significantly associated with reduced levels of *MARCO* mRNA in PBMCs stimulated with *Mtb*. For cytokine production, PBMCs were activated and produced pro-inflammatory cytokines TNF-α and IL-1β in response to both TDM and *Mtb* lysate. The anti-inflammatory cytokine IL-10 was induced by *Mtb* lysate stimulation, but not TDM (Figure 5.7C). In TDM or *Mtb* lysate stimulated cells, there was no significant association of the two SNP genotypes with TNF-α, IL-1β and IL-10 levels (Figure 5.7D-E for rs2278589, and F-G for rs6751745).

Collectively, these data showed that the AG genotype of rs2278589 and rs6751745 in *MARCO* was not associated with *MARCO* mRNA expression or cytokine concentrations in PBMCs, but it was associated with reduced phagocytosis activated via TDM and β-glucan in macrophages.

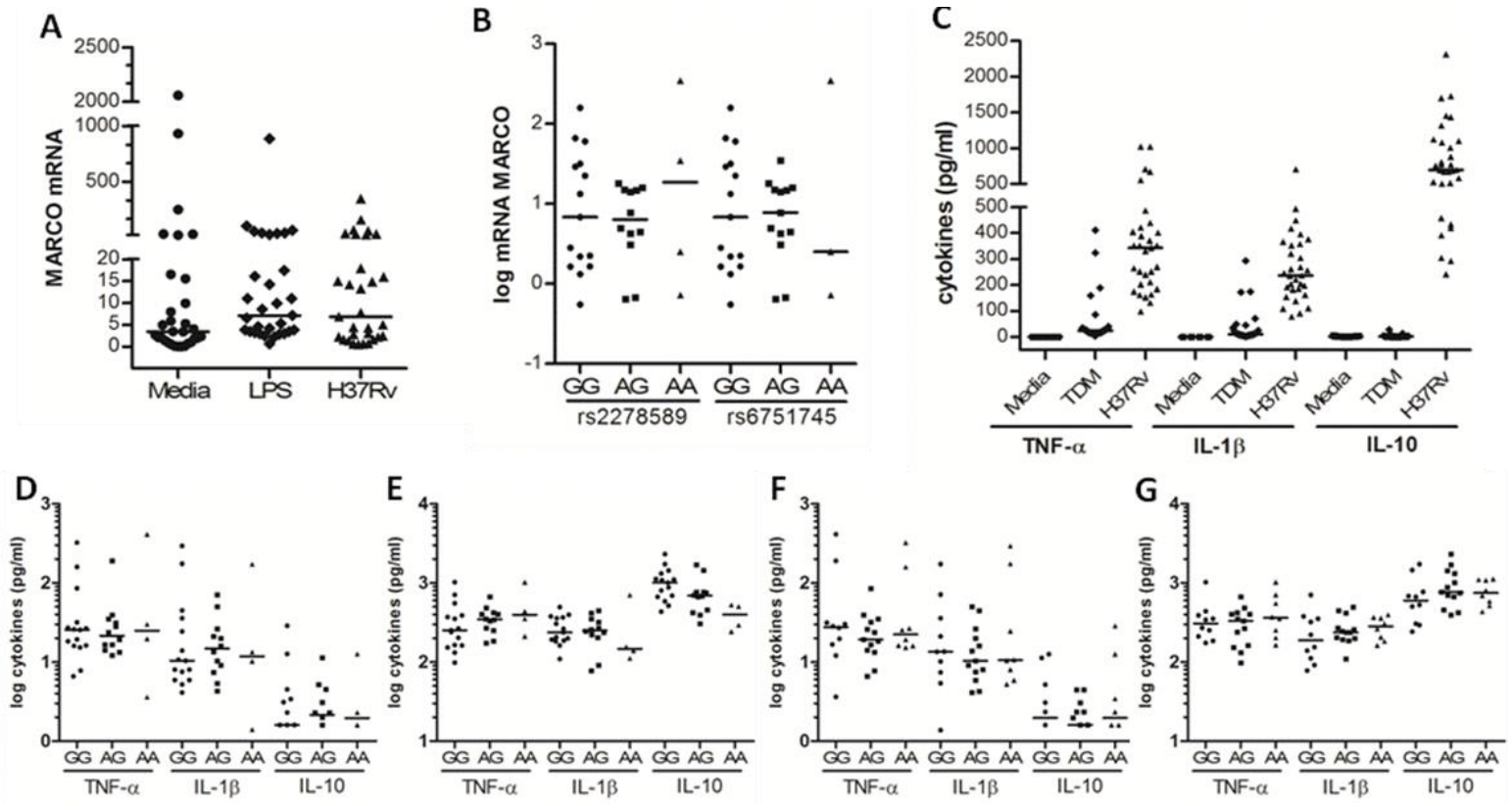

Figure 5.7 *MARCO* polymorphisms and variation in mRNA expression or cytokine production from healthy subjects

(A) mRNA was isolated from monocytes stimulated with Media, LPS at 100 ng/ml or *Mtb* whole cell lysate at 5µg/ml. *MARCO* mRNA expression was measured and normalizes to GAPDH. (B) Association of MARCO mRNA expression from cells stimulated with *Mtb* whole cell lysate was analysed with SNPs in *MARCO*: rs2278589 (4 AA, 12 AG, 15 GG), P= 0.068 and rs6751745 (3 AA, 13 AG, 15 GG), P= 0.039. (C) Cytokines were measured from monocytes stimulated with media alone, TDM at 100µg/ml or *Mtb* whole cell lysate at 25µg/ml. Cytokines from cells stimulated with TDM (D) or *Mtb* whole cell lysate (E) were analysed with SNP rs2278589 (4 AA, 12 AG, 15 GG). Cytokines from cells stimulated with TDM (F) or *Mtb* whole cell lysate (G) were analysed with SNP rs6751745 (3 AA, 13 AG, 15 GG). Data were collected from duplicate samples. Bars in plots represent median values. Comparisons across three genotypes were performed by using one-way ANOVA.

5.4 Discussion

I found, among three genes examined, that polymorphisms in *MARCO* (rs2278589 and rs6751745) were associated with increased susceptibility to pulmonary TB and severe chest radiography abnormality. The SNP genotypes were also associated with a reduction of phagocytosis of beads coated with pathogen-derived ligands, TDM from *Mtb*. Our results suggest that these polymorphisms may regulate phagocytosis of *Mtb*, and impairment of phagocytic ability could increase susceptibility to, and severity of, pulmonary TB. The *MARCO* genotypes were preferentially associated with Beijing rather than Indo-Oceanic or Euro-American lineage, which implies that *MARCO* genotype may increase the susceptibility to tuberculosis particularly of the Beijing lineage.

This is the first study investigating the association of *DECTIN-1* polymorphisms in TB susceptibility, however I did not observe any association. Consistent with our findings in our Vietnamese population, a genetic study in South African coloured (SAC) population did not find an association between *MINCLE* SNPs with TB either[201]. Although *DECTIN-1* and *MINCLE* may not be associated with TB susceptibility, its function in the human immune system cannot be discounted[306,315,316,321,332]. Since *Mtb* engages a wide range of host receptors to initiate the immune response [36,87,120], it is possible that the influence of *DECTIN-1* and *MINCLE* SNPs on disease susceptibility could be compensated by other receptors.

Scavenger receptors on human monocytes have been found to bind to β-glucan[333], and *MARCO* on macrophages treated with CpG-containing oligodeoxynucleotides (CpG-ODN), a ligand for TLR9) has been found to participate in the uptake of zymosan (which is derived from β-glucan)[334]. In line with these findings, I observed the

association of *MARCO* SNPs with phagocytosis of β-glucan beads similar to TDM beads, suggesting that β-glucan might be a ligand for *MARCO*.

MARCO plays a key role in bacterial phagocytosis and clearance[325,330,335]. Recognition of TDM by MARCO, in conjunction with TLR2/CD4, activates transcriptional expression of immunity genes[336] and cytokine production[294]. However, no studies have yet shown the influence of *MARCO* genetic variation on the antimicrobial activity of macrophages such as phagocytosis or immune response. In this study, I found that *MARCO* SNPs rs2278589 and rs6751745 were not associated with gene expression and cytokine production in PBMCs but were associated with reduced phagocytosis of beads coated with pathogen-derived ligands, TDM or β-glucan in macrophages. I found that *MARCO* polymorphisms were not associated with cytokine production while in murine studies, macrophages from *Marco*-deficient mice were associated with a reduction of TNFα, IL-6 and IL-1β cytokine production. The difference in the study design could account for the differences seen in cytokine production between these two studies. I used human PBMCs, whereas in study of Bowdish *et al.*[294] murine macrophages were used. In the macrophages from knockout mice, *Marco* was absent, potentially having a major impact. In our study, MARCO was still produced, albeit a variant of *MARCO* with an unknown and potentially smaller impact. Another reason for the difference may be the limited numbers of samples in our study once stratified by genotype.

MARCO is involved in phagocytosis of bacteria, a step in pathogenesis which may be important in the development of pulmonary TB in the early phase of infection. The heterozygous genotypes of two *MARCO* SNPs were associated with reduced macrophage phagocytic function. The impairment of phagocytosis at the beginning of infection reduces the number of macrophages infected with *Mtb*, which then limits

microbial killing and antigen presentation to lymphocytes[275,293]. The consequence of this could be the inadequate induction of innate and adaptive immune responses against *Mtb*, potentially increasing the susceptibility to active disease. Deficient responses could also lead to increased microbial replication, which could manifest as severe abnormalities on CXR, as observed in TB patients carrying the heterozygous genotypes. Together, our data suggest that TB susceptibility and disease severity in patients with the *MARCO* AG genotype may be due to impairment of *Mtb* phagocytosis.

Our results show that variations in human *MARCO* gene were associated with susceptibility to pulmonary TB in the Vietnamese Kinh population. The associated intronic SNPs rs6748401 and rs2278589 are part of a wide haplotype block, suggesting they are markers in high LD with the unknown causative SNP(s). Two *MARCO* SNPs (rs17009726 or rs4491733) were previously associated with TB susceptibility in the Han Chinese Beijing and Gambian populations[326,327], however I did not observe any association with these SNPs in our TB population. Conversely, the associated SNPs (rs6748401 and rs2278589) described in this study were not associated in the Gambian population and were not genotyped in the Chinese population. The discrepancy in our results may be due to different population LD structure. The frequencies of the associated SNPs found in the three studies were very different based on the 1000 Genomes Project (http://www.ncbi.nlm.nih.gov/projects/SNP; rs17009726 minor allele frequency in African 0.0008, Ad Mixed American 0.0014, European 0.0060, East Asian 0.1210 and South Asian 0.1483 super populations) and overall linkage (D' plots) across the *MARCO* SNPs in three populations are visually different (figure 5.5 and [326,327]). LD in the Vietnamese Kinh population across this gene region contains larger haplotype blocks with more SNPs compared to both the Han Chinese (HCB) and Gambian

populations. The differing population structures in this gene region may account for the inability to replicate individual SNP associations, however the accumulated evidence across these populations suggests that *MARCO* variation contributes to pulmonary TB susceptibility.

The remarkable emergence of Beijing lineage worldwide, including Vietnam, supports the hypothesis that the variation in the scavenger receptor *MARCO*, which binds *Mycobacterium* and promotes macrophage internalization, might support the emergence of the Beijing lineages. Our data shows associations of both *MARCO* variants with *Mtb* lineage and TB susceptibility suggesting potential role of host-pathogen co-evolution, as reported previously with *TLR2*, *EREG,* and *NRAMP1*[20,199,337]. Our associated SNPs may be markers of non-synonymous structural variants of MARCO that effects ability to bind ligands from Beijing lineage strains, reducing phagocytosis and increasing susceptibility to TB. Host-pathogen co-evolution in tuberculosis needs to be studied on a larger scale with respect to patients and genes, coupled with functional studies to determine the underlying mechanisms.

In conclusion, out of the three phagocytic genes examined, *MARCO* is likely to play an important role in TB susceptibility. Our results suggest that *MARCO* polymorphisms may regulate phagocytosis of *Mtb*, influence pathogen clearance and thus increase susceptibility to and severity of pulmonary tuberculosis. The results also suggest that *MARCO* genotype and Beijing strains may interact to increase the risk of pulmonary tuberculosis.

Chapter 6

VIRULENCE OF *MTB* CLINICAL STRAINS AND ITS ASSOCIATION TO BACTERIA GENOTYPE AND HOST IMMUNE RESPONSE

6.1 Introduction

Together with host genetic and physiological factors, the virulence of *Mtb* strains is thought to contribute to TB susceptibility[338]. Understanding *Mtb* virulence and its determinants could help us to understand how the bacteria survive from host defense to cause disease, which is important in regard to efforts at TB control and improvement of TB treatment.

There are different models and measurements to evaluate the virulence of *Mtb*. It can be assessed experimentally by the *Mtb* burden in the organs of infected animals such as mice or guinea pigs, or ability to cause the lung pathology or the death of the host. Many studies have shown that virulent *Mtb* strains are associated with the rapid growth in the lung, severe lung histopathology and the earlier death of infected animals[51,58,338]. *Mtb* virulence can also be gauged by intracellular growth in macrophage model *in vitro*, including murine or human macrophage cell lines or primary macrophages. In these models, the virulent *Mtb* strains are shown to grow more rapidly than avirulent or attenuated bacteria[260,290,339]. *Mtb* is obligate pathogen that requires human infection to replicate and spread, hence the ability to transmit is also considered as a measurement for *Mtb* virulence. The more transmissible a bacteria is, higher the virulence it is[66]. As an intracellular bacterium, *Mtb* also needs to escape from macrophages for new infection. Therefore, many studies have showed that host cell cytotoxicity is associated with the *Mtb* virulence[47,69,340].

Pro-inflammatory cytokine signaling is crucial for the host immune response against infection of intracellular pathogens such as *Mtb*[341]. Insufficient amount of these cytokine could increase the susceptibility to TB[14]. In consistency with this, virulent *Mtb* strains are demonstrated to reduce production of inflammatory cytokines and induce

production of anti-inflammatory cytokines in the host[51,53,61]. It could be that, by biasing the host immunity towards a non-protective response, the virulent *Mtb* strains are able to rapidly grow and lead to the disease development.

Thanks to the development of new molecular biology techniques, *Mtb* has been known to have a wide range of genetic variation determined by deletion, repetition and polymorphisms on the genome[342]. Based on these variations, *Mtb* isolates were globally categorized into 7 main lineages, comprising East-Asian/Beijing, Indo-Oceanic, East African-Indian, Euro-American, *M. africanum* West African-1 and 2 and Ethipoian[38]. Some of these lineages are present worldwide while others are restricted to specific global regions. A number of studies have indicated that such genetic diversity influences the transmissibility and virulence of clinical *Mtb* isolates, host immune response and clinical picture they evoke[20,66,70,343]. However, to my knowledge, analysis of the virulence of clinical isolates have mainly been restricted to a very few isolates.

In this study, I evaluated the variation in virulence indicated by the host cell lysis of a large number of clinical *Mtb* isolates. I hypothesized that there was variation in the virulence among different clinical *Mtb* strains and the variation was associated with distinct host immune responses and lineage-specific strains.

6.2 Study design

159 clinical *Mtb* isolates were collected from PTB patients from district TB control units in HCMC, Vietnam between January 2015 and October 2016 (see Section 2.8.2). Among them, 84 patients participated in the study of antimicrobial function of macrophages in TB (Chapter 4). I established the infection of these isolates at MOI 1 in human macrophage cell lines (see Section 2.8.3). To assess *Mtb* virulence, host cell

lysis of infected macrophages was monitored daily under a light microscopy (see Section 2.8.6). The stability of *Mtb* virulence after *in vitro* serial passages or in primary hMDM was also examined. The cytokine expression in hMDM infected with *Mtb* clinical isolates was measured (see Section 2.9.3) to investigate the association of macrophage responses and *Mtb* virulence. I also studied whether *Mtb* growth rate or strain genetic factor determines the virulence phenotypes. *In vitro* growth rate of bacteria was measured as detailed in section 2.8.4. *Mtb* strains were genotyped by LSP to identify the global lineages as detailed in Section 2.12.

6.3 Results

6.3.1 Diversity in virulence of different *Mtb* clinical isolates

To examine the variation in virulence of different *Mtb* strains, 159 clinical isolates and the lab strain H37Rv, as a reference, were used to infect the human macrophage-like cell line, PMA-treated THP-1, and the host cell lysis was observed during 6 days post infection (Figure 6.1). During the first two days of infection, infected macrophages were observed to be still adherent and intact as were the controls. However after 3 days, several isolates induced cell death more readily than others, with up to 50 % cells infected with these strains being lysed. From day 4 and afterwards, there was significant variation on the level of cell lysis of THP1 infected with different isolates, which ranged from 0 % to 100 %. Up to day 6 I still observed different patterns where macrophages infected with a number of isolates were lysed completely whereas macrophages infected with other isolates remained intact. These results suggested that different isolates could have specific interaction with macrophages, leading to different outcomes of cell lysis. As such, cell lysis could be used as a maker for bacterial virulence.

Regarding host cell lysis at day 6 post-infection, I grouped clinical isolates into three different phenotypes of virulence: high virulence when ≥ 90 % infected cells were lysed, low virulence when ≤ 5 % infected cells were lysed, and moderate virulence for the remainder. Among 159 clinical isolates examined, 36 isolates (22.6 %) had low virulence phenotype, 49 isolates (30.8 %) had high virulence phenotype and 74 isolates (46.6 %) had moderate phenotype. The lab strain H37Rv exhibited the moderate virulence in THP-1 model, which caused 50 % macrophage lysis. I evaluated the virulence phenotype of *Mtb* on day 6 because it provided sufficient time to observe macrophage-*Mtb* interaction clearly through host cell lysis, enabling us to distinguish the isolates with really low or high virulent phenotypes.

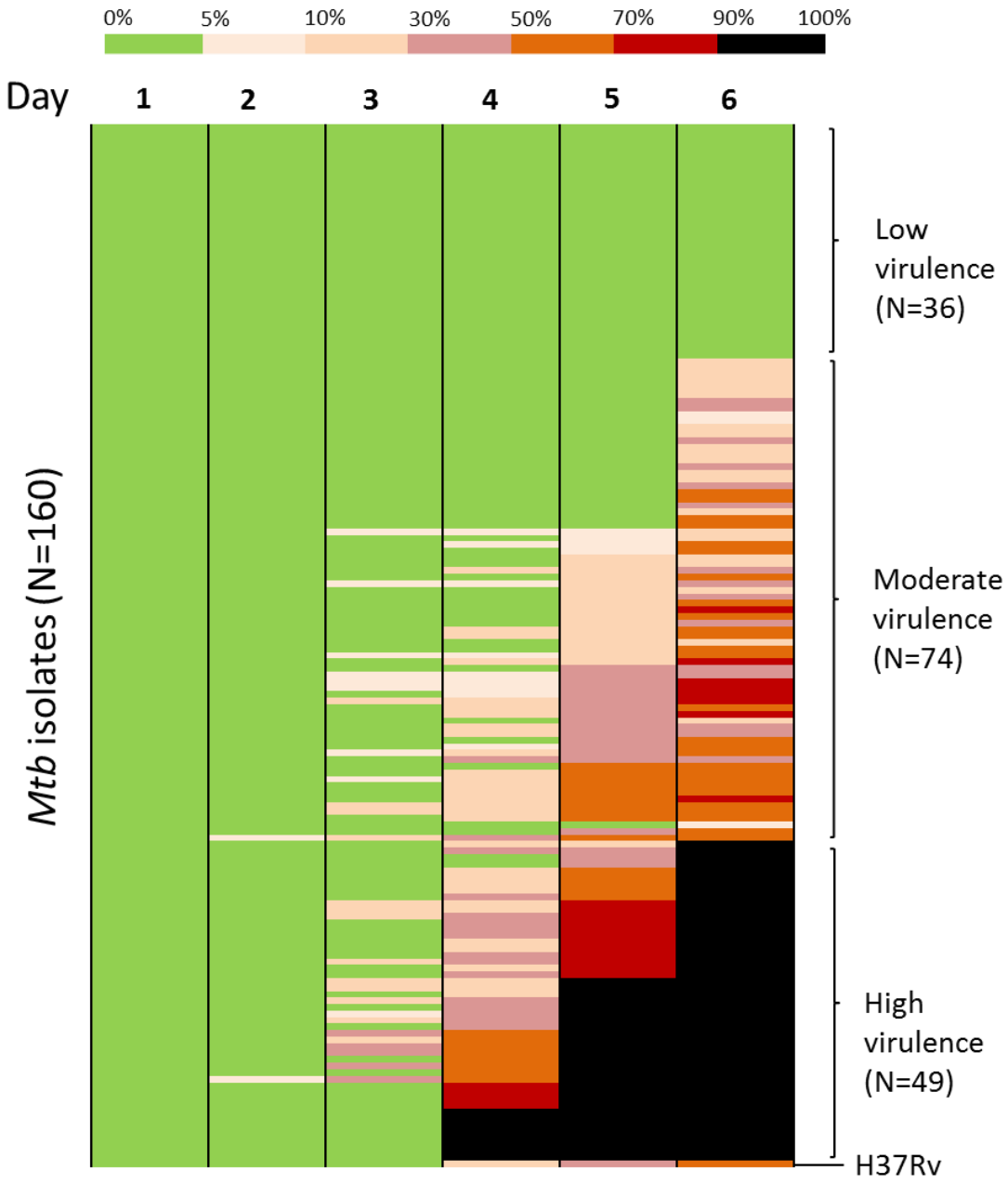

Figure 6.1 Heat map of THP-1 cell lysis induced by different *Mtb* clinical isolates over 6-day post-infection

Color from green to red represents the proportion of THP-1 lysis, ranging from 0-5 % to 90-100%. The strains that caused cell lysis up to 90-100 % at day 6 (in red) were clustered as a group of high virulence phenotype, while to 0-5 % as a group of low virulence (in green) and the remainder as a group of moderate virulence.

6.3.2 Consistency of virulence phenotype of clinical isolates during *in vitro* passages

It has been observed that *in vitro* serial passages of microorganisms may produce important changes in their genetic and phenotypic characteristics[344]. In *Mtb*, multiple *in vitro* subcultures of the laboratory strain H37Rv can reduce its ability to synthesize the cell wall lipid phthiocerol dimycocerosate (PDIM), an important *Mtb* virulence factor. This loss is irreversible and related to genetic change, particularly the deletion of two operons, namely *drr* and *pps*[345]. Hence, I examined whether the variation in the virulent phenotype observed was genetically stable through *in vitro* serial passage. I was very interested in the two extreme phenotypes of low and high virulence. Hence, I randomly selected approximately 20% isolates representative each group of phenotypes that were 8 strains with low, 14 strains with high and 7 strains including H37Rv with moderate virulence. These isolates were serially passaged 10 times within 3 months; bacteria from passage 1st, 3rd, 7th and the last 10th were used to infect THP-1 and cell lysis was daily monitored (Figure 6.2).

Among 8 low virulence isolates, five isolates (62.5 %) showed consistently low virulence during passages, two isolates (isolates 6 and 8) (25 %) changed the phenotype from low to moderate at the passage 10th. One isolate (isolate 19) (12.5 %) showed moderate virulence at passage 1st but remained low virulence from passage 3rd and afterwards, indicating that these changes were possibly minor variation among experiments. For the group of high virulence, 9 out of 14 (64.3 %) isolates remained high virulence during passages. In 5 isolates (isolates 114, 115, 126, 145, and 157) I observed inconsistently minor variations in virulence from high to high medium, and at the passage 10th all of these isolates exhibit high virulence, indicating that this could be

possibly experiment-to-experiment variation. No isolates with moderate virulence (including H37Rv) remained consistent phenotype across initial screening and different passages. Among them, three isolates (isolate 50, 75, and 108) maintained the same phenotype while other isolates were variable across four passages because they are at borderline of phenotype grouping. To conclude, I observed distinct virulent phenotypes among different clinical isolates during serial passages, the isolates with low and high virulence remain stable while the moderate virulent isolates were likely to be variable across experiments.

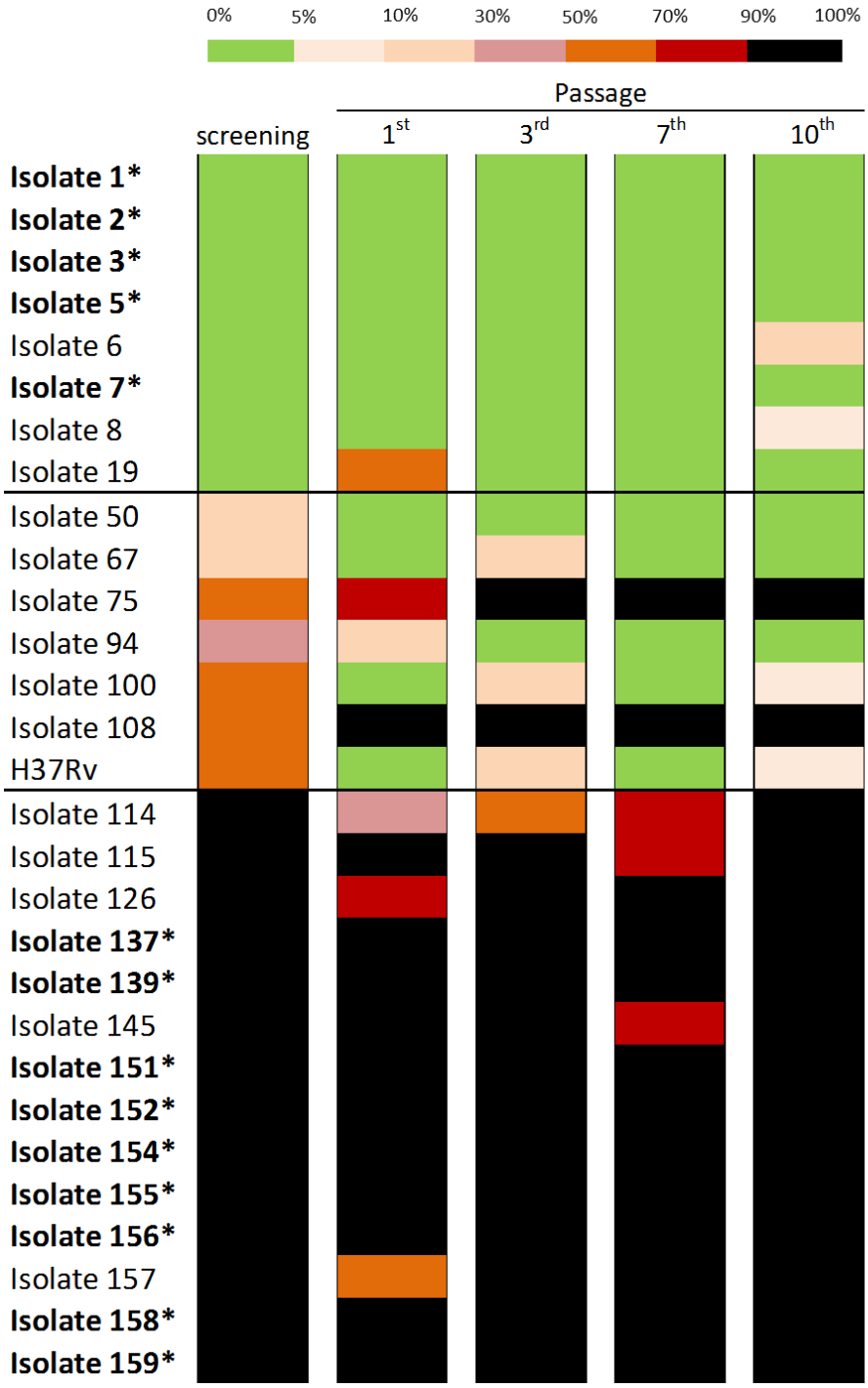

Figure 6.2 Heat map of THP-1 cell lysis induced by *Mtb* clinical isolates at day 6 post-infection from different *in vitro* passages

Color from green to red represents the percentage of THP-1 lysis, ranging from 0-5 % to 90-100 %. The strains that caused cell lysis at day 6 up to 90-100 % were considered as high virulence phenotype (in red), 0-5 % as low virulence (in green) and the remainder as moderate virulence. The isolates whose phenotype was consistent thorough screening and passages are indicated in bold with a superscripted star.

6.3.3 Validation of virulence phenotype of *Mtb* clinical isolates in hMDM

THP-1 cells treated with PMA differentiate into mature macrophages that have been indicated to behave similarly to primary hMDM in their bacterial growth control and immune response to *Mtb* infection[346,347]. However, PMA treatment is also considered as a confounding variable due to the fact that it activates the cells and produce TNF-α production, which could produce some undesirable response. Given this point, it is important that the results obtained with THP-1 cell line should be validated by *in vivo* studies or in hMDM cells for the results to be conclusive[347]. Therefore, I examined whether the difference in virulence of clinical isolates observed in THP-1 could be re-produced in hMDM. Twenty-nine isolates including H37Rv at passage 10th, which were examined for the stability of virulent phenotype during *in vitro* serial passages, were used to infect hMDM from three healthy volunteers, and the percentages of cell lysis were daily assessed. In comparison to THP-1 cells, the lysis of hMDM was slower. For cells infected with a group of highly virulent isolates, complete destruction of THP-1 cells was observed at day 6 post-infection while that of hMDM was observed at day 12 (Figure 6.3). Therefore, the virulence phenotype of clinical isolates in infected hMDM was classified based on the level of cell lysis on day 12. Those were grouped for low virulence when they had ≤ 5 % of infected cells lysed, for high virulence when ≥ 90% of infected cells lysed, and the remainder was moderate virulence.

Six out of eight (75 %) low virulent isolates in THP-1 exhibited consistently low virulence in hMDM from three subjects while an isolate (isolate 19) (12.5 %) changed phenotype from low in THP-1 to moderate in hMDM. Isolate 6 with low virulence in THP-1 showed a variation from low to moderate virulence among hMDM from 3

subjects, which could be possibly resulted from response variation among subjects or experimental variation. Among 14 isolates with high virulence in THP-1, 11 isolates (78.6 %) showed consistently high virulence phenotype in hMDM from 3 subjects whereas 3 isolates (21.4 %) changed to moderate phenotype. In moderate phenotype in THP-1, isolate 50 and H37Rv (28.6 %) showed consistently low virulence while isolate 108 (14 %) showed consistently high virulence in hMDM. Two isolates 67 and 75 (28.6 %) remained moderate virulence in hMDM whereas other two isolates 94 and 100 (28.6 %) had phenotypic variation among different subjects. Altogether, these results indicate that majority (≥ 75 %) of isolates having low or high virulence in THP-1 conserved their phenotypes in hMDM while less consistent between these two cell types was observed in isolates having moderate virulence.

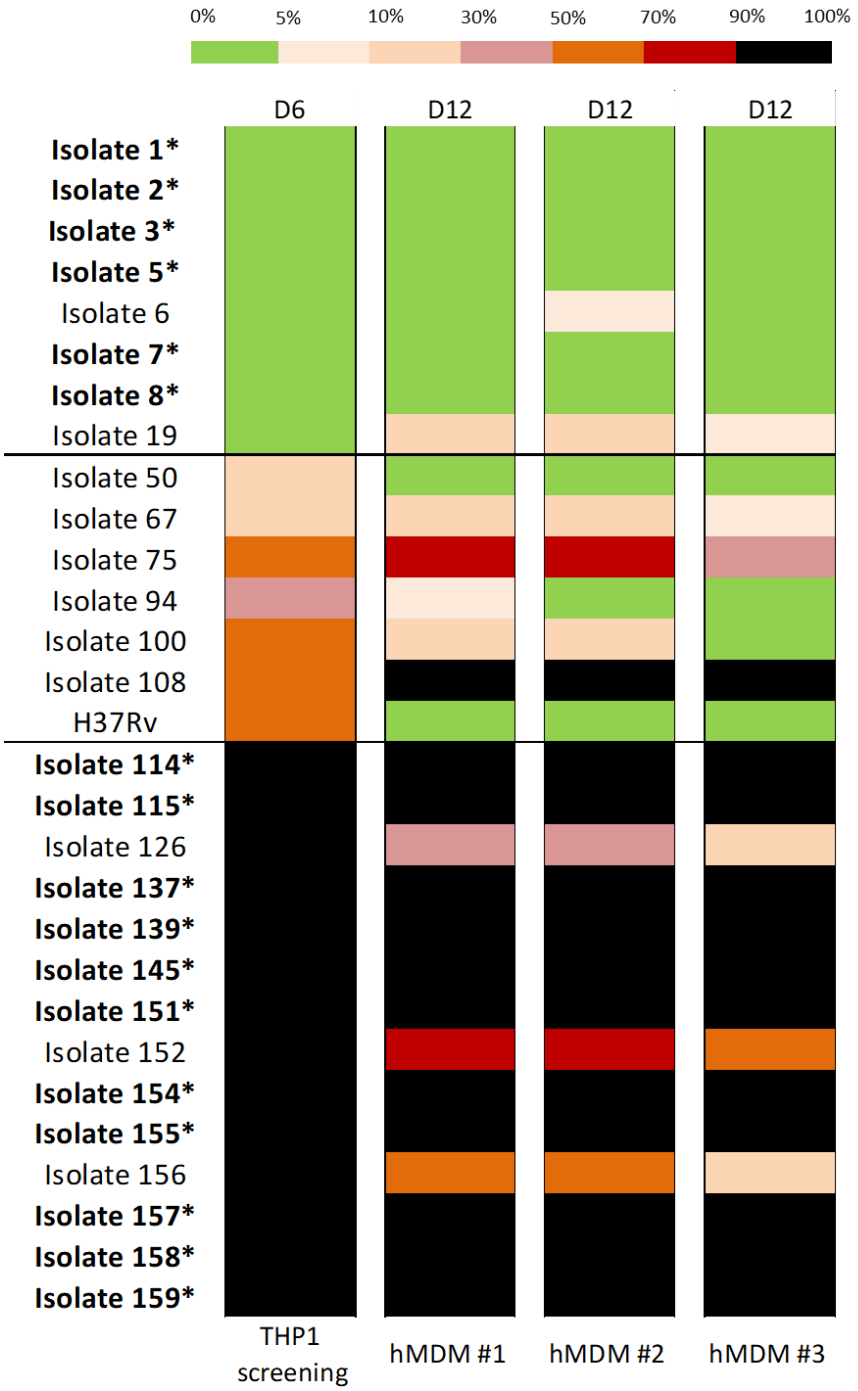

Figure 6.3 Heat map of cell lysis at day 12 post-infection induced by *Mtb* clinical isolates in hMDM from 3 subjects

Color from green to red represents the percentage of hMDM lysis, ranging from 0-5 % to 90-100 %. The strains that caused cell lysis at day 12 up to 90-100 % were considered as high virulence phenotype (in red), 0-5 % as low virulence phenotype (in green) and the remainder as moderate virulence phenotype. The isolates whose phenotype was consistent thorough screening in THP-1 cells and hMDM from different subjects were indicated in bold with a superscripted star.

6.3.4 Association of *Mtb* virulence phenotype and cytokine response

Several studies have revealed that *Mtb* strains with high virulence phenotype, which is indicated by their rapid intracellular growth in macrophage or by high lethality of infected animals, are able to suppress the host pro-inflammatory cytokine responses[53,66,343]. Such reduced immune responses might contribute to more rapid disease progression and transmission of these *Mtb* strains[61,60]. I hypothesized that the different virulence phenotypes in our study were associated with distinct patterns of host cytokine response. To answer this hypothesis, I infected hMDM from three healthy volunteers with each of 29 *Mtb* isolates, which were examined for consistency in virulent phenotype in both THP-1 cells and hMDM, and analyzed for production of pro-inflammatory cytokine.

It was noted that in hMDM model, 8 isolates showed low virulence phenotype, 9 showed moderate virulence and 12 showed high virulence phenotype. Table 6.1 showed cytokine expression from infected hMDM and highlighted two observations. First, I observed a variation in cytokine production from three groups of virulence phenotype (greyed rows). Second, there was also variation in cytokine production among three independent subjects in response to infection (greyed column). Since low or high virulent phenotype remained consistently through *in vitro* serial passages or in different experimental models, I was interested in examining the influence of these two distinct phenotypes on cytokine response against the infection. The results showed that hMDM from two out of three individuals infected with high virulence isolates produced significantly higher level of IL-1β than that infected with low virulence isolates (S1, P=0.002 and S2, P= 0.0002) (Figure 6.4A). A similar trend was observed in the third individual, but was not statistically difference (P= 0.11). In contrast to IL-1β, the release

of IL-6 and TNF-α by hMDM infected with high virulence isolates were clearly reduced compared to the low virulence isolates (Figure 6.4 B, C). These results were observed in 2 out of 3 subjects (TNF-α, S2, P= 0.03 and S3, P= 0.003; IL-6, S2, P= 0.02 and S3, P= 0.002). Analyses of cytokine production in all three subjects showed a significantly high concentration of IL-1β but low concentrations of IL-6 and TNF-α in high virulence isolates (IL-1β, P= 0.0001; IL-6, P= 0.002; and TNF- α, P= 0.006). (Figure 6.4D).

Table 6.1 Cytokines response in hMDM infected with clinical isolates from different virulence phenotypes

		Isolates/ Phenotypes			
Cytokine	**Subject[a]**	**All (n = 29)**	**Low (n= 8)**	**Moderate (n = 9)**	**High (n = 12)**
IL-1β (pg/ml)	**S1**	23.7 (36.1-45.9)	19.4 (15.7-25.6)	30.0 (26.1-42.1)	48.7 (42.8-56.1)
	S2	36.6 (33.4-64.3)	31.7 (27.8-33.5)	36.5 (34.0-53.5)	67.2 (39.9-80.3)
	S3	17.3 (14.5-21.3)	15.8 (12.9-19.7)	16.2 (14.5-17.5)	20.7 (15.8-26.6)
	S1, S2, and S3	19.1 (31.3-45.5)	15.7 (21.2-33.2)	17.4 (28.5-17.4)	24.8 (42.9-64.0)
IL-6 (pg/ml)	**S1**	110.6 (147-177.0)	206.3 (110.8-290.2)	133.0 (98.3-177.0)	147.7 (113.8-162.5)
	S2	207.8 (183.8-351.3)	599.7 (251.2-877.7)	220.8 (194.2-344.9)	182.3 (161.0-194.3)
	S3	349.8 (292.1-736.6)	882.7 (582.7-1093.6)	342.4 (292.1-736.6)	307.8 (230.2-358.3)
	S1, S2, and S3	163.0 (217.6-350.5)	249.9 (387.5-873.9)	176.7 (86.7-343.6)	148.7 (182.3-271.2)
TNF-α (pg/ml)	**S1**	83.6 (110.2-180.9)	148.1 (105.2-166.4)	117.8 (83.3-181.1)	107.2 (84.5-148.1)
	S2	251.6 (180.0-435.2)	489.9 (280.8-585.0)	251.6 (183.2-465.8)	208.6 (170.3-261.9)
	S3	212.0 (160.1-490.5)	537.7 (326.0-662.0)	233.8(189.1-435.5)	161.2 (139.2-192.2)
	S1, S2, and S3	133.8 (184.2-329.4)	160.5 (264.6-555.7)	142.7 (51.8-329.2)	109.7 (160.8-212.6)

[a]Cytokines were measured in infected hMDM collected from different subjects

Data were represented by median (interquartile range)

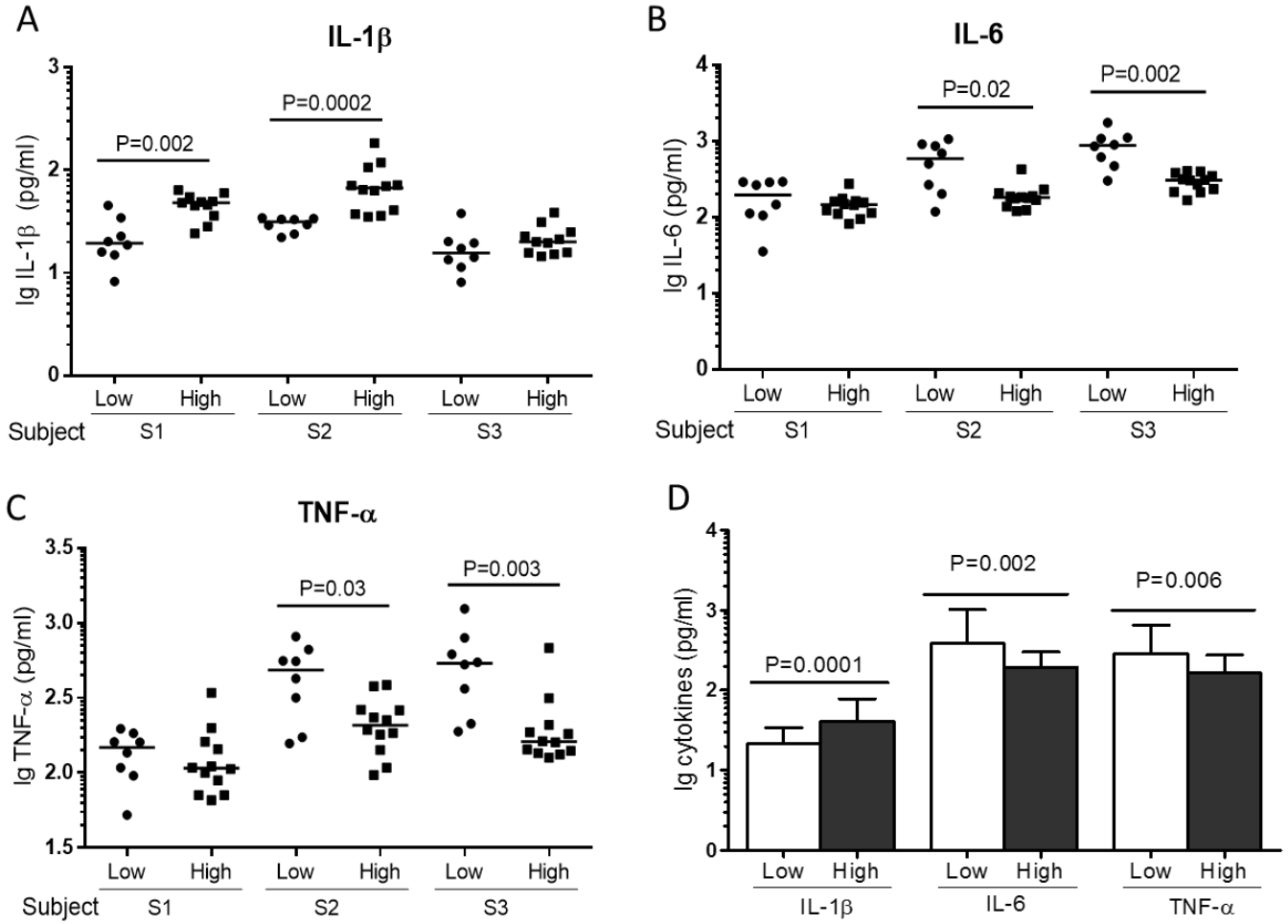

Figure 6.4 Cytokine response in hMDM infected with low or high virulent *Mtb* clinical isolates

(A) IL-1β, (B) IL-6, and (C) TNF-α expression by hMDM infected with low virulence *Mtb* (n= 8) or high virulence *Mtb* (n= 12) from three independent subjects. Bars in plots represent median values. (D) Average cytokine responses by infected hMDM from three subjects. Bars represent the mean value of cytokines with standard deviation. Comparisons across two virulent phenotypes were performed using Mann-Whitney U test.

6.3.5 Association of in vitro growth rate and virulent phenotype of *Mtb* clinical isolates

Several previous studies have suggested that rapid destruction of infected macrophages could result from effective intracellular replication[152,259,290]. *Mtb* growth in liquid broth is likely to have positive correlation with its intracellular growth[343] whereas other studies have showed that the *in vitro* growth in media does not influence bacterial growth inside the macrophages[339]. Therefore, I examined whether the intrinsic growth of bacteria in liquid media, where there is without nutrient limitations and immune pressure, could influence bacterial virulence. The OD_{600} of *Mtb* culture has a strong correlation with the CFU (see Section 3.2.5), hence I cultured *Mtb* isolates in liquid 7H9T broth and evaluated bacterial growth by OD measurement.

The $\log_2$ of OD_{600} value of 159 isolates and H37Rv was plotted over the 20-day period; overall I observed an increased number of bacteria during 20 days of measurement. As I anticipated, there was a wide variation in the growth curve among clinical isolates, ranging within 4 units of $\log_2$. Growth curves of many clinical strains were above the curve of H37Rv from day 6 (Figure 6.5). To compare the growth among different isolates, I determined a growth rate that was expressed as the slope of the line plotted in Figure 6.5. Approximately 20 % of them had growth rate 1.5-2 times higher than H37Rv while 12 % had significantly lower growth rate than lab strain (Figure 6.6A). I then investigated whether these distinct growth rates determined virulence of clinical isolates. There was no difference in growth rate between isolates with low, high or moderate virulence (P= 0.36) (Figure 6.6B). The growth rates of 29 isolates representative of three groups of virulence at 1^{st}, 3^{rd}, 7^{th} passage were also examined (Figure 6.6C, D, E). As previously presented, the low and high phenotypes were

conserved during *in vitro* passages. However, no statistical difference was observed among growth rate of low, high and moderate virulent isolates (1st: P= 0.15, 3nd: P= 0.47, and 7th: P= 0.14) (Figure 6.6 C-E). These results confirmed that *in vitro* growth rate of *Mtb* did not contribute to host cell lysis. They also imply that outcome of *Mtb* infection is more likely determined by the interaction between macrophage and pathogen.

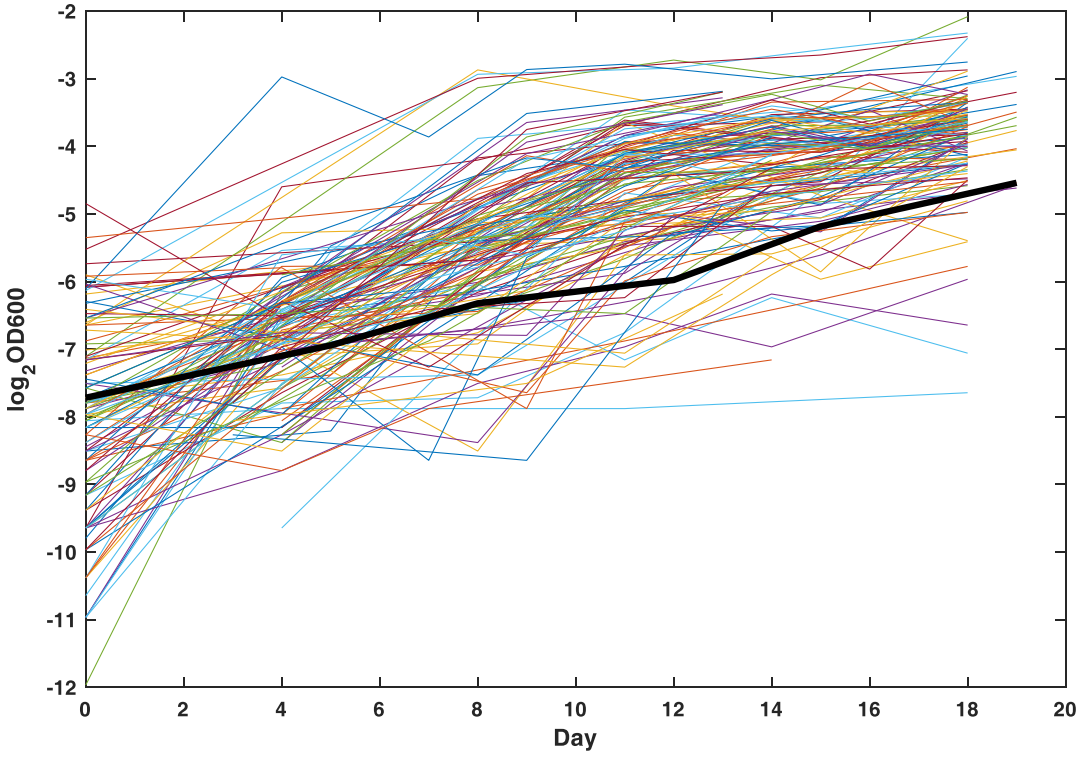

Figure 6.5 Growth curves of *Mtb* clinical isolates and H37Rv in 7H9T broth at the initial screening

The growth of bacteria (n= 160) was monitored by measuring the OD at 600nm. The growth curve of H37Rv was indicated in black thick line.

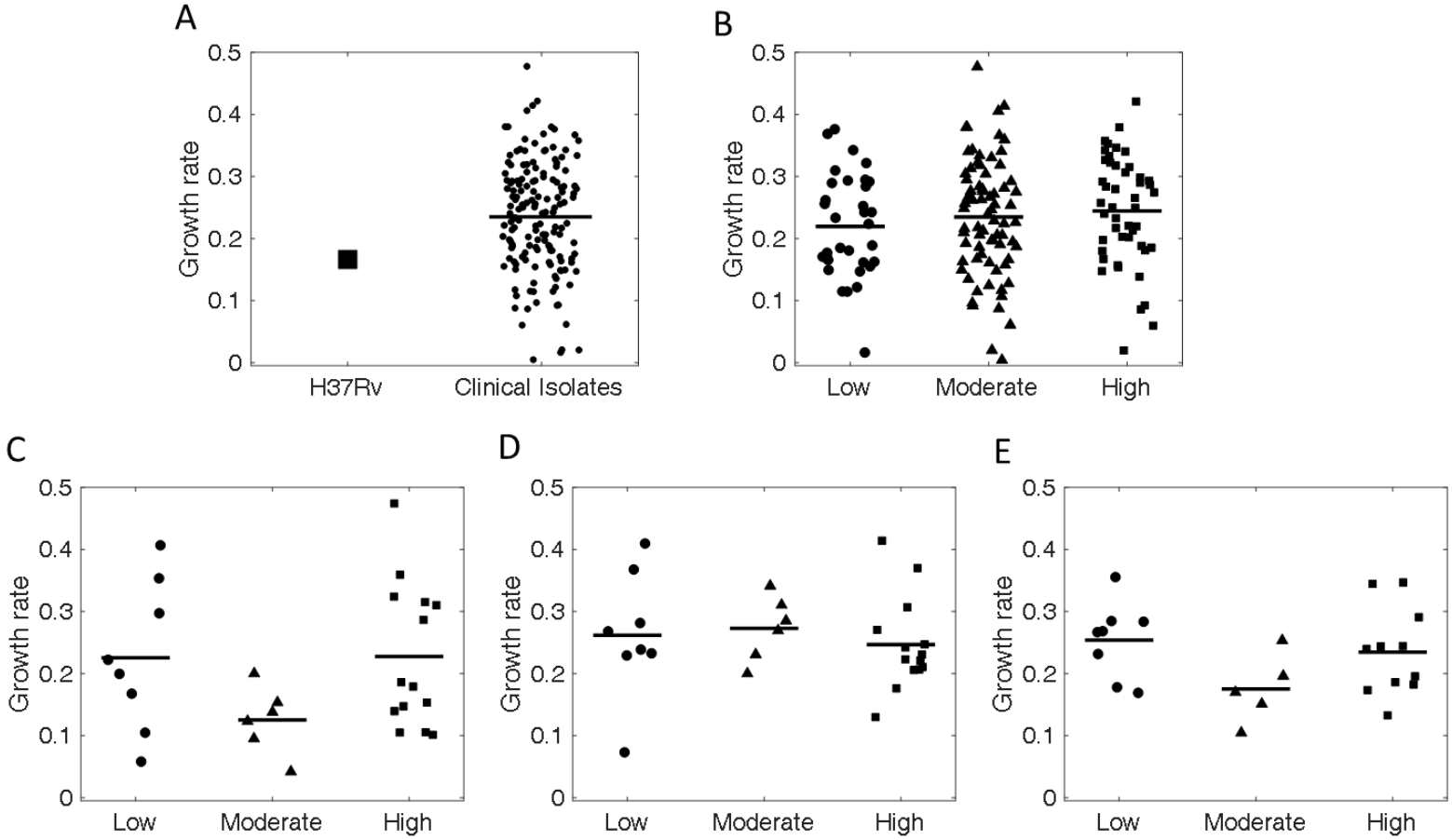

Figure 6.6 Growth rate of *Mtb* clinical isolates in 7H9T broth

The growth rate of H37Rv and 159 clinical isolates (A) or of isolates with low (n= 36), moderate (n= 75) and high (n= 49) (B) at the initial screening were plotted. The growth rate of isolates with low (N= 8), moderate (N= 6), and high (N= 14) at passage 1st (C), 3rd (D), 7th (E) were plotted. P value was determined using Kruskal-Wallis test. All P-value >0.05.

6.3.6 Association of *Mtb* lineages and virulence phenotype of clinical isolates

The *Mtb* genotype has been demonstrated to influence the intracellular growth or pathogenicity of bacteria. The East-Asian/Beijing strains have been associated with rapid intracellular growth in cellular model[48,343], high mortality in infected animals[56], as well as drug resistance[70]. Therefore, I hypothesized that the East Asian/Beijing lineage is associated with the virulent phenotype of clinical isolates.

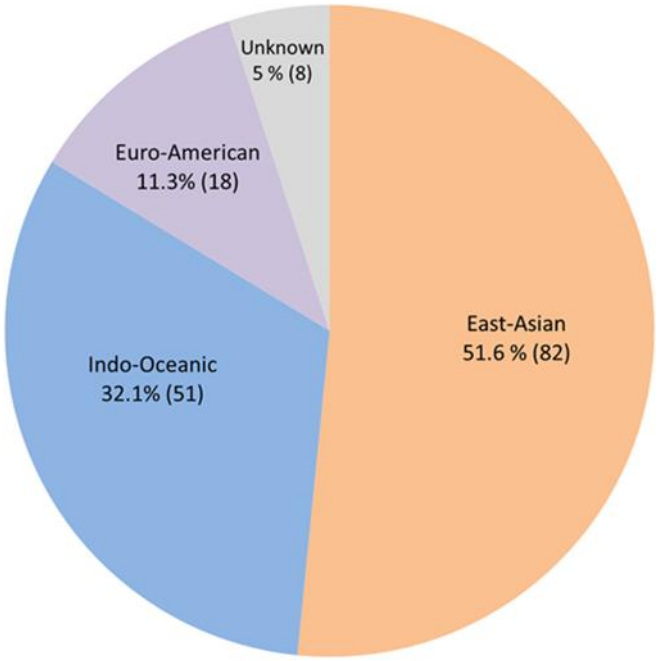

Figure 6.7 Proportion of *Mtb* lineages in 159 clinical isolates

I genotyped 159 *Mtb* isolates by LPS typing. In line with previous reports[20,70], three main *Mtb* lineages that are known in Vietnam were observed in our isolate collection. Indo-oceanic lineage, with RD239 deleted, represented 49/159 (31%) of isolates. East Asian/Beijing lineage, with RD105 deleted, represented 80/159 (50%) of isolates. Euro-American, pks 7bp deletion, was the least popular with 11% of isolates (Figure 6.7). There was a small proportion (5%) of undefined isolates that failed to generate a

product on repeated PCR for the two RD regions despite generating for other PCR products. To investigate the association of virulence phenotype and East Asian/Beijing lineages versus other lineages, I combined Euro-American, Indo-Oceanic and unknown group as non-Beijing lineages. The frequencies of East Asian/Beijing isolates with low, moderate and high virulence were 13/82 (15.9 %), 36/82 (43.9 %) and 33/82 (40.2 %), respectively, while there were 23/77 (29.9 %), 48/77 (49.4 %) and 16/77 (20.8 %) isolates with low, moderate, and high virulence, respectively, in non-Beijing lineages. When I compared the frequencies of *Mtb* genotypes contributing to each virulence phenotype, I found an influence of East Asian/Beijing lineage on virulence phenotype of *Mtb* (P= 0.01) and more closely, this lineage was associated with high virulence phenotype compared to low virulence (P= 0.004, OR= 3.65, 95%CI= 1.48-9.02) or to moderate virulence (P= 0.04, OR= 2.18, 95%CI= 1.03-4.61) (Table 6.2).

Table 6.2 East Asian/Beijing strain was associated with high virulence phenotype

Phenotypes	**Low** (n = 36)	**Moderate** (n= 74)	**High** (n= 49)
Non-Beijing (n, %)	23 (29.9)	38 (49.4)	16 (20.8)
East-Asia/Beijing (n, %)	13 (15.9)	36 (43.9)	33 (40.2)
Low vs. Moderate vs. High (P)	**0.01**		
Low vs. Moderate (P) OR (95%CI)	0.21 1.68 (0.74-3.80)		
Moderate vs. High (P) OR (95%CI)	**0.04** 2.18 (1.03-4.61)		
Low vs. High (P) OR (95%CI)	**0.004** 3.65 (1.48-9.02)		

P: P value, were determined by using Chi-square test

OR (95%CI): odds ratio (95% confidence interval)

6.4 Discussion

In this study, I accessed *Mtb* virulence in a large sample set of 159 isolates from pulmonary TB patients by examining host cell lysis in macrophage models. I observed a wide range in cell lysis and regarding its extent, these *Mtb* clinical isolates were classified as being of low, moderate and high virulence. The extreme phenotypes of being low or high virulence in infected THP-1 cells were highly conserved during *in vitro* serial passages or in different model such as hMDM. I also confirmed that the high virulent isolates were associated with low production of TNF-α and IL-6. In consistent with previous studies, I clearly demonstrated that the East-Asian/Beijing lineage was associated with the high virulence phenotype, which strongly indicates that the lineage-specific genetics could be the factor determining the interaction of macrophage and *Mtb*.

The lysis of THP-1 cells induced by different *Mtb* isolated varied widely, ranging from no or very less cells lysed to 100% cells lysed after 6 days of infection. Such an outcome mirrored the diversity in the bacterial virulence which spanned a spectrum from low to high. Comparison of isolates with extreme phenotypes such as low and high virulence could enable us to further understand the determinants as well as the biological mechanism for bacterial virulence, which may contribute to TB treatment and disease control. Therefore, to discriminate the distinct phenotypes, the isolates with low virulence phenotype were defined by no capacity to lyse cells or lysing cells up to 5 % while the high virulence induced the cell lysis ≥ 90 %.

Our study indicated that the levels of cytokines released by infected hMDM were highly variable in response to different strains. Nevertheless, there was a correlation of

cytokines induced by *Mtb* clinical isolates and their virulence. I observed lower concentration of IL-6 and TNF-α and higher IL-1β level among isolates with high virulence than in isolates with low virulence. The results on IL-6 and TNF-α has been consistent with the findings in previous study that demonstrated the correlation of low level of these cytokines and high necrotic cell death in THP-1 cells infected with K-strain, a high virulent and transmitted *Mtb*[47]. Such a low inflammatory response has been observed in strains that are considered to be highly virulent due to rapid growth of *Mtb* in macrophages[260,343], or high ability to cause tissue damage[57] and early death in infected mice[53], or highly transmissible[66]. Suppression of the pro-inflammatory cytokine response is likely to be a mechanism for survival and transmission of highly virulent bacteria because by avoiding the host protective immune response, the high virulent bacteria can rapidly replicate, leading to cell disruption for bacterial release. In addition, the cell lysis is known to release variety of cellular components that could enhance the influx of immune cells from the host, including neutrophils, that aggravate pathology by collateral tissue damage contributing to lung necrosis[69]. Therefore, it would be important to further examine the correlation of *Mtb* virulence and lung lesions in the patients.

In this study, I observed an increased IL-1β concentration in high virulence phenotypes whereas many previous studies have demonstrated the reduced level of IL-1β produced by either murine or human macrophages infected with highly virulent mycobacteria[51,68,348]. Previous studies also have shown the increase level of IL-1β in virulent *Mtb* compared to BCG[349] or in East Asian/Beijing compared to H37Rv or Euro-American[67]. It has been demonstrated that the increased production of IL-1β in

macrophages infected with *Mtb* is dependent on caspase-1, a protease to cleave pro IL-1β to active form rather than due to the alteration in IL-1β transcription or level of pro IL-1β [350]. Caspase-1 is also known to induce the host cell lysis which is accompanied by the release of IL-1β[351,352]. Therefore, the increased production of IL-1β in high virulence isolates could be involved in their alternative mechanism of inducing cell lysis which is dependent on caspase-1. Further examination on the level of caspase-1 in macrophages infected with low and high virulence isolates could help to elucidate the mechanism of bacterial virulence.

There are many studies indicating the lineage-specific virulence of *Mtb* strains. Different models of infection with East Asian/Beijing genotype have suggested that this genotype leads to a hypervirulent phenotype compared with other strains such as Euro-American or East Africa-Indian[51,54]. The East Asian/Beijing also causes a great concern because of its high prevalence and its association with multi-drug resistance[70]. A recent study has revealed the Beijing lineage is associated with high level of transmissions in Ho Chi Minh city, Vietnam[353]. In this study, I observed an association of clinical East Asian/ Beijing isolates with rapid cell lysis in macrophage models, which accumulatively demonstrates the hypervirulent phenotype of East Asian/Beijing genotype. The host cell lysis probably serves as an exit strategy which may help to explain why this genotype is likely to rapidly progress to active TB disease and has high transmission. Even though the East Asian/Beijing genotype is predominantly associated with high virulence, I still observed a proportion of East Asian/Beijing isolates with low virulence, which is in line with previous observation of virulent variation within East Asian/Beijing strains[56,57,69].

Recent studies have indicated that *Mtb* has ability to cause phagosome rupture accompanied with the translocation intro the cytosol, which results in the host cell death[251]. The strains that lack the ESX-1 secretion system, such as BCG or mutant *Mtb,* fail in inducing phagosome rupture and cell death, which is reversed when the ESX-1 is restored in these bacteria[251,252]. A recent study has reported a clinical isolate that has a defect in the ESX-1 secretion system due to the insertion mutation in eccCa1 gene, one of component genes related to EXS-1[354]. This isolates is unable to disrupt the phagosome lysosome in THP-1 cells and associated with a mild pathology in lung of infected mice. A comparison on 12 ESX-1–associated genes on genomes of 143 clinical isolates and H37Rv has revealed that 26 isolates (18%) show critical mutations that are likely to prevent or diminish ESX-1 secretion[354]. A study using TEM has found that different *Mtb* clinical isolates have variations in intracellular niche preference which could be phagosome or cytosol[253]. Therefore, the difference in ability to rupture phagosomes, which is influenced by the variation on ESX-1-associated genes, could explain for the low or high level of host cell lysis which is associated with low or high virulence of clinical isolates.

In conclusion, there is a wide variation on the bacterial virulence among different clinical *Mtb* isolates, which is associated with cytokine response and bacterial lineages. More specifically, high virulence isolates predominantly belong to East Asian/Beijing genotype and are able to suppress the expression of inflammatory cytokines of IL-6 and TNF-α in infected macrophage. The molecular mechanisms which could potentially contribute to variation in virulence between strains are not fully understood. Future

comparative genomic studies could be essential to shed light on discovering the determinants of such phenotypic differences.

Chapter 7

CONCLUSION AND FUTURE RESEARCH

TB in humans is very complex with a wide range of pathology and clinical manifestations. Approximately one third of human population is latently infected with *Mtb*, but only 10% of them develop active TB disease during their lifetime. The lung is the favorable place for *Mtb* to develop the disease, however the bacteria can hematogenously spread to other organs or tissues where it causes extra-pulmonary TB, of which TBM is the most severe form. There are differences in clinical complications among PTB patients or among TBM patients. Some PTB patients have bloody cough or very severe lung damage while some TBM patients have very severe disease and are at high risk of death. To successfully control TB, I need to understand the factors that influence the susceptibility to pulmonary or extra-pulmonary TB, the disease severity, and the treatment outcome. For that reason, for this thesis I studied how the variations in host cellular and genetic factors, and the diversity in the virulence of *Mtb* strains, influence TB susceptibility.

The antimicrobial activities of macrophages are achieved due to phagosomal maturation. Bacteria are killed mainly by the extremely acidic and protease-enriched environment that is achieved within the lysosome by fusion with multiple intra-vesicles, such as from the early or late endosomal system, the secretory system (including secretory lysosomes), and even the endoplasmic reticulum. All these components and proteins can affect the function of phagosome, therefore it could be misleading if the antimicrobial activities of macrophages are accessed by the presence of protein-markers only[275]. Previous studies have developed bead-based assays to assess in real-time the alterations in the kinetics of phagosomal physiology that directly indicate their influence to intracellular growth of bacteria[271,273,275,291]. In **Chapter 3,** I adopted and modified the

reporter beads specific for phagocytosis, acidification and proteolysis. Our beads were coated with TDM, an immunogenic component of *Mtb*'s cell wall recognized by MARCO and MINCLE receptor and with β-glucan, a fungi's cell wall component recognized by DECTIN-1 receptor. Hence, I could study the macrophage antimicrobial activity induced by pathways initiated by these receptors. The assays exploiting these reporter beads revealed the high ability in bead uptake of macrophage cell lines. I also observed the kinetics of acidification and proteolysis in macrophage cell lines that are similar to previous reports. Most importantly, our bead-based assays showed the consistent repetitive results in macrophage cell lines. They also revealed the heterogeneity in the phagosomal activities among different host that may help to explain the difference in TB susceptibility in host populations. The *Mtb* reporter strain expressing fluorescent protein generated in this study provided us a sensitive and rapid method to study the bacterial growth within the macrophages as well ability of macrophages to inhibit intracellular bacterial growth. The fluorescence intensity was correlative of bacterial viability and it allowed us to observe the difference in the outcome of macrophage-bacteria interaction when macrophage cell lines were infected with *Mtb* at different MOI. The bead-based assays could not only be exploited to study the macrophage antimicrobial activities in TB pathogenesis but also could be modified to study such macrophage function in the pathogenesis of other infectious diseases caused by intracellular pathogens. Likewise, the model of bacterial expressing fluorescent protein could be generated for other intracellular bacteria to study the pathogen-host cell interactions or to follow the course of infections in animal models.

In **Chapter 4**, I exploited the bead-based assays established in chapter 3 to study whether the macrophage antimicrobial activities are associated with TB susceptibility. The acidification and proteolysis of hMDM collected from individuals with LTB were lower than that from patients with active TB when the macrophages were incubated with beads coated with either IgG, TDM or β-glucan. In response to the infection of live *Mtb* reporter strains, the proteolysis activity of hMDM from both LTB and ATB groups were significantly decreased compared to the resting macrophages. Consequently, the intracellular bacterial loads were increased, resulting in the necrotic death of infected hMDM from both LTB and ATB groups after 4 day post infection and afterwards. Our results indicated that *Mtb* can modulate the antimicrobial activities of macrophages to benefit their survival. The observation of no difference in antimicrobial activities of macrophage between LTB and ATB or between PTB and TBM in response to *Mtb* infection suggests that macrophage activities alone do not count for the development of different TB clinical phenotypes. Lu *et al*. have showed the efficiency of antibodies from people with LTB in enhancing the killing ability of macrophages against *Mtb*[183]. It is also known that the T cells can either drive the macrophage towards M1 activation state that has enhanced antimicrobial functions or direct cytolysis of *Mtb*-infected macrophages, resulting the control of *Mtb* growth[181,355]. Thus there could be difference in the T cells response which results in the protection from TB in some people and TB progression in others. It would be essential to further examine whether the incorporation of T cells or antibody and macrophage from LTB and ATB could help to understand the immunological mechanism in TB protection or TB development, which may allow us to predict the susceptibility to TB so that individuals at risk could be efficiently treated for

TB elimination. Although the ligand-coated beads are limited in reflecting the complicated interaction between antimicrobial functions of macrophages and live *Mtb*, this model suggests for the differences in macrophage antimicrobial functions driven by distinct immunogenic ligands and their associated pathways in host. More specifically, TDM is likely to inhibit the macrophage antimicrobial function, which may benefit for *Mtb* survival and causing disease[247,309]. The results could further help for the development of new class of anti-*Mtb* compounds that target the bacterial proteins/lipids that modulate the host immune response.

Host genetic variation has been reported to be an important factor for the susceptibility to TB[20,328,329]. In **Chapter 5**, I found that among variations of three receptor genes involved in macrophage phagocytosis, two SNPs rs2278589 and rs6751745 on *MARCO* genes were strongly associated with susceptibility to PTB as well as susceptible to infection with Beijing strains during the development of PTB. Such associations were possibly resulted from the association of these two *MARCO* SNPs with the reduced macrophage phagocytosis at the beginning of infection. The impaired phagocytosis then could limit the macrophage killing activity and antigen presentation that may lead to the increased susceptibility to active TB. The deficient response could also result in increased bacterial replication, which could manifest as severe lung abnormality. The two *MARCO* SNPs do not influence the *MARCO* transcription or change the protein sequence hence they could be the markers of functional variants that affect ability to bind bacterial ligands, reducing phagocytosis and increasing the disease susceptibility. Further study on sequencing *MARCO* gene would help to identify such causative mutations, which can allow us to understand the molecular mechanism of phagocytosis

impairment which could help in TB prevention and treatment. The *MARCO* SNPs rs2278589 and rs6751745 were found to be associated with the severe lung damage which may prolong the treatment time hence a further examination on the association of *MARCO* SNPs and time to smear conversion could help for host-directed therapy.

In **chapter 6**, I studied the virulence of *Mtb* in a large number of isolates from PTB patients by examining the cell lysis of infected macrophages. I observed a spectrum of host cytotoxicity which could allow *Mtb* strains to be grouped as low, high and moderate phenotypes of virulence. I demonstrated that high virulent *Mtb* strains are associated with severe host cytotoxicity and reduced inflammatory cytokines while the low virulent strains fail to promote the host cell death and induce strong immune response. These results are consistent with previous studies of *Mtb* virulence reflected by rapid intracellular growth or high mortality of infected animals. It is likely that the reduced inflammatory response facilitates *Mtb* to multiply and lyse macrophages, so that *Mtb* could escape, infect other new cells and establish new infection. The difference in the virulence of *Mtb* strains was determined by their genetic background, of which Beijing genotype was strongly associated with high virulence while non-Beijing genotype was predominantly being low virulent. However, I still observed a proportion of Beijing isolates also being low virulent and a proportion of non-Beijing isolates being high virulent. The variation in the ESX-1 region of *Mtb* genome is thought to be related to distinct ability in inducing phagosome rupture[251,252], which thereby may lead to different extent of cell death. Hence, it would be important to study the phagosome rupture of *Mtb* strains with low and high virulence in order to understand the underlying cellular mechanism of such different phenotypes. With the emerge of next generation

sequencing technologies coupled with advances in bioinformatics analysis in a genome era nowadays, whole genome sequencing (WGS) of bacteria would provide an invaluable tool in diagnosis and understanding insight bacterial pathogens, including their evolution, pathogenesis, and the design of related therapeutic interventions[356–358]. Therefore, the comparison of WGS of low and high virulent isolates of Beijing and non-Beijing isolates would allow us to identify the specific genetic determinants for *Mtb* virulence.

In conclusion, the findings from this thesis contribute to the current understanding of the influence of host and bacterial factors to the TB susceptibility and clinical manifestations of TB infection. They also provide foundation for further studies on improving TB prevention and treatment of TB.

References

1. Daniel, T. M. The history of tuberculosis. *Respir. Med.* **100,** 1862–70 (2006).
2. Bos, K. I. *et al.* Pre-Columbian mycobacterial genomes reveal seals as a source of New World human tuberculosis. *Nature* **514,** 494–497 (2014).
3. Frith, J. & others. History of tuberculosis. Part 1-Phthisis, consumption and the white plague. **22,** 29–35 (2014).
4. World Health Organization. Global Tuberculosis Report 2015. *World Heal. Organ.* (2015).
5. World Health Organization. Global Tuberculosis Report 2016. *World Heal. Organ.* (2016).
6. World Health Organization. Global Tuberculosis Report 2007: Global tuberculosis control - surveillance, planning, financing. *World Heal. Organ.* (2007).
7. World Health Organization. Tuberculosis and HIV. *http://www.who.int/hiv/topics/tb/en/*
8. World Health Organization. Tuberculosis. *http://www.who.int/mediacentre/factsheets/fs104/en/*
9. M Vree *et al.* Low tuberculosis notification in mountainous Vietnam is not due to low case detection: a cross-sectional survey. *BMC Infect. Dis.* **7,** 109 (2007).
10. Hoa, N. B. *et al.* National survey of tuberculosis prevalence in Viet Nam. *Bull. World Heal. Organ. HO* **88,** 273–280 (2010).
11. Trinh, Q. M. *et al.* Tuberculosis and HIV co-infection in Vietnam. *Int. J. Infect. Dis.* **46,** 56–60 (2016).
12. Cambier, C. J. *et al.* Mycobacteria manipulate macrophage recruitment through coordinated use of membrane lipids. *Nature* **505,** 218–222 (2014).
13. Andrews, J. R. *et al.* Risk of Progression to Active Tuberculosis Following

Reinfection With *Mycobacterium tuberculosis*. *Clin. Infect. Dis.* **54,** 784–791 (2012).

14. van Crevel, R., Ottenhoff, T. H. M. & van der Meer, J. W. M. Innate immunity to *Mycobacterium tuberculosis*. *Adv. Exp. Med. Biol.* **531,** 241–247 (2003).

15. Gengenbacher, M. & Kaufmann, S. H. E. *Mycobacterium tuberculosis*: success through dormancy. *FEMS Microbiol. Rev.* **36,** 514–32 (2012).

16. Esmail, H. *et al.* Characterization of progressive HIV-associated tuberculosis using 2-deoxy-2-[18F]fluoro-d-glucose positron emission and computed tomography. *Nat. Med.* **22,** 1090–1093 (2016).

17. Cardona, P.-J. Reactivation or reinfection in adult TB: Is that the question? *Int. J. mycobacteriology* **5,** 400–407 (2016).

18. van Rie, A. *et al.* Exogenous Reinfection as a Cause of Recurrent Tuberculosis after Curative Treatment. *N. Engl. J. Med.* **341,** 1174–1179 (1999).

19. Verver, S. *et al.* Rate of Reinfection Tuberculosis after Successful Treatment Is Higher than Rate of New Tuberculosis. *Am. J. Respir. Crit. Care Med.* **171,** 1430–1435 (2005).

20. Caws, M. *et al.* The influence of host and bacterial genotype on the development of disseminated disease with *Mycobacterium tuberculosis*. *PLoS Pathog.* **4,** e1000034 (2008).

21. World Health Organization. *Definitions and reporting framework for tuberculosus-2013 revision.* (2013).

22. American Thoraic Soceity. Diagnostic standards and classification of tuberculosis. *Am Rev Respir Dis* **142,** 725–735 (1990).

23. Zumla, A., Raviglione, M., Hafner, R. & Fordham von Reyn, C. Tuberculosis. *N. Engl. J. Med.* **368,** 745–755 (2013).

24. Hosoglu, S. *et al.* Predictors of outcome in patients with tuberculous meningitis. *Int. J. Tuberc. Lung Dis.* **6,** 64–70 (2002).

25. Combs, D. L., O'Brien, R. J. & Geiter, L. J. USPHS tuberculosis short-course chemotherapy trial 21: Effectiveness, toxicity, and acceptability. The report of final results. *Ann. Intern. Med.* **112,** 397–406 (1990).

26. Török, M. E. & Farrar, J. J. When to Start Antiretroviral Therapy in HIV-Associated Tuberculosis. *N. Engl. J. Med.* **365,** 1538–1540 (2011).

27. AIDSinfo. Guidelines for the Use of Antiretroviral Agents in HIV-1-Infected Adults and Adolescents. Available at: https://aidsinfo.nih.gov/guidelines/html/1/adult-and-adolescent-arv-guidelines/27/tb-hiv. (Accessed: 11th July 2017)

28. World Health Organisation. WHO treatment guidelines for drug- resistant tuberculosis 2016. *WHO Press. Geneva, Switz.* (2016).

29. Cohen, J. Easier cure for resistant TB. *Science* **355,** 677–677 (2017).

30. Molina-Torres, C. A. *et al.* Effect of serial subculturing on the genetic composition and cytotoxic activity of *Mycobacterium tuberculosis*. *J. Med. Microbiol.* **59,** 384–391 (2010).

31. Mangtani, P. *et al.* Protection by BCG vaccine against tuberculosis: A systematic review of randomized controlled trials. *Clin. Infect. Dis.* **58,** 470–480 (2014).

32. Colditz, G. A. *et al.* Efficacy of BCG vaccine in the prevention of tuberculosis. Meta-analysis of the published literature. *JAMA* **271,** 698–702 (1994).

33. Warren, R. M. *et al.* Differentiation of *Mycobacterium tuberculosis* complex by PCR amplification of genomic regions of difference. *Int. J. Tuberc. Lung Dis.* **10,** 818–822 (2006).

34. Traag, B. A. *et al.* Do mycobacteria produce endospores? *Proc. Natl. Acad. Sci. U. S. A.* **107,** 878–81 (2010).

35. Lamont, E. A., Bannantine, J. P., Armién, A., Ariyakumar, D. S. & Sreevatsan, S. Identification and characterization of a spore-like morphotype in chronically starved *Mycobacterium avium subsp. paratuberculosis* cultures. *PLoS One* **7,** e30648 (2012).

36. Kleinnijenhuis, J., Oosting, M., Joosten, L. A. B., Netea, M. G. & Van Crevel, R. Innate Immune Recognition of *Mycobacterium tuberculosis*. *Clin. Dev. Immunol.* **2011,** 1–12 (2011).

37. Gagneux, S. Genetic Diversity in *Mycobacterium tuberculosis*. *Curr. Top. Microbiol. Immunol.* **6,** (2013).

38. Gagneux, S. & Small, P. M. Global phylogeography of *Mycobacterium tuberculosis* and implications for tuberculosis product development. *Lancet Infect. Dis.* **7,** 328–337 (2007).

39. Chernick, V. A new evolutionary scenario for the *Mycobacterium tuberculosis* complex. *Pediatr. Pulmonol.* **38,** 1 (2004).

40. Gagneux, S. *et al.* Variable host-pathogen compatibility in *Mycobacterium tuberculosis*. *Proc. Natl. Acad. Sci.* **103,** 2869–2873 (2006).

41. Comas, I. *et al.* Population Genomics of *Mycobacterium tuberculosis* in Ethiopia Contradicts the Virgin Soil Hypothesis for Human Tuberculosis in Sub-Saharan Africa. *Curr. Biol.* **25,** 3260–3266 (2015).

42. Parwati, I., van Crevel, R. & van Soolingen, D. Possible underlying mechanisms for successful emergence of the *Mycobacterium tuberculosis* Beijing genotype strains. *Lancet Infect. Dis.* **10,** 103–111 (2010).

43. Anh, D. D. *et al. Mycobacterium tuberculosis* Beijing genotype emerging in vietnam. *Emerg. Infect. Dis.* **6,** 302–305 (2000).

44. Buu, T. N. *et al.* The Beijing genotype is associated with young age and multidrug-resistant tuberculosis in rural Vietnam. *Int. J. Tuberc. Lung Dis.* **13,** 900–906 (2009).

45. Coscolla, M. & Gagneux, S. Consequences of genomic diversity in *Mycobacterium tuberculosis*. *Semin. Immunol.* **26,** 431–444 (2014).

46. Casadevall, A. & Pirofski, L. Host-Pathogen Interactions: The Attributes of Virulence. *J. Infect. Dis.* **184,** 337–344 (2001).

47. Sohn, H. *et al.* Induction of cell death in human macrophages by a highly virulent Korean isolate of *Mycobacterium tuberculosis* and the virulent strain H37Rv. *Scand. J. Immunol.* **69,** 43–50 (2009).

48. Li, Q. *et al.* Differences in Rate and Variability of Intracellular Growth of a Panel of *Mycobacterium tuberculosis* Clinical Isolates within a Human Monocyte Model. *Infect. Immun.* **70,** 6489 (2002).

49. Bhatia, A. L. A Comparison of the Virulence in Guinea-pigs of South Indian and British Tubercle Bacilli. *Tubercle.* **41,** 1–22 (1960).

50. Naganathan, N. *et al.* Virulence of tubercle bacilli isolated from patients with tuberculosis in Bangalore, India. *Tubercle* **67,** 261–267 (1986).

51. Reiling, N., Homolka, S. & Walter, K. Clade-Specific Virulence Patterns of *Mycobacterium tuberculosis* Complex Strains in Human Primary Macrophages and Aerogenically Infected Mice. **4,** 1–10 (2013).

52. Manca, C. *et al. Mycobacterium tuberculosis* CDC1551 induces a more vigorous host response in vivo and in vitro, but is not more virulent than other clinical isolates. *J. Immunol.* **162,** 6740–6746 (1999).

53. Manca, C. *et al.* Virulence of a *Mycobacterium tuberculosis* clinical isolate in mice is determined by failure to induce Th1 type immunity and is associated with induction of IFN-alpha /beta. *Proc. Natl. Acad. Sci. U. S. A.* **98,** 5752–7 (2001).

54. Via, L. E. *et al.* Differential virulence and disease progression following *Mycobacterium tuberculosis* complex infection of the common marmoset (callithrix jacchus). *Infect. Immun.* **81,** 2909–2919 (2013).

55. Theus, S., Eisenach, K., Fomukong, N., Silver, R. F. & Cave, M. D. Beijing family *Mycobacterium tuberculosis* strains differ in their intracellular growth in THP-1 macrophages. *Int. J. Tuberc. Lung Dis.* **11,** 1087–1093 (2007).

56. Palanisamy, G. S. *et al.* Clinical strains of *Mycobacterium tuberculosis* display a wide range of virulence in guinea pigs. *Tuberculosis* **89,** 203–209 (2009).

57. Aguilar L, D. *et al. Mycobacterium tuberculosis* strains with the Beijing

genotype demonstrate variability in virulence associated with transmission. *Tuberculosis* **90,** 319–325 (2010).

58. Dormans, J. *et al.* Correlation of virulence, lung pathology, bacterial load and delayed type hypersensitivity responses after infection with different *Mycobacterium tuberculosis* genotypes in a BALB/c mouse model. *Clin. Exp. Immunol.* **137,** 460–8 (2004).

59. Pheiffer, C., Betts, J. C., Flynn, H. R., Lukey, P. T. & van Helden, P. Protein expression by a Beijing strain differs from that of another clinical isolate and *Mycobacterium tuberculosis* H37Rv. *Microbiology* **151,** 1139–1150 (2005).

60. Reed, M. B. *et al.* A glycolipid of hypervirulent tuberculosis strains that inhibits the innate immune response. *Nature* **431,** 84–7 (2004).

61. Portevin, D., Gagneux, S., Comas, I. & Young, D. Human macrophage responses to clinical isolates from the *Mycobacterium tuberculosis* complex discriminate between ancient and modern lineages. *PLoS Pathog.* **7,** (2011).

62. Tanveer, M., Hasan, Z., Kanji, A., Hussain, R. & Hasan, R. Reduced TNF-α and IFN-γ responses to Central Asian strain 1 and Beijing isolates of *Mycobacterium tuberculosis* in comparison with H37Rv strain. *Trans. R. Soc. Trop. Med. Hyg.* **103,** 581–587 (2009).

63. Manca, C. *et al.* Differential Monocyte Activation Underlies Strain-Specific *Mycobacterium tuberculosis* Pathogenesis. *Infect. Immun.* **72,** 5511–5514 (2004).

64. Comas, I. & Gagneux, S. A role for systems epidemiology in tuberculosis research. *Trends Microbiol.* **19,** 492–500 (2011).

65. Marquina-Castillo, B. *et al.* Virulence, immunopathology and transmissibility of selected strains of *Mycobacterium tuberculosis* in a murine model. *Immunology* **128,** 123–133 (2009).

66. Theus, S. A., Cave, M. D. & Eisenach, K. D. Intracellular macrophage growth rates and cytokine profiles of *Mycobacterium tuberculosis* strains with different transmission dynamics. *J. Infect. Dis.* **191,** 453–60 (2005).

67. Krishnan, N. *et al. Mycobacterium tuberculosis* lineage influences innate immune response and virulence and is associated with distinct cell envelope lipid profiles. *PLoS One* **6,** (2011).

68. van Laarhoven, A. *et al.* Low induction of proinflammatory cytokines parallels evolutionary success of modern strains within the *Mycobacterium tuberculosis* beijing genotype. *Infect. Immun.* **81,** 3750–3756 (2013).

69. Ribeiro, S. C. M. *et al. Mycobacterium tuberculosis* strains of the modern sublineage of the Beijing family are more likely to display increased virulence than strains of the ancient sublineage. *J. Clin. Microbiol.* **52,** 2615–24 (2014).

70. Thwaites, G. *et al.* Relationship between *Mycobacterium tuberculosis* genotype and the clinical phenotype of pulmonary and meningeal tuberculosis. *J. Clin. Microbiol.* **46,** 1363–1368 (2008).

71. de Jong, B. C. *et al.* Progression to active tuberculosis, but not transmission, varies by *Mycobacterium tuberculosis* lineage in The Gambia. *J. Infect. Dis.* **198,** 1037–43 (2008).

72. Drobniewski, F. *et al.* Drug-resistant tuberculosis, clinical virulence, and the dominance of the Beijing strain family in Russia. *Jama* **293,** 2726–31 (2005).

73. Hesseling, A. C. *et al.* Mycobacterial genotype is associated with disease phenotype in children. *Int. J. Tuberc. Lung Dis.* **14,** 1252–8 (2010).

74. Kong, Y. *et al.* Association between *Mycobacterium tuberculosis* Beijing/W lineage strain infection and extrathoracic tuberculosis: Insights from epidemiologic and clinical characterization of the three principal genetic groups of M. tuberculosis clinical isolates. *J. Clin. Microbiol.* **45,** 409–14 (2007).

75. Visser, M. E. *et al.* Baseline predictors of sputum culture conversion in pulmonary tuberculosis: Importance of cavities, smoking, time to detection and w-beijing genotype. *PLoS One* **7,** (2012).

76. Parwati, I. *et al. Mycobacterium tuberculosis* Beijing genotype is an independent risk factor for tuberculosis treatment failure in Indonesia. *J. Infect. Dis.* **201,** 553–

7 (2010).

77. Lan, N. T. N. *et al. Mycobacterium tuberculosis* Beijing Genotype and Risk for Treatment Failure and Relapse, Vietnam. *Emerg. Infect. Dis.* **9,** 1633–1635 (2003).

78. Huyen, M. N. T. *et al.* Tuberculosis relapse in vietnam is significantly associated with *Mycobacterium tuberculosis* beijing genotype infections. *J. Infect. Dis.* **207,** 1516–1524 (2013).

79. Sun, Y.-J., Lee, a S. G., Wong, S.-Y. & Paton, N. I. Association of *Mycobacterium tuberculosis* Beijing genotype with tuberculosis relapse in Singapore. *Epidemiol. Infect.* **134,** 329–332 (2006).

80. Nicol, M. P. *et al.* Distribution of strain families of *Mycobacterium tuberculosis* causing pulmonary and extrapulmonary disease in hospitalized children in Cape Town, South Africa. *J. Clin. Microbiol.* **43,** 5779–5781 (2005).

81. Borgdorff, M. W., Van Deutekom, H., De Haas, P. E. W., Kremer, K. & Van Soolingen, D. *Mycobacterium tuberculosis*, Beijing genotype strains not associated with radiological presentation of pulmonary tuberculosis. *Tuberculosis* **84,** 337–340 (2004).

82. Fieschi, C. *et al.* Low penetrance, broad resistance, and favorable outcome of interleukin 12 receptor beta1 deficiency: medical and immunological implications. *J. Exp. Med.* **197,** 527–35 (2003).

83. Altare, F. *et al.* Impairment of mycobacterial immunity in human interleukin-12 receptor deficiency. *Science* **280,** 1432–1435 (1998).

84. Vergne, I., Chua, J., Singh, S. B. & Deretic, V. Cell Biology of *Mycobacterium tuberculosis* Phagosome. *Annu. Rev. Cell Dev. Biol.* **20,** 367–394 (2004).

85. Hirsch, C. S., Ellner, J. J., Russell, D. G. & Rich, E. A. Complement receptor-mediated uptake and tumor necrosis factor-alpha-mediated growth inhibition of *Mycobacterium tuberculosis* by human alveolar macrophages. *J. Immunol.* **152,** (1994).

86. Rooyakkers, A. W. J. & Stokes, R. W. Absence of complement receptor 3 results in reduced binding and ingestion of *Mycobacterium tuberculosis* but has no significant effect on the induction of reactive oxygen and nitrogen intermediates or on the survival of the bacteria in resident and interfe. *Microb. Pathog.* **39,** 57–67 (2005).

87. Zimmerli, S., Edwards, S. & Ernst, J. D. Selective receptor blockade during phagocytosis does not alter the survival and growth of *Mycobacterium tuberculosis* in human macrophages. *Am. J. Respir. Cell Mol. Biol.* (2012).

88. Hu, C., Mayadas-Norton, T., Tanaka, K., Chan, J. & Salgame, P. *Mycobacterium tuberculosis* infection in complement receptor 3-deficient mice. *J. Immunol.* **165,** 2596–602 (2000).

89. Goyal, S., Klassert, T. E. & Slevogt, H. C-type lectin receptors in tuberculosis: what we know. *Med. Microbiol. Immunol.* **205,** 513–535 (2016).

90. Taylor, M. E. in *Mammalian Carbohydrate Recognition Systems* 105–121 (Springer Berlin Heidelberg, 2001). doi:10.1007/978-3-540-46410-5_6

91. Tailleux, L. *et al.* DC-SIGN is the major *Mycobacterium tuberculosis* receptor on human dendritic cells. *J. Exp. Med.* **197,** 121–127 (2003).

92. Kang, P. B. *et al.* The human macrophage mannose receptor directs *Mycobacterium tuberculosis* lipoarabinomannan-mediated phagosome biogenesis. *J. Exp. Med.* **202,** 987–99 (2005).

93. Geijtenbeek, T. B. H. *et al.* Mycobacteria target DC-SIGN to suppress dendritic cell function. *J. Exp. Med.* **197,** 7–17 (2003).

94. Murphy, J. E., Tedbury, P. R., Homer-Vanniasinkam, S., Walker, J. H. & Ponnambalam, S. Biochemistry and cell biology of mammalian scavenger receptors. *Atherosclerosis* **182,** 1–15 (2005).

95. Peiser, L. & Gordon, S. The function of scavenger receptors expressed by macrophages and their role in the regulation of inflammation. *Microbes Infect.* **3,** 149–159 (2001).

96. Montoya, D. *et al.* Divergence of macrophage phagocytic and antimicrobial programs in leprosy. *October* **6,** 343–353 (2009).

97. Bermudez, L. E., Parker, A. & Goodman, J. R. Growth within macrophages increases the efficiency of Mycobacterium avium in invading other macrophages by a complement receptor-independent pathway. *Infect. Immun.* **65,** 1916–1925 (1997).

98. Haworth, R. *et al.* The macrophage scavenger receptor type A is expressed by activated macrophages and protects the host against lethal endotoxic shock. *J. Exp. Med.* **186,** 1431–9 (1997).

99. Pedroza González, A. *et al.* In situ analysis of lung antigen-presenting cells during murine pulmonary infection with virulent *Mycobacterium tuberculosis*. *Int. J. Exp. Pathol.* **85,** 135–145 (2004).

100. Józefowski, S., Sobota, A., Pawłowski, A. & Kwiatkowska, K. *Mycobacterium tuberculosis* lipoarabinomannan enhances LPS-induced TNF-a production and inhibits NO secretion by engaging scavenger receptors. *Microb. Pathog.* **50,** 350–359 (2011).

101. Drage, M. G. *et al.* TLR2 and its co-receptors determine responses of macrophages and dendritic cells to lipoproteins of *Mycobacterium tuberculosis*. *Cell. Immunol.* **258,** 29–37 (2009).

102. Guilliams, M., Bruhns, P., Saeys, Y., Hammad, H. & Lambrecht, B. N. The function of Fcγ receptors in dendritic cells and macrophages. *Nat. Rev. Immunol.* **14,** 94–108 (2014).

103. Armstrong, J. A. & Hart, P. D. Phagosome-Lysosome interactions in cultured macrophages infected with virulent tubercle bacilli. *J. Exp. Med.* **142,** (1975).

104. Kumar, S. K., Singh, P. & Sinha, S. Naturally produced opsonizing antibodies restrict the survival of *Mycobacterium tuberculosis* in human macrophages by augmenting phagosome maturation. *Open Biol.* **5,** 150171 (2015).

105. Farhat, K. *et al.* Heterodimerization of TLR2 with TLR1 or TLR6 expands the

ligand spectrum but does not lead to differential signaling. *J. Leukoc. Biol.* **83,** 692–701 (2008).

106. Nilsen, N. J. *et al.* Cellular trafficking of lipoteichoic acid and Toll-like receptor 2 in relation to signaling: role of CD14 and CD36. *J. Leukoc. Biol.* **84,** 280–91 (2008).

107. Jones, B. W. *et al.* Different Toll-like receptor agonists induce distinct macrophage responses. *J. Leukoc. Biol.* **69,** 1036–44 (2001).

108. Stamm, C. E., Collins, A. C. & Shiloh, M. U. Sensing of *Mycobacterium tuberculosis* and consequences to both host and bacillus. *Immunol. Rev.* **264,** 204–219 (2015).

109. Kiemer, A. K. *et al.* Attenuated activation of macrophage TLR9 by DNA from virulent mycobacteria. *J. Innate Immun.* **1,** 29–45 (2008).

110. Drennan, M. B. *et al.* Toll-Like Receptor 2-Deficient Mice Succumb to *Mycobacterium tuberculosis* Infection. *Am. J. Pathol.* **164,** 49–57 (2004).

111. Abel, B. *et al.* Toll-like receptor 4 expression is required to control chronic *Mycobacterium tuberculosis* infection in mice. *J. Immunol.* **169,** 3155–3162 (2002).

112. Reiling, N. *et al.* Cutting edge: Toll-like receptor (TLR)2- and TLR4-mediated pathogen recognition in resistance to airborne infection with *Mycobacterium tuberculosis*. *J. Immunol.* **169,** 3480–3484 (2002).

113. Shim, T. S., Turner, O. C. & Orme, I. M. Toll-like receptor 4 plays no role in susceptibility of mice to *Mycobacterium tuberculosis infection*. *Tuberculosis* **83,** 367–371 (2003).

114. Thuong, N. T. T. *et al.* A polymorphism in human TLR2 is associated with increased susceptibility to tuberculous meningitis. *Genes Immun.* **8,** 422–428 (2007).

115. Weikert, L. F. *et al.* SP-A enhances uptake of bacillus Calmette-Guérin by macrophages through a specific SP-A receptor. *Am. J. Physiol.* **272,** L989-95

(1997).

116. Tenner, A. J., Robinson, S. L., Borchelt, J. & Wright, J. R. Human pulmonary surfactant protein (SP-A), a protein structurally homologous to C1q, can enhance FcR- and CR1-mediated phagocytosis. *J. Biol. Chem.* **264,** 13923–13928 (1989).

117. Gaynor, C. D., McCormack, F. X., Voelker, D. R., McGowan, S. E. & Schlesinger, L. S. Pulmonary surfactant protein A mediates enhanced phagocytosis of *Mycobacterium tuberculosis* by a direct interaction with human macrophages. *J. Immunol.* **155,** 5343–51 (1995).

118. Pugin, J. *et al.* CD14 is a pattern recognition receptor. *Immunity* **1,** 509–516 (1994).

119. Lewthwaite, J. C. *et al. Mycobacterium tuberculosis* Chaperonin 60 . 1 Is a More Potent Cytokine Stimulator a CD14-Binding Domain. **2,** 7349–7355 (2001).

120. Peterson, P. K. *et al.* CD14 receptor-mediated uptake of nonopsonized *Mycobacterium tuberculosis* by human microglia. *Infect. Immun.* **63,** 1598–1602 (1995).

121. Eruslanov, E. B. *et al.* Neutrophil Responses to *Mycobacterium tuberculosis* Infection in Genetically Susceptible and Resistant Mice. *Infect. Immun.* **73,** 1744–1753 (2005).

122. Fulton, S. a, Reba, S. M., Martin, T. D. & Boom, W. H. Neutrophil-Mediated Mycobacteriocidal Immunity in the Lung during *Mycobacterium bovis* BCG Infection in C57BL / 6 Mice. *Infect. Immun.* **70,** 5322–5327 (2002).

123. Pedrosa, J. *et al.* Neutrophils Play a Protective Nonphagocytic Role in Systemic *Mycobacterium tuberculosis* Infection of Mice. *Infect. Immun.* **68,** 577–583 (2000).

124. Kisich, K. O., Higgins, M., Diamond, G. & Heifets, L. Tumor Necrosis Factor Alpha Stimulates Killing of *Mycobacterium tuberculosis* by Human Neutrophils. *Infect. Immun.* **70,** 4591–4599 (2002).

125. Yang, C.-T. *et al.* Neutrophils Exert Protection in the Early Tuberculous

Granuloma by Oxidative Killing of Mycobacteria Phagocytosed from Infected Macrophages. *Cell Host Microbe* **12,** 301–312 (2012).

126. Tan, B. H. *et al.* Macrophages Acquire Neutrophil Granules for Antimicrobial Activity against Intracellular Pathogens. *J. Immunol.* **177,** 1864–1871 (2006).

127. Braian, C., Hogea, V. & Stendahl, O. ***Mycobacterium tuberculosis*-** Induced Neutrophil Extracellular Traps Activate Human Macrophages. *J. Innate Immun.* **5,** 591–602 (2013).

128. Gopal, R. *et al.* S100A8/A9 proteins mediate neutrophilic inflammation and lung pathology during tuberculosis. *Am. J. Respir. Crit. Care Med.* **188,** 1137–1146 (2013).

129. Wolf, A. J. *et al. Mycobacterium tuberculosisMycobacterium tuberculosis* infects dendritic cells with high frequency and impairs their function in vivo. *J Immunol* **179,** 2509–2519 (2007).

130. Mihret, A., Mamo, G., Tafesse, M., Hailu, A. & Parida, S. Dendritic Cells Activate and Mature after Infection with *Mycobacterium tuberculosis*. *BMC Res. Notes* **4,** 247 (2011).

131. Tascon, R. E. *et al. Mycobacterium tuberculosis*-activated dendritic cells induce protective immunity in mice. *Immunology* **99,** 473–480 (2000).

132. Tian, T., Woodworth, J., Sköld, M. & Behar, S. M. In vivo depletion of CD11c+ cells delays the CD4+ T cell response to *Mycobacterium tuberculosis* and exacerbates the outcome of infection. *J. Immunol.* **175,** 3268–3272 (2005).

133. Madan-Lala, R. *et al. Mycobacterium tuberculosis* impairs dendritic cell functions through the serine hydrolase Hip1. *Biophys. Chem.* **192,** 4263–4272 (2014).

134. Wolf, A. J. *et al.* Initiation of the adaptive immune response to *Mycobacterium tuberculosis* depends on antigen production in the local lymph node, not the lungs. *J. Exp. Med.* **205,** 105–15 (2008).

135. Allen, M. *et al.* Mechanisms of control of *Mycobacterium tuberculosis* by NK

cells: Role of glutathione. *Front. Immunol.* **6,** 1–9 (2015).

136. Perussia, B. The Cytokine Profile of Resting and Activated NK Cells. *Methods* **9,** 370–378 (1996).

137. Wang, R., Jaw, J. J., Stutzman, N. C., Zou, Z. & Sun, P. D. Natural killer cell-produced IFN-γ and TNF-α induce target cell cytolysis through up-regulation of ICAM-1. *J. Leukoc. Biol.* **91,** 299–309 (2012).

138. Harshan, K. V & Gangadharam, P. R. In vivo depletion of natural killer cell activity leads to enhanced multiplication of *Mycobacterium avium* complex in mice. *Infect. Immun.* **59,** 2818–21 (1991).

139. Brill, K. J. *et al.* Human Natural Killer Cells Mediate Killing of Intracellular *Mycobacterium tuberculosis* H37Rv via Granule-Independent Mechanisms. *Infect. Immun.* **69,** 1755–1765 (2001).

140. Yoneda, T. & Ellner, J. J. CD4 T cell and natural killer cell-dependent killing of *Mycobacterium tuberculosis* by human monocytes. *Am. J. Respir. Crit. Care Med.* **158,** 395–403 (1998).

141. Lu, C.-C. *et al.* NK cells kill mycobacteria directly by releasing perforin and granulysin. *J. Leukoc. Biol.* **96,** 1–11 (2014).

142. Romagnani, S. T-cell subsets (Th1 versus Th2). *Ann. Allergy, Asthma Immunol.* **85,** 9–21 (2000).

143. Kidd, P. Th1 / Th2 Balance Th1 / Th2 Balance : The Hypothesis , its Limitations , and Implications for Health and Disease. *Altern. Med. Rev.* **8,** 223–242 (2003).

144. Liu, X., Fang, L., Guo, T. B., Mei, H. & Zhang, J. Z. Drug targets in the cytokine universe for autoimmune disease. *Trends Immunol.* **34,** 120–128 (2013).

145. Casarini, M. *et al.* Cytokine Levels Correlate with a Radiologic Score in Active Pulmonary Tuberculosis. *Am. J. Respir. Crit. Care Med.* (2012).

146. Henderson, R. A., Watkins, S. C. & Flynn, J. L. Activation of human dendritic cells following infection with *Mycobacterium tuberculosis*. *J. Immunol.* **159,**

(1997).

147. Roca, F. J. & Ramakrishnan, L. TNF dually mediates resistance and susceptibility to mycobacteria via mitochondrial reactive oxygen species. *Cell* **153,** 521–534 (2013).

148. Harris, J., Hope, J. C. & Keane, J. Tumor Necrosis Factor Blockers Influence Macrophage Responses to *Mycobacterium tuberculosis*. *J. Infect. Dis.* **198,** 1842–1850 (2008).

149. Harris, J. & Keane, J. How tumour necrosis factor blockers interfere with tuberculosis immunity. *Clin. Exp. Immunol.* **161,** 1–9 (2010).

150. Roach, D. R. *et al.* TNF Regulates Chemokine Induction Essential for Cell Recruitment, Granuloma Formation, and Clearance of Mycobacterial Infection. *J. Immunol.* **168,** 4620–4627 (2002).

151. Kindler, V., Sappino, A. P., Grau, G. E., Piguet, P. F. & Vassalli, P. The inducing role of tumor necrosis factor in the development of bactericidal granulomas during BCG infection. *Cell* **56,** 731–740 (1989).

152. Tobin, D. M. *et al.* Host genotype-specific therapies can optimize the inflammatory response to mycobacterial infections. *Cell* **148,** 434–446 (2012).

153. Law, K. *et al.* Increased Release of Interleukin-1β, Interleukin-6, and Tumor Necrosis Factor-α by Bronchoalveolar Cells Lavaged from Involved Sites in Pulmonary Tuberculosis. *Am J Respir Crit Care Med* **153,** 799–804 (1996).

154. Chensue SW, Warmington KS, Berger AE & Tracey DE. Immunohistochemical demonstration of interleukin-1 receptor antagonist protein and interleukin-1 in human lymphoid tissue and granulomas. *Am. J. Pathol.* **140,** 269–275 (1992).

155. Mayer-Barber, K. *et al.* Innate and adaptive interferons suppress IL-1α and IL-1β production by distinct pulmonary myeloid subsets during *Mycobacterium tuberculosis* infection. *Immunity* **35,** 1023–1034 (2011).

156. Yamada, H., Mizumo, S., Horai, R., Iwakura, Y. & Sugawara, I. Protective role of interleukin-1 in mycobacterial infection in IL-1 alpha/beta double-knockout

mice. *Lab. Invest.* **80,** 759–67 (2000).

157. Schenk, M. *et al.* Interleukin-1β triggers the differentiation of macrophages with enhanced capacity to present mycobacterial antigen to T cells. *Immuology* **141,** 174–180 (2013).

158. Awomoyi, A. a *et al.* Polymorphism in IL1B: IL1B–511 association with tuberculosis and decreased lipopolysaccharide-induced IL-1β in IFN-γ primed ex-vivo whole blood assay. *J. Endotoxin Res.* **11,** 281–6 (2005).

159. Hall, N. B. *et al.* Polymorphisms in TICAM2 and IL1B are associated with TB. *Genes Immun.* **16,** 127–133 (2015).

160. Saunders, B. M., Frank, A. A., Orme, I. M. & Cooper, A. M. Interleukin-6 induces early gamma interferon production in the infected lung but is not required for generation of specific immunity to *Mycobacterium tuberculosis* infection. *Infect. Immun.* **68,** 3322–3326 (2000).

161. Ladel, C. H. *et al.* Lethal tuberculosis in interleukin-6-deficient mutant mice. *Infect. Immun.* **65,** 4843–4849 (1997).

162. Cavalcanti, Y. V. N., Brelaz, M. C. A., Neves, J. K. D. A. L., Ferraz, J. C. & Pereira, V. R. A. Role of TNF-alpha, IFN-gamma, and IL-10 in the development of pulmonary tuberculosis. *Pulm. Med.* **2012,** (2012).

163. Flynn, J. L. *et al.* An essential role for interferon γ in resistance to *Mycobacterium tuberculosis* infection. *J. Exp. Med.* **178,** 2249–2254 (1993).

164. Schaible, U. E., Sturgill-Koszycki, S., Schlesinger, P. H. & Russell, D. G. Cytokine activation leads to acidification and increases maturation of *Mycobacterium avium*-containing phagosomes in murine macrophages. *J. Immunol* **160,** 1290–1296. (1998).

165. Via, L. E. *et al.* Effects of cytokines on mycobacterial phagosome maturation. *J. Cell Sci.* **111 (Pt 7,** 897–905 (1998).

166. Hostetter, J. M., Steadham, E. M., Haynes, J. S., Bailey, T. B. & Cheville, N. F. Cytokine effects on maturation of the phagosomes containing Mycobacteria

avium subspecies paratuberculosis in J774 cells. *FEMS Immunol. Med. Microbiol.* **34,** 127–134 (2002).

167. MacMicking, J. D. Immune Control of Tuberculosis by IFN- -Inducible LRG-47. *Science (80-.).* **302,** 654–659 (2003).

168. Cooper, B. A. M. *et al.* Disseminated Tuberculosis in Interferon gamma Gene-disrupted Mice. *J. Exp. Med.* **178,** 2243–2247 (1993).

169. Newport, M. J. *et al.* A mutation in the interferon-gamma receptor gene and susceptibility to mycobacterial infection. *N. Engl. J. Med.* **335,** 1941–1949 (1996).

170. Lee, S. W. *et al.* Interferon gamma polymorphisms associated with susceptibility to tuberculosis in a Han Taiwanese population. *J. Microbiol. Immunol. Infect.* **48,** 376–380 (2015).

171. Banning, U., Verheyen, J., Bonig, H. & Korholz, D. Interleukin 10 Inhibits TNF-Alpha Production in Human Monocytes Independently of Interleukin 12 and Interleukin 1 Beta. *Immunol. Invest.* **28,** 165–175 (1999).

172. Bobadilla, K. *et al.* Human phagosome processing of *Mycobacterium tuberculosis* antigens is modulated by interferon-γ and interleukin-10. *Immunology* **138,** 34–46 (2013).

173. O'Leary, S., O'Sullivan, M. P. & Keane, J. IL-10 blocks phagosome maturation in *Mycobacterium tuberculosis*-infected human macrophages. *Am. J. Respir. Cell Mol. Biol.* **45,** 172–180 (2011).

174. CDC | TB | Fact Sheets. Tuberculin Skin Testing for TB. Available at: https://www.cdc.gov/tb/publications/factsheets/testing/skintesting.htm. (Accessed: 8th July 2017)

175. Serbina, N. V & Flynn, J. O. A. L. CD8+ T Cells Participate in the Memory Immune Response to *Mycobacterium tuberculosis*. *Infect. Immun.* **69,** 4320–4328 (2001).

176. Lin, P. L. *et al.* CD4 T Cell Depletion Exacerbates Acute *Mycobacterium*

tuberculosis While Reactivation of Latent Infection Is Dependent on Severity of Tissue Depletion in Cynomolgus Macaques. *AIDS Res. Hum. Retroviruses* **28,** 1693–1702 (2012).

177. Saunders, B. M., Frank, A. A., Orme, I. M. & Cooper, A. M. CD4 is required for the development of a protective granulomatous response to pulmonary tuberculosis. *Cell. Immunol.* **216,** 65–72 (2002).

178. Scanga, C. A. *et al.* Depletion of CD4(+) T cells causes reactivation of murine persistent tuberculosis despite continued expression of interferon gamma and nitric oxide synthase 2. *J. Exp. Med.* **192,** 347–58 (2000).

179. Lin, P. L. & Flynn, J. L. CD8 T cells and *Mycobacterium tuberculosis* infection. *Semin Immunopathol.* **37,** 239–249 (2015).

180. Woodworth, J. S., Wu, Y. & Behar, S. M. *Mycobacterium tuberculosis*-specific CD8+ T cells require perforin to kill target cells and provide protection in vivo. *J. Immunol.* **181,** 8595–8603 (2008).

181. Carranza, C. *et al. Mycobacterium tuberculosis* growth control by lung macrophages and CD8 cells from patient contacts. *Am. J. Respir. Crit. Care Med.* **173,** 238–245 (2006).

182. Casadevall, A. & Ph, D. Clinical Implications of Basic Research Antibodies to *Mycobacterium tuberculosis*. *N. Engl. J. Med.* **376,** 283–285 (2017).

183. Lu, L. L. *et al.* A Functional Role for Antibodies in Tuberculosis. *Cell* **167,** 1–11 (2016).

184. Zimmermann, N. *et al.* Human isotype-dependent inhibitory antibody responses against *Mycobacterium tuberculosisMycobacterium tuberculosis*. *EMBO Mol Med* **8,** 1325–1339 (2016).

185. Ramakrishnan, L. Revisiting the role of the granuloma in tuberculosis. *Nat. Rev. Immunol.* **12,** 352–366 (2012).

186. Ulrichs, T. *et al.* Human tuberculous granulomas induce peripheral lymphoid follicle-like structures to orchestrate local host defence in the lung. *J. Pathol.*

204, 217–228 (2004).

187. Volkman1, H. E. *et al.* Tuberculous Granuloma Induction via Interaction of a Bacterial Secreted Protein with Host Epithelium. *Science (80-.).* **327,** 466–469 (2010).

188. Russell, D. G., Cardona, P., Kim, M. & Allain, S. Foamy macrophages and the progression of the human TB granuloma. *Nat. Immunol.* **10,** 943–948 (2010).

189. Dutta, N. K. & Karakousis, P. C. Latent tuberculosis infection: myths, models, and molecular mechanisms. *Microbiol. Mol. Biol. Rev.* **78,** 343–71 (2014).

190. Russell, D. G. *Mycobacterium tuberculosisMycobacterium tuberculosis* and the intimate discourse of a chronic infection. *Immunol. Rev.* **240,** 252–268 (2011).

191. Berrington, W. R. & Hawn, T. R. *Mycobacterium tuberculosis*, macrophages, and the innate immune response: Does common variation matter? *Immunol. Rev.* **219,** 167–186 (2007).

192. Hattersley, A. T. & McCarthy, M. I. What makes a good genetic association study? *Lancet* **366,** 1315–1323 (2005).

193. Quesniaux, V. *et al.* Toll-like receptor pathways in the immune responses to mycobacteria. *Microbes Infect.* **6,** 946–959 (2004).

194. Tobin, D. M. *et al.* The lta4h locus modulates susceptibility to mycobacterial infection in zebrafish and humans. *Cell* **140,** 717–30 (2010).

195. Patnala, R., Clements, J. & Batra, J. Candidate gene association studies: a comprehensive guide to useful in silico tools. *BMC Genet.* **14,** 39 (2013).

196. International, T. & Consortium, H. The International HapMap Project. *Nature* **426,** 789–796 (2003).

197. Ha, N.-T., Freytag, S. & Bickeboeller, H. Coverage and efficiency in current SNP chips. *Eur. J. Hum. Genet.* **22,** 1124–1130 (2014).

198. Hawn, T. R. *et al.* A polymorphism in Toll-interleukin 1 receptor domain containing adaptor protein is associated with susceptibility to meningeal

tuberculosis. *J. Infect. Dis.* **194,** 1127–1134 (2006).

199. Thuong, N. T. T. *et al.* Epiregulin (EREG) variation is associated with susceptibility to tuberculosis. *Genes Immun.* **13,** 275–81 (2012).

200. Li, H. T., Zhang, T. T., Zhou, Y. Q., Huang, Q. H. & Huang, J. SLC11A1 (formerly NRAMP1) gene polymorphisms and tuberculosis susceptibility: A meta-analysis. *Int. J. Tuberc. Lung Dis.* **10,** 3–12 (2006).

201. Bowker, N. *et al.* Polymorphisms in the Pattern Recognition Receptor Mincle Gene (CLEC4E) and Association with Tuberculosis. *Lung* **194,** 763–767 (2016).

202. Azad, A. K., Sadee, W. & Schlesinger, L. S. Innate immune gene polymorphisms in tuberculosis. *Infect. Immun.* **80,** 3343–3359 (2012).

203. Flannagan, R. S., Cosío, G. & Grinstein, S. Antimicrobial mechanisms of phagocytes and bacterial evasion strategies. *Nat. Rev. Microbiol.* **7,** 355–66 (2009).

204. Gordon, S. & Taylor, P. R. Monocyte and macrophage heterogeneity. *Nat. Rev. Immunol.* **5,** 953–964 (2005).

205. Rohde, K., Yates, R. M., Purdy, G. E. & Russell, D. G. *Mycobacterium tuberculosis* and the environment within the phagosome. *Immunol. Rev.* **219,** 37–54 (2007).

206. C. Vinh, D. & Holland, S. M. *Phagocyte-Pathogen Interaction: Macrophages and the Host response to Infection*. (ASM Press American Society for Microbiology, 2009).

207. Vazquez-Torres, A. *et al. Salmonella* pathogenicity island 2-dependent evasion of the phagocyte NADPH oxidase. *Science (80-.).* **287,** 1655–1658 (2000).

208. Miller, B. H. *et al.* Mycobacteria Inhibit Nitric Oxide Synthase Recruitment to Phagosomes during Macrophage Infection. *Infect. Immun.* **72,** 2872–2878 (2004).

209. Benoit, M., Desnues, B. & Mege, J.-L. Macrophage polarization in bacterial infections. *J. Immunol.* **181,** 3733–3739 (2008).

210. Aderem, a & Underhill, D. M. Mechanisms of phagocytosis in macrophages. *Annu. Rev. Immunol.* **17,** 593–623 (1999).

211. Desjardins, M. Biogenesis of phagolysosomes: the 'kiss and run' hypothesis. *Trends Cell Biol.* **5,** 183–186 (1995).

212. Desjardins, M., Nzala, N. N., Corsini, R. & Rondeau, C. Maturation of phagosomes is accompanied by changes in their fusion properties and size-selective acquisition of solute materials from endosomes. *J. Cell Sci.* **110 (Pt 1,** 2303–2314 (1997).

213. Bucci, C. *et al.* The small GTPase rab5 function as a regulatory factor in the early endocytic pathway. *Cell* **70,** 715–728 (1992).

214. Desjardins, M., Huber, L. A., Parton, R. G. & Griffiths, G. Biogenesis of phagolysosomes proceeds through a sequential series of interactions with the endocytic apparatus. *J. Cell Biol.* **124,** 677–688 (1994).

215. Rink, J., Ghigo, E., Kalaidzidis, Y. & Zerial, M. Rab conversion as a mechanism of progression from early to late endosomes. *Cell* **122,** 735–749 (2005).

216. Harrison, R. E., Bucci, C., Vieira, O. V., Schroer, T. A. & Grinstein, S. Phagosomes Fuse with Late Endosomes and/or Lysosomes by Extension of Membrane Protrusions along Microtubules: Role of Rab7 and RILP. *Mol. Cell. Biol.* **23,** 6494–6506 (2003).

217. Beauregard, K. E., Lee, K.-D., Collier, R. J. & Swanson, J. A. pH-dependent Perforation of Macrophage Phagosomes by Listeriolysin O from *Listeria monocytogenes*. *J. Exp. Med.* **186,** 1159–1163 (1997).

218. Sturgill-Koszycki, S. *et al.* Lack of acidification in Mycobacterium phagosomes produced by exclusion of the vesicular proton-ATPase. *Science (80-.).* **263,** 678–681 (1994).

219. Stewart, G. R., Patel, J., Robertson, B. D., Rae, A. & Young, D. B. Mycobacterial mutants with defective control of phagosomal acidification. *PLoS Pathog.* **1,** 0269–0278 (2005).

220. Pethe, K. *et al.* Isolation of *Mycobacterium tuberculosis* mutants defective in the arrest of phagosome maturation. *Proc. Natl. Acad. Sci.* **101,** 13642–13647 (2004).

221. Lehrer, R. I., Lichtenstein, A. K. & Ganz, T. Defensins: Antimicrobial and Cytotoxic Peptides of Mammalian Cells. *Annu. Rev. Immunol.* **11,** 105–128 (1993).

222. Arnett, E., Lehrer, R. I., Pratikhya, P., Lu, W. & Seveau, S. Defensins enable macrophages to inhibit the intracellular proliferation of *Listeria monocytogenesListeria monocytogenes*. *Cell. Microbiol.* **13,** 635–651 (2011).

223. Sow, F. B. *et al.* Expression and localization of hepcidin in macrophages: a role in host defense against tuberculosis. *J. Leukoc. Biol.* **82,** 934–45 (2007).

224. Finbow, M. E. & Harrison, M. A. The vacuolar H + -ATPase: a universal proton pump of eukaryotes. *Biochem. J.* **324,** 697–712 (1997).

225. Mellman, I. The importance of being acid: the role of acidification in intracellular membrane traffic. *J. Exp. Biol.* **172,** 39–45 (1992).

226. Yates, R. M., Hermetter, A. & Russell, D. G. The kinetics of phagosome maturation as a function of phagosome/lysosome fusion and acquisition of hydrolytic activity. *Traffic* **6,** 413–420 (2005).

227. Segal, A. W. How Neutrophils Kill Microbes. *Annu. Rev. Immunol.* **23,** 197–223 (2005).

228. Quinn, M. T. & Gauss, K. A. Structure and regulation of the neutrophil respiratory burst oxidase: comparison with nonphagocyte oxidases. *J. Leukoc. Biol.* **76,** 760–81 (2004).

229. Vazquez-Torres, A., Jones-Carson, J., Mastroeni, P., Ischiropoulos, H. & Fang, F. C. Antimicrobial actions of the NADPH phagocyte oxidase and inducible nitric oxide synthase in experimental salmonellosis. I. Effects on microbial killing by activated peritoneal macrophages in vitro. *J. Exp. Med.* **192,** 227–36 (2000).

230. Sasada, M. & Johnston, R. B. Macrophage microbicidal activity. Correlation between phagocytosis-associated oxidative metabolism and the killing of Candida by macrophages. *J. Exp. Med.* **152,** 85–98 (1980).

231. Webb, J. L., Harvey, M. W., Holden, D. W. & Evans, T. J. Macrophage Nitric Oxide Synthase Associates with Cortical Actin but Is Not Recruited to Phagosomes. *Infect. Immun.* **69,** 6391–6400 (2001).

232. Knowles, R. G. & Moncada, S. Nitric oxide synthases in mammals. *Biochem. J.* **298,** 249–58 (1994).

233. Chan, J., Xing, Y., Magliozzo, R. S. & Bloom, B. R. Killing of Virulent *Mycobacterium tuberculosis* by Reactive Nitrogen Intermediates Produced by Activated Murine Macrophages. *J. Exp. Med* **175,** 1111–1122 (1992).

234. Schneemann, M. & Schoeden, G. Macrophage biology and immunology: man is not a mouse. *J. Leukoc. Biol.* **81,** 579–579 (2006).

235. Jung, J. Y. *et al.* The intracellular environment of human macrophages that produce nitric oxide promotes growth of mycobacteria. *Infect. Immun.* **81,** 3198–3209 (2013).

236. Cellier, M. F., Courville, P. & Campion, C. Nramp1 phagocyte intracellular metal withdrawal defense. *Microbes Infect.* **9,** 1662–1670 (2007).

237. Shin, D.-M. & Jo, E.-K. Antimicrobial Peptides in Innate Immunity against Mycobacteria. *Immune Netw.* **11,** 245–52 (2011).

238. DENIS, M. Killing of *Mycobacterium tuberculosis* within human monocytes: activation by cytokines and calcitriol. *Clin. Exp. Immunol.* **84,** 200–206 (1991).

239. Podinovskaia, M., Lee, W., Caldwell, S. & Russell, D. G. Infection of macrophages with *Mycobacterium tuberculosis* induces global modifications to phagosomal function. *Cell. Microbiol.* **15,** 843–859 (2013).

240. Wong, D., Bach, H., Sun, J., Hmama, Z. & Av-Gay, Y. *Mycobacterium tuberculosis* protein tyrosine phosphatase (PtpA) excludes host vacuolar-H+-ATPase to inhibit phagosome acidification. *Proc. Natl. Acad. Sci. U. S. A.* **108,**

19371–6 (2011).

241. Xu, S. *et al.* Intracellular trafficking in *Mycobacterium tuberculosis* and Mycobacterium avium-infected macrophages. *J. Immunol.* **153,** 2568–2578 (1994).

242. Kyei, G. B. *et al.* Rab14 is critical for maintenance of *Mycobacterium tuberculosis* phagosome maturation arrest. *EMBO J.* **25,** 5250–5259 (2006).

243. Via, L. E. *et al.* Arrest of mycobacterial phagosome maturation is caused by a block in vesicle fusion between stages controlled by rab5 and rab7. *J. Biol. Chem.* **272,** 13326–13331 (1997).

244. Yates, R. M. & Russell, D. G. Phagosome maturation proceeds independently of stimulation of toll-like receptors 2 and 4. *Immunity* **23,** 409–717 (2005).

245. Mwandumba, H. C. *et al. Mycobacterium tuberculosis* resides in nonacidified vacuoles in endocytically competent alveolar macrophages from patients with tuberculosis and HIV infection. *J. Immunol.* **172,** 4592–4598 (2004).

246. Fratti, R. A., Chua, J., Vergne, I. & Deretic, V. *Mycobacterium tuberculosis* glycosylated phosphatidylinositol causes phagosome maturation arrest. *Proc. Natl. Acad. Sci. U. S. A.* **100,** 5437–42 (2003).

247. Axelrod, S. *et al.* Delay of phagosome maturation by a mycobacterial lipid is reversed by nitric oxide. *Cell. Microbiol.* **10,** 1530–1545 (2008).

248. Denis, M. Growth of Mycobacterium avium in human monocytes: identification of cytokines which reduce and enhance intracellular microbial growth. *Eur. J. Immunol.* **21,** 391–395 (1991).

249. Sibling, L. D., Franzblau, S. G. & Krahenbuhl, J. L. Intracellular fate of Mycobacterium leprae in normal and activated mouse macrophages. *Infect. Immun.* **55,** 680–685 (1987).

250. van der Wel, N. *et al.* M. tuberculosis and M. leprae translocate from the phagolysosome to the cytosol in myeloid cells. *Cell* **129,** 1287–98 (2007).

251. Simeone, R. *et al.* Phagosomal Rupture by *Mycobacterium tuberculosis* Results in Toxicity and Host Cell Death. *PLoS Pathog.* **8,** e1002507 (2012).

252. Houben, D. *et al.* ESX-1-mediated translocation to the cytosol controls virulence of mycobacteria. *Cell. Microbiol.* **14,** 1287–1298 (2012).

253. Jamwal, S. V *et al.* Mycobacterial escape from macrophage phagosomes to the cytoplasm represents an alternate adaptation mechanism. *Sci. Rep.* **6,** 23089 (2016).

254. Simeone, R. *et al.* Cytosolic Access of *Mycobacterium tuberculosis*: Critical Impact of Phagosomal Acidification Control and Demonstration of Occurrence In Vivo. *PLOS Pathog.* **11,** e1004650 (2015).

255. Pires, D. *et al.* Role of Cathepsins in *Mycobacterium tuberculosis* Survival in Human Macrophages. *Sci. Rep.* **6,** 32247 (2016).

256. Noss, E. H., Harding, C. V. & Boom, W. H. *Mycobacterium tuberculosis* Inhibits MHC Class II Antigen Processing in Murine Bone Marrow Macrophages. *Cell. Immunol.* **201,** 63–74 (2000).

257. Behar, S. M. *et al.* Apoptosis is an innate defense function of macrophages against *Mycobacterium tuberculosis*. *Mucosal Immunol.* **4,** 279–87 (2011).

258. Gardner, E. M. *et al.* Efferocytosis is an innate antibacterial mechanism. **6,** 145–155 (2009).

259. Lerner, T. R. *et al. Mycobacterium tuberculosis* replicates within necrotic human macrophages. *J. Clin. Invest.* **216,** 583–594 (2017).

260. Park, J. S., Tamayo, M. H., Gonzalez-Juarrero, M., Orme, I. M. & Ordway, D. J. Virulent clinical isolates of *Mycobacterium tuberculosis* grow rapidly and induce cellular necrosis but minimal apoptosis in murine macrophages. *J. Leukoc. Biol.* **79,** 80–86 (2006).

261. Srinivasan, L., Ahlbrand, S. & Briken, V. Interaction of *Mycobacterium tuberculosis* with Host Cell Death Pathways. *Cold Spring Harb. Perspect. Med.* **4,** a022459–a022459 (2014).

262. Chen, M. *et al.* Lipid mediators in innate immunity against tuberculosis: opposing roles of PGE_2 and LXA_4 in the induction of macrophage death. *J. Exp. Med.* **205,** 2791–2801 (2008).

263. Marais, S. *et al.* Tuberculous meningitis: a uniform case definition for use in clinical research. *Lancet Infect. Dis.* **10,** 803–812 (2010).

264. Thwaites, G. E. *et al.* Dexamethasone for the Treatment of Tuberculous Meningitis in Adolescents and Adults. *N. Engl. J. Med.* **351,** 1741–1751 (2004).

265. Whitehorn, J. *et al.* Genetic variants of MICB and PLCE1 and associations with non-severe dengue. *PLoS One* **8,** e59067 (2013).

266. Dunstan, S. J. *et al.* Variation in human genes encoding adhesion and proinflammatory molecules are associated with severe malaria in the Vietnamese. *Genes Immun.* **13,** 503–8 (2012).

267. Dunstan, S. J. *et al.* A TNF region haplotype offers protection from typhoid fever in Vietnamese patients. *Hum. Genet.* **122,** 51–61 (2007).

268. Oxford Immunotec. T-SPOT.TB Training guide. **8,** 1–8 (2011).

269. ATCC. THP-1 ATCC® TIB-202™. Available at: https://www.atcc.org/Products/All/TIB-202.aspx#culturemethod. (Accessed: 28th February 2017)

270. ATCC. J774A.1 ATCC ® TIB-67™ Mus musculus ascites reticulum cell. Available at: https://www.atcc.org/Products/All/TIB-67.aspx#culturemethod.

271. Podinovskaia M. & Russell, D. *Detection and quantification of microbial manipulation of phagosomal function*. *Methods in Cell Biology* **126,** (Methods in Cell Biology, 2015).

272. Yates, R. M., Hermetter, A., Taylor, G. a. & Russell, D. G. Macrophage activation downregulates the degradative capacity of the phagosome. *Traffic* **8,** 241–250 (2007).

273. Yates, R. M. & Russell, D. G. Real-time spectrofluorometric assays for the

lumenal environment of the maturing phagosome. *Methods Mol. Biol.* **445,** 311–25 (2008).

274. Jambo, K. C. *et al.* Small alveolar macrophages are infected preferentially by HIV and exhibit impaired phagocytic function. *Mucosal Immunol.* **7,** 1116–26 (2014).

275. Russell, D. G., Vanderven, B. C., Glennie, S., Mwandumba, H. & Heyderman, R. S. The macrophage marches on its phagosome: dynamic assays of phagosome function. *Nat. Rev. Immunol.* **9,** 594–600 (2009).

276. Carroll, P. *et al.* Sensitive detection of gene expression in mycobacteria under replicating and non-replicating conditions using optimized far-red reporters. *PLoS One* **5,** (2010).

277. Baqir, M. *et al.* Cigarette smoke decreases MARCO expression in macrophages: Implication in Mycoplasma pneumoniae infection. *Respir. Med.* **102,** 1604–1610 (2008).

278. Illumina. GoldenGate Assay Workflow. *Illumina, Inc.* 1–2 (2006).

279. Balding, D. J. & Balding, D. J. A tutorial on statistical methods for population association studies. *Nat. Rev. Genet.* **7,** 781–91 (2006).

280. Lewis, C. Genetic association studies: design, analysis and interpretation. *Brief. Bioinform.* **3,** 146–153 (2002).

281. Tsolaki, A. G. *et al.* Genomic deletions classify the Beijing/W strains as a distinct genetic lineage of *Mycobacterium tuberculosis*. *J. Clin. Microbiol.* **43,** 3185–91 (2005).

282. Donnelly, L. E. & Barnes, P. J. Defective phagocytosis in airways disease. *Chest* **141,** 1055–1062 (2012).

283. Taylor, A. E. *et al.* Defective macrophage phagocytosis of bacteria in COPD. *Eur. Respir. J.* **35,** 1039–1047 (2010).

284. Berenson, C. S., Kruzel, R. L., Eberhardt, E. & Sethi, S. Phagocytic dysfunction

of human alveolar macrophages and severity of chronic obstructive pulmonary disease. *J. Infect. Dis.* **208,** 2036–45 (2013).

285. Ghigo, E. *et al.* Link between impaired maturation of phagosomes and defective Coxiella burnetii killing in patients with chronic Q fever. *J. Infect. Dis.* **190,** 1767–72 (2004).

286. Brighenti, S. & Lerm, M. How *Mycobacterium tuberculosis* Manipulates Innate and Adaptive Immunity – New Views of an Old Topic. *Underst. Tuberc. – Anal. Orig. Mycobacterium Tuberc. Pathog.* 208–234 (2012). doi:urn:nbn:se:liu:diva-75444 LA - English

287. Huynh, K. K. *et al.* LAMP proteins are required for fusion of lysosomes with phagosomes. *EMBO J.* **26,** 313–324 (2007).

288. Kelley, V. A. & Schorey, J. S. Mycobacterium's arrest of phagosome maturation in macrophages requires Rab5 activity and accessibility to iron. *Mol. Biol. Cell* **14,** 3366–77 (2003).

289. Borlace, G. N., Jones, H. F., Keep, S. J., Butler, R. N. & Brooks, D. A. Helicobacter pylori phagosome maturation in primary human macrophages. *Gut Pathog.* **3,** 3 (2011).

290. Welin, A., Raffetseder, J., Eklund, D., Stendahl, O. & Lerm, M. Importance of Phagosomal Functionality for Growth Restriction of *Mycobacterium tuberculosis* in Primary Human Macrophages. *J. Innate Immun.* **3,** 508–518 (2011).

291. Podinovskaia, M. *et al.* Dynamic quantitative assays of phagosomal function. *Curr. Protoc. Immunol.* 1–14 (2013). doi:10.1002/0471142735.im1434s102

292. Nüsse, O. Biochemistry of the phagosome: the challenge to study a transient organelle. *ScientificWorldJournal.* **11,** 2364–81 (2011).

293. Fujiwara, N. & Kobayashi, K. Macrophages in inflammation. *Curr. Drug Targets. Inflamm. Allergy* **4,** 281–6 (2005).

294. Bowdish, D. M. E. *et al.* MARCO, TLR2, and CD14 are required for macrophage cytokine responses to mycobacterial trehalose dimycolate and

Mycobacterium tuberculosis. *PLoS Pathog.* **5,** e1000474 (2009).

295. Brown, G. D. & Gordo, S. A new receptor for beta-glucans. *Nature* **413,** 36 (2001).

296. Shaner, N. C., Steinbach, P. A. & Tsien, R. Y. A guide to choosing fluorescent proteins. *Nat. Methods* **2,** 905–909 (2005).

297. Doherty, G. P., Bailey, K. & Lewis, P. J. Stage-specific fluorescence intensity of GFP and mCherry during sporulation In Bacillus Subtilis. *BMC Res. Notes* **3,** 303 (2010).

298. Proskuryakov, S. Y., Konoplyannikov, A. G. & Gabai, V. L. Necrosis: A specific form of programmed cell death? *Exp. Cell Res.* **283,** 1–16 (2003).

299. Vanderven, B. C., Yates, R. M. & Russell, D. G. Intraphagosomal measurement of the magnitude and duration of the oxidative burst. *Traffic* **10,** 372–378 (2009).

300. Repasy, T. *et al.* Intracellular Bacillary Burden Reflects a Burst Size for *Mycobacterium tuberculosis* In Vivo. *PLoS Pathog.* **9,** e1003190 (2013).

301. Al-Orainey, I. O. Diagnosis of latent tuberculosis: Can we do better? *Ann. Thorac. Med.* **4,** 5–9 (2009).

302. Styblo, K. Recent advances in epidemiological research in tuberculosis. *Adv. Tuberc. Res.* **20,** 1–63 (1980).

303. Flynn, J. L., Chan, J. & Lin, P. L. Macrophages and control of granulomatous inflammation in tuberculosis. *Mucosal Immunol.* **4,** 271–278 (2011).

304. Sturgill-koszycki, S., Schaible, U. E. & Russell, D. G. Mycobacterium-containing phagosomes. *EMBO J.* **15,** 6960–6968 (1996).

305. de Chastellier, C., Forquet, F., Gordon, A. & Thilo, L. Mycobacterium requires an all-around closely apposing phagosome membrane to maintain the maturation block and this apposition is re-established when it rescues itself from phagolysosomes. *Cell. Microbiol.* **11,** 1190–1207 (2009).

306. Schoenen, H. *et al.* Cutting edge: Mincle is essential for recognition and

adjuvanticity of the mycobacterial cord factor and its synthetic analog trehalose-dibehenate. *J. Immunol.* **184,** 2756–2760 (2010).

307. Willment, J. A. *et al.* The human β-glucan receptor is widely expressed and functionally equivalent to murine Dectin-1 on primary cells. *Eur. J. Immunol.* **35,** 1539–1547 (2005).

308. Rybicka, J. M., Balce, D. R., Khan, M. F., Krohn, R. M. & Yates, R. M. NADPH oxidase activity controls phagosomal proteolysis in macrophages through modulation of the lumenal redox environment of phagosomes. *Proc. Natl. Acad. Sci. U. S. A.* **107,** 10496–10501 (2010).

309. Indrigo, J., Hunter, R. L. & Actor, J. K. Cord factor trehalose 6,6'-dimycolate (TDM) mediates trafficking events during mycobacterial infection of murine macrophages. *Microbiology* **149,** 2049–2059 (2003).

310. Taylor, P. R. *et al.* The beta-glucan receptor, dectin-1, is predominantly expressed on the surface of cells of the monocyte/macrophage and neutrophil lineages. *J. Immunol.* **169,** 3876–3882 (2002).

311. Underhill, D. M., Rossnagle, E., Lowell, C. a, Simmons, R. M. & Dc, W. Dectin-1 activates Syk tyrosine kinase in a dynamic subset of macrophages for reactive oxygen production. *Blood* **106,** 2543–2550 (2005).

312. Herre, J. *et al.* Dectin-1 uses novel mechanisms for yeast phagocytosis in macrophages. *Blood* **104,** 4038–4045 (2004).

313. Shin, D. M. *et al.* Mycobacterium abscessus activates the macrophage innate immune response via a physical and functional interaction between TLR2 and dectin-1. *Cell. Microbiol.* **10,** 1608–1621 (2008).

314. Lee, H.-M. *et al.* Innate immune responses to Mycobacterium ulcerans via toll-like receptors and dectin-1 in human keratinocytes. *Cell. Microbiol.* **11,** 678–92 (2009).

315. Lee, H. M., Yuk, J. M., Shin, D. M. & Jo, E. K. Dectin-1 is inducible and plays an essential role for mycobacteria-induced innate immune responses in airway

epithelial cells. *J Clin Immunol* **29,** 795–805 (2009).

316. Rothfuchs, A. G. *et al.* Dectin-1 Interaction with *Mycobacterium tuberculosis* Leads to Enhanced IL-12p40 Production by Splenic Dendritic Cells. *J. Immunol.* **179,** 3463–3471 (2007).

317. Yadav, M. & Schorey, J. S. The beta-glucan receptor dectin-1 functions together with TLR2 to mediate macrophage activation by mycobacteria. *Blood* **108,** 3168–3175 (2006).

318. Yamasaki, S. *et al.* Mincle is an ITAM-coupled activating receptor that senses damaged cells. *Nat Immunol* **9,** 1179–1188 (2008).

319. Brown, G. D., Marakalala, M. J. & Graham, L. M. The role of Syk/CARD9-coupled C-type lectin receptors in immunity to *Mycobacterium tuberculosis* infections. *Clin. Dev. Immunol.* **2010,** 567571 (2010).

320. Behler, F. *et al.* Role of Mincle in alveolar macrophage-dependent innate immunity against mycobacterial infections in mice. *J. Immunol.* **189,** 3121–9 (2012).

321. Ishikawa, E. *et al.* Direct recognition of the mycobacterial glycolipid, trehalose dimycolate, by C-type lectin Mincle. *J. Exp. Med.* **206,** 2879–2888 (2009).

322. Lee, W. *et al.* Neutrophils Promote Mycobacterial Trehalose Dimycolate-Induced Lung Inflammation via the Mincle Pathway. *PLoS Pathog.* **8,** (2012).

323. van der Laan, L. J. *et al.* Regulation and functional involvement of macrophage scavenger receptor MARCO in clearance of bacteria in vivo. *J. Immunol.* **162,** 939–47 (1999).

324. Ito, S. *et al.* Roles of a macrophage receptor with collagenous structure (MARCO) in host defense and heterogeneity of splenic marginal zone macrophages. *Archives of histology and cytology* **62,** 83–95 (1999).

325. Benard, E. L., Roobol, S. J., Spaink, H. P. & Meijer, A. H. Phagocytosis of mycobacteria by zebrafish macrophages is dependent on the scavenger receptor Marco, a key control factor of pro-inflammatory signalling. *Dev. Comp.*

Immunol. **47,** 223–233 (2014).

326. Bowdish, D. M. *et al.* Genetic variants of MARCO are associated with susceptibility to pulmonary tuberculosis in a Gambian population. *BMC Med. Genet.* **14,** 47 (2013).

327. Ma, M.-J. *et al.* Genetic Variants in MARCO Are Associated with the Susceptibility to Pulmonary Tuberculosis in Chinese Han Population. *PLoS One* **6,** e24069 (2011).

328. Thuong, N. T. T. *et al.* Identification of tuberculosis susceptibility genes with human macrophage gene expression profiles. *PLoS Pathog.* **4,** e1000229 (2008).

329. Thuong, N. T. T. *et al.* MARCO variants are associated with phagocytosis, pulmonary tuberculosis susceptibility and Beijing lineage. *Genes Immun.* **17,** 1–7 (2016).

330. Arredouani, M. *et al.* The scavenger receptor MARCO is required for lung defense against pneumococcal pneumonia and inhaled particles. *J. Exp. Med.* **200,** 267–72 (2004).

331. Thelen, T. *et al.* The class A scavenger receptor, macrophage receptor with collagenous structure, is the major phagocytic receptor for Clostridium sordellii expressed by human decidual macrophages. *J. Immunol.* **185,** 4328–4335 (2010).

332. Lang, R. Recognition of the mycobacterial cord factor by Mincle: Relevance for granuloma formation and resistance to tuberculosis. *Front. Immunol.* **4,** 1–7 (2013).

333. Rice, P. J. *et al.* Human monocyte scavenger receptors are pattern recognition receptors for (1->3)- β -D-glucans. *J. Leukoc. Biol.* **72,** 140–146 (2002).

334. Józefowski, S., Yang, Z., Marcinkiewicz, J. & Kobzik, L. Scavenger receptors and β-glucan receptors participate in the recognition of yeasts by murine macrophages. *Inflamm. Res.* **61,** 113–26 (2012).

335. Dorrington, M. G. *et al.* MARCO is required for TLR2- and Nod2-mediated responses to Streptococcus pneumoniae and clearance of pneumococcal

colonization in the murine nasopharynx. *J. Immunol.* **190,** 250–8 (2013).

336. Sakamoto, K. *et al.* Mycobacterial trehalose dimycolate reprograms macrophage global gene expression and activates matrix metalloproteinases. *Infect. Immun.* **81,** 764–776 (2013).

337. van Crevel, R. *et al.* Infection with *Mycobacterium tuberculosis* Beijing genotype strains is associated with polymorphisms in SLC11A1/NRAMP1 in Indonesian patients with tuberculosis. *J. Infect. Dis.* **200,** 1671–1674 (2009).

338. Dunn, P. L. & North, R. J. Virulence ranking of some *Mycobacterium tuberculosis* and Mycobacterium bovis strains according to their ability to multiply in the lungs, induce lung pathology, and cause mortality in mice. *Infect. Immun.* **63,** 3428–3437 (1995).

339. Zhang, M., Gong, J., Lin, Y. & Barnes, P. F. Growth of virulent and avirulent *Mycobacterium tuberculosis* strains in human macrophages. *Infect. Immun.* **66,** 794–9 (1998).

340. McDonough, K. A. & Kress, Y. Cytotoxicity for lung epithelial cells is a virulence-associated phenotype of *Mycobacterium tuberculosis*. *Infect. Immun.* **63,** 4802–4811 (1995).

341. Mogensen, T. H. Pathogen recognition and inflammatory signaling in innate immune defenses. *Clin. Microbiol. Rev.* **22,** 240–273 (2009).

342. Coscolla, M. & Gagneux, S. Does M. tuberculosis genomic diversity explain disease diversity? *Drug Discov. Today Dis. Mech.* **7,** e43–e59 (2010).

343. Sarkar, R., Lenders, L., Wilkinson, K. A., Wilkinson, R. J. & Nicol, M. P. Modern lineages of *Mycobacterium tuberculosis* exhibit lineage-specific patterns of growth and cytokine induction in human monocyte-derived macrophages. *PLoS One* **7,** e43170 (2012).

344. Somerville, G. A. *et al.* In vitro serial passage of Staphylococcus aureus: changes in physiology, virulence factor production, and agr nucleotide sequence. *J. Bacteriol.* **184,** 1430–7 (2002).

345. Domenech, P. & Reed, M. B. Rapid and spontaneous loss of phthiocerol dimycocerosate (PDIM) from *Mycobacterium tuberculosis* grown in vitro: implications for virulence studies. *Microbiology* **155,** 3532–3543 (2009).

346. Stokes, R. W. & Doxsee, D. The receptor-mediated uptake, survival, replication, and drug sensitivity of *Mycobacterium tuberculosis* within the macrophage-like cell line THP-1: a comparison with human monocyte-derived macrophages. *Cell. Immunol.* **197,** 1–9 (1999).

347. Castañón, M. & E, M.-C. Comparative evaluation of in vitro human macrophage models for mycobacterial infection study. *Pathog Dis.* **74,** 1–7 (2016).

348. Koo, M.-S., Subbian, S. & Kaplan, G. Strain specific transcriptional response in *Mycobacterium tuberculosis* infected macrophages. *Cell Commun. Signal.* **10,** 2 (2012).

349. Novikov, A. *et al. Mycobacterium tuberculosis* triggers host type I IFN signaling to regulate IL-1β production in human macrophages. *J. Immunol.* **187,** 2540–7 (2011).

350. Krishnan, N., Robertson, B. D. & Thwaites, G. Pathways of IL-1β secretion by macrophages infected with clinical *Mycobacterium tuberculosis* strains. *Tuberculosis* **93,** 538–547 (2013).

351. Cervantes, J., Nagata, T., Uchijima, M., Shibata, K. & Koide, Y. Intracytosolic *Listeria monocytogenesListeria monocytogenes* induces cell death through caspase-1 activation in murine macrophages. *Cell. Microbiol.* **10,** 41–52 (2008).

352. Sun, G. W., Lu, J., Pervaiz, S., Cao, W. P. & Gan, Y. H. Caspase-1 dependent macrophage death induced by Burkholderia pseudomallei. *Cell. Microbiol.* **7,** 1447–1458 (2005).

353. Holt, K. E. *et al.* Genomic analysis of *Mycobacterium tuberculosis* reveals complex etiology of tuberculosis in Vietnam including frequent introduction and transmission of Beijing lineage and positive selection for EsxW Beijing variant. *http://www.biorxiv.org/content/early/2016/12/07/092189* 1–16 (2016).

354. Clemmensen, H. S. *et al.* An attenuated *Mycobacterium tuberculosis* clinical strain with a defect in ESX-1 secretion induces minimal host immune responses and pathology. *Sci. Rep.* **7,** 46666 (2017).

355. Munk, M. E. & Emoto, M. Functions of T-cell subsets and cytokines in mycobacterial infections. *Eur. Respir. J. Suppl.* **20,** 668s–675s (1995).

356. Walker, T. M. *et al.* Whole-genome sequencing for prediction of *Mycobacterium tuberculosis* drug susceptibility and resistance: A retrospective cohort study. *Lancet Infect. Dis.* **15,** 1193–1202 (2015).

357. Takiff, H. E. & Feo, O. Clinical value of whole-genome sequencing of *Mycobacterium tuberculosis*. *Lancet Infect. Dis.* **15,** 1077–1090 (2015).

358. Kwong, J. C., McCallum, N., Sintchenko, V. & Howden, B. P. Whole genome sequencing in clinical and public health microbiology. *Pathology* **47,** 199–210 (2015).

APPENDIX

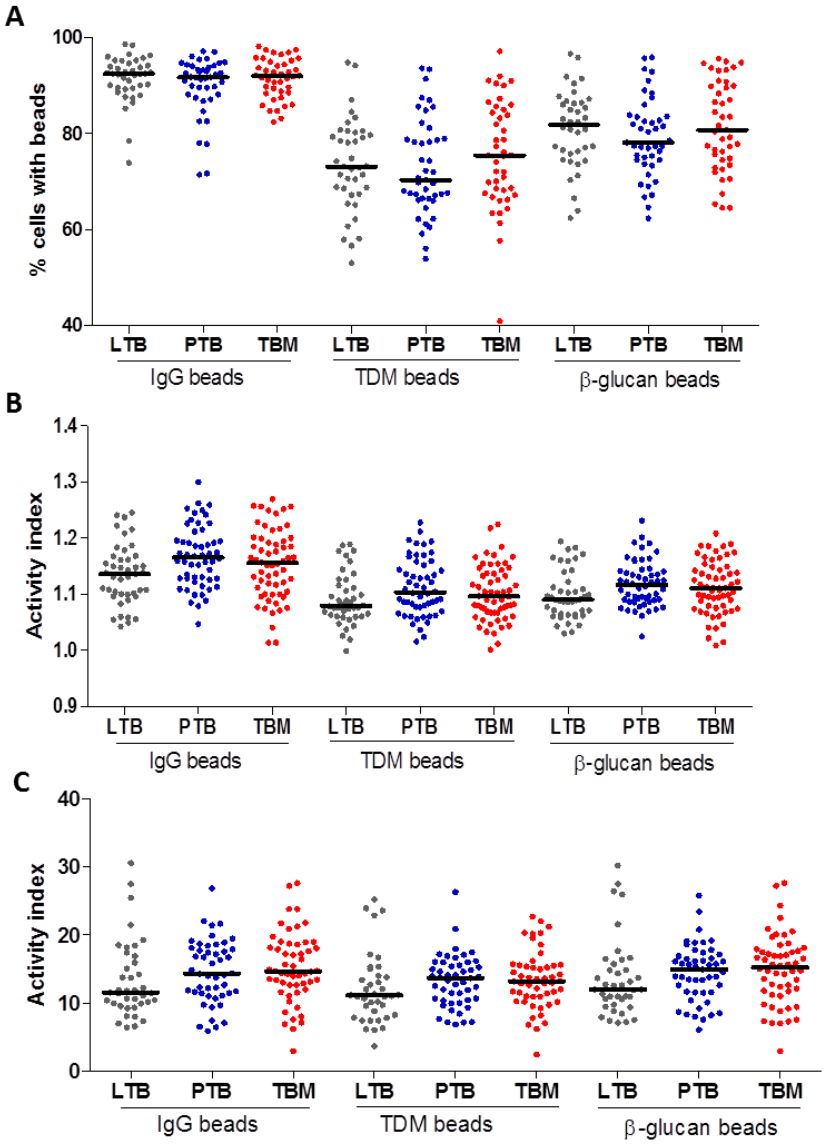

Supplementary figure 4.1 Macrophage activities in PTB and TBM individuals

Monocyte-derived macrophages from subjects with LTB, PTB, and TBM at day 7 were treated with reporter beads coated with either IgG, TDM or β-glucan. (A) Phagocytosis of macrophages from LTB (n= 39), PTB (n= 42) and TBM (n= 42), (B) Acidification Activity index at 60 min in macrophage from LTB (n= 43), PTB (n= 54) and TBM (n= 60) and (C) Proteolysis Activity index at 210 min upon beat treatment in macrophage from LTB (n= 42), PTB (n= 52) and TBM (n= 59). Bars in the plots represent median values. To compare activity of macrophages from PTB and TBM individuals, P-value was determined using Mann-Whitney U test.

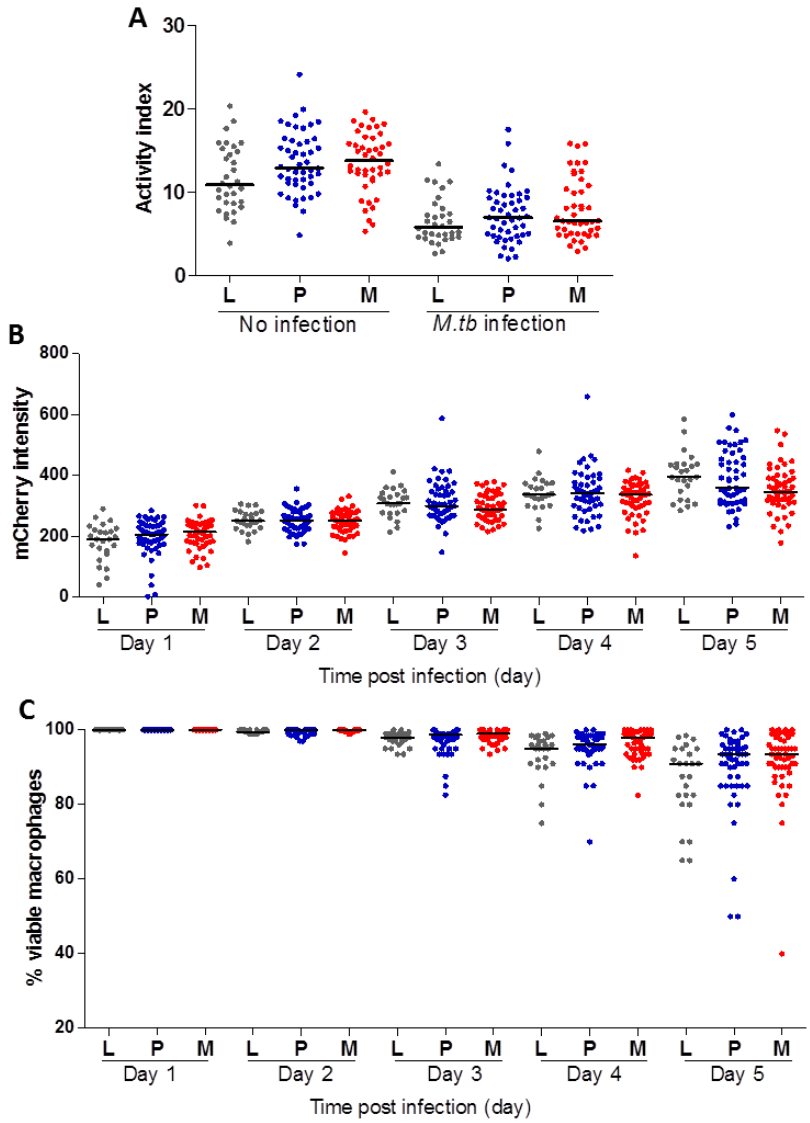

Supplementary figure 4.2 Proteolysis activity and killing ability of macrophages from PTB and TBM individuals during *Mtb* infection

Macrophages derived from cryopreserved monocytes from subjects with LTB, PTB and TBM at day 5 were infected with reporter *Mtb* at MOI 1 or left uninfected. (A) Proteolytic Activity index of infected macrophages from LTB (n= 32), PTB (n= 48), and TBM (n= 44) individuals at 210 min. At day 2 post infection, macrophages were treated with reporter beads coated with IgG to measure proteolytic activity. (B, C) The bacteria intracellular growth during 5 days of infection was assessed by the mCherry intensity readout (B) and the viability of infected macrophages (C) from LTB (n= 26), PTB (n= 52) and TBM (n= 53). L indicates LTB, P indicates PTB, M indicates TBM. Bars in the plot represent median values. To compare activity of macrophages from PTB and TBM individuals, P-value was determined using Mann-Whitney U test.

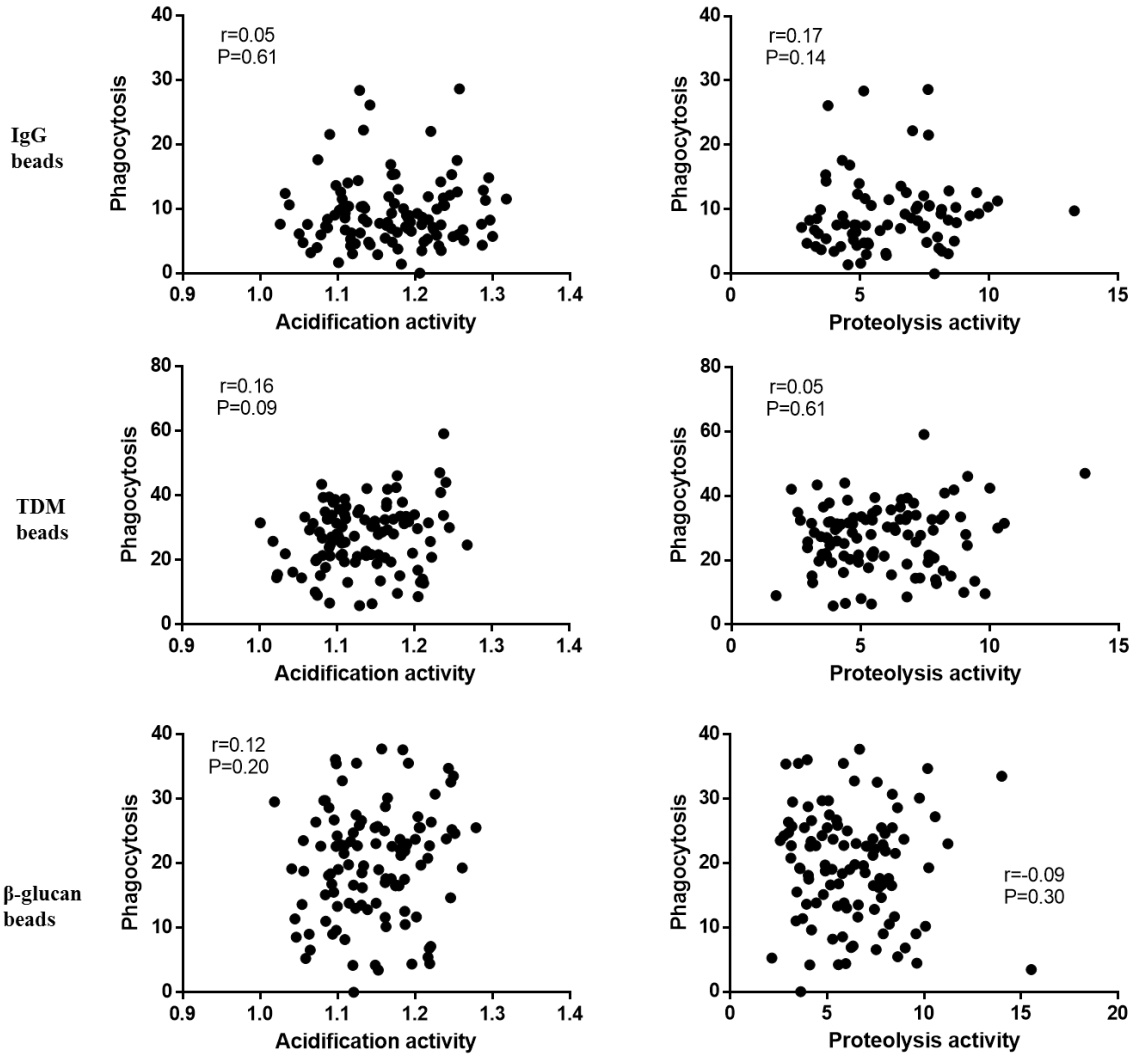

Supplementary figure 4.3 Correlation between phagocytosis and acidification or proteolysis activities in macrophages treated with beads coated with either IgG, TDM or β-glucan (G-I). Macrophages were from LTB and ATB combined. r: correlation coefficient